university of groningen
faculty of science and engineering



Multi-agent network games with applications in smart electric mobility

Carlo Cenedese



This dissertation has been completed in fulfillment of the requirements of the Dutch Institute of Systems and Control (DISC) for graduate study.



This research is supported by the Netherlands Organization for Scientific Research (NWO-vidi-14134).

This thesis was prepared with the LaTeXdocumentation system.

Copyright © 2021 by Carlo Cenedese.

All rights reserved. No part of the material protected by this copyright notice may be reproduced or utilized in any form or by any means, electronic or mechanical, including photocopying, recording or by any information storage and retrieval system, without written permission from the copyright owner.



rijksuniversiteit
groningen

Multi-agent network games with applications in smart electric mobility

PhD Thesis

to obtain the degree of PhD at the
University of Groningen,
on the authority of the
Rector Magnificus Prof. C. Wijmenga,
and on accordance with
the decision by the College of Deans

This thesis will be defended in public on
16 April 2021 at 11:00 hours

by

Carlo Cenedese

born on 13 June 1991
in Treviso, Italy

Supervisors:
Prof. M. Cao
Prof. J.M.A. Scherpen
External Supervisor:
Prof. S. Grammatico (Technische Universiteit Delft)
Assessment committee:
Prof. L. Pavel (University of Toronto)
Prof. A. Ferrara (University of Pavia)
Prof. D. Bauso (Rijksuniversiteit Groningen)

To my beloved family
my parents Diego and Liviana
and my brother Nicola.

Acknowledgments

The past four years have been a period of great growth for me, during which I have learned a lot from many amazing people, some of which I have the pleasure to define friends nowadays. Therefore, let me start this thesis by giving due thanks to the people without whom this adventure would not have been the same.

I start by thanking my supervisor Prof. Ming Cao, for giving me the chance to perform my PhD at the prestigious University of Groningen. You gave me a great number of opportunities to develop from an academic and personal point of view. You always trusted and empowered me, starting from giving me the lead of the TAs of in the Robotics course all the way to the presentation performed for the royal family. I always appreciated the freedom you gave me in exploring the topics in which I was more interested, allowing me to find my way in the broad field of research on systems and control without putting pressure on me. By you I have learned the power and importance of the words to convey efficiently a message. You have always aim at the highest standard and pushed me to do better, I will always keep that in mind throughout my future works. To my second supervisor Prof. Jacquelien M. A. Scherpen, I want to express my appreciation. During the research projects in which we collaborated I had the pleasure to entertaining with you in challenging and thriving discussions. I respect you not only from a research but also from a human point of view. During these years, you have always put a lot of effort in making the group a welcoming place in which ideas can thrive and I am sure everyone is grateful for this. I could not choose a better place for the start of my research career. My external (and daily) supervisor Prof. Sergio Grammatico has always been a guide and an example of how cutting-edge research should be carried out. I have great admiration for you not only for how greatly involved you are in all the projects of your students but also for the impressive technical skills that always allowed you to steer me in the right direction. I enjoyed our meeting, you keep challenged me to approach new topics by stepping out of my research comfort zone. If I learned how to tackle a complex problem by emending everything not essential, then I have to thank your guidance. Finally, from a human point of view, I am grateful for all the advice that you have given me any time I asked for an honest opinion or help.

I want to thank the members of the assessment committee Prof. Lacra Pavel, Prof. Antonella Ferrara and Prof. Dario Bauso for taking the time of reading my thesis and providing interesting comments.

My two paranymphs and dear friends Michele Cucuzzella and Pablo B. Rosales deserve an acknowledgment for helping me in this final part of my journey. I want

to thank Michele for the nice collaborations and the development of the works on smart-mobility that made me discover a new and attractive topic on which I am sure we will collaborate again in the future. I can not speak of our amazing trips. In Miami, with Henk van Waarde my favorite mathematician together with Mark Jeeninga. In Nice, with Prof. Yu Kawano that always made me laugh with his unique sense of humor, and that I also have to thank for helping me to place the firsts important milestones of my PhD (he knows English very well). In Naples and the Capri, during which we have guided Alain Govaert through the beauties of our motherland. I am deeply grateful to Alain for numerous things from the trip we had in Germany to the introduction to potential games, but most of all for the kindness and friendship he showed me during some very difficult moments I have passed in the past years. Even though I did not manage to collaborate with Pablo on research topics, he is a very important part of my experience in Groningen. I share a lot of nice memories with him, like the football match we have seen in Amsterdam and the subsequent night spent at the airport. Together, with his wife Celia they form a heart-warming couple and I cannot thank them enough for all the fun we had together, I have always felt welcome in your company. He, together with the other members of the Mexican "gang" have been a constant in my most enjoyable memories in Groningen. In fact, I am grateful to all of them. To Hildeberto J. Kojakhmetov for the poker nights and the basketball matches together with Yuzhen Qin, Shuai Feng, and Qingkai Yang. To Rodolfo Reyez-Baéz, for showing me how to combine fun and hard work. To Marco Vasquez Beltran, for always been so kind and lighthearted. Moreover, I want to thank Lorenzo Zino not only for the nice project on which we collaborated but also for all the memorable dinners we had together. I also feel lucky to have met Ben Ye, a great and clever guy whith whom I have spent a lot of time, and I even manage to teach him how to cook proper carbonara. Iurii Kapitaniuk and Weijia Yao have been of great help in supporting me during the Robotics course and it was a pleasure to collaborate in developing the experiment that we presented to the royal family (I will not forget those moments). I also highly appreciate Emin Martirosyan for being my office mate, a tough guy with a golden heart. I also want to thank Tábitha Esteves and Carmen Chan for always being able to lighten the mood and have fun. In general, I am deeply regretful to all the members of DTPA, SMS and ODS for creating the best environment in which I could have hoped to work.

Next, I can not mention my foster research group, i.e., the group of Prof. S. Grammatico at the Delft Center for Systems and Control, TU Delft. During these years I have traveled so many times to Delft that it seems like a second home. I highly appreciated the technical discussions that all of us had every Thursday and the more light ones during the coffee breaks. A special thanks go to Filippo Fabiani, Barbara Franci, and Mattia Bianchi with whom I have built a nice friendship and always manage to make me laugh. One of the most important colleagues that I had in these years is Giuseppe Belgioioso. I have always seen him as a big brother-in-research since we manage to achieve numerous results together on the topic of monotone operators. He helped me many times with brilliant intuitions and discussions. Our paths crossed several times, in Padova, at the times of the Master, in Paris, in Turin, and, once again, here in Zürich; I have always enjoyed the time we have spent together.

I would also like to thank all the people that helped me in these first months of my new Swiss adventure: Giuseppe and Igrid, Nicoló Pagan, and Enrico Mion. They helped me to navigate this difficult period and I am grateful for this.

When I moved to the Netherlands I have left many important people in Italy that had and always will have a special place in life. My childhood friends that make me feel like no time has passed every time I go back home: Franceso De Lazzer, Francisco Martearena, Carlo Giacomin, Giorgio Segato, Davide Vignotto, Matteo Giacomin, Antonio Sartor, Filippo Atzori, and Emiliano Tintinaglia. I also want to thank Enrica Rossi and Chiara Zambon for always being there when I needed to talk or just to hang out.

This journey would have been different and less enjoyable if I hadn't found along the way Marta Nardo, a very special person that gave me a new perspective and her love and support motivated me to achieve this personal milestone represented by this thesis.

Finally, I foremost have to be grateful to my family and relatives for supporting me. I want to thank my brother Nicola; even though we are so different, I have always looked up to him as an example for his determination and incredible skills in whatever he decides to do. I could not have a better brother. Last but not least, my parents Liviana and Diego witnessed my change during these four years and encouraged me to always chase my dreams. I hope that in the future I will manage to create something half as good as they did with our family, they will always be a role model to me.

Carlo Cenedese
Groningen
March 2021

Contents

Acknowledgment **vii**

List of Abbreviations xv

List of Symbols xvii

1 Overview **1**

1.1 Introduction to multi-agent network games 2

1.2 Structure of the thesis 5

I Multi-agent network games via operator theory **11**

2 Asynch. and time-varying proximal network games **13**

2.1 Introduction 14

2.2 Mathematical setup and problem formulation 15

2.3 Proximal dynamics 17

2.4 Numerical simulations 23

2.5 Conclusion and outlook 26

2.6 Appendix 28

3 Equilibrium seeking design in proximal network games **33**

3.1 Introduction 34

3.2 Proximal dynamics under coupling constraints 35

3.3 Proximal dynamics under time-varying coupling constraints 39

3.4 Simulations 44

3.5 Conclusion and outlook 48

3.6 Appendix 49

4 Asynchronous networked GNE seeking **57**

4.1 Introduction . . . 58

4.2 Problem formulation . . . 59

4.3 Synchronous distributed GNE seeking algorithm . . . 62

4.4 Asynchronous, distributed algorithm with edge variables (AD-GEED) 66

4.5 Asynchronous, distributed algorithm with node variables (AD-GENO) 69

4.6 Simulations . . . 70

4.7 Conclusion . . . 75

4.8 Appendix . . . 76

II Decision making via potential game theory **81**

5 Relative Best Response dynamics **83**

5.1 Introduction . . . 84

5.2 h-Relative Best Response dynamics . . . 86

5.3 Convergence for finite games . . . 91

5.4 Convergence of convex games . . . 93

5.5 Networks of best and h-relative best responders . . . 95

5.6 Competing products with network effects . . . 96

5.7 Conclusion and final remarks . . . 100

6 Charging coordination for plug-in electric vehicles **101**

6.1 Introduction . . . 102

6.2 PEVs scheduling and charge as a system of mixed-logical-dynamical systems . . . 103

6.3 Translating the logical implications into mixed-integer linear constraints . . . 106

6.4 PEVs charge coordination as a generalized mixed-integer potential game . . . 109

6.5 Numerical simulations . . . 112

6.6 Conclusion and outlook . . . 115

6.7 Appendix . . . 116

7 Highway congestion control via smart electric mobility 117
7.1 Introduction . . . 118
7.2 Cell Transmission Model with Charging Station . . . 120
7.3 Decision making process . . . 123
7.4 Formulation of the mixed-integer game . . . 132
7.5 Cell Transmission Model (CTM) traffic control scheme . . . 134
7.6 CTM identification . . . 137
7.7 Decision process' parameters selection . . . 143
7.8 Numerical results . . . 145
7.9 Sensitivity analysis . . . 150
7.10 Policy recommendation . . . 154
7.11 Conclusion . . . 155
7.12 Appendix . . . 157

8 Conclusion and Outlook 159
8.1 Part I: Multi-agent network games via operator theory . . . 160
8.2 Part II: Decision making via potential game theory . . . 162

A Monotone operators and fixed point theory 165
A.1 Operators . . . 165
A.2 Nonexpansive operators . . . 166
A.3 Monotone Operators . . . 167
A.4 Nonexpansiveness and monotonicity of relevant operators . . . 169
A.5 Fixed point iterations . . . 171
A.6 Zero finding algorithms . . . 172

B Graph theory 175
B.1 Graphs . . . 175
B.2 Relevant matrices . . . 176
B.3 Perron–Frobenious theory . . . 178

C Potential game theory 181
C.1 Potential functions . . . 181
C.2 Improvement paths . . . 182

Bibliography 197

Summary **199**

About the Author **203**

List of Abbreviations

r2s	road-to-station
s2r	station-to-road
ε-GNE	ε-Generalized Nash equilibrium (ε-GNE)
h-RBR	h-Relative Best Response
AFIP	Approximate Finite Improvement Property
ATDM	Active Traffic Demand Management
AVG	averaged
BR	Best Response
BSI	Bilateral Symmetric Interaction
CON	contractive
CS	Charging Station
CTM	Cell Transmission Model
ENWE	Extended Network Equilibrium
EV	Electric Vehicle
FB	forward-backward operator splitting
FIP	Finite Improvement Property
FNE	firmly nonexpansive
FoRB	forward-reflected-backward operator splitting
g2v	grid-to-vehicle
GAE	generalized aggregative equilibrium
GNE	generalized Nash equilibrium
GNEP	generalized Nash equilibrium problem
GNWE	Generalized Network Equilibrium
GS	Gauss-Southwell
GVI	generalized variational inequality
HO	Highway Operator
i.i.d.	independent and identically distributed
KKT	Karush-Kuhn-Tucker conditions
LIP	Lipschitz continuous
MI-GPG	Mixed-Integer Generalized Potential Game
MINE	ε-Mixed-Integer Nash Equilibrium
MIP	Mixed-Integer Programming
MLD	Mixed-Logical-Dynamical
MON	monotone
MPC	Model Predictive Control
n–ENWE	normalized Extended Network Equilibrium
NDW	Nationaal Dataportaal Wegverkeer
NE	Nash equilibrium
NEP	Nash equilibrium problem
NEX	nonexpansive
NWE	Network Equilibrium
p-ENWE	persistent Extended Network Equilibrium
p-GNWE	persistent Generalized Network Equilibrium
p-NWE	persistent Network Equilibrium

PEV	Plug-in Electric Vehicle
PF	Perron-Frobenius
pFB	preconditioned forward-backward algorithm
PG	pseudo-gradient mapping
pn-ENWE	persistent normalized Extended Network Equilibrium
PPA	proximal-point algorithm
PPP	preconditioned proximal-point algorithm
PS	pseudo-subdifferential mapping
Q-NE	quasi-nonexpansive
RBR	Relative Best Response
SMON	strongly monotone
sMON	strictly monotone
SoC	State of Charge
sPC	stricly pseudo-contractive
TDM	Traffic Demand Management
v-GAE	variational generalized aggregative equilibrium
v-GNE	variational generalized Nash equilibrium
v2g	vehicle-to-grid
VI	variational inequality

List of Symbols

Basic Operators and Relations

$\cdot$	general placeholder
$:=$	right-hand side defines the left-hand side
$\mid$	such that (or given)
$\in$	left-hand side is an element of right-hand side
$\exists$	there exists
$\forall$	for all
$\Rightarrow$	implies
$\Leftrightarrow$	if and only if
$\rightrightarrows$	maps to a set
$\mapsto$	maps to a value

Set, Spaces and Set Operators

$\mathbb{N}$	set of natural numbers
$\mathbb{Z}$	set of integer numbers
$\mathbb{B}$	set $\{0, 1\}$
$\mathbb{R}$	set of real numbers
$\overline{\mathbb{R}}$	set of extended real numbers, i.e., $\overline{\mathbb{R}} := \mathbb{R} \cup \{\infty\}$
$\mathbb{R}_{\geq 0}(\mathbb{R}_{\leq 0})$	set of nonnegative (nonpositive) real numbers
$\mathbb{R}_{>0}(\mathbb{R}_{<0})$	set of positive (negative) real numbers
$\mathbb{R}^n$	set of real n-dimensional vectors
$\mathbb{R}^{n\times m}$	set of the matrices with dimension $n \times m$ with real elements
$A \cup B$	union of the sets A and B
$A \cap B$	intersection of the sets A and B
$A \subset B$	A is subset of B
$A \subseteq B$	A is a subset or equal to B
$A \setminus B$	set of elements of A but not in B
$A \times B$	Cartesian product of the sets A and B
$\prod_{i=1}^{N} A_i$	$:= A_1 \times \ldots \times A_N$, Cartesian product of $A_1, \ldots, A_N$
$\operatorname{conv}(A)$	convex hull of the set A
$\operatorname{conv}(A_1, \ldots, A_N)$	$:= \left\{a_1 x_1 + \ldots + a_N x_N \mid \sum_{i=1}^{N} a_i = 1, a_i \in \mathbb{R}_{\geq 0}, x_i \in \mathcal{S}_i, \forall i \in \{1, \ldots, N\}\right\}$ convex hull of the union

Operations on Vectors and Matrices

$\mathbf{0}$	matrix/vector with all elements equal to 0
$\mathbf{1}$	matrix/vector with all elements equal to 1
$v^\top$	transpose of the vector v

v_i	i-th component of the vector v
$\|v\|$	2-norm of the vector v
$\|v\|_\infty$	∞-norm of the vector v
$\mathrm{col}(v_1, \dots, v_N)$	$:= [v_1^\top, \dots, v_N^\top]^\top$ stacked vector of vectors
$\mathrm{diag}(v_1, \dots, v_N)$	diagonal matrix with $v_1, \dots, v_N$ on the diagonal
$(v_k)_{k\in\mathbb{N}}$	ordered sequence of vectors v_k
$v \perp w$,	with $v, w \in \mathbb{R}^n$, if $v_i w_i = 0$ for all $i \in \{1, \dots, n\}$
$M^\top$	transpose of the matrix M
M^{-1}	inverse of the matrix M
$[M]_{i,j} = M_{i,j}$	element in position (i, j) of the matrix M
$s_{\min}(M), s_{\max}(M)$	minimum, maximum singular value of M
$\lambda_{\min}(M), \lambda_{\max}(M)$	minimun, maximum eigenvalue of the matrix M
$\|M\|$	$:= s_{\max}(M)$, 2-matrix norm
$\|M\|_\infty$	$:= \max_i \sum_{j=1}^n \|M_{i,j}\|$, ∞-matrix norm
$M_1 \otimes M_2$	Kronecker productof the matrices M_1 and M_2
$M \succ (\succeq) \mathbf{0}$	M is positive (semi)definite
$\ker(M)$	kernel (null space) of the matrix M
$\max^k(A)$	set of the k unique highest values in A
$\langle \cdot, \cdot \rangle_M$	weighted inner product, i.e., $\langle x, y \rangle_M = x^\top M y$
$\| \cdot \|_M$	M-induced norm, i.e., $\|x\|_M = \langle x, x \rangle_M$
$\mathcal{H}_M$	Hilbert space with inner product $\langle \cdot, \cdot \rangle_M$
$\Gamma_0(\mathcal{H})$	Set of proper lower semicontinuous convex functions from $\mathcal{H}$ to $]-\infty, +\infty]$

Game Theory

x_i	strategy of agent i
$\boldsymbol{x}$	$:= \mathrm{col}(x_1, \dots, x_N)$, collective strategy
$\boldsymbol{x}_{-i}$	$:= \mathrm{col}(x_1, \dots, x_{i-1}, x_{i+1}, \dots, x_N)$
$(\boldsymbol{x}_{-i}, z)$	$:= \mathrm{col}(x_1, \dots, x_{i-1}, z, x_{i+1}, \dots, x_N)$
J_i	cost function of agent i
π_i	cost function of agent i
Ω_i	local strategy set of agent i

Operator Theory

Id	identity operator
ι_Ω	indicator function of the set Ω, [14, Eq. 1.41]
$\mathrm{J}_F := (\mathrm{Id} + F)^{-1}$	resolvent operator of the mapping F, [14, Def. 23.1]
prox_f	proximal operator of the function f, [14, Def. 12.23]
proj_Ω	projection onto the set Ω, [14, Def. 3.8]
N_Ω	normal cone operator of the set Ω, [14, Def. 6.38]
$\mathrm{dom}(F)$	domain of the operator F

$\mathrm{fix}(F)$	fixed-point set of the operator F
$\mathrm{range}(F)$	range of the operator F
$\mathrm{zer}(F)$	zero set of the operator F
∂f	subdifferential of the function f , [14, Def. 16.1]
∇f	gradient of the differentiable function f

1 Overview

This first chapter is dedicated to introducing the concept of multi-agent network game and it discusses its role in various applications that will become more and more relevant with the predicted increasing complexity of engineering, social, and economic systems. Then, we discuss the main research objectives on which we concentrate in the works proposed in this thesis. In the end, the structure of the dissertation is discussed and we provide an introduction to all the remaining chapters.

1.1 Introduction to multi-agent network games

In modern society, every part of daily life is highly connected. Most of the actions performed require some sort of interactions among humans and/or machines that can reciprocally influence. An illustrative example can be the discussion among individuals, in which everyone involved affects the opinion of everyone else. The advent of social networks drastically changed these interactions, not only by making the number of people involved gargantuan but also by moderating them via an algorithm that may foster some opinions over others [4, 59]. Another example of this growing complexity can be spotted in competitions among companies. Markets are highly interconnected and influence each other directly and indirectly, a lot of effort was put into studying their interdependence, e.g., [50, 102] , and even more flourishing is the field of designing possible policies to moderate them [165]. The recurring trends among these examples are the increment in the number of "agents" involved, their interdependence, and the possible presence of an external policymaker (e.g. the service provider). Arguably one of the most complex problems that present all these features is smart mobility in highly populated cities. It is characterized by a highly unpredictable environment, in which many services have to act in synergy to offer diverse transportation methods and fulfill different necessities of the end-users [64, 135]. Smart mobility is one of the key aspects that make up the foundations of a "smart city", which is probably a climax of complex and interconnected systems [23].

Noncooperative game theory is a key branch in the science of strategic decision making. Originally invented in 1944 by John von Neumann and Oskar Morgenstern [170], it found during the years a plethora of applications in diverse research fields, spanning from economics [2, 113] to psychology [51]. It became a useful tool to model complex systems, in which a set of rational agents interact selfishly with one another [152]. A missing feature in classical game theory was the ability to model the interaction of one agent with only a specific subset of other individuals. In many cases, the decision of an individual (or player) is influenced only by a small subset of all participants. This gap was bridged by the introductions of network games, namely games in which the interactions are described via a network structure, and the payoff of a player is defined solely by the actions of its neighbors, i.e., those directly connected with it. The classical literature on this topic is broad and many significant results have been achieved during the years. In [127], the framework of potential games was exploited to analyze several applications like congestion games. In more recent works [86, 97, 90, 107], the authors considered more involved, yet specific, games of which they carried out a complete characterization. Almost all these *classical* results, rely on the assumption that the players' actions can be represented by a scalar and that no complex coupling constraints among players are present. To address these limitations, several recent papers proposed the use of variational inequalities [166, 124, 128, 142] and operator theory [19, 99, 146, 177]. In fact, these powerful mathematical tools allow studying elegantly and compactly constrained network games in which the agent's actions can be modeled via multi-dimensional variables. In particular, this approach is suitable if one is interested in analyzing the convergence properties of the game at hand, rather than completely characterize its equilibria. To the interested reader, we refer to [143] and reference

there in for a discussion on the differences of the two approaches. The work in this thesis belongs to the second framework since the applications mentioned above are complex and the constraints are a key feature that is necessary to describe them. Network games are successful in modeling individuals that naturally aim at maximizing their local interests, rather than seeking social welfare. It is of particular interest because it allows us to design the local interactions between the players, while providing us the necessary mathematical tools to analyze the emerging behavior. In many real-world problems, an unregulated approach, as the one described so far, may emphasize the disparity among players, and the final result might even be detrimental for everyone involved. For this reason, a relevant research topic is the policy-making problem [37]. An external policymaker may be interested in influencing the actions of the players to promote a certain collective behavior, for example, to make cooperation profitable. These policies are usually easy to enforce since they are based on the selfishness of the player and do not require any sort of collaboration, which is intrinsically lacking in many of the problems aforementioned.

The emphasis of this thesis is on both aspects of multi-agents network games, i.e., the evolution analysis of the strategies in the game, and the design of policies to enforce some desired collective behavior. In particular, as an application, we focus on the smart mobility of Plug-in Electric Vehicle (PEV), also called e-mobility. This is a thriving topic and we design policies nudging the users to adopt a virtuous behavior. A game-theoretic perspective allows us to rigorously model and estimate the future effects of the proposed interventions, rather than analyzing them *a posteriori*. Throughout the dissertation, we also investigate and design the dynamics that define the future strategy selected by the players. Asynchronous update rules are one of the pivotal themes of the works presented. Multi-agent network games arise also in the context of parallel computation, where the efficiency and robustness of an algorithm are crucial aspects. As highlighted in [25], there are many advantages in the design of asynchronous dynamics to solve these problems, rather than relying on synchronous ones; next, we list the two that are the most important.

(i) *Reduction of the synchronization penalty.* If an algorithm adopts a synchronous update without assuming the presence of a common global clock, then a synchronization protocol must be carried out by the players. This usually translates into more communications, worsening the performances.

(ii) *Reduction of the effects of bottlenecks.* An asynchronous algorithm allows agents with different computational capabilities to update at different rates. This leads to a low idle time. In comparison, the presence of a single slow agent taking part in a synchronous update may cripple the overall performance.

In real-world phenomena, the evolution of complex systems is often asynchronous, since there are few cases in which synchronicity is inherited in the problem. Therefore, asynchronous dynamics may also have greater modeling power than their synchronous counterparts.

Research objectives

The discussion above framed the context in which our research is positioned. The main research objectives of this thesis can be concisely summarized by the following two statements.

- Exploit multi-agent network games to model and analyze complex large-scale and highly connected complex system.
- Design algorithms or policies that lead towards players' coordination and achieve a desirable equilibrium point.

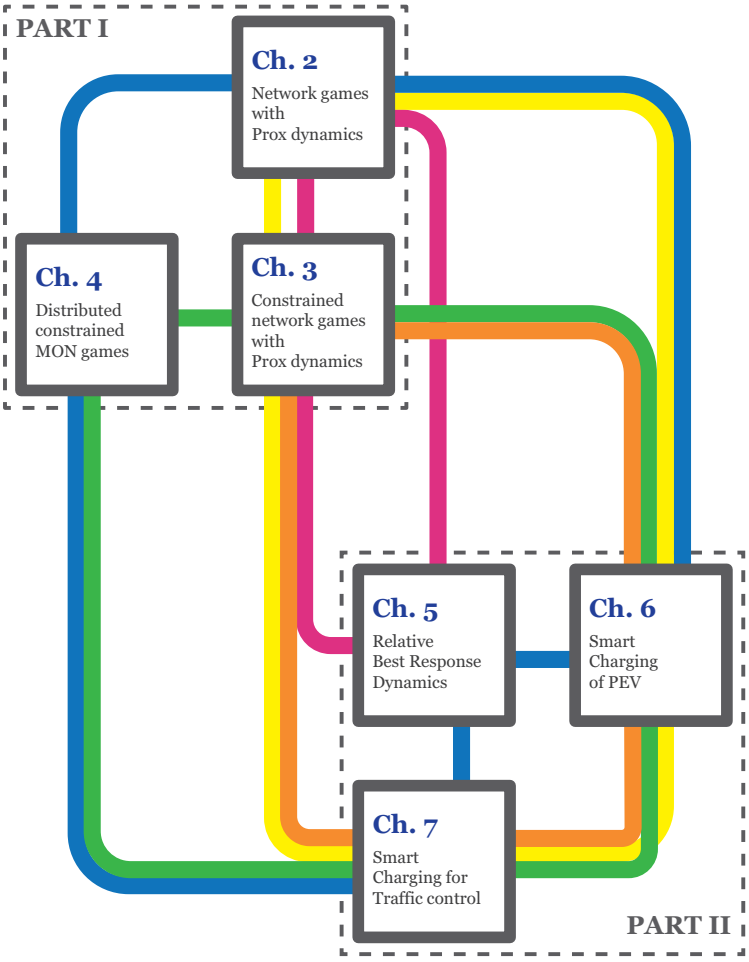

Figure 1.1: Link between the chapters in the thesis based on topics (represented via the same color scheme as in Table 1.1).

1.2 Structure of the thesis

Throughout the whole thesis, there are several connections among the chapters based on the different topics considered, a schematic representation of which can be seen in Figure 1.1 and Table 1.1. The most recurring theme is the analysis of asynchronous dynamics; it is interesting to notice their different derivations in the problems in Part I and Part II. In the former, we start from synchronous dynamics and consequently generalize it to address an asynchronous update. In Part II instead, the chosen framework of potential games drives us to develop asynchronous dynamics, since they well describe the problem at hand, and the theoretical results better support this kind of dynamics. In the following chapters, we are going to present several (semi-)decentralized algorithms. A semi-decentralized structure suits the best in those cases in which the agents connect with a third party to gather information, or the presence of a policy-maker is required. On the other hand, a fully decentralized algorithm describes better those problems in which the sole interactions occurring are among the decision makers, e.g., in the context of competition over a free and unregulated market. In Appendices A, B and C, we review the mathematical background that are used in both Part I and II of the thesis. Specifically, in Appendix A we collect some of the most important results on operator theory, heavily employed in Part I. We focus on the properties of nonexpansiveness and monotonicity of an operator, and then we propose a selection of the most popular fixed points iterations and zero-finding algorithms. Appendix B presents some classical results and definitions of graph theory that are useful throughout the whole thesis. Lastly, Appendix C introduces the different types of potential games, the concept of finite improvement path and some convergence results for mixed integer potential games. These concepts embody the theoretical cornerstone on which Part II is founded. We conclude the thesis by discussing the future development and interesting research challenges associated with the topics debated in the dissertation.

Table 1.1: Connection between the chapters based on topics.

	Part I			Part II		
	Ch. 2	Ch. 3	Ch. 4	Ch. 5	Ch. 6	Ch. 7
Network/Aggregative game	⊖	⊖			⊖	⊖
Asynchronous dynamics	⊕		⊕	⊕	⊕	⊕
Time/State-varying	✶	✶		✶		
Constrained dynamics		⊗	⊗		⊗	⊗
Semi decentralized		◇			◇	◇

1.2.1 Part I: Multi-agent network games via operator theory

In this first part of the dissertation, we analyze different instances of multi-agent network games subject to various types of dynamics, constraints, and network topologies. The first two chapters focus on games that adopt proximal type dynamics subject to local and coupling constraints, respectively. Chapter 4 instead assumes a more general setup in which the cost function in the game is not required to satisfy any particular structure, but is subject to some regularity assumptions. In this case, we focus on the efficiency and scalability of the asynchronous iterative algorithm developed to seek the equilibrium of the game.

– **Chapter 2** –

In this chapter, we introduce network games subject to proximal dynamics and local constraints. The communication network is described by a directed graph, and we prove that the players' strategies converge to a NE of the game under myopic Best Response (BR). Moreover, we generalize this setup to allow for an asynchronous update of the player and possible delays in the communication. We analytically characterize the maximum delay under which we can ensure the convergence of the strategies to a NE. Furthermore, we consider a time-varying communication network and discuss under which conditions the modified dynamics converge. We conclude by simulating the evolution of two classical models of opinion dynamics, i.e., the DeGroot and the Friedkin-Johnsen models; in fact, they can be seen as particular examples of network games.

This chapter is based on the following publications:

- C. Cenedese, Y. Kawano, S. Grammatico, and M. Cao, "Towards Time-Varying Proximal Dynamics in Multi-Agent Network Games," 2018 IEEE 57th Conference on Decision and Control Miami (CDC), pages 4378–4383, doi:10.1109/CDC.2018.8619670
- C. Cenedese, G. Belgioioso, Y. Kawano, S. Grammatico and M. Cao, "Asynchronous and time-varying proximal type dynamics multi-agent network games," 2020 IEEE Transaction on Automatic Control (TAC), doi:10.1109/TAC.2020.3011916

– **Chapter 3** –

This can be seen as the direct follow-up of the results developed in Chapter 2. We consider the generalized Nash equilibrium problem for network games adopting proximal dynamics and subject to both static and time-varying communication network. The key difference is the presence of (possibly time-varying) affine coupling constraints among the players. For the case with a static communication network, we take inspiration from the classical results in Appendix A to develop a preconditioned and modified version of the PPA, called Prox-GNWE. This iterative equilibrium-seeking algorithm ensures global convergence to a Generalized Network Equilibrium (GNWE) of the constrained game. In the more general case of time-varying constraints

and communication networks, the existence of an equilibrium is not guaranteed. Therefore, we discuss the possible assumptions that are required to ensure the feasibility of the problem. Then, the time-varying version of Prox-GNWE is developed, i.e., TV-Prox-GNWE. Finally, we validate both algorithms applying them to the problems of constrained consensus and distributed model fitting.

This chapter is based on the following publications:

- C. Cenedese, G. Belgioioso, Y. Kawano, S. Grammatico and M. Cao, "Asynchronous and time-varying proximal type dynamics multi-agent network games," 2020 IEEE Transaction on Automatic Control (TAC), doi: 10.1109/TAC.2020.3011916.
- C. Cenedese, G. Belgioioso, S. Grammatico and M. Cao, "Time-varying constrained proximal type dynamics in multi-agent network games," 2020 19th European Control Conference Saint Petersburg (ECC), pp. 148–153, doi: 10.23919/ECC51009.2020.9143683.

– **Chapter 4** – ⊕ ⊗

The algorithms developed in Chapter 3 are based on a semi-decentralized structure, in which a central coordinator collects information from the players and broadcasts some global variable to drive them to coordinate. In this chapter, we develop a fully decentralized asynchronous algorithm for strongly monotone games in which the cost functions are assumed to be differentiable. The final algorithm, called AD-GENO, is obtained as a result of a preconditioned FB splitting. The novelty of this work lies in the preconditioning, which allows achieving an algorithm that is not only faster than the others available in the literature but also more scalable since it requires the number of auxiliary variables to increase linearly with the number of players. We conclude the analysis with a comparison of the performances of the discussed algorithms applied to a constrained Cournot game.

This chapter is based on the following publications:

- C. Cenedese, G. Belgioioso, S. Grammatico and M. Cao, "An asynchronous, forward-backward, distributed generalized Nash equilibrium seeking algorithm," 2019 18th European Control Conference Naples (ECC), pp. 3508–3513, doi: 10.23919/ECC.2019.8795952.
- C. Cenedese, G. Belgioioso, S. Grammatico and M. Cao, "An asynchronous distributed and scalable generalized Nash equilibrium seeking algorithm for strongly monotone games," 2020 European Journal of Control, doi: 10.1016/j.ejcon.2020.08.006.

1.2.2 Part II: Decision making processes via potential game theory

In the second part of the thesis, we mostly focus on modeling decision making processes in which there is a human in the loop. We first propose novel dynamics

to describe the partial rationality of the decision makers and then we model two problems related to the smart mobility of PEVs. In these applications, the game-theoretic approach allows us to design an optimal policy that can achieve global benefits, even when the players act selfishly. From a technical point of view, all these results are achieved employing results derived from the field of potential game theory, see Appendix C.

– **Chapter 5** –

Two well-known dynamics for noncooperative games are the myopic BR and the imitation dynamics. The former models perfectly rational agents, while in the latter players simply copy the strategy of whoever performs the best. In Chapter 5, we propose novel dynamics that aspire to model partial rationality of the agents, we called it h-Relative Best Response (h-RBR). The players limit their possible actions to those chosen by the h best performers in their neighborhood. Among these, they select the one they are going to adopt based on their interest. We prove the convergence of multi-agent network games subject to h-RBR dynamics to a GNE. Specifically, the convergence is guaranteed for generalized ordinal potential games in the case of finite games, and for weighted potential games in the case of convex games. Interestingly, if one considers a network with a mixture of best responders and relative best responders, then our convergence results still hold. Furthermore, we show via simulations that these dynamics may model different degrees of rationality by varying the value of the parameter h.

This chapter is based on the following publications:

- A. Govaert, C. Cenedese, S. Grammatico and M. Cao, "Relative Best Response Dynamics in finite and convex Network Games,"2019 IEEE 58th Conference on Decision and Control Nice (CDC), pp. 3134–3139, doi: 10.1109/CDC40024.2019.9029821.
- C. Cenedese, A. Govaert, S. Grammatico and M. Cao, "Rationality and social influence in network games," (in preparation).

– **Chapter 6** –

The rising number of PEVs in the market creates an increment of the energy demand throughout the days, and, in particular, this leads to a growth of high energy demand peaks, that compromise an optimal energy supply. For this reason, we propose in this chapter an energy price policy that aims at incentivizing the PEV owners to charge during the hours in which the demand is lower. The price dynamically changes in accordance with the total demand that the grid has to satisfy at that particular moment. This creates a coupling between the PEV. Consequently, the PEVs have to solve a mixed integer aggregative noncooperative game to compute the optimal charging schedule. We take advantage of the integer variables to model various complex constraints that model and limit the charging behavior of the players. As done in Chapter 3, we consider a semi-decentralized structure in which the PEVs communicate with the grid to receive the energy price. We show that

this game is an exact potential game and thus the sequential better response dynamics lead the agent to an ε-Mixed-Integer Nash Equilibrium (MINE) of the game.

This chapter is based on the following publications:

- C. Cenedese, F. Fabiani, M. Cucuzzella, J. M. A. Scherpen, M. Cao and S. Grammatico, "Charging plug-in electric vehicles as a mixed-integer aggregative game," 2019 IEEE 58th Conference on Decision and Control Nice (CDC), pp. 4904–4909, doi: 10.1109/CDC40024.2019.9030152.

– **Chapter 7** – 

In this final technical chapter of the dissertation, we start from an idea that recalls the one introduced in Chapter 6, but, in this case, we create a policy for the charging of PEVs that acts as an Active Traffic Demand Management (ATDM) for a highway stretch. Specifically, we consider the problem of alleviating the traffic congestion by incentivizing the PEV owners to stop at a Charging Station (CS) during the moments of high congestion. The incentive consists of a discount of the energy price that changes proportionally to the congestion level. The decision making process of the drivers is carefully modeled as a mixed integer potential game and the traffic evolution is estimated via the CTM. This approach allows us to craft a policy, which makes the charging schedule that creates a congestion alleviation the most profitable for the PEVs on the highways. This work is the first that links the energy market to the transportation facilities and provides rigorous analysis of the produced effects. For this reason, we introduce the novel concepts of "road-to-station" and "station-to-road" flows, and consider mixed integer variables to describe a wide collection of interactions among drivers. The theoretical framework is then tested using real-world data obtained from the Nationale Databank Wegverkeersgegevens (NDW). We show via simulations that this policy manages to align the global interest with the local one of the single drivers. In fact, it is capable of reducing the congestion peaks and reduce the overall travel time for all the drivers on the highways, on top of providing an advantageous service to the PEV owners. Finally, we discuss what is the best policy that can be implemented for the current situation and how it might change in the future, due to the trends observed in the market.

This chapter is based on the following publications:

- C. Cenedese, M. Cucuzzella, J. M. A. Scherpen, S. Grammatico and M. Cao, "Highway Traffic Control via Smart e-Mobility – Part I: Theory," 2021 IEEE Transaction on Intelligent Transportation Systems (under review).
- C. Cenedese, M. Cucuzzella, J. M. A. Scherpen, S. Grammatico and M. Cao, "Highway Traffic Control via Smart e-Mobility – Part II: Case Study," 2021 IEEE Transaction on Intelligent Transportation Systems (under review).

Part I

Multi-agent network games via operator theory

2

Asynchronous and time-varying proximal dynamics in network games

In this chapter, we study proximal type dynamics in the context of multi-agent network games. These dynamics arise in different applications, since they describe distributed decision making in multi-agent networks, e.g., in opinion dynamics, distributed model fitting and network information fusion, where the goal of each agent is to seek an equilibrium using local information only. We analyze several conjugations of this class of games, providing convergence results. Specifically, we look into synchronous/asynchronous dynamics with a time-invariant communication network and synchronous dynamics with time-varying communication networks. Finally, we validate the theoretical results via numerical simulations on opinion dynamics.

2.1 Introduction

2.1.1 Multi-agent decision making over networks

Multi-agent decision making over networks is currently a vibrant research area in the systems-and-control community, with applications in several domains, such as smart grids [65, 99], traffic and information networks [108], social networks [93, 72], consensus and flocking groups [38], robotics [47] and sensor networks [121], [159]. The main benefit that each decision maker, in short, *agent*, achieves from the use of a distributed computation and communication, is to keep its own data private and to exchange information with selected agents only. Essentially, in networked multi-agent systems, the states (or decisions) of some agents evolve as a result of *local decision making*, e.g. local constrained optimization, and *distributed communication* with some neighboring agents, via a communication network. Usually, the agents aim to reach a collective equilibrium state, where no one can benefit from changing its state at that equilibrium.

Multi-agent dynamics over networks embody the natural extension of distributed optimization and equilibrium seeking problems in network games. In the past decade, this field has thrived and a wide range of results were developed. Some examples of constrained convex optimization problems, subject to homogeneous constraint sets, are studied in [137], where uniformly bounded subgradients and complete communication graphs with uniform weights are considered; while in [114], the cost functions are assumed to be differentiable with Lipschitz continuous and uniformly bounded gradients; and, more generally, in [82], convergence is proven via *vanishing* step sizes.

Solutions for nooncoperative games over networks subject to local convex constraints have been developed, e.g., in [141], under strongly convex quadratic costs and time-invariant communication graphs; in [110] [155], with differentiable cost functions with Lipschitz continuous gradients, strictly convex cost functions, and undirected, possibly time-varying, communication graphs; and in [47], where the communication is ruled by a possibly time-varying digraph and the cost functions are assumed to be convex. In some recent works, researchers have developed algorithms to solve games over networks subject to asynchronous updates of the agents: among others, in [177, 40], the game is subject to affine coupling constraints, and the cost functions are differentiable, while the communication graph is assumed to be undirected.

To the best of the our knowledge, the main works that extensively focus on multi-agent network games with proximal dynamics are [99, 47], where the authors consider local convex costs and quadratic proximal terms, time-invariant and time-varying communication graphs, but subject to some technical restrictions.

2.1.2 Contribution

Next, we highlight the novelties and main contribution presented in this chapter with respect to the literature referenced above:

- We prove that a row-stochastic adjacency matrix describing a strongly connected graph with self-loops is an averaged operator in the Hilbert space weighted by its left Perron-Frobenius (PF) eigenvector (Lemma 2.2). This result is significant itself and fundamental to generalize the work in [141].
- We prove global convergence of synchronous proximal dynamics in network games under time-invariant directed communication graph (hence described by a row-stochastic adjacency matrix). This extends the results in [99, 47].
- We establish global convergence for asynchronous proximal dynamics and synchronous proximal dynamics over time-varying networks. The former setup is considered here for the first time. The latter is studied in [99] for undirected communication graph (hence doubly-stochastic adjacency matrix), and in [47] via a dwell-time restriction.

2.2 Mathematical setup and problem formulation

We consider a set of N agents (or players), where the state (or strategy) of each agent $i \in \mathcal{N} := \{1, \dots, N\}$ is denoted by $x_i \in \mathbb{R}^n$. The set $\Omega_i \subset \mathbb{R}^n$ represents all the feasible states of agent i, hence it is used to model its local constraints, i.e., $x_i \in \Omega_i$. Throughout the chapter, we assume compactness and convexity of the local constraint set Ω_i.

Standing Assumption 2.1 (Convexity)**.** *For each $i \in \mathcal{N}$, the set $\Omega_i \subset \mathbb{R}^n$ is non-empty, compact and convex.* □

We consider rational (or myopic) agents, namely, each agent i aims at minimizing a local cost function g_i that we assume convex and with the following structure.

Standing Assumption 2.2 (Proximal cost functions)**.** *For each $i \in \mathcal{N}$, the function $g_i : \mathbb{R}^n \times \mathbb{R}^n \to \overline{\mathbb{R}}$ is defined by*

$$J_i(x_i, z_i) := f_i(x_i) + \iota_{\Omega_i}(x_i) + \tfrac{1}{2}\|x_i - z_i\|^2, \tag{2.1}$$

where $\bar{f}_i := f_i + \iota_{\Omega_i} : \mathbb{R}^n \to \overline{\mathbb{R}}$ is a lower semi-continuous, proximal friendly and convex function. □

We emphasize that Standing Assumption 2.2 requires neither the differentiability of the local cost function, nor the Lipschitz continuity and boundedness of its gradient. The *proximal-friendly* structure of $\bar{f}_i$ ensures that agent i can efficiently minimize (2.1), see [54, Table 10.2] for some examples of this class of functions. In (2.1), the function $\bar{f}_i$ is local to agent i and models the local objective that the player would pursue if no coupling between agents is present. The quadratic term $\frac{1}{2}\|x_i - z_i\|^2$ penalizes the distance between the state of agent i and a given z_i, precisely defined later. This term is referred in the literature as *regularization* (see [14, Ch. 27]), since it makes $J_i(\cdot, z_i)$ strictly convex, even though $\bar{f}_i$ is only lower semi-continuous, see [14, Th. 27.23].

We assume that the agents can communicate through a network structure, described by a weighted digraph $\mathcal{G} = (\mathcal{N}, A)$, see Appendix B. The communication links between the agents are represented by the weighted adjacency matrix $A \in \mathbb{R}^{N\times N}$ defined as $[A]_{ij} := a_{i,j}$. For all $i, j \in \mathcal{N}$, $a_{i,j} \in [0, 1]$ denotes the weight that agent i assigns to the state of agent j. If $a_{i,j} = 0$, then the state of agent i is independent from that of agent j. The set of agents with whom agent i communicates is called neighborhood and denoted by $\mathcal{N}_i$. The following assumption formalizes the communication network via a digraph and the associated adjacency matrix.

Standing Assumption 2.3 (Row stochasticity and self-loops)**.** *The communication graph is strongly connected. The matrix $A = [a_{i,j}]$ is row stochastic, i.e., $a_{i,j} \geq 0$ for all $i, j \in \mathcal{N}$, and $\sum_{j=1}^{N} a_{i,j} = 1$, for all $i \in \mathcal{N}$. Moreover, A has strictly-positive diagonal elements, i.e., $\min_{i\in\mathcal{N}} a_{i,i} =: \underline{a} > 0$.* □

In our setup, the variable z_i in (2.1) represents the average state among the neighbors of agent i, weighted through the adjacency matrix, i.e., $z_i := \sum_{j=1}^{N} a_{i,j}x_j$. Therefore, the cost function of agent i is $J_i\big(x_i, a_{i,i}x_i + \sum_{j\neq i}^{N} a_{i,j}x_j\big)$. Note that a *coupling* between the agents emerges in the local cost function, since the second argument of the J_i's depends on the strategy of (some of) the other agents.

We consider a population of rational agents that update their states/strategies, at each time instant k, according to the following myopic dynamics:

$$x_i(k+1) = \operatorname{argmin}_{y\in\mathbb{R}^n} \; J_i\left(y, \textstyle\sum_{j=1}^{N} a_{i,j}x_j(k)\right) . \tag{2.2}$$

These dynamics are relatively simple, yet arise in diverse research areas. Next, we recall some popular problems in the literature where the emergent dynamics are a special case of (2.2).

1. *Opinion dynamics:* In [144], the authors study the Friedkin-Johnsen model, that is an extension of the DeGroot's model [62]. The update rule in [144, Eq. 1] is effectively the best response of a game with cost functions equal to

$$J_i(x_i, z) := \tfrac{1-\mu_i}{\mu_i}\|x_i - x_i(0)\|^2 + \iota_{[0,1]^n}(x_i) + \|x_i - z\|^2 \tag{2.3}$$

   where $\mu_i \in [0, 1]$ represents the stubbornness of the player. Thus, [144, Eq. 1] is a special case of (2.2).

2. *Distributed model fitting:* One of the most common tasks in machine learning is model fitting and in fact several algorithms are proposed in literature, e.g. [183, 164]. The idea is to identify the parameters x of a linear model $Bx = b$, where B and b are obtained via experimental data. If there is a large number of data, i.e., B is a tall matrix, then the distributed counterpart of these algorithms are presented in [31, Sec. 8.2]. In particular, [31, Eq. 8.3] can be rewritten as a constrained version of (2.2). The cost function is defined by

$$g(x_i, z) := \ell_i(B_i x_i - b_i) + r(z) ,$$

where A_i and b_i represent the i-th block of available data,and x_i is the local estimation of the parameters of the model. Here, ℓ_i is a loss function and r is the regularization function $r(z) \coloneqq \frac{1}{2}\|x_i - z\|$. Finally, the arising game is subject to the constraint that at the equilibrium $x_i = x_j$ for all $i \in \mathcal{N}$.

3. *Constrained consensus:* if the cost function of the game in (2.2) is chosen with $f_i = 0$ for all $i \in \mathcal{N}$, then we retrive the projected consensus algorithm studied in [137, Eq. 3] to solve the problem of constrained consensus. To achieve the convergence to the consensus, it is required the additional assumption that $\text{int}(\cap_{i\in\mathcal{N}}\Omega_i) \neq \varnothing$, see [137, Ass. 1].

In this chapter, we focus on games under local constraints only, an apply our convergence results to classical opinion dynamics models. In Chapter 3, we study the more general case of games under both local and coupling constraints and show the effectiveness of the algorithms developed to solve the problems of constrained consensus and distributed model fitting.

Next, we introduce the concept of equilibrium of interest for this class of games. The collective strategy profiles that are stationary points of the dynamics in (2.2) are called *network equilibria*, and are formalized next.

Definition 2.1 (Network equilibrium [99, Def. 1])**.** The collective vector $\bar{\boldsymbol{x}} = \text{col}(\bar{x}_1, \dots, \bar{x}_N)$ is a Network Equilibrium (NWE) if, for all $i \in \mathcal{N}$,

$$\bar{x}_i = \text{argmin}_{y\in\mathbb{R}^n} \; J_i\left(y, \textstyle\sum_{j=1}^N a_{i,j}\bar{x}_j\right) . \tag{2.4}$$

□

We remark that the set of NWE directly depends on both the communication topology and on the specific weights $a_{i,j}$ of the adjacency matrix. Moreover, if there are no self loops, i.e., $a_{i,i} = 0$ for all i, then (2.2) are best-response dynamics and NWE correspond to Nash equilibria [99, Rem. 1].

2.3 Proximal dynamics

In this section, we study three different types of proximal dynamics, namely synchronous, asynchronous and time-varying. While for the former two, we can study and prove convergence to an NWE, the last one does not ensure convergence. Thus, we propose a modified version of the dynamics with the same equilibria of the original game.

2.3.1 Synchronous proximal dynamics

As a first step, we exploit the structure of the cost function J_i in (2.1) to rephrase the dynamics in (2.2) by means of the proximity operator [14, Ch. 12.4] as

$$x_i(k+1) = \text{prox}_{\bar{f}_i}\big(\textstyle\sum_{j=1}^N a_{i,j}\, x_j(k)\big), \;\; \forall k \in \mathbb{N}. \tag{2.5}$$

In compact form, they read as

$$\boldsymbol{x}(k+1) = \mathbf{prox}_{\boldsymbol{f}}(\boldsymbol{A}\,\boldsymbol{x}(k))\,, \tag{2.6}$$

where the matrix $\boldsymbol{A} := A \otimes I_n$ represents the interactions among agents, and the operator $\mathbf{prox}_{\boldsymbol{f}}$ is defined as

$$\mathbf{prox}_{\boldsymbol{f}}(\boldsymbol{y}) \coloneqq \mathrm{col}(\mathrm{prox}_{\bar{f}_1}(y_1), \dots, \mathrm{prox}_{\bar{f}_N}(y_N)).$$

Remark 2.1. *Definition 2.1 can be equivalently cast in terms of fixed points of the operator on the left-hand side of* (2.6)*. In fact, a collective vector $\overline{\boldsymbol{x}}$ is an NWE if and only if $\overline{\boldsymbol{x}} \in \mathrm{fix}(\mathbf{prox}_{\boldsymbol{f}} \circ \boldsymbol{A})$. Under Assumptions 2.1 and 2.2, fix $\big(\mathbf{prox}_{\boldsymbol{f}} \circ \boldsymbol{A}\big)$ is non-empty [160, Th. 4.1.5], i.e., there always exists an NWE, thus the convergence problem is well posed.* □

The following lemma shows that a row-stochastic matrix A is an AVG operator in $\mathcal{H}_Q$, where $Q \coloneqq \mathrm{diag}(\bar{q})$ and $\bar{q}$ is the left PF eigenvector of A, see Appendix B. We always consider the normalized PF eigenvector, i.e., $q = \bar{q}/\|\bar{q}\|$.

Lemma 2.2 (Averagedness and left PF eigenvector)**.** *Let Assumption 3 hold true, i.e, A be row stochastic, $\underline{a} > 0$ be its smallest diagonal element and $q = \mathrm{col}(q_1, \dots, q_N)$ its left PF eigenvector. Then, the following hold:*

(i) A is η-AVG in $\mathcal{H}_Q$, with $Q \coloneqq \mathrm{diag}(q_1, \dots, q_N)$ and $\eta \in (0, 1 - \underline{a})$;

(ii) The operator $\mathbf{prox}_{\boldsymbol{f}} \circ \boldsymbol{A}$ is $\frac{1}{2-\eta}$–AVG in $\mathcal{H}_Q$.

If A is doubly-stochastic, (i) and (ii) hold with $Q = I$. □

Now, we are ready to present the first result, the global convergence of the proximal dynamics in (2.6) to an NWE.

Theorem 2.3 (Convergence of proximal dynamics)**.** *For any $\boldsymbol{x}(0) \in \boldsymbol{\Omega}$, the sequence $(\boldsymbol{x}(k))_{k\in\mathbb{N}}$ generated by the proximal dynamics in* (2.6) *converges to an NWE.* □

Remark 2.2. *Theorem 2.3 extends [99, Th. 1], where the matrix A is assumed to be doubly stochastic [99, Ass. 1, Prop. 2]. In that case, $\mathbf{1}_N$ is the left PF eigenvector of A and the matrix Q is set as the identity matrix, see Lemma 2.2.* □

Remark 2.3. *In [99, Sec. VIII-A] the authors study, via simulations, an application of* (2.2) *to opinion dynamics. In particular, they conjecture the convergence of the dynamics in the case of a row-stochastic weighted adjacency matrix. Theorem 2.3 theoretically supports the convergence of this class of dynamics.* □

The presence of self-loops in the communication (Assumption 2.3) is critical for the convergence of the dynamics in (2.6). In fact, we present next a simple example of a two player game, in which the dynamics fail to converge due to the lack of self-loops.

Example 2.4. Consider the two player game, in which the state of each agent is scalar and $\bar{f}_i \coloneqq \iota_\Omega$, for $i = 1, 2$. The set Ω is an arbitrarily big compact subset of $\mathbb{R}$, in which the dynamics of the agents are invariant. The communication network is described by the doubly-stochastic adjacency matrix $A = \left[\begin{smallmatrix} 0 & 1 \\ 1 & 0 \end{smallmatrix}\right]$, defining a strongly connected graph without self-loops. In this example, the dynamics in (2.6) reduce to $\boldsymbol{x}(k+1) = A\boldsymbol{x}(k)$. Hence, convergence does not take place for all $\boldsymbol{x}(0) \in \boldsymbol{\Omega}$. □

If $\underline{a} = 0$, i.e., the self-loop requirement in Standing Assumption 2.3 is not met, the convergence may be restored by relaxing the dynamics in (2.2) via the so-called Krasnosel'skii-Mann iteration [14, Sec. 5.2],

$$\boldsymbol{x}(k+1) = (1-\alpha)\boldsymbol{x}(k) + \alpha\, \mathbf{prox}_{\boldsymbol{f}}(\boldsymbol{A}\,\boldsymbol{x}(k))\,, \tag{2.7}$$

where $\alpha \in (0, 1)$. These new dynamics share the same fixed points of (2.6), namely, the set of NWE (Remark 2.1).

Corollary 2.4. *For any $\boldsymbol{x}(0) \in \boldsymbol{\Omega}$ and for $\min_{i\in\mathcal{N}} a_{i,i} \geq 0$, the sequence $(\boldsymbol{x}(k))_{k\in\mathbb{N}}$ generated by the dynamics in (2.7) converges to an NWE.* □

2.3.2 Asynchronous proximal dynamics

The dynamics introduced in (2.6) assume that all the agents update synchronously. Here, we study a more realistic case in which they behave asynchronously. To model the asynchronous updates we adopt the same mathematical framework as in [177, 130, 30]. Specifically, we assume that each agent i has a local Poisson clock with the rate τ_i and updates independently from the rest every time the clock ticks. It is convenient for the analysis to consider a virtual Poisson clock that ticks every time one of the agents updates, so it has rate $\tau = \sum_{i\in\mathcal{N}} \tau_i$. We denote by Z_k the k-th tick of the global clock, and by k the time interval $[Z_{k-1}, Z_k)$. We assume that only one agent updates during each time slot. Then, we denote by $i_k \in \mathcal{N}$ the agent starting its update during the time slot k. According to this setup, at each time instant k, only one agent $i_k \in \mathcal{N}$ updates its state according to (2.5), while the remainders keep their state unchanged, i.e.,

$$x_i(k+1) = \begin{cases} \mathrm{prox}_{\bar{f}_i}\big(\sum_{j=1}^N a_{i,j} x_j(k)\big), & \text{if } i = i_k, \\ x_i(k), & \text{otherwise.} \end{cases} \tag{2.8}$$

Next, we derive a compact form for the dynamics above. Define H_i as the matrix of all zeros except for $[H_i]_{ii} = 1$, and also $\boldsymbol{H}_i := H_i \otimes I_n$. Then, we define the set $\boldsymbol{H} := \{\boldsymbol{H}_i\}_{i\in\mathcal{N}}$ as the collection of these N matrices. We denote by ζ_k an i.i.d. random variable that takes values in $\boldsymbol{H}$, with $\mathbb{P}[\zeta_k = \boldsymbol{H}_i] = \tau_i/\tau$, for all $i \in \mathcal{N}$. If

$\zeta_k = \boldsymbol{H}_i$, it means that agent i is updating at time k, while the others maintain their strategies unchanged. With this notation in mind, the dynamics in (2.6) are modified to model asynchronous updates,

$$\boldsymbol{x}(k+1) = \boldsymbol{x}(k) + \zeta_k\big(\mathbf{prox}_{\boldsymbol{f}}(\boldsymbol{A}\,\boldsymbol{x}(k)) - \boldsymbol{x}(k)\big)\,. \tag{2.9}$$

We remark that (2.9) represents the natural asynchronous counterpart of the dynamics in (2.6). In fact, the update above is equivalent to (2.5) for the active agent at time $k \in \mathbb{N}$.

Each agent $i \in \mathcal{N}$ has a public and private memory. If the player is not performing an update, the strategies stored in the two memories coincide. During an update, instead, the public memory stores the strategy of the agent before the update has started, while in the private one there is the value that is modified during the computations. When the update is completed, the value in the public memory is overwritten by that in the private memory. This assumption ensures that all the reads of agent i's public memory, performed by its neighbours $j \in \mathcal{N}_i$, are always consistent, see [147, Sec. 1.2] for technical details.

We consider the case in which the computation time for the update is not negligible, therefore the strategies that agent i reads from each neighbor $j \in \mathcal{N}_i$ may be outdated of $\varphi_j(k) \in \mathbb{N}$ time intervals. The maximum delay is assumed uniformly upper bounded.

Assumption 2.4 (Bounded maximum delay)**.** *The delays are uniformly upper bounded, i.e.,* $\sup_{k\in\mathbb{N}} \max_{i\in\mathcal{N}} \varphi_i(k) \leq \overline{\varphi} < \infty$*, for some* $\overline{\varphi} \in \mathbb{N}$*.* □

The dynamics describing the asynchronous update with delays are cast in a more compact form as

$$\boldsymbol{x}(k+1) = \boldsymbol{x}(k) + \zeta_k\big(\mathbf{prox}_{\boldsymbol{f}}(\boldsymbol{A}\,\hat{\boldsymbol{x}}(k)) - \hat{\boldsymbol{x}}(k)\big)\,, \tag{2.10}$$

where $\hat{\boldsymbol{x}} = \mathrm{col}(\hat{x}_1, \ldots, \hat{x}_N)$ is the vector of possibly delayed strategies. Notice that each agent i has always access to the most up to date value of its own strategy, i.e., $\hat{x}_i = x_i$. We stress that the dynamics in (2.10) coincide with (2.9) when no delay is present, i.e., if $\overline{\varphi} = 0$.

The following theorem claims the global convergence (in probability) of (2.10) to an NWE when the maximum delay $\overline{\varphi}$ is small enough.

Theorem 2.5 (Convergence of asynchronous dynamics)**.** *Let Assumption 2.4 hold true,* $p_{\min} := \min_{i\in\mathcal{N}} \tau_i/\tau$ *and*

$$\overline{\varphi} < \tfrac{N\sqrt{p_{\min}}}{2(1-\underline{\alpha})} - \tfrac{1}{2\sqrt{p_{\min}}}\,. \tag{2.11}$$

Then, for any $\boldsymbol{x}(0) \in \boldsymbol{\Omega}$*, the sequence* $(\boldsymbol{x}(k))_{k\in\mathbb{N}}$ *generated by* (2.10) *converges almost surely to some* $\bar{\boldsymbol{x}} \in \mathrm{fix}(\mathbf{prox}_{\boldsymbol{f}} \circ \boldsymbol{A})$*, namely, an NWE.* □

Remark 2.5. *If $\bar{\varphi} = 0$, then the convergence can be established also in the more general case in which multiple agents update at the exact same time instant, by relying on random block-coordinate updates for fixed-point iterations, as introduced in [53]. Specifically, one can define 2^N different operators T_j, $j \in \{1, \dots, 2^N\}$, each triggering the update of a different combination of agents. The dynamics become a particular case of [53, Eq. 3.17] and the convergence follows from [53, Cor. 3.8].* □

If the maximum delay does not satisfy (2.11), the convergence of the dynamics in (2.10) is not guaranteed. Nevertheless, it can be restored by introducing a time-varying scaling factor $\psi_k \in (0, 1)$ in the dynamics:

$$\boldsymbol{x}(k+1) = \boldsymbol{x}(k) + \psi_k \zeta_k \big(\mathbf{prox}_{\boldsymbol{f}}(\boldsymbol{A}\, \hat{\boldsymbol{x}}(k)) - \hat{\boldsymbol{x}}(k) \big) . \tag{2.12}$$

The next theorem proves that the modified dynamics converges, if the scaling factor is chosen small enough.

Theorem 2.6. *Let Assumption 2.4 hold true and set*

$$0 < \psi_k < \tfrac{N p_{\min}}{(2\bar{\varphi}\sqrt{p_{\min}}+1)(1-\underline{a})}, \quad \forall k \in \mathbb{N}. \tag{2.13}$$

Then, for any $\boldsymbol{x}(0) \in \boldsymbol{\Omega}$, the sequence $(\boldsymbol{x}(k))_{k\in\mathbb{N}}$ generated by (2.12) converges almost surely to some $\bar{\boldsymbol{x}} \in \mathrm{fix}(\mathbf{prox}_{\boldsymbol{f}} \circ \boldsymbol{A})$, namely, an NWE. □

Now, if the value of $\underline{a}$ is not globally known by all the agents, one may consider a more conservative bound,

$$0 < \psi_k < \tfrac{N p_{\min}}{(2\bar{\varphi}\sqrt{p_{\min}}+1)}, \quad \forall k \in \mathbb{N}\,, \tag{2.14}$$

which is independent of $\underline{a}$. Furthermore, since at each time instant k only one agent updates its state, the agents do not need to coordinate with each other to agree on the relaxation sequence $(\psi_k)_{k\in\mathbb{N}}$. Thus, the dynamics in (2.12) remain distributed.

Remark 2.6. *An interesting particular case arises when all the agents have the same update rate, i.e., $p_{\min} = 1/N$. In this case, the bound on the maximum delay becomes $\bar{\varphi} < \frac{\underline{a}\sqrt{N}}{2(1-\underline{a})}$, that grows when $\underline{a}$ or the population size N increases. In (2.14), the scaling coefficient can be chosen as $\psi_k < \frac{\sqrt{N}}{(2\bar{\varphi}+\sqrt{N})}$. It follows that $\bar{\varphi}$ is the only global parameter that the agents must know a priori to compute ψ_k.* □

2.3.3 Time-varying proximal dynamics

A challenging problem related to the (synchronous) dynamics in (2.6) is studying their convergence when the communication network varies over time, i.e., the associated adjacency matrix A is time dependent. In particular, we assume that, at each time instant $k \in \mathbb{N}$, the communications between the players is described by a strongly connected digraph, $\mathcal{G}_k = (\mathcal{N}, A(k))$, where $A(k)$ is the adjacency

matrix at time k. The set of all the neighbors of agent i at time k is denoted by $\mathcal{N}_i(k) \coloneqq \{j \,|\, a_{i,j}(k) > 0\}$.

The update rules in (2.6) reflect this new setup and become

$$\boldsymbol{x}(k+1) = \mathbf{prox}_{\boldsymbol{f}}(\boldsymbol{A}(k)\,\boldsymbol{x}(k))\,, \tag{2.15}$$

where $\boldsymbol{A}(k) = A(k) \otimes I_n$, and $A(k)$ is the adjacency matrix at time instant k.

As in [99, Ass. 4,5], we assume *persistent stochasticity* of the sequence $(\boldsymbol{A}(k))_{k\in\mathbb{N}}$, that can be seen as the time-varying counterpart of Standing Assumption 2.3.

Assumption 2.5 (Persistent row stochasticity and self-loops)**.** *For all $k \in \mathbb{N}$, the adjacency matrix $\boldsymbol{A}(k)$ is row stochastic and describes a strongly connected graph. Furthermore, there exists $\overline{k} \in \mathbb{N}$ such that, for all $k > \overline{k}$, the matrix $\boldsymbol{A}(k)$ satisfies* $\inf_{k>\overline{k}} \min_{i\in\mathcal{N}}[A(k)]_{ii} =: \underline{a} > 0$. □

The concept of NWE in Definition 2.1 is bound to the particular communication network considered. In the case of a time-varying communication topology, we focus on a different class of equilibria, namely, those invariant with respect to changes in the communication topology.

Definition 2.7 (Persistent NWE [99, Ass. 3])**.** A collective vector $\bar{\boldsymbol{x}}$ is a persistent Network Equilibrium (p-NWE) of (2.15) if there exists some positive constant $\overline{k} > 0$, such that

$$\bar{\boldsymbol{x}} \in \mathcal{E} := \cap_{k>\overline{k}} \operatorname{fix}\big(\mathbf{prox}_{\boldsymbol{f}}(\boldsymbol{A}(k)\,\boldsymbol{x}(k))\big)\,. \tag{2.16}$$

□

Next, we assume the existence of a p-NWE.

Assumption 2.6 (Existence of a p-NWE)**.** *The set of p-NWE of* (2.15) *is non-empty, i.e., $\mathcal{E} \neq \varnothing$.* □

We note that when the mappings $\operatorname{prox}_{\bar{f}_i}$'s have a common fixed point[1], i.e., $\cap_{i\in\mathcal{N}} \operatorname{fix}(\operatorname{prox}_{\bar{f}_i}) \neq \varnothing$, then our convergence problem boils down to the setup studied in [89]. In this case, [89, Th. 2] can be applied to the dynamics in (2.15) to prove convergence to a p-NWE, $\bar{\boldsymbol{x}} = \mathbf{1} \otimes \overline{x}$, where $\bar{x}$ is a common fixed point of the proximal operators $\operatorname{prox}_{\bar{f}_i}$'s. For example, this additional condition holds true when $\bar{f}_i = \iota_{\Omega_i}$, for all $i \in \mathcal{N}$, and $\cap_{i\in\mathcal{N}} \Omega_i \neq \varnothing$, namely, the constrained consensus framework considered in [137], and in the classical consensus setup [28], i.e., $\Omega_i = \mathbb{R}^n$, for all $i \in \mathcal{N}$.

However, if this additional assumption is not met, then convergence is not guaranteed. In fact, a priori there is no common space in which $\mathbf{prox}_{\boldsymbol{f}} \circ \boldsymbol{A}(k)$ posses the AVG propriety for every $k \in \mathbb{N}$, thus we cannot infer the convergence of the dynamics in (2.15) under arbitrary switching topologies. In some special cases, a

[1] Equivalently, when the cost functions $\bar{f}_i$'s have a common minimizer.

common space can be found, e.g. if all the adjacency matrices are doubly stochastic as in [99, Th. 3].

Next, we propose modified dynamics with convergence guarantees to a p-NWE, for every switching sequence, i.e.,

$$\boldsymbol{x}(k+1) = \mathbf{prox}_{\boldsymbol{f}}\big([I + \boldsymbol{Q}(k)(\boldsymbol{A}(k) - I)]\,\boldsymbol{x}(k)\big)\,. \tag{2.17}$$

These new dynamics are obtained by replacing $\boldsymbol{A}(k)$ in (2.15) with $I+\boldsymbol{Q}(k)(\boldsymbol{A}(k)-I)$, where $\boldsymbol{Q}(k)$ is chosen as in Theorem 2.3. Remarkably, this key modification makes the resulting operators $\big(\mathbf{prox}_{\boldsymbol{f}} \circ \big(I + \boldsymbol{Q}(k)(\boldsymbol{A}(k) - I)\big)\big)_{k\in\mathbb{N}}$ AVG in the same space, i.e., $\mathcal{H}_I$, for all $A(k)$ satisfying Assumption 2.3, as explained in Appendix 2.6.3. Moreover, the change of dynamics does not lead to extra communications between the agents, since the matrix $\boldsymbol{Q}(k)$ is block diagonal and it does not modify the fixed points of the mapping.

The following theorem shows that the modified dynamics in (2.17), subject to arbitrary switching of communication topology, converge to a p-NWE, for any initial condition.

Theorem 2.8 (Convergence of time-varying dynamics)**.** *Let Assumptions 2.5, 2.6 hold true. Then, for any $\boldsymbol{x}(0) \in \boldsymbol{\Omega}$, the sequence $(\boldsymbol{x}(k))_{k\in\mathbb{N}}$ generated by* (2.17) *converges to some $\bar{\boldsymbol{x}} \in \mathcal{E}$, with $\mathcal{E}$ as in* (2.16)*, namely, a p-NWE of* (2.15)*.* □

We clarify that in general, the computation of $Q(k)$ associated to each $A(k)$ requires global information on the communication network. Therefore, this solution is suitable for the case of switching between a finite set of adjacency matrices, for which the associated matrices $Q(k)$ can be computed offline.

Nevertheless, for some network structures the left PF eigenvector is known or it can be explicitly computed locally. If the matrix $A(k)$ is symmetric, hence doubly-stochastic, or if each agent i knows the weight that its neighbours assign to the information it communicates, the i-th component of $q(k)$ can be computed as $\lim_{t\to\infty}[A(k)^\top]_i^t x = q_i(k)$, for any $x \in \mathbb{R}^N$ [35, Prop. 1.68]. Moreover, if each agent i has the same out and in degree, denoted by $d_i(k)$, and the weights in the adjacency matrix are chosen as $[A(k)]_{ij} = \frac{1}{d_i(k)}$, then the left PF eigenvector is $q(k) := \mathrm{col}((d_i(k)/\sum_{j=1}^N d_j(k))_{i\in\mathcal{N}})$. In other words, in this case each agent must only know its out-degree to compute its component of $q(k)$.

2.4 Numerical simulations

2.4.1 Synchronous/asynchronous Friedkin and Johnsen model

As mentioned in Section 2.2, the problem studied in this chapter arises often in the field of opinion dynamics. Next, we consider the standard Friedkin and Johnsen model, introduced in [87]. The state $x_i(k)$ of each player represents its opinion on n independent topics at time k. An opinion is represented with a value between

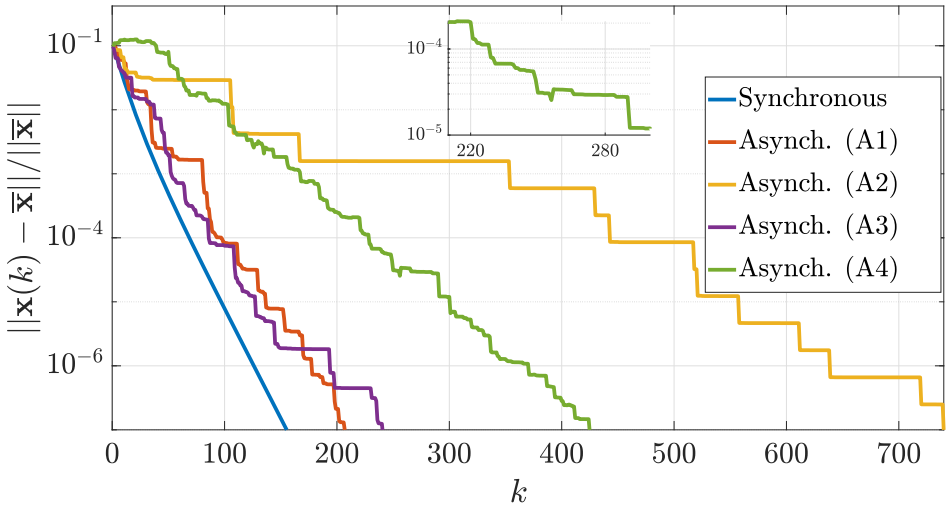

Figure 2.1: Comparison between the convergence of the Friedkin and Johnsen model subject to synchronous and asynchronous update. In the latter case the different type of updates (A1), (A2), (A3) and (A4) are considered. For a fair comparison we have assumed that the synchronous dynamics update once every N time instants.

0 and 1, hence $\Omega_i := [0,1]^n$. The opinion $[x_i]_j = 1$ if agent i completely agrees on topic j, and 0 if it disagrees. Each agent is stubborn with respect to its initial opinion $x_i(0)$ and $\mu_i \in (0,1]$ defines how much its opinion is bound to it. Namely, $\mu_i = 0$ represents a *fully stubborn* player, while $\mu_i = 1$ a *follower*. In the following, we present the evolution of the synchronous and asynchronous dynamics (2.6) and (2.10), respectively, where the cost function is as in (2.3).

We considered $N = 10$ agents discussing on $n = 3$ topics. The communication network and the weights that each agent assigns to the neighbours are randomly drawn, with the only constraint of satisfying Assumption 2.3. The initial condition is also a random vector $\boldsymbol{x}(0) \in [0,1]^{nN}$. Half of the players are somehow stubborn $\mu = 0.1$ and the remaining are more incline to follow the opinion of the others, i.e., $\mu = 0.5$. For the asynchronous dynamics, we consider three scenarios.

(A1) There is no delay in the information and the probability of update is uniform between the players, hence $\overline{\varphi} = 0$ and $p_{\min} = 1/N = 0.1$.

(A2) There is no delayed information and the agents update with different rates, so $\overline{\varphi} = 0$ and $p_{\min} = 0.0191 \neq 1/N$. In particular, we consider the case of a sensible difference between the rates to highlight the contrast with (A1) and (A3).

(A3) We consider an uniform probability of update and a maximum delay of two time instants, i.e., $p_{\min} = 1/N = 0.1$ and $\overline{\varphi} = 2$. The values of the maximum delay is chosen in order to fulfil condition (2.11).

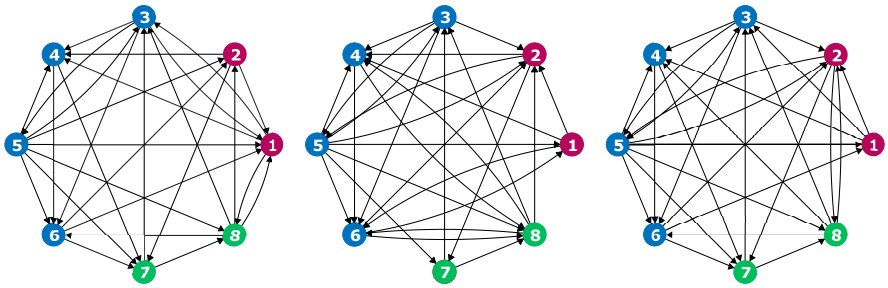

Figure 2.2: The three different communication networks between which the agents switch.

(A4) We consider the same setup as in (A3) but in this case with $\overline{\varphi} = 50$. Notice that our theoretical results do not guarantee the convergence of these dynamics.

In Figure 2.1, it can be seen how the convergence of the synchronous dynamics (A1) and the asynchronous ones (A3) are similar. The delay affects the convergence speed if it exceeds the theoretical upper bound in (2.11), as in (A4). It is worthy to notice that, even a big delay does not seem to lead to instability, while it can produce a sequence that does not converge monotonically to the equilibrium, see the zoom in Figure 2.1. The slowest convergence is obtained in case of a non uniform rate of update, i.e., (A2). From the simulation it seems that the uniform update probability produces always the fastest convergence.

2.4.2 Time-varying DeGroot model with bounded confidence

In this section, we consider a modified time varying version of the DeGroot model [62], where each agent is willing to change its opinion up to a certain extent. This model can describe the presence of extremists in a discussion. In the DeGroot model, the cost function $\bar{f}_i$ in (2.1), reduces to $\bar{f}_i = \iota_{\Omega_i}$ for all $i \in \mathcal{N}$. We consider $N = 8$ agents discussing on one topic, hence the state x_i is a scalar.

The agents belong to three different categories, that we call: *positive extremists, negative extremists and neutralists*. This classification is based on the local feasible decision set.

- *Positive (negative) extremists*: the agents agree (disagree) with the topic and are not open to drastically change their opinion, i.e., $\Omega_i = [0.75, 1]$ ($\Omega_i = [0, 0.25]$).
- *Neutralists*: the agents do not have a strong opinion on the topic, so their opinions vary from 0 to 1, i.e., $\Omega_i = [0, 1]$.

Our setup is composed of two negative extremists (agent 1 and 2), four neutralists (agents 3-6) and two positive extremists (agents 7 and 8). We assume that, at each

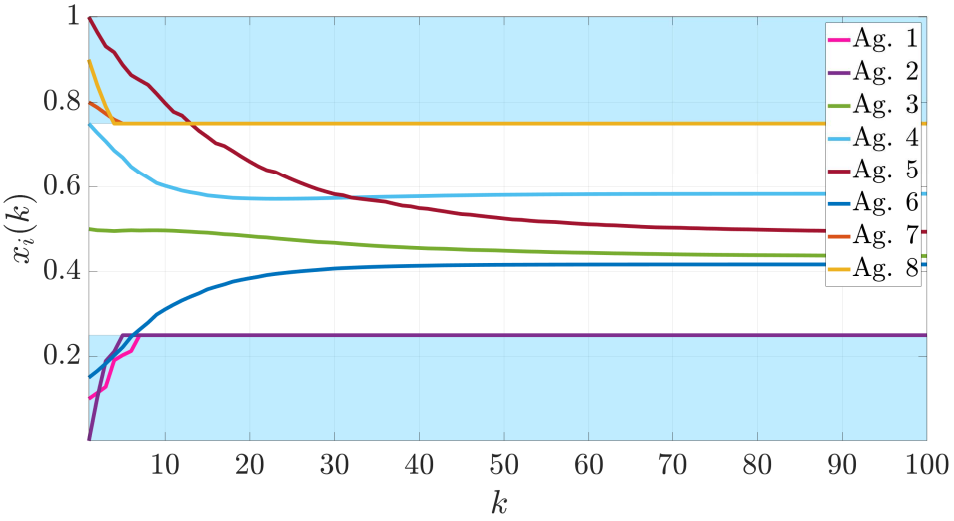

Figure 2.3: The evolution of the opinion $x_i(k)$ of each agent $i \in \mathcal{N}$. The light blue top and bottom regions represents the local feasible sets of positive and negative extremists, respectively.

time instant, the agents can switch between three different communication network topologies, depicted in Figure 2.2.

The dynamics in (2.17) can be rewritten, for a single agent $i \in \mathcal{N}$, as

$$x_i(k+1) = \mathrm{proj}_{\Omega_i}\big((1-q_i(k))x_i(k) + q_i(k)[A(k)]_i\boldsymbol{x}(k)\big).$$

From this formulation, it is clear how the modification of the original dynamics (2.15) results into an inertia of the players to change their opinion.

We have proven numerically that Assumption 2.6 is satisfied and that the unique p-NWE of the game is

$$\bar{\boldsymbol{x}} = \big[0.25,\ 0.25,\ 0.44,\ 0.58,\ 0.49,\ 0.41,\ 0.75,\ 0.75\big]^\top.$$

In Figure 2.3 the evolution of the players' opinion are reported, as expected, the dynamics converge to the unique p-NWE $\bar{\boldsymbol{x}}$.

2.5 Conclusion and outlook

For the class of multi-agent network games, proximal type dynamics converge, provided that the communication network is strongly connected. We proved that their asynchronous counterparts also converge, and that they are robust to bounded delayed information. If each agent has the possibility to arbitrarily choose the communications weights with its neighbours, then proximal dynamics converge

even if the communication network varies over time. When the problem at hand can be recast as a proximal type dynamics, the results achieved directly provide the solution of the game, as shown in the numerical examples proposed.

2.6 Appendix

2.6.1 Proof of Theorem 2.3

Firstly, we introduce the following auxiliary lemma.

Lemma 2.9. *Let $P \in \mathbb{R}^{N\times N}$, $[P]_{ij} := p_{ij}$ be a non negative matrix that satisfies*

$$P\mathbf{1}_N = \mathbf{1}_N, \iff \textstyle\sum_{j\in\mathcal{N}} p_{ij} = 1 \tag{2.18}$$

$$q^\top P \le q^\top \iff \textstyle\sum_{i\in\mathcal{N}} q_i p_{ij} \le q_j, \tag{2.19}$$

where $q \in \mathbb{R}^N_{>0}$. Then P is NEX in $\mathcal{H}_Q$, with $Q = \mathrm{diag}(q)$. □

Proof. To ease the notation we adopt $\sum_j(\cdot) := \sum_{j\in\mathcal{N}}(\cdot)$ and $\sum_j\sum_{k<j}(\cdot) := \sum_{j\in\mathcal{N}}\sum_{k\in(1,\dots,j-1)}(\cdot)$ in the following.

Next, we exploit (2.19) to compute

$$\begin{aligned} x^\top P^\top QPx - x^\top Qx &= \textstyle\sum_i q_i \left(\sum_j p_{ij}x_j\right)^2 - \sum_j q_j x_j^2 \\ &\le \textstyle\sum_i q_i \left(\left(\sum_j p_{ij}x_j\right)^2 - \sum_j p_{ij}x_j^2\right). \end{aligned} \tag{2.20}$$

Notice that for all $i \in \mathcal{N}$ it holds $\sum_j p_{ij}x_j^2 = \sum_j p_{ij}(\sum_k p_{ik})x_j^2$, furthermore this implies that

$$\left(\textstyle\sum_j p_{ij}x_j\right)^2 - \sum_j p_{ij}x_j^2 = -\sum_j\sum_{k<j} p_{ij}p_{ik}(x_j - x_k)^2 \tag{2.21}$$

Since the matrix P is supposed non negative and from (2.20) and (2.21), it follows that

$$x^\top P^\top QPx - x^\top Qx \le -\textstyle\sum_j\sum_{k<j} p_{ij}p_{ik}(x_j - x_k)^2 \le 0\,.$$

Therefore, P is NEX in $\mathcal{H}_Q$ from [16, Lemma 3 (ii)]. ■

Proof of Lemma 2.2

(i) From Standing Assumption 2.3, A is marginally stable, with no eigenvalues on the boundary of the unit disk but semi-simple eigenvalues at 1. A can be rewrite as $A = (1-\eta)\mathrm{Id}+\eta B$ with $\eta \in (1-\underline{a}, 1)$, hence $B \ge 0$ and is row stochastic. The graph associated to B has the same edges of that to A, so it is strongly connected and B irreducible. The PF theorem for irreducible matrix, see Appendix B, ensures the existence of a vector q satisfying (2.19) for B. Therefore, Lemma 2.9 can be applied to B, implying that B is NEX in $\mathcal{H}_Q$ where $Q = \mathrm{diag}(q) \succ 0$. By construction, this implies that the linear operator A is η–AVG in the same space [14, Def. 4.33]. This directly implies that $\boldsymbol{A} = A \otimes I_n$ is η–AVG in $\mathcal{H}_{\boldsymbol{Q}}$, with $\boldsymbol{Q} = Q \otimes I_n$.

(ii) From point (i), we know that A is η–AVG in $\mathcal{H}_Q$. For all $i \in \mathcal{N}$, define $q_i := [Q]_{ii}$ and recall that $\text{prox}_{\bar{f}_i}$ is FNE in $\mathcal{H}_{I_n}$ since $\bar{f}_i$ is convex from Assumption 2.2. Hence, from [14, Prop. 4.4. (iv)] for all $x, y \in \mathbb{R}^n$, it holds that

$$\|\text{prox}_{\bar{f}_i}(x) - \text{prox}_{\bar{f}_i}(y)\|^2 \leq \langle x - y,\, \text{prox}_{\bar{f}_i}(x) - \text{prox}_{\bar{f}_i}(y)\rangle. \tag{2.22}$$

The following inequality shows that $\mathbf{prox_f}$ is FNE in $\mathcal{H}_{\boldsymbol{Q}}$. For all $\boldsymbol{x} = \text{col}(\{x_i\}_{i=1}^N)$, $\boldsymbol{y} = \text{col}(\{y_i\}_{i=1}^N) \in \mathbb{R}^{nN}$,

$$\begin{aligned}\|\mathbf{prox_f}(\boldsymbol{x}) - \mathbf{prox_f}(\boldsymbol{y})\|_{\boldsymbol{Q}}^2 &= \sum_{i=1}^N q_i \|\text{prox}_{\bar{f}_i}(x_i) - \text{prox}_{\bar{f}_i}(y_i)\|^2 \\ &\leq \textstyle\sum_{i=1}^N q_i \langle x_i - y_i,\, \text{prox}_{\bar{f}_i}(x_i) - \text{prox}_{\bar{f}_i}(y_i)\rangle \\ &= \langle \boldsymbol{x} - \boldsymbol{y},\, \mathbf{prox_f}(\boldsymbol{x}) - \mathbf{prox_f}(\boldsymbol{y})\rangle_{\boldsymbol{Q}},\end{aligned}$$

The second step follows from (2.22). It follows from [14, Prop. 4.44] that the composition $\mathbf{prox_f} \circ \boldsymbol{A}$ is AVG in $\mathcal{H}_{\boldsymbol{Q}}$ with constant $\frac{1}{2-\eta}$, since $\mathbf{prox_f}$ and $\boldsymbol{A}$ are, respectively, $\frac{1}{2}$- and η-AVG in $\mathcal{H}_{\boldsymbol{Q}}$.
If the matrix A is doubly stochastic, then its left PF eigenvector is $\mathbf{1}$, see Appendix B. By applying the result just attained in (ii), we conclude that $\mathbf{prox_f} \circ \boldsymbol{A}$ is $\frac{1}{2-\eta}$-AVG in $\mathcal{H}_I$. ■

Proof of Theorem 2.3

From Lemma 2.2(ii), we know that the operator $\mathbf{prox_f} \circ \boldsymbol{A}$ is AVG in $\mathcal{H}_{\boldsymbol{Q}}$ with constant $\frac{1}{2-\eta}$ and $\eta > 1 - \underline{a}$. Therefore the convergence of the iteration in (2.6) follows by [14, Prop. 5.16]. ■

Proof of Corollary 2.4

The convergence follows directly from [14, Th. 5.15] and the fact that the considered $\boldsymbol{A}$ is NEX in the space $\mathcal{H}_{\boldsymbol{Q}}$, by Lemma 2.9. ■

2.6.2 Proof of Section 2.3.2

Since the dynamics in (2.12) are a special case of (2.10), we first prove Theorem 2.6 and successively derive the proof of Theorem 2.5 exploiting a similar reasoning.

Proof of Theorem 2.6

From Theorem 2.3, we know that the operator $T := \mathbf{prox_f} \circ \boldsymbol{A}$ is η-AVG in the space $\mathcal{H}_{\boldsymbol{Q}}$ with $\eta \in (1 - \underline{a}, 1)$. Therefore, it can be written as $T = (1-\eta)\text{Id} + \eta\overline{T}$ where $\overline{T}$ is a suitable NEX operator in $\mathcal{H}_{\boldsymbol{Q}}$. Notice that $\text{fix}(\overline{T}) = \text{fix}(T)$. Substituting this formulation of T in (2.12) leads to

$$\boldsymbol{x}(k+1) = \boldsymbol{x}(k) + \psi_k \eta \zeta_k \big(\overline{T} - \text{Id}\big)\hat{\boldsymbol{x}}(k)\,. \tag{2.23}$$

Since $\overline{T}$ is NEX in $\mathcal{H}_{\boldsymbol{Q}}$, [147, Lemma 13 and 14] can be applied to the dynamics in (2.23). Therefore, if we choose $\psi_k \in \big(0, \frac{Np_{\min}}{(2\overline{\varphi}\sqrt{p_{\min}}+1)(1-\underline{a})}\big)$, the sequence generated by the dynamics in (2.23) are bounded and converge almost surely to a point $\overline{\boldsymbol{x}} \in \operatorname{fix}(\overline{T}) = \operatorname{fix}(\mathbf{prox}_{\boldsymbol{f}} \circ \boldsymbol{A})$. The proof is completed recalling that the set of fixed points of $\mathbf{prox}_{\boldsymbol{f}} \circ \boldsymbol{A}$ coincides with the set of NWE, by Remark 2.1. ■

Proof of Theorem 2.5

The dynamics (2.10) coincide with (2.12), when $\psi_k = 1$ for all $k \in \mathbb{N}$, therefore if $\frac{Np_{\min}}{(2\overline{\varphi}\sqrt{p_{\min}}+1)(1-\underline{a})} > 1$, then the convergence is guaranteed from Theorem 2.6. From easy computation it can be seen that this condition is equivalent to (2.11), and this conclude the proof. ■

2.6.3 Proofs of Section 2.3.3

First, we propose two preliminary lemmas

Lemma 2.10. *Let $P := p \in \mathbb{R}^{N\times N}$ and $[P]_{ij} = p_{ij}$ be a non negative, row-stochastic matrix. If there exists a vector $w \in \mathbb{R}^N_{\geq 0}$ such that $w^\top P = w^\top$, then the matrix*

$$\overline{P} := I + \mu \operatorname{diag}(w)(P - I), \tag{2.24}$$

where $0 \leq \mu \leq \frac{1}{\max_{i\in\mathcal{N}}(1-p_{ii})w_i}$, is non negative and doubly stochastic. If $\mu < \frac{1}{\max_{i\in\mathcal{N}}(1-p_{ii})w_i}$, then the diagonal elements of $\overline{P}$ are positive. □

Proof. Since w is a left eigenvector of P it holds that $w^\top P = w^\top$. To prove the first part of the lemma we have to show that $\overline{P}\mathbf{1} = \mathbf{1}$ and $\mathbf{1}^\top\overline{P} = \mathbf{1}^\top$, hence

$$\overline{P}\mathbf{1} = \mathbf{1} - \mu w + \mu \operatorname{diag}(w)P\mathbf{1} = \mathbf{1}\,. \tag{2.25}$$

Analogously, $\mathbf{1}^\top\overline{P} = \mathbf{1}^\top - \mu w^\top + \mu w^\top P = \mathbf{1}^\top$, where the last equality is achieved using the properties of w. So, from the relations above we conclude that $\overline{P}$ is doubly stochastic.

Now we prove that all the element of $\overline{A}$ are non negative if $0 \leq \mu \leq \overline{w}$. The diagonal elements of $\overline{P}$ are $\overline{p}_{ii} := 1 - \mu w_i + \mu w_i p_{ii}$ the off diagonal ones are instead $\overline{p}_{ij} := \mu w_i p_{ij}$, $\forall i, j \in \mathcal{N}$. From simple calculations, it follows that if $0 \leq \mu \leq \frac{1}{\max_{i\in\mathcal{N}}(1-p_{ii})w_i}$ then $\overline{P}$ is a non negative matrix.

If $\mu < \frac{1}{\max_{i\in\mathcal{N}}(1-p_{ii})w_i}$ then $\overline{p}_{ii} > 0$ for all $i \in \mathcal{N}$, hence $\overline{P}$ is doubly stochastic, with positive diagonal elements. ■

In the next corollary we consider the case of a matrix A satisfying Standing Assumption 2.3. It shows that the transformation (2.24) does not change the set of fixed points of A. Furthermore, it also provides the coefficient of averagedness of $\overline{A}$. We show that if A satisfies Standing Assumption 2.3, then (2.24) does not change the fixed points of A.

Lemma 2.11. *Let the matrix A satisfies Standing Assumption 2.3 and Q as in Theorem 2.3. Then the matrix*

$$\overline{A} := I + Q(A - I) \tag{2.26}$$

is doubly stochastic with self-loops and the following statements hold:

(i) $\operatorname{fix}(\overline{A}\cdot) = \operatorname{fix}(A\cdot)$*;*

(ii) $\overline{A}$ *satisfies Standing Assumption 2.3;*

(iii) $\overline{A}$ *is* χ*-AVG in* $\mathcal{H}$ *with* $\chi \in (\max_{i\in\mathcal{N}}(1 - a_{i,i})q_i, 1)$.□

Proof. (i) The definition in (2.26) is equivalent to $\overline{A} = (I - Q) + QA$. Therefore $\operatorname{fix}(\overline{A}) = \operatorname{fix}(A)$, since $Q \succ 0$.

(ii) The matrix $\overline{A}$ is in the form of (2.24) with $\mu = 1$ and, since

$$1 < \frac{1}{\max_{i\in\mathcal{N}}(1 - a_{i,i}(k))} \leq \frac{1}{\max_{i\in\mathcal{N}}(1 - a_{i,i}(k))q_i}\,.$$

It satisfies the assumption of Lemma 2.10, thus $\overline{A}$ is doubly stochastic with self-loops. Finally, since A satisfies Standing Assumption 2.3, the graph defined by $\overline{A}$ is also strongly connected, therefore also $\overline{A}$ satisfies Standing Assumption 2.3.

(iii) To prove that $\overline{A}$ is χ-AVG with $\chi \in (\max_{i\in\mathcal{N}}(1 - a_{i,i})q_i, 1)$, we can also apply [99, Lem. 9] or use the same argument as in the proof of Lemma 2.2. ■

Proof of Theorem 2.8

From Corollary 2.11, each matrix $\overline{A} := I + \mu\boldsymbol{Q}(k)(\boldsymbol{A}(k) - I)$ is $(\mu(k)\max_{i\in\mathcal{N}}(1 - a_{i,i}(k))q_i(k))$-AVG in $\mathcal{H}_I$. Since $\mathbf{prox}_{\boldsymbol{f}}$ is FNE in $\mathcal{H}_I$, the operator $\mathbf{prox}_{\boldsymbol{f}} \circ \overline{\boldsymbol{A}}(k)$ is $\frac{1}{2-\hat{\eta}(k)}$ where $\hat{\eta}(k) := \mu(k)\max_{i\in\mathcal{N}}(1 - a_{i,i}(k))q_i(k)$, [14, Prop. 4.44]. All the operators used in the dynamics are AVG in the same space $\mathcal{H}_I$, therefore the global convergence follows from [14, Cor. 5.19], since all the cluster point of $(\boldsymbol{x}(k))_{k\in\mathbb{N}}$ lay in $\mathcal{E}$. ■

3

Equilibrium seeking design in proximal network games

In this chapter, we carry out the analysis on constrained multi-agent network games. We first focus on games subject to affine coupling constraints, and then we generalize them to the case of time-varying constraints and communication networks. For the former problem, we propose an iterative equilibrium seeking algorithm (Prox-GNWE), using only local information, that converges to a generalized Nash equilibrium of the game. In the second case, the concept of persistent equilibrium is introduced and the assumptions considered to solve the problem are discussed and motivated. Then, we present a modified version of the previous algorithm (TV-Prox-GNWE) that converges to a special class of game equilibria. Its derivation is motivated by several examples, showing that the original game dynamics fail to converge. To validate the theoretical results, we present two possible applications for the introduced algorithms, namely a distributed model fitting and a constrained consensus problem.

3.1 Introduction

In Section 2.1, we discussed the importance of multi-agent network games in many different applications. There are several problems in which the action of a player is restricted by those of the others. These restrictions are called *coupling constraints* and arise in many problems, e.g., in the context of smart grids it is common to limit the total energy that the prosumers can purchase [65]. These constraints transform the problem into a GNEP and consequently require a different analysis.

In this chapter, we study, not only games subject to static constraints, but also multi-agent network games in which the communication network and the constraints between the agents are both time-varying. Multi-agent network games arise from the well established field of distributed optimization and equilibrium seeking over networks. In the past years, several results were proposed for optimization problems subject to a time-varying communication network: in [131] the subgradients of the cost functions are bounded and the communication is described by a sequence of strongly connected directed graphs, while in [132] the cost functions are assumed to be continuously differentiable and a linearly convergent algorithm is designed under the assumption of a time-varying undirected communication network. Another approach, explored in [117], is to construct a game, whose emerging behavior solves the optimization problems. In this case, the cost functions are differentiable and the communication is ruled by an undirected time-varying graph connected over time.

The problem of noncooperative multi-agent games, subject to coupling constrains, was firstly studied in [79], under the assumptions of continuously differentiable cost functions and no network structure between the agents. In the past years, several researchers focused on this class of problems providing a range of results for games over networks, e.g., in [176, 20, 40] where the communication network is always assumed to be undirected, while the cost functions are chosen either differentiable or continuously differentiable. Moreover, some researchers also focused on the class of noncooperative games over time-varying communication networks, in particular on the unconstrained case. For example, in [110] differentiable and strictly convex cost functions with Lipschitz continuous gradient were considered, where the sequence of time-varying communication networks was assumed repeatedly strongly connected, and the associated adjacency matrices are doubly stochastic.

3.1.1 Main contribution

A complete formulation of multi-agent network games, subject to proximal type dynamics, can be found in [99] where the unconstrained case is studied for a time-varying strongly connected communication network, described by a doubly stochastic adjacency matrix. In [47] and Chapter 2, the condition on the double stochasticity of the adjacency matrix was relaxed, in the first case by means of a dwell time. Notice that these types of games can also be rephrased as paracontracions; in this framework, the work in [89] provided convergence for repeatedly jointly connected digraphs. Iterative equilibrium seeking algorithms were developed for constrained

multi-agent network games in [99] under the assumption of a static communication network.

The contribution of this chapter is twofold. In the first part we tackle the problem of multi-agent network games subject to coupling constraints by formalizing the problem using operator theory and then, we derive an iterative equilibrium seeking algorithm (Prox-GNWE) that is proven to converge globally to an equilibrium of the game. In the second part, we generalize the problem by considering constrained multi-agent network games subject to time-varying communication networks. We first discuss the convergence of the game and motivate the technical assumptions needed to ensure the existence of an equilibrium. Moreover, we develop a generalization of teh previous algorithm called TV-Prox-GNWE that achieves global convergence for the game at hand. Finally, we conclude the chapter by showing two applications of the algorithms developed for the problems of distributed model fitting and constrained consensus, introduced in Section 2.2.

3.2 Proximal dynamics under coupling constraints

3.2.1 Problem formulation

In the remainder of the chapter, we assume the same standing assumptions introduced in Chapter 2 for the case of games subject only to local constraints. Starting from the setup described in Section 2.2, we generalize it to address M affine separable coupling constraints between the agents. The set of all the strategies profiles that satisfy both the local and coupling constraints is called the *collective feasible decision set*, and it is defined as

$$\boldsymbol{\mathcal{X}} := \boldsymbol{\Omega} \cap \{\boldsymbol{x} \in \mathbb{R}^{nN} \,|\, C\boldsymbol{x} \leq c\} \tag{3.1}$$

where $C \in \mathbb{R}^{M \times nN}$ and $c \in \mathbb{R}^M$. For every agent $i \in \mathcal{N}$, the set of local strategies satisfying the coupling constraints reads as

$$\mathcal{X}_i(\boldsymbol{x}_{-i}) := \left\{ y \in \mathbb{R}^n \,|\, C_i y + \sum_{\substack{j=1 \\ j \neq i}}^{N} C_j x_j \leq c \right\}. \tag{3.2}$$

Standing Assumption 3.1. *For all $i \in \mathcal{N}$, the local feasible decision set $\Omega_i \cap \mathcal{X}_i(\boldsymbol{x}_{-i})$ satisfies Slater's condition.* □

The original game formulation, described by the dynamics in (2.5), changes to consider also the coupling constraints, i.e.,

$$\forall i \in \mathcal{N} : \begin{cases} \operatorname{argmin}_{y \in \mathbb{R}^n} & \bar{f}_i(y) + \frac{1}{2} \left\| y - \sum_{j=1}^{N} a_{i,j} x_j \right\|^2 \\ \text{s.t.} & y \in \mathcal{X}_i(\boldsymbol{x}_{-i}). \end{cases} \tag{3.3}$$

Hence, the correspondent myopic dynamics read as

$$x_i(k+1) = \operatorname{argmin}_{y \in \mathcal{X}_i(\boldsymbol{x}_{-i}(k))} J_i\left(y, \textstyle\sum_{j=1}^{N} a_{i,j} x_j(k)\right) . \tag{3.4}$$

For the game in (3.4), the concept of equilibrium point is non trivial. A popular equilibrium notion for constrained game is the, so called, GNWE. Loosely speaking, a profile strategy $\bar{\boldsymbol{x}}$ is a GNWE of the game, if no player i can change its strategy to another *feasible* one while decreasing its local cost J_i.

Definition 3.1 (Generalized Network Equilibrium)**.** A collective vector $\overline{\boldsymbol{x}}$ is a GNWE for the game in (3.3) if, for all $i \in \mathcal{N}$,

$$\overline{x}_i = \operatorname{argmin}_{y \in \mathcal{X}_i(\boldsymbol{x}_{-i})} J_i\left(y, \textstyle\sum_{j=1}^{N} a_{i,j} \overline{x}_j\right) . \qquad \square$$

Notice that, if A does not have self-loops, the definition of GNWE coincides with that of GNE, see [79].

The following example shows that the dynamics in (3.1) fail to converge even for simple coupling constraints.

Example 3.1 (Non-convergence)**.** Consider a 2-player game, defined as in (3.3), where, for $i \in \{1, 2\}$, $x_i \in \mathbb{R}$ and the local feasible decision set is defined as $\mathcal{X}_i(u) := \{v \in \mathbb{R} \,|\, u+v = 0\} = \{-u\}$. The game is jointly convex since the collective feasible decision set is described by the convex set $\boldsymbol{\mathcal{X}} := \{\boldsymbol{x} \in \mathbb{R}^2 \,|\, x_1 + x_2 = 0\}$. The parallel myopic best response dynamics are described in closed form as the discrete-time linear system:

$$\begin{bmatrix} x_1(k+1) \\ x_2(k+1) \end{bmatrix} = \begin{bmatrix} 0 & -1 \\ -1 & 0 \end{bmatrix} \begin{bmatrix} x_1(k) \\ x_2(k) \end{bmatrix}, \tag{3.5}$$

which is not globally convergent, e.g., consider $x_1(0) = x_2(0) = 1$. $\square$

The myopic dynamics of the agents fail to converge, and thus we rephrase them into some analogues pseudo-collaborative ones. The players aim to minimize their local cost functions, while at the same time coordinate with the other agents to satisfy the coupling constraints. Toward this end, we first dualize the problem and transform it into an auxiliary (extended) network game [56, Ch. 3]. Finally, we design a semi-decentralized iterative algorithm that ensures the convergence of these dynamics to a GNWE.

Let us now introduce the dual variable $\lambda_i \in \mathbb{R}^M_{\geq 0}$ for each player $i \in \mathcal{N}$, and define the concept of Extended Network Equilibrium (ENWE) arising from this new problem structure.

Definition 3.2 (Extended Network Equilibrium)**.** The pair $(\overline{\boldsymbol{x}}, \overline{\boldsymbol{\lambda}})$, is an ENWE for the game in (3.3) if, for every $i \in \mathcal{N}$, it satisfies

$$\overline{x}_i = \operatorname{argmin}_{y \in \mathbb{R}^n} \; J_i\left(y, \textstyle\sum_{j=1}^{N} a_{i,j} \overline{x}_j\right) + \overline{\lambda}_i^\top C_i y, \tag{3.6a}$$

$$\overline{\lambda}_i = \operatorname{argmin}_{\xi \in \mathbb{R}^M_{\geq 0}} \; -\xi^\top (C\overline{\boldsymbol{x}} - c) . \tag{3.6b}$$

$\square$

To find an GNWE of the game in (3.3), we assume the presence of a central coordinator. It broadcasts to all agents an auxiliary variable σ that each agent i uses to compute its local dual variable λ_i. Namely, every agent i applies a scaling factor $\alpha_i \in [0,1]$ to σ to attain its dual variable, i.e. $\lambda_i = \alpha_i \sigma$. The values of the scaling factor represent a split of the burden that the agents experience to satisfy the constraints, hence $\sum_{i=1}^{N} \alpha_i = 1$. These game equilibrium problems were studied for the first time in the seminal work of Rosen [152], where the author introduces the notion of *normalized equilibrium*. We specialize this equilibrium idea for the problem at hand, introducing the notion of normalized Extended Network Equilibrium (n–ENWE).

Definition 3.3 (normalized-ENWE)**.** The pair $(\overline{\boldsymbol{x}}, \overline{\sigma})$, is an n–ENWE for the game in (3.3), if for all $i \in \mathcal{N}$ it satisfies

$$\overline{x}_i = \text{argmin}_{y \in \mathbb{R}^n} \; J_i\left(y, \sum_{j=1}^{N} a_{i,j} \overline{x}_j\right) + \alpha_i \, \overline{\sigma}^\top C_i y, \tag{3.7a}$$

$$\overline{\sigma} = \text{argmin}_{\varsigma \in \mathbb{R}^M_{\geq 0}} \; -\varsigma^\top (C\overline{\boldsymbol{x}} - c), \tag{3.7b}$$

where $\alpha_i > 0$. □

From (3.7a) - (3.7b), one can see that the class of n–ENWE is a particular instance of GNWE and, at the same time, a generalization of the case in which all the agents adopt the same dual variable, hence $\alpha_i = 1/M$, for all $i \in \mathcal{N}$. This latter case is widely studied in the literature, since it implies an equal split between the agents of the burden to satisfy the constraints [176, 18].

Next, we recast the n–ENWE described by the two inclusions (3.7a) – (3.7b) as a fixed point of a suitable mappings. In fact, (3.7a) can be equivalently rewritten as

$$\overline{\boldsymbol{x}} = \mathbf{prox}_{\boldsymbol{f}}(\boldsymbol{A}\boldsymbol{x} - \boldsymbol{\Lambda} C^\top \overline{\sigma}) \,,$$

where $\boldsymbol{\Lambda} = \text{diag}((\alpha_i)_{i \in \mathcal{N}}) \otimes I_n$, while (3.7b) holds true if and only if $\overline{\sigma} = \text{proj}_{\mathbb{R}^M}(\overline{\sigma} + C\overline{\boldsymbol{x}} - c)$.

To combine in a single operator (3.7a) and (3.7b), we first introduce two mappings, i.e.,

$$\boldsymbol{\mathcal{R}} := \text{diag}(\mathbf{prox}_{\boldsymbol{f}}, \; \text{proj}_{\mathbb{R}^M_{\geq 0}}) \tag{3.8}$$

and the affine mapping $\boldsymbol{\mathcal{G}} : \mathbb{R}^{nN+M} \to \mathbb{R}^{nN+M}$ defined as

$$\boldsymbol{\mathcal{G}}(\cdot) := \boldsymbol{G} \cdot + \begin{bmatrix} \mathbf{0} \\ c \end{bmatrix} := \begin{bmatrix} \boldsymbol{A} & -\boldsymbol{\Lambda} C^\top \\ C & I \end{bmatrix} \cdot - \begin{bmatrix} \mathbf{0} \\ c \end{bmatrix} . \tag{3.9}$$

The composition of these two operators provides a compact definition of the n–ENWE for the game in (3.3). In fact, a point $(\overline{\boldsymbol{x}}, \overline{\sigma})$ is an n–ENWE if and only if $\text{col}(\overline{\boldsymbol{x}}, \overline{\sigma}) \in \text{fix}(\boldsymbol{\mathcal{R}} \circ \boldsymbol{\mathcal{G}})$; indeed the explicit computation of $\boldsymbol{\mathcal{R}} \circ \boldsymbol{\mathcal{G}}$ retrieves exactly (3.7a) and (3.7b).

The following lemmas show that an n–ENWE is also a GNWE by proving that a fixed point of $\boldsymbol{\mathcal{R}} \circ \boldsymbol{\mathcal{G}}$ is a GNWE.

Lemma 3.4 (GNWE as fixed point)**.** *Let Assumption 3.1 hold true. Then, the following statements are equivalent:*

(i) $\overline{\boldsymbol{x}}$ *is a GNWE for the game in* (3.3)*;*

(ii) $\exists \overline{\sigma} \in \mathbb{R}^M$ *such that* $\operatorname{col}(\overline{\boldsymbol{x}}, \overline{\sigma}) \in \operatorname{fix}(\boldsymbol{\mathcal{R}} \circ \boldsymbol{\mathcal{G}})$. □

Lemma 3.5 (Existence of a GNWE)**.** *Let Assumption 3.1 hold true. There always exists a GNWE for the game in* (3.3)*.* □

The two lemmas above are direct consequences of [99, Lem. 2, Prop. 2] respectively, so the proofs are omitted.

3.2.2 Algorithm derivation (Prox-GNWE)

In this section, we describe the iterative algorithm seeking GNWE (Prox-GNWE) for the game in (3.3). The set of fixed points of the operator $\boldsymbol{\mathcal{R}} \circ \boldsymbol{\mathcal{G}}$ can be expressed as the set of zeros of other suitable operators, as formalized next.

Lemma 3.6 ([14, Prop. 26.1 (iv)])**.** *Let* $\boldsymbol{\mathcal{B}} := F \times N_{\mathbb{R}^M_{\geq 0}}$*, with* $F := \prod_{i=1}^N \partial \bar{f}_i$*. Then,* $\operatorname{fix}(\boldsymbol{\mathcal{R}} \circ \boldsymbol{\mathcal{G}}) = zer(\boldsymbol{\mathcal{B}} + \mathrm{Id} - \boldsymbol{\mathcal{G}})$. □

Several algorithms are available in the literature to find a zero of the sum of two monotone operators, the most common being presented in [14, Ch. 26]. We opted for a variant of the preconditioned PPP that allows for non-self-adjoint preconditioning [32, Eq. 4.18]. It results in a proximal type update with inertia that resembles the original myopic dynamics studied. The resulting algorithm is here called Prox-GNWE and it is described in (3.10a) – (3.10d) where, for all the variables introduced, we adopted the notation $x^+ := x(k+1)$ and $x = x(k)$, for the sake of compactness. The complete derivation of the algorithm is reported in Appendix 3.6.1. Prox-GNWE is composed of three main steps:

1. a local gradient descend (3.10a), done by each agent,
2. a gradient ascend (3.10b), performed by the coordinator,
3. and finally an inertia step (3.10c) – (3.10d).

The parameters in Prox-GNWE are selected such that the following inequalities are satisfied:

$$\begin{aligned} r_i - a_{i,i} < \delta_i^{-1} \leq \gamma^{-1} - r_i - a_{i,i}, \quad \forall i \in \mathcal{N}, \\ p_j < \beta \leq \gamma^{-1} - p_j, \end{aligned} \tag{3.11}$$

$$\forall i \in \mathcal{N}: \quad \tilde{x}_i = \operatorname{prox}_{\frac{\delta_i}{\delta_i+1}\bar{f}_i}\left(\tfrac{\delta_i}{\delta_i+1}\left(\tfrac{1}{\delta_i}x_i + \textstyle\sum_{j=1}^{N} a_{i,j}x_j - \alpha_i C_i^\top \sigma\right)\right) \tag{3.10a}$$

$$\tilde{\sigma} = \operatorname{proj}_{\mathbb{R}^M_{\geq 0}}\left(\sigma + \tfrac{1}{\beta}(C\boldsymbol{x} - c)\right) \tag{3.10b}$$

$$\forall i \in \mathcal{N}: \quad x_i^+ = x_i + \gamma\left[\delta_i(\tilde{x}_i - x_i) + \textstyle\sum_{j=1}^{N} a_{i,j}(\tilde{x}_j - x_j) - \alpha_i C_i^\top(\tilde{\sigma} - \sigma)\right] \tag{3.10c}$$

$$\sigma^+ = \sigma + \gamma\left[\beta(\tilde{\sigma} - \sigma) + C(\tilde{\boldsymbol{x}} - \boldsymbol{x})\right] \tag{3.10d}$$

where

$$\begin{aligned} r_i &\coloneqq \tfrac{1}{2}\textstyle\sum_{\substack{j=1\\ j\neq i}}^{N}(a_{i,j} + a_{ji}) + (1+\alpha_i)\|C_i^\top\|_\infty, \\ p_j &\coloneqq (1+\alpha_i)\max_{j\in\{1,\dots,N\}}\|C_j^\top\|_\infty . \end{aligned} \tag{3.12}$$

We note that, if γ is chosen small enough, then the right inequalities in (3.11) always hold. On the other hand, γ is the step size of the algorithm, thus a smaller value can affect the convergence speed. The formal derivation of these bounds is reported in Appendix 3.6.1.

We also remark that (3.10a) – (3.10d) require two rounds of communications between an agent i and its neighbours: one to obtain the value of $x_j(k)$ in (3.10a) and the second to gather $\tilde{x}_j(k)$ for all $j \in \mathcal{N}_i$ in (3.10c). Finally, we conclude the section by establishing global convergence of the sequence generated by Prox-GNWE to a GNWE of the game in (3.3).

Theorem 3.7 (Convergence Prox-GNWE)**.** *Set $\alpha_i = q_i$, for all $i \in \mathcal{N}$, with q_i being the i-th element of the left PF eigenvector of A, and choose δ_i, β, γ satisfying* (3.11)*. Then, for any initial condition, the sequence $(\boldsymbol{x}(k))_{k\in\mathbb{N}}$ generated by* (3.10a) – (3.10d)*, converges to a GNWE of the game in* (3.3)*.* □

3.3 Proximal dynamics under time-varying coupling constraints

3.3.1 Mathematical formulation

In this second part of the chapter, we tackle the more general problem of multi-agent network games subject to M time-varying affine and separable coupling constraints, and a time-varying network topology.

For an agent $i \in \mathcal{N}$, at time instant $k \in \mathbb{N}$, the time-varying set of strategies satisfying the coupling constraints, given the other agents' strategies $\boldsymbol{x}_{-i}$, defined in (3.2) becomes a time-varying set and it reads as

$$\mathcal{X}_i(\boldsymbol{x}_{-i}, k) \coloneqq \left\{ y \in \mathbb{R}^n \,|\, C_i(k)y + \sum_{\substack{j=1 \\ j\neq i}}^{N} C_j(k)x_j(k) \leq c(k) \right\}$$

where $C_j(k) \in \mathbb{R}^{M\times n}$ and $c(k) \in \mathbb{R}^M$ are the time-varying counterparts of the matrices in (3.2).

Similarly, also the set of collective feasible decisions in 3.1 becomes time-varying due to the constraints, hence

$$\boldsymbol{\mathcal{X}}(k) \coloneqq \boldsymbol{\Omega} \cap \left\{ \boldsymbol{x} \in \mathbb{R}^{Nn} | \boldsymbol{C}(k)\boldsymbol{x} \leq c(k) \right\} \tag{3.13}$$

where $\boldsymbol{C}(k) \coloneqq [C_1(k), \dots, C_N(k)] \in \mathbb{R}^{M\times Nn}$ and $\boldsymbol{\Omega} \coloneqq \prod_{i=1}^{N} \Omega_i$.

Next, Standing Assumption 3.1 is restated in a more general form to address the time-dependency of $\boldsymbol{\mathcal{X}}(k)$.

Standing Assumption 3.2. *For all $i \in \mathcal{N}$ and $k \in \mathbb{N}$, the collective feasible decision set $\boldsymbol{\mathcal{X}}(k)$ satisfies Slater's condition.* □

Notice that in the case of static constraints, Standing Assumption 3.2 coincides with Standing Assumption 3.1.

The cost function minimized by the agents does not change in this new setup, therefore Standing Assumption 2.2 remains unchanged. As done in Section 2.3.3, the time-varying communication network is described by a weighted row-stochastic adjacency matrix $A(k)$, and it is assumed to satisfy Assumption 2.5. Therefore, for every $k \in \mathbb{N}$, the resulting weighted digraph is strongly connected with self-loops.

The myopic best response dynamics describing the decision process of the agents for all $k \in \mathbb{N}$ and $i \in \mathcal{N}$ read as

$$x_i(k+1) = \operatorname{argmin}_{y\in\mathcal{X}_i(\boldsymbol{x}_{-i},k)} \; J_i\left(y, \textstyle\sum_{j=1}^{N} a_{i,j}(k)x_j(k)\right) . \tag{3.14}$$

The interaction of the N players, using dynamics (3.14), defines the following noncooperative network game, for all $k \in \mathbb{N}$, as

$$\forall i \in \mathcal{N} : \begin{cases} \operatorname{argmin}_{y\in\mathbb{R}^n} & f_i(y) + \frac{1}{2}\left\| y - \sum_{j=1}^{N} a_{i,j}(k)x_j(k) \right\|^2 \\ \text{s.t.} & y \in \Omega_i \cap \mathcal{X}_i(\boldsymbol{x}_{-i}, k) \,. \end{cases} \tag{3.15}$$

3.3.2 Equilibrium concept and convergence

The idea of equilibrium introduced in Section 3.2, i.e., the GNWE, cannot be directly applied to (3.15). In fact, every variation in the communication network generates a different game, with its own set of GNWE. Therefore, the equilibria in which we are interested in are those invariant to the changes in the communication; they take the name of persistent Generalized Network Equilibrium (p-GNWE).

Definition 3.8 (persistent GNWE)**.** A collective vector $\bar{\boldsymbol{x}} = \text{col}((\bar{x}_i)_{i\in\mathcal{N}})$ is a p-GNWE for the game (3.15), if there exists some $\bar{k} > 0$, such that for all $i \in \mathcal{N}$,

$$\bar{x}_i = \bigcap_{k\geq\bar{k}} \quad \text{argmin}_{y\in\mathcal{X}(\bar{\boldsymbol{x}}_{-i},k)} J_i\left(y, \textstyle\sum_{j=1}^{N} a_{i,j}(k)\bar{x}_j\right). \tag{3.16}$$

□

We have defined both the game and the set of equilibria we are interested in. Let us now elaborate on the convergence properties of the game in (3.15), focusing three examples highlighting different aspects of these dynamics. In Example 3.1 we have shown that the dynamics in (3.14) can fail to converge to an equilibrium point, even in the case of a static communication network, where the existence of a GNWE is guaranteed by [99, Prop. 4]. Next, we show first a case in which the existence of a p-GNWE is not guaranteed and then an example showing that the game in (3.15) converges.

Example 3.2 (Equilibirum existence)**.** Consider a 2-player game without local or coupling constraints and scalar strategies. The communication network can vary between the two graphs described respectively by the adjacency matrices $A_1 = \begin{bmatrix} 1/2 & 1/2 \\ 1/2 & 1/2 \end{bmatrix}$ and $A_2 = \begin{bmatrix} 1/3 & 2/3 \\ 1/3 & 2/3 \end{bmatrix}$. The cost functions of the agents are in the form of (2.1), where the local part is chosen as $\bar{f}_i(x_i) = \frac{1}{2}\|x_i - i\|^2$, for $i \in \{1, 2\}$. For each communication network, there exists only one equilibrium point of the game, i.e., $\boldsymbol{x}_{A_1} = [5/4\,,\ 7/4]^\top$ and $\boldsymbol{x}_{A_2} = [4/3\,,\ 11/6]^\top$, when respectively A_1 or A_2 is adopted. So, the set of p-GNWE of the game is empty, leading the dynamics to oscillate between $\boldsymbol{x}_{A_1}$ and $\boldsymbol{x}_{A_2}$. □

Example 3.3 (Convergence)**.** Once again, consider the 2-player game, where for a player $i \in \{1, 2\}$ the local feasible set is $\Omega_i = [-1, 1]$ and $f_i(x_i) = 0$. The collective feasible decision set is defined as

$$\boldsymbol{\mathcal{X}}(k) \coloneqq \{\boldsymbol{x} \in [-1, 1]^2 \,|\, m(k) \leq x_1 + x_2\}$$

where $m(k) \in [-1, -0.25]$. We choose $A(k)$ satisfying Standing Assumption 2.3 and it is doubly stochastic, for every time instant $k \in \mathbb{N}$. If the strategy profile belongs to the consensus subspace $\mathcal{C}$, both agents achieve the minimum of their cost functions, and therefore all those points are equilibria of the unconstrained game. Furthermore, for the set $\hat{\mathcal{C}} = \{u \in \mathbb{R}^2 \,|\, u = \alpha\mathbf{1}^\top,\ \alpha \in [-0.25, 1]\}$, it always holds that $\hat{\mathcal{C}} \subseteq \mathcal{C} \cap \boldsymbol{\mathcal{X}}$, and hence they are p-GNWE of the game. Assume that at $\bar{k} > 0$, $m(\bar{k}) = -0.25$, then, for all $k > \bar{k}$, the dynamics reduce to $\boldsymbol{x}(k + 1) = A(k)\boldsymbol{x}(k)$, therefore the profile strategy will converge to a point in $\hat{\mathcal{C}}$, i.e., to a p-GNWE of the game. □

3.3.3 Primal-dual characterization

In order to establish convergence for the dynamics in (3.14), we recast them as pseudo-collaborative ones introducing the dual variable $\lambda_i \in \mathbb{R}^M_{\geq 0}$, for each player

$i \in \mathcal{N}$. The equilibrium concept is also adapted to address this change, so we introduce the persistent Extended Network Equilibrium (p-ENWE).

Definition 3.9 (persistent ENWE)**.** The pair $(\overline{\boldsymbol{x}}, \overline{\boldsymbol{\lambda}})$, is a p-ENWE for the game in (3.15) if there exists $\bar{k} > 0$ such that, for every $i \in \mathcal{N}$,

$$\begin{aligned} \overline{x}_i &= \bigcap_{k \geq \bar{k}} \operatorname{argmin}_{y \in \mathbb{R}^n} \; J_i\left(y, \textstyle\sum_{j=1}^N a_{i,j}(k)\overline{x}_j\right) + \overline{\lambda}_i^\top C_i(k) y, \\ \overline{\lambda}_i &= \bigcap_{k \geq \bar{k}} \operatorname{argmin}_{\xi \in \mathbb{R}^M_{\geq 0}} \; -\xi^\top (C(k)\overline{\boldsymbol{x}} - c(k)) \,. \end{aligned} \tag{3.17}$$

□

In order to develop an iterative algorithm seeking p-ENWE of the game, we propose the same semi-decentralized structure introduced in Section 3.2. The central coordinator broadcasts an auxiliary variable $\sigma \in \mathbb{R}^M$ to each agent i, that uses this information to compute its local dual variable as $\lambda_i := \alpha_i(k)\sigma(k)$, where $\alpha_i(k) \in [0, 1]$ is a possibly time-varying factor.

This idea leads to the definition of the persistent normalized Extended Network Equilibrium (pn-ENWE).

Definition 3.10 (persistent normalized-ENWE)**.** The pair $(\overline{\boldsymbol{x}}, \overline{\sigma})$, is a pn-ENWE for the game in (3.15), if it exists $\bar{k} > 0$, such that for all $i \in \mathcal{N}$ it satisfies

$$\begin{aligned} \overline{x}_i &= \bigcap_{k \geq \bar{k}} \operatorname{argmin}_{y \in \mathbb{R}^n} \; J_i\left(y, \textstyle\sum_{j=1}^N a_{i,j}(k)\overline{x}_j\right) + \alpha_i(k)\, \overline{\sigma}^\top C_i(k) y, \\ \overline{\sigma} &= \bigcap_{k \geq \bar{k}} \operatorname{argmin}_{\varsigma \in \mathbb{R}^M_{\geq 0}} \; -\varsigma^\top (\boldsymbol{C}(k)\overline{\boldsymbol{x}} - c(k)), \end{aligned} \tag{3.18}$$

with $\alpha_i(k) > 0$. □

The following lemma shows that a pn-ENWE is also a p-GNWE, and vice versa.

Lemma 3.11 (p-GNWE as fixed point)**.** *The following statements are equivalent:*

(i) $\overline{\boldsymbol{x}}$ *is a p-GNWE for the game in* (3.15)*;*

(ii) $\exists \overline{\sigma} \in \mathbb{R}^M$ *and* $\bar{k} > 0$ *such that* $\operatorname{col}(\overline{\boldsymbol{x}}, \overline{\sigma}) \in \mathcal{E}$*, where* $\mathcal{E}$ *is the set of all the pn-GNWE of the game* (3.15)*.* □

We omit the demonstration of the lemma, since it follows the same steps as that in [99, Lem. 2].

3.3.4 On the existence of persistent equilibria

Next,we elaborate on the problem of the existence of a p-GNWE for the game in (3.15). In general, there is no guarantee that such an equilibrium exists, as shown in Example 3.2. The literature dealing with similar problems is split on how to handle this problem. Namely, two possible solutions are considered to proceed with the analysis. The first one supposes *a priori* the existence of at least one p-GNWE in the game. This assumption does not restrict the original problem, since the convergence can be established only for the cases in which this assumption holds. However, it can be difficult to check if it is satisfied in practice. This approach is the one chosen in this work and it is usually adopted when the focus is more on theoretical results, see [14, Cor. 5.19], [55, Prop. 3.1], [99, Ass. 3] and [43, Ass. 6].

Standing Assumption 3.3 (Existence of a pn-ENWE)**.** *The set of pn-ENWE of* (3.15) *is non-empty, hence* $\mathcal{E} \neq \varnothing$ *.* □

On the other hand, an alternative assumption considers only those games in which the N local cost functions share at least one common fixed point. This implies that at least one point in the consensus subspace is an equilibrium invariant to the change of the communication network. If, at the same time, this point is also feasible, then it is a p-GNWE of the game. This assumption is clearly stronger than the previous one. Nevertheless, it is easier to check in practice, since it only requires the analysis of the cost functions of the agents, as shown in Example 3.3. Mainly for this reason, it is widely spread throughout the literature, where it is either implicitly verified, as in [137], or explicitly required [89, Ass in Th. 2] .

3.3.5 TV-Prox-GNWE and convergence result

We finally present the main result of this chapter, namely an iterative and decentralized algorithm converging to a pn-ENWE of the game in (3.15). We call it TV-Prox-GNWE and it is described by (3.19a)–(3.19d), while its derivation is proposed in the Appendix 3.6.3.

$$\forall i \in \mathcal{N} \,:\, \tilde{x}_i = \operatorname{prox}_{\frac{\delta_i(k)}{\delta_i(k)+1}\bar{f}_i}\left(\tfrac{\delta_i(k)}{\delta_i(k)+1}\left(\tfrac{1}{\delta_i(k)}x_i + \textstyle\sum_{j=1}^{N} a_{i,j}(k)x_j - \alpha_i(k)C_i^\top(k)\sigma\right)\right) \tag{3.19a}$$

$$\tilde{\sigma} = \operatorname{proj}_{\mathbb{R}^M_{\geq 0}}\left(\sigma + \tfrac{1}{\beta(k)}\left(C(k)\boldsymbol{x} - c(k)\right)\right) \tag{3.19b}$$

$$\forall i \in \mathcal{N} \,:\, x_i^+ = x_i + \gamma(k)q_i(k)\Big[\delta_i(k)(\tilde{x}_i - x_i) + \textstyle\sum_{j=1}^{N} a_{i,j}(k)(\tilde{x}_j - x_j) - \alpha_i(k)C_i^\top(k)\left(\tilde{\sigma} - \sigma\right)\Big] \tag{3.19c}$$

$$\sigma^+ = \sigma + \gamma(k)\big[\beta(k)(\tilde{\sigma} - \sigma) + C(k)(\tilde{\boldsymbol{x}} - \boldsymbol{x})\big] \tag{3.19d}$$

In the algorithm several parameters are involved. In the following, we provide the bounds that must be respected during the choice of their values to ensure convergence. Towards this end, let us redefine the matrix $\boldsymbol{A}(k)$ via a diagonal matrix, an upper and a lower triangular matrix, i.e., $\boldsymbol{A}(k) = \boldsymbol{A}_{\mathrm{ut}}(k) + \boldsymbol{A}_{\mathrm{d}}(k) + \boldsymbol{A}_{\mathrm{lt}}(k)$, where $\boldsymbol{A}_{\mathrm{ut}}$ and $\boldsymbol{A}_{\mathrm{lt}}$ always have zeros diagonal elements. For each time instant $k \in \mathbb{N}$, the parameters in TV-Prox-GNWE are selected such that the following inequalities hold:

$$\min_{i\in\mathcal{N}}(\delta_i^{-1} + a_{i,i}) \geq \|\boldsymbol{A} - \boldsymbol{A}_{\mathrm{d}}\| + \|\boldsymbol{C}^\top - \boldsymbol{\Lambda}\boldsymbol{C}^\top\| \tag{3.20a}$$

$$\max_{i\in\mathcal{N}}(2q_i(\delta_i^{-1} + a_{i,i})) < R + \gamma^{-1} \tag{3.20b}$$

$$R \coloneqq 2\|\boldsymbol{Q}\boldsymbol{A}_{\mathrm{ut}} + \boldsymbol{A}_{\mathrm{lt}}\boldsymbol{Q}\| + \|\boldsymbol{Q}(\boldsymbol{C}^\top - \boldsymbol{\Lambda}\boldsymbol{C}^\top)\|$$

$$\beta \geq \tfrac{1}{2}\|\boldsymbol{C} - \boldsymbol{C}\boldsymbol{\Lambda}\| \tag{3.20c}$$

$$\beta < \tfrac{1}{2}\big(\gamma^{-1} - \|\boldsymbol{C} - \boldsymbol{C}\boldsymbol{\Lambda}\|\big) \tag{3.20d}$$

where $\boldsymbol{\Lambda}(k) \coloneqq \mathrm{diag}((\alpha_i(k))_{i\in\mathcal{N}}) \otimes I_n$ and $\boldsymbol{Q}(k) \coloneqq \mathrm{diag}((q_i(k))_{i\in\mathcal{N}}) \otimes I_n$, with q_i being the i-th element of the left PF eigenvector of $A(k)$. Also in this case, we omitted the time dependency of the matrices to ease the notation. The bounds in (3.20c) – (3.20d) implicitly lead to a condition on the maximum value of the step size γ, namely $\gamma \leq \frac{1}{2}\|\boldsymbol{C} - \boldsymbol{C}\boldsymbol{\Lambda}\|^{-1}$.

Similarly to Prox-GNWE, also TV-Prox-GNWE in (3.19), is composed of three main steps: a proximal gradient descend, performed by every agent (3.19a), a dual ascend done by the central coordinator (3.19b) and a correction step, in (3.19c) – (3.19d), that balances the asymmetricity of the weights in the directed network, i.e., $a_{i,j} \neq a_{j,i}$.

The main technical result of the chapter is the following theorem, where we establish global convergence of the sequence generated by the TV-Prox-GNWE to a p-GNWE of the game in (3.15).

Theorem 3.12. *For all $i \in \mathcal{N}$ and $k \in \mathbb{N}$, set $\alpha_i(k) = q_i(k)$, with $q_i(k)$ the i-th element of the left PF eigenvector of $A(k)$, and choose $\delta_i(k)$, $\beta(k)$ and γ satisfying* (3.20)*. Then, for any initial condition, the sequence $(\boldsymbol{x}(k))_{k\in\mathbb{N}}$ generated by* (3.19) *converges to a p-GNWE of the game in* (3.15)*.* □

3.4 Simulations

3.4.1 Distributed model fitting

The following simulation applies Prox-GNWE to solve a problem of distributed model fitting. Namely, we develop a distributed implementation of the LASSO algorithm, previously presented in Section 2.2.

First, we introduce the problem by describing the classical centralized formulation, for a complete description refer to [164]. Consider a large number of data $\tilde{y} \in \mathbb{R}^d$,

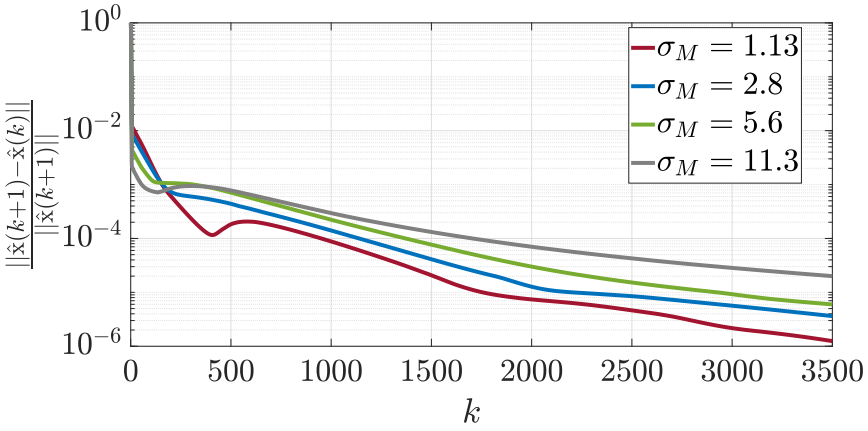

Figure 3.1: Trajectory of $\frac{\|\hat{\boldsymbol{x}}(k+1)-\hat{\boldsymbol{x}}(k)\|}{\|\hat{\boldsymbol{x}}(k+1)\|}$ generated via Prox-GNWE. The different maximum noise variances σ_M adopted identify the different curves.

where $d = 500$, affected by an additive normal Gaussian noise; the true model that generates them is assumed to be linear and in the form $Bx = y$, where $B \in \mathbb{R}^{d\times n}$ is the covariate matrix; $x \in \mathbb{R}^n$ the real parameters of the model, with $n = 6$; and y the model outputs not affected by the noise. Hereafter, the matrix B is assumed to be known. The LASSO algorithm computes the parameters' estimation $\hat{x} \in \mathbb{R}^n$ that minimizes the cost

$$f(\hat{x}) \coloneqq \|B\hat{x} - \tilde{y}\|_2^2 + \|\hat{x}\|_1 .$$

We focus now on the distributed counterpart of the LASSO, already analized in the literature, see [123]. In our setup, we assume $N = 5$ agents, each one measuring a subset $\tilde{y}_i \in \mathbb{R}^{200}$ of $\tilde{y}$, and communicating via a network described by the adjacency matrix $\boldsymbol{A}$, satisfying Standing Assumption 2.3. Accordingly, each agent i knows the local covariate matrix $B_i \in \mathbb{R}^{200\times 6}$ associated to the measurements $\tilde{y}_i \in \mathbb{R}^{200}$. The noise affecting the data set of each agent i, is assumed Gaussian with zero mean and variance σ_i. It models the different precision of each agent in measuring the data. The variance σ_i is randomly drawn between $[0, \sigma_M]$. In the following, we propose simulations for four different values of σ_M, namely 0.5%, 1.25%, 2.5% and 5% of the maximum value of y, i.e., the values of $\sigma_M \coloneqq \{1.13, 2.8, 5.6, 11.3\}$.

The problem ca be rephrased as an instance of the game in (3.3), where, for all agent $i \in \mathcal{N}$, the local cost function is $f_i(\hat{x}_i) \coloneqq \|B_i\hat{x}_i - \tilde{y}_i\|_2^2 + \|\hat{x}_i\|_1$, where $\hat{x}_i$ is the local estimation of the model parameters. On the other hand, let $\hat{\boldsymbol{x}} = \mathrm{col}((\hat{x}_i)_{i\in\mathcal{N}})$, then the aggregative term $\|\hat{x}_i - \boldsymbol{A}\hat{\boldsymbol{x}}\|^2$ leads to a better fit of the model, when the weights in the matrix $\boldsymbol{A}$ are chosen inversely proportional to the noise variance of each agent. To enforce the consensus between all the local estimations $\hat{x}_i$, i.e., $\hat{x}^* \coloneqq \hat{x}_i(\infty)$ for all $i \in \mathcal{N}$, we impose the constraint $\boldsymbol{L}\hat{\boldsymbol{x}} = 0$, where $\boldsymbol{L} \coloneqq L \otimes I_n$ and L is the Laplacian matrix associated to the communication network. The resulting game can be solved via Prox-GNWE, that provides a distributed version of the LASSO algorithm. In particular, it generates a sequence $(\hat{\boldsymbol{x}}(k))_{k\in\mathbb{N}}$ converging asymptotically to a solution of the model fitting problem.

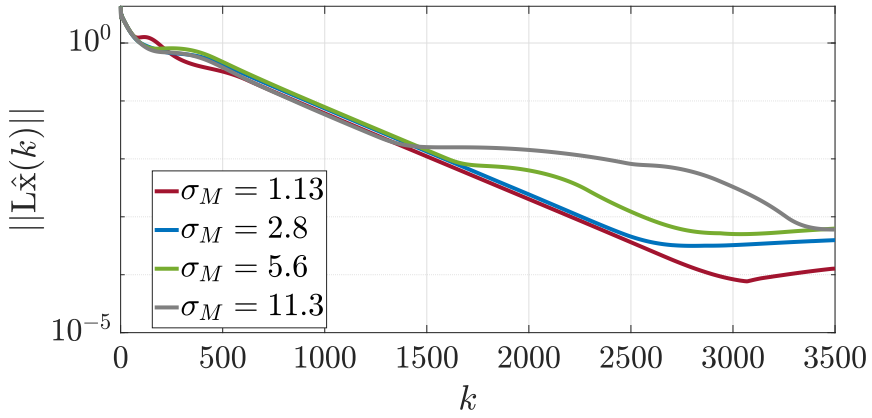

Figure 3.2: Constraint violation $\|\boldsymbol{L}\hat{\boldsymbol{x}}(\boldsymbol{k})\|$ of the collective vector $\hat{\boldsymbol{x}}(k)$ for each iteration k. The different maximum noise variances σ_M adopted identify the different curves.

In Figure 3.1, it is shown the trajectory of $\frac{\|\hat{\boldsymbol{x}}(k+1)-\hat{\boldsymbol{x}}(k)\|}{\|\hat{\boldsymbol{x}}(k+1)\|}$ where $\hat{\boldsymbol{x}}(k)$ is the collective vectors of the parameters estimations obtained via Prox-GNWE at iteration k; this quantity describes the relative variation of the estimations between two iterations of the algorithms. Notice that the sequence converges asymptotically, but, as expected, a greater noise variance σ_M leads to a slower rate of convergence.

The constraint violation, i.e., $\|\boldsymbol{L}\hat{\boldsymbol{x}}(\boldsymbol{k})\|$, at every iteration k of the algorithm are reported in Figure 3.2; the constraints fulfilment is achieved asymptotically. Also in this case, the use of more noisy measurements $\tilde{y}$ leads to a slower asymptotic convergence of the local estimations $\hat{x}_i$ to consensus. Finally, for every iteration

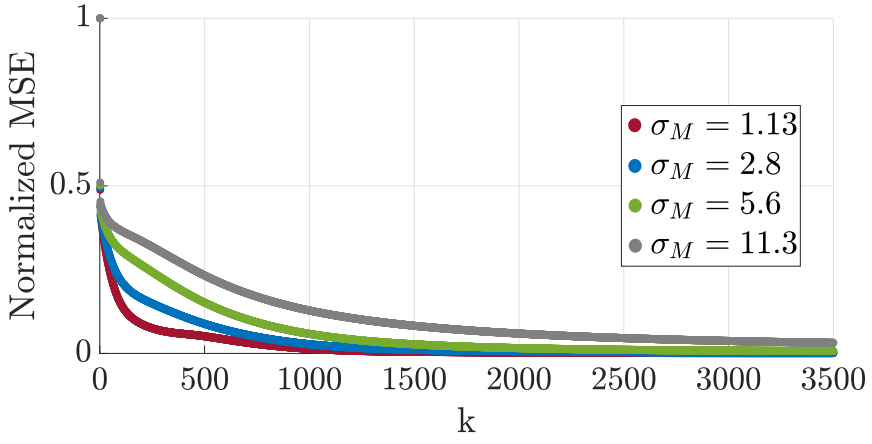

Figure 3.3: Trajectory of the normalized average MSE of the estimated model with respect to the real one, for every iteration $k \in \mathbb{N}$. The different maximum noise variances σ_M adopted identify the different curves.

k, consider the output of the estimated model $\hat{y}_i(k) = B\hat{x}_i(k)$, for all $i \in \mathcal{N}$; the average of the mean squared values (MSE) of all the local estimations is computed as MSE $\coloneqq \frac{1}{N}\sum_{i\in\mathcal{N}}\|\hat{y}_i(k) - y\|^2$. This value can be used as an index of the quality of the estimation. In Figure 3.3, we report the normalized MSE for different values of σ_M. The increment of σ_M causes a slower reduction of the MSE, i.e., a higher number of iterations to achieve a good parameters estimations. On the other hand, if a small noise affects the data, already after 1000 iterations the parameters obtained perform almost as good as the final ones. The study of this curves emphasizes the trade-off between a good parameters' estimation and a fast converging algorithm.

3.4.2 Constrained consensus

Next, we apply TV-Prox-GNWE to solve a constrained consensus problem. We consider a game with $N = 15$ agents, where the strategy of every agent i is $x_i \in \mathbb{R}^5$, and its local feasible decision set is $\Omega_i \in [m_i, M_i]$, with m_i and M_i randomly drawn respectively from $[-100, -5]$ and $[5, 100]$. The local cost function is equal to $f_i(x_i) = \iota_{\Omega_i}(x_i)$. The adjacency matrices, descibing the communication network at every time instant k, are randomly generated and define digraphs of the type small-word, satisfying Standing Assumption 2.3. The coupling constraints are used to force the strategies towards the consensus subspace and are in the form $|x_i(k) - x_j(k)| \leq s(k)\mathbf{1}$, for every $i, j \in \mathcal{N}$, where $s(k) > 0$ and it is decreasing over time. Notice that in this case the *multiplier graph* is complete, see [176]. Finally, the parameters of the algorithm are chosen such that they always satisfy (3.20).

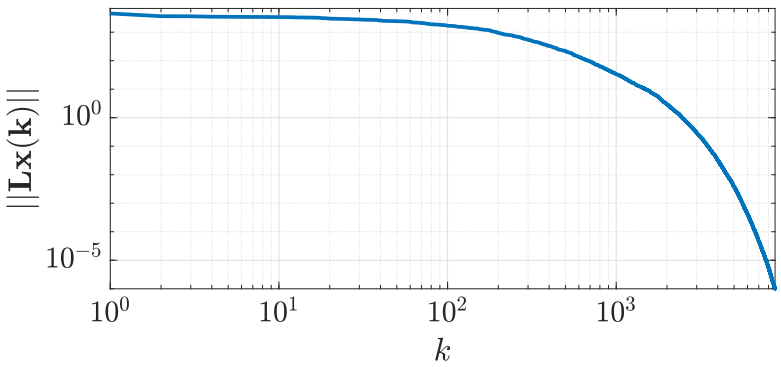

Figure 3.4: Convergence of the strategy profile $\boldsymbol{x}(k)$ to the consensus subspace. The matrix $\boldsymbol{L}$ is the Laplacian matrix associated to the multiplier graph.

The trajectory of the profile strategy generated by TV-Prox-GNWE converges to the consensus subspace, this is shown in Fig. 3.4, by means of the Laplacian matrix $\boldsymbol{L}$ of the multiplier graph. The initial strategy profile $\boldsymbol{x}(0)$ is randomly chosen in $\boldsymbol{\Omega}$. As expected from the result in Theorem 3.12, the constraints are satisfied asymptotically, see Fig. 3.5.

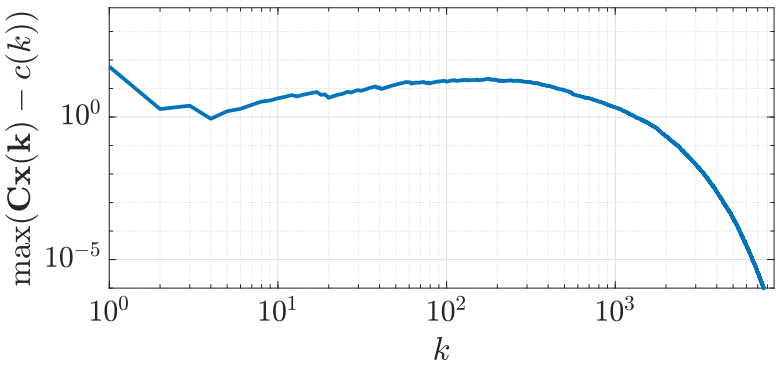

Figure 3.5: Asymptotic satisfaction of the time-varying affine coupling constraints $\boldsymbol{C}\boldsymbol{x}(k) \leq c(k)$.

3.5 Conclusion and outlook

In multi-agent network games, subject to time-varying coupling constraints and time-varying communication networks, described by strongly connected digraphs, agents can fail to converge when they adopt proximal type dynamics. We developed two iterative equilibrium seeking algorithms that ensure the global convergence of the agents' strategies to a normalized (persistent) equilibrium of the game, when it exists. In particular, we discussed the assumptions that are required in order to ensure the existence of an equilibrium point of the game. For the case of static coupling constraints we propose Prox-GNWE, while for the more general case of time-varying constraints and communication networks we designed TV-Prox-GNWE, we apply these algorithms to solve the problem of distributed model fitting and the problem of constraint consensus.

3.6 Appendix

3.6.1 Derivation of Prox-GNWE

Here, we propose the complete derivation of Prox-GNWE. To ease the notation, we define $\boldsymbol{\mathcal{A}} := \boldsymbol{\mathcal{B}} + \mathrm{Id} - \boldsymbol{\mathcal{G}}$, $\boldsymbol{\varpi} := \mathrm{col}(\boldsymbol{x}(k), \sigma(k))$ and $\boldsymbol{\varpi}^+ := \mathrm{col}(\boldsymbol{x}(k+1), \sigma(k+1))$. Consider the following non-symmetric preconditioning matrix

$$\Phi := \begin{bmatrix} \boldsymbol{\delta}^{-1} + \boldsymbol{A} & -\boldsymbol{\Lambda} C^\top \\ C & \beta I_M \end{bmatrix} \tag{3.21}$$

where $\boldsymbol{\delta} := \mathrm{diag}((\delta_i)_{i\in\mathcal{N}}) \otimes I_n$, $\delta_i \in \mathbb{R}_{>0}$ and $\beta \in \mathbb{R}_{>0}$.

The update rule of the modified PPP algorithm [32, Eq. 4.18], reads as

$$\tilde{\boldsymbol{\varpi}} = \mathrm{J}_{\Phi^{-1}\boldsymbol{\mathcal{A}}}\boldsymbol{\varpi} \tag{3.22a}$$

$$\boldsymbol{\varpi}^+ = \boldsymbol{\varpi} + \gamma\Phi(\tilde{\boldsymbol{\varpi}} - \boldsymbol{\varpi}) \tag{3.22b}$$

where $\mathrm{J}_{\Phi^{-1}\boldsymbol{\mathcal{A}}} := \mathrm{J}_{U^{-1}(\boldsymbol{\mathcal{A}}+S)}(\mathrm{Id} + U^{-1}S)$ and $\gamma \in > 0$.

Let us define its *self-adjoint* and *skew symmetric* components as $U := (\Phi + \Phi^\top)/2$ and $S := (\Phi - \Phi^\top)/2$.
We choose the parameters $\boldsymbol{\delta}$ and β to ensure that $U \succ 0$ and $\|U\| \leq \gamma^{-1}$, where γ will be the step-size of the algorithm. This can be done through the *Gerschgorin Circle Theorem* [84, Th. 2]. The resulting bounds are reported in (3.11).

Remark 3.4. *The set of fixed points of the mapping defining the whole update in* (3.22a)–(3.22b)*, coincides with* $\mathrm{zer}(\boldsymbol{\mathcal{A}})$*, [32, Proof of Th. 4.2]* . □

Next, we proceed to compute the explicit formulation of the algorithm. First, we focus on (3.22a) , so

$$\tilde{\boldsymbol{\varpi}} = \mathrm{J}_{U^{-1}(\boldsymbol{\mathcal{A}}+S)}(\mathrm{Id} + U^{-1}S)\boldsymbol{\varpi} \tag{3.23a}$$

$$\tilde{\boldsymbol{\varpi}} + U^{-1}(\boldsymbol{\mathcal{A}} + S)\tilde{\boldsymbol{\varpi}} \ni \boldsymbol{\varpi} + U^{-1}S\boldsymbol{\varpi} \tag{3.23b}$$

$$\mathbf{0} \in U(\tilde{\boldsymbol{\varpi}} - \boldsymbol{\varpi}) + \boldsymbol{\mathcal{A}}\tilde{\boldsymbol{\varpi}} + S(\tilde{\boldsymbol{\varpi}} - \boldsymbol{\varpi}) \tag{3.23c}$$

$$\mathbf{0} \in \Phi(\tilde{\boldsymbol{\varpi}} - \boldsymbol{\varpi}) + \boldsymbol{\mathcal{A}}\tilde{\boldsymbol{\varpi}} \tag{3.23d}$$

Solving the first row block of (3.23d), i.e. $\mathbf{0} \in (\boldsymbol{\delta}^{-1} + \boldsymbol{A})(\tilde{\boldsymbol{x}} - \boldsymbol{x}) - \boldsymbol{\Lambda} C^\top(\tilde{\sigma} - \sigma) + F(\tilde{\boldsymbol{x}}) + \tilde{\boldsymbol{x}} - \boldsymbol{A}\tilde{\boldsymbol{x}} + \boldsymbol{\Lambda} C^\top\tilde{\sigma}$, leads to

$$\begin{aligned} \mathbf{0}_{nN} &\in \boldsymbol{\delta}^{-1}(\tilde{\boldsymbol{x}} - \boldsymbol{x}) - \boldsymbol{A}\boldsymbol{x} + \boldsymbol{\Lambda} C^\top\sigma + F(\tilde{\boldsymbol{x}}) + \tilde{\boldsymbol{x}} \\ \mathbf{0}_{nN} &\in (\boldsymbol{\delta}^{-1} + I)\tilde{\boldsymbol{x}} + F(\tilde{\boldsymbol{x}}) - \boldsymbol{\delta}^{-1}\boldsymbol{x} - \boldsymbol{A}\boldsymbol{x} + \boldsymbol{\Lambda} C^\top\sigma \end{aligned}$$

with a slight abuse of notation let us define $\frac{1}{\boldsymbol{\delta}^{-1}+1} := \mathrm{diag}\left(\left(\frac{1}{\boldsymbol{\delta}_i^{-1}+1}\right)_{i\in\mathcal{N}}\right) \otimes I_n$ then we obtain

$$\begin{aligned} \mathbf{0}_{nN} &\in \tilde{\boldsymbol{x}} + \tfrac{1}{\boldsymbol{\delta}^{-1}+1}F(\tilde{\boldsymbol{x}}) + \tfrac{1}{\boldsymbol{\delta}^{-1}+1}\left[\boldsymbol{\Lambda} C^\top\sigma - \boldsymbol{\delta}^{-1}\boldsymbol{x} - \boldsymbol{A}\boldsymbol{x}\right] \\ \tilde{\boldsymbol{x}} &= \mathrm{J}_{\frac{1}{\boldsymbol{\delta}^{-1}+1}F}\left(\tfrac{1}{\boldsymbol{\delta}^{-1}+1}\left[\boldsymbol{\delta}^{-1}\boldsymbol{x} + \boldsymbol{A}\boldsymbol{x} - \boldsymbol{\Lambda} C^\top\sigma\right]\right) \end{aligned} \tag{3.24}$$

The second row block instead reads as $\mathbf{0} \in C(\tilde{\boldsymbol{x}}-\boldsymbol{x})+\beta(\tilde{\sigma}-\sigma)+N_{\mathbb{R}^M_{\geq 0}}(\tilde{\sigma})+\tilde{\sigma}-C\tilde{\boldsymbol{x}}+c$, and leads to

$$\mathbf{0}_M \in -C\boldsymbol{x} + \beta(\tilde{\sigma} - \sigma) + N_{\mathbb{R}^M_{\geq 0}}(\tilde{\sigma}) + c \tag{3.25a}$$

$$\tilde{\sigma} = \mathrm{J}_{N_{\mathbb{R}^M_{\geq 0}}}\left(\sigma + \tfrac{1}{\beta}(C\boldsymbol{x} - c)\right) \tag{3.25b}$$

The final formulation of Prox-GNWE, presented in (3.10a) – (3.10d), is obtained combining (3.24) and (3.25b) with (3.22b).

3.6.2 Convergence proof of Prox-GNWE

Before proving the global convergence of Prox-GNWE, we first propose an auxiliary lemma.

Lemma 3.13. *Let $\boldsymbol{\Lambda} = \boldsymbol{Q}$ with $\boldsymbol{Q}$ is chosen in accordance with Theorem 2.3. Then the mapping $\mathrm{Id} - \boldsymbol{\mathcal{G}}$ from (3.9) is maximally monotone in $\mathcal{H}_{\overline{\boldsymbol{Q}}}$ where $\overline{\boldsymbol{Q}} = \mathrm{diag}(\boldsymbol{Q}, I_M)$.* □

Proof. The mapping $\mathrm{Id} - \boldsymbol{\mathcal{G}}$ is monotone if and only if $2\overline{\boldsymbol{Q}} - (\boldsymbol{G}^\top\overline{\boldsymbol{Q}} + \overline{\boldsymbol{Q}}\boldsymbol{G}) \succeq 0$ (by [100, Lemma 3]).

$$\begin{aligned} 2\overline{\boldsymbol{Q}} - (\boldsymbol{G}^\top\overline{\boldsymbol{Q}} + \overline{\boldsymbol{Q}}\boldsymbol{G}) &\succeq 0 \\ 2\overline{\boldsymbol{Q}} - \left(\begin{bmatrix} \boldsymbol{A}^\top\boldsymbol{Q} & \boldsymbol{Q}C^\top \\ -C\boldsymbol{Q} & I \end{bmatrix} + \begin{bmatrix} \boldsymbol{Q}\boldsymbol{A} & -\boldsymbol{Q}C^\top \\ \boldsymbol{Q}C & I \end{bmatrix}\right) &\succeq 0 \\ \begin{bmatrix} 2\boldsymbol{Q} - \left(\boldsymbol{A}^\top\boldsymbol{Q} + \boldsymbol{Q}\boldsymbol{A}\right) & 0 \\ 0 & 0 \end{bmatrix} &\succeq 0 \end{aligned} \tag{3.26}$$

The last inequality in (3.26) holds if and only if $\mathrm{Id} - \boldsymbol{A}$ is monotone in $\mathcal{H}_{\boldsymbol{Q}}$. The matrix $\boldsymbol{Q}$ is chosen as in Theorem 2.3, thus $\boldsymbol{A}$ is η-AVG in $\mathcal{H}_{\boldsymbol{Q}}$ with $\eta \in (0, 1-\underline{a})$. From [14, Example 20.7] we conclude that $\mathrm{Id}-\boldsymbol{A}$ is monotone. Therefore, also $\mathrm{Id}-\boldsymbol{\mathcal{G}}$ is monotone. Finally, since we considered a bounded linear operator we conclude the maximally monotonicity of $\mathrm{Id} - \boldsymbol{\mathcal{G}}$ in $\mathcal{H}_{\overline{\boldsymbol{Q}}}$ invoking [14, Example 20.34]. ■

Proof of Theorem 3.7

By Lemma 3.13, we know that $\mathrm{Id} - \boldsymbol{\mathcal{G}}$ is maximally monotone. Using a reasoning similar to the one in the proof if Theorem 2.3, we conclude that $\boldsymbol{\mathcal{R}}$ is firmly nonexpansive in $\mathcal{H}_{\overline{\boldsymbol{Q}}}$. The domain of the operator $\boldsymbol{\mathcal{R}}$ is the entire space, thus applying [15, Prop. 23.8(iii)] we deduce that $\boldsymbol{\mathcal{B}}$ is maximally monotone.
The mapping $\boldsymbol{\mathcal{B}} + \mathrm{Id} - \boldsymbol{\mathcal{G}}$ is the sum of two maximally monotone operators, so [14, Corollary 25.5(i)] ensures the maximal monotonicity of the sum. The step sizes $\boldsymbol{\delta}$ and β are chosen as in (3.11), hence U is positive definite.

Applying [32, Th. 4.2] ensures the convergence of the sequence generated by the update rule (3.22a) – (3.22b) to a point in $\mathrm{zer}(\boldsymbol{\mathcal{B}} + \mathrm{Id} - \boldsymbol{\mathcal{G}})$. The proof is concluded invoking Lemma 3.4 and 3.6. ■

3.6.3 Derivation of TV-Prox-GNWE

Here, we propose the main steps to derive the iterative algorithm TV-Prox-GNWE. The omitted calculations resemble the ones used to attain Prox-GNWE.

Equilibria reformulation

The set of pn-ENWE, defined by the two equalities in (3.18), can be equivalently rephrased as the set of fixed points of a suitable mappings. Similarly to what we have done for the case of a static network, we exploit in the following two operators, namely $\boldsymbol{\mathcal{R}}$, defined in (3.8), and the affine one $\boldsymbol{\mathcal{G}}_k : \mathbb{R}^{nN+M} \to \mathbb{R}^{nN+M}$ defined as

$$\begin{aligned} \boldsymbol{\mathcal{G}}_k(\cdot) &:= \boldsymbol{G} \cdot + \begin{bmatrix} \mathbf{0} \\ c(k) \end{bmatrix} \\ &:= \begin{bmatrix} \boldsymbol{A}(k) & -\boldsymbol{\Lambda}(k)\boldsymbol{C}^\top(k) \\ C(k) & I \end{bmatrix} \cdot - \begin{bmatrix} \mathbf{0} \\ c(k) \end{bmatrix} . \end{aligned} \tag{3.27}$$

In (3.18), the first equality is equivalent to

$$\overline{\boldsymbol{x}} = \bigcap_{k>\bar{k}} \mathbf{prox}_{\boldsymbol{f}}(\boldsymbol{A}(k)\boldsymbol{x} - \boldsymbol{\Lambda}(k)\boldsymbol{C}^\top(k)\overline{\sigma}) ,$$

where $\boldsymbol{A}(k) \coloneqq A(k) \otimes I_n$ and $\boldsymbol{\Lambda}(k) = \mathrm{diag}((\alpha_i(k))_{i\in\mathcal{N}}) \otimes I_n$. The second equality holds true if and only if $\overline{\sigma} = \mathrm{proj}_{\mathbb{R}^M}(\overline{\sigma} + \boldsymbol{C}(k)\overline{\boldsymbol{x}} - c(k))$.

As a result, the dynamics of the game can be cast as

$$\begin{bmatrix} \boldsymbol{x}(k+1) \\ \sigma(k+1) \end{bmatrix} = \boldsymbol{\mathcal{R}} \circ \boldsymbol{\mathcal{G}}_k \left(\begin{bmatrix} \boldsymbol{x}(k) \\ \sigma(k) \end{bmatrix} \right) . \tag{3.28}$$

Once again, we exploit this new compact form to describe the set of pn-ENWE via the fixed points of $\boldsymbol{\mathcal{R}} \circ \boldsymbol{\mathcal{G}}_k$. In particular, by Definiton 3.10, a pair $(\bar{\boldsymbol{x}}, \bar{\sigma})$ is a pn-ENWE of the game in (3.15) if and only if $\mathrm{col}((\bar{\boldsymbol{x}}, \bar{\sigma})) \in \cap_{k>\bar{k}} \mathrm{fix}(\boldsymbol{\mathcal{R}} \circ \boldsymbol{\mathcal{G}}_k)$. Furthermore, from Lemma 3.11, we also know that a pn-ENWE is a p-GNWE of the original game. So, we focus on the design of an algorithm converging to the subset $\mathcal{E}$ for which we can take advantage of this new formulation. First we notice that also in this case the fixed point problem is equivalent to a zero finding one for a suitable operator.

Lemma 3.14 ([14, Prop. 26.1 (iv)])**.** *Let* $\boldsymbol{\mathcal{B}} := F \times N_{\mathbb{R}^M_{\geq 0}}$, *with* $F := \prod_{i=1}^N \partial \bar{f}_i$. *Then,*

$$\mathrm{fix}\,(\boldsymbol{\mathcal{R}} \circ \boldsymbol{\mathcal{G}}_k) = zer\,(\boldsymbol{\mathcal{A}}_k) ,$$

where $\boldsymbol{\mathcal{A}}_k \coloneqq \boldsymbol{\mathcal{B}} + \mathrm{Id} - \boldsymbol{\mathcal{G}}_k$. □

Modified proximal point algorithm

Next, we describe the main steps used to develop the iterative algorithm solving the zero finding problem associated to the operator $\boldsymbol{\mathcal{A}}_k$, and, as a consequence, the original one of finding pn-ENWE of (3.15). The update rule is a preconditioned version of the proximal point algorithm proposed in [32, Eq. 4.18], after defining $\boldsymbol{\varpi} := \mathrm{col}(\boldsymbol{x}(k), \sigma(k))$ and $\boldsymbol{\varpi}^+ := \mathrm{col}(\boldsymbol{x}(k+1), \sigma(k+1))$, it can be rewritten as

$$\tilde{\boldsymbol{\varpi}} = \mathrm{J}_{\Phi^{-1}(k)\boldsymbol{\mathcal{A}}_k}\boldsymbol{\varpi} \tag{3.29a}$$

$$\boldsymbol{\varpi}^+ = \boldsymbol{\varpi} + \gamma(k)\bar{\boldsymbol{Q}}(k)\Phi(k)(\tilde{\boldsymbol{\varpi}} - \boldsymbol{\varpi}) \tag{3.29b}$$

where and $\gamma(k) > 0$ is the step-size of the algorithm and $\bar{\boldsymbol{Q}}(k) := \mathrm{diag}(\boldsymbol{Q}(k), I)$, and $\boldsymbol{Q}(k) := \mathrm{diag}((q_i(k))_{i\in\mathcal{N}}) \otimes I_n$, with q_i being the i-th element of the left PF eigenvector of $A(k)$.

The preconditioning matrix is chosen as

$$\Phi(k) := \begin{bmatrix} \boldsymbol{\delta}^{-1}(k) + \boldsymbol{A}(k) & -\boldsymbol{\Lambda}(k)C(k)^\top \\ C(k) & \beta(k)I_M \end{bmatrix} \tag{3.30}$$

where $\beta(k) \in \mathbb{R}_{>0}$ and $\boldsymbol{\delta}(k) := \mathrm{diag}((\delta_i(k))_{i\in\mathcal{N}}) \otimes I_n$. The *self-adjoint* and *skew symmetric* components are defined as $U(k) := (\Phi(k) + \Phi^\top(k))/2$ and $S(k) := (\Phi(k) - \Phi^\top(k))/2$. Due to the non symmetric preconditioning the resolvent operator takes the form

$$\mathrm{J}_{\Phi^{-1}(k)\boldsymbol{\mathcal{A}}_k} := \mathrm{J}_{U^{-1}(k)(\boldsymbol{\mathcal{A}}_k + S(k))}(\mathrm{Id} + U^{-1}(k)S(k)) \,.$$

The parameters $\boldsymbol{\delta}(k)$ and $\beta(k)$ in the preconditioning have to be chosen such that $U(k) \succ 0$ and $\|\bar{\boldsymbol{Q}}(k)U(k)\| \leq \gamma^{-1}(k)$. The resulting bounds are reported in (3.20).

Using a reasoning akin to the one in [32, Proof of Th. 4.2], one can show that, at every time instant k, the set of fixed points of the mapping describing the update in (3.29a)-(3.29b) coincides with $\mathrm{zer}(\boldsymbol{\mathcal{A}}_k)$.

Finally, we are ready for the complete derivation of the algorithm by explicitly compute the local update rules of the agents and of the central coordinator. We omit the time dependency in the following formulas.

First, we focus on (3.29a) , so

$$\tilde{\boldsymbol{\varpi}} = \mathrm{J}_{U^{-1}(\boldsymbol{\mathcal{A}}+S)}(\mathrm{Id} + U^{-1}S)\boldsymbol{\varpi} \tag{3.31a}$$

$$\mathbf{0} \in \Phi(\tilde{\boldsymbol{\varpi}} - \boldsymbol{\varpi}) + \boldsymbol{\mathcal{A}}\tilde{\boldsymbol{\varpi}} \tag{3.31b}$$

By solving the first row block of (3.31b), i.e. $\mathbf{0} \in (\boldsymbol{\delta}^{-1} + \boldsymbol{A})(\tilde{\boldsymbol{x}} - \boldsymbol{x}) - \boldsymbol{\Lambda}C^\top(\tilde{\sigma} - \sigma) + F(\tilde{\boldsymbol{x}}) + \tilde{\boldsymbol{x}} - \boldsymbol{A}\tilde{\boldsymbol{x}} + \boldsymbol{\Lambda}C^\top\tilde{\sigma}$, we obtain

$$\begin{aligned} \mathbf{0}_{nN} &\in \boldsymbol{\delta}^{-1}(\tilde{\boldsymbol{x}} - \boldsymbol{x}) - \boldsymbol{A}\boldsymbol{x} + \boldsymbol{\Lambda}C^\top\sigma + F(\tilde{\boldsymbol{x}}) + \tilde{\boldsymbol{x}} \\ \mathbf{0}_{nN} &\in (\boldsymbol{\delta}^{-1} + I)\tilde{\boldsymbol{x}} + F(\tilde{\boldsymbol{x}}) - \boldsymbol{\delta}^{-1}\boldsymbol{x} - \boldsymbol{A}\boldsymbol{x} + \boldsymbol{\Lambda}C^\top\sigma \,. \end{aligned}$$

Let us define, with a small abuse of notation, the matrix $\frac{1}{\delta^{-1}+1} \coloneqq \operatorname{diag}\left(\left(\frac{1}{\boldsymbol{\delta}_i^{-1}+1}\right)_{i\in\mathcal{N}}\right)\otimes I_n$, then we attain

$$\begin{aligned}\mathbf{0}_{nN} &\in \tilde{\boldsymbol{x}} + \tfrac{1}{\boldsymbol{\delta}^{-1}+1}F(\tilde{\boldsymbol{x}}) + \tfrac{1}{\boldsymbol{\delta}^{-1}+1}\left[\boldsymbol{\Lambda}C^\top\sigma - \boldsymbol{\delta}^{-1}\boldsymbol{x} - \boldsymbol{A}\boldsymbol{x}\right]\\ \tilde{\boldsymbol{x}} &= \mathrm{J}_{\frac{1}{\boldsymbol{\delta}^{-1}+1}F}\left(\tfrac{1}{\boldsymbol{\delta}^{-1}+1}\left[\boldsymbol{\delta}^{-1}\boldsymbol{x} + \boldsymbol{A}\boldsymbol{x} - \boldsymbol{\Lambda}C^\top\sigma\right]\right)\,. \end{aligned} \tag{3.32}$$

The second row block instead reads as $\mathbf{0} \in C(\tilde{\boldsymbol{x}}-\boldsymbol{x})+\beta(\tilde{\sigma}-\sigma)+N_{\mathbb{R}^M_{\geq 0}}(\tilde{\sigma})+\tilde{\sigma}-C\tilde{\boldsymbol{x}}+c$, and leads to

$$\mathbf{0}_M \in -C\boldsymbol{x} + \beta(\tilde{\sigma}-\sigma) + N_{\mathbb{R}^M_{\geq 0}}(\tilde{\sigma}) + c \tag{3.33a}$$

$$\tilde{\sigma} = \mathrm{J}_{N_{\mathbb{R}^M_{\geq 0}}}\left(\sigma + \tfrac{1}{\beta}(C\boldsymbol{x} - c)\right) \tag{3.33b}$$

Combining (3.32) and (3.33b) together with (3.29b), leads to the final formulation for the TV-Prox-GNWE, its dynamics are shown in (3.19a) – (3.19d).

3.6.4 Convergence proof of TV-Prox-GNWE

In order to simplify the proofs proposed in the following, let us introduce some useful definition that will be adopted thorough the whole section. We define the two scalars L_k and m_k, where the former is the Lipschitz constant of $S(k)$ and the latter is such that $m_k\|x\|^2 < \langle U(k)x, x\rangle$, this also implies that $\|U^{-1}(k)\| \leq m_k^{-1}$. Next, we define the time-varying matrix $K(k) \coloneqq \overline{\boldsymbol{Q}}_k U(k)$ and the scalars $\rho \coloneqq m_k^{-1}L_k$, $q_m \coloneqq \min_i[\overline{\boldsymbol{Q}}_k]_{ii}$ and $M_k \geq \|U(k)\|$. Notice that, without loss of generality, we can always choose the normalized version of the left PF eigenvector $q(k)$ of the matrix $A(k)$, so $\max_i[\overline{\boldsymbol{Q}}_k]_{ii} \leq 1$.

In the following, we also omit the time dependency of the operators when this does not create to ambiguities. The proofs follow similar steps to the ones in [32, Prop.2.1 and 4.2], where the case of a static communication network is considered.

Lemma 3.15. *For all $k \in \mathbb{N}$, consider the time-varying operator*

$$\mathcal{T}_\Phi \coloneqq \mathrm{J}_{\Phi^{-1}\boldsymbol{\mathcal{A}}} + U^{-1}S(\mathrm{J}_{\Phi^{-1}\boldsymbol{\mathcal{A}}} - \mathrm{Id})\,, \tag{3.34}$$

then the following hold:

(i) $\mathcal{T}_\Phi$ is quasi-nonexpansive in the space $\mathcal{H}_K$,

(ii) if $L_k \leq m_k$, then $\operatorname{fix}(\mathcal{T}_\Phi) = \operatorname{zer}(\boldsymbol{\mathcal{A}})$. □

Proof. (i) From the proof of Lemma 3.13, the operator $\boldsymbol{\mathcal{A}} \coloneqq \boldsymbol{\mathcal{B}} + \mathrm{Id} - \boldsymbol{\mathcal{G}}_k$ is maximally monotone in $\mathcal{H}_{\overline{\boldsymbol{Q}}}$ for all $k \in \mathbb{N}$. The operator S is also maximally monotone, since it is a skew-symmetric matrix, [14, Ex. 20.30]. Next, we define the two auxiliary operators $\mathcal{M} = U^{-1}(\boldsymbol{\mathcal{A}} + S)$ and $\mathcal{D} = -U^{-1}S$. It is easy to

see that $\mathcal{A}$ is monotone and $\mathcal{D}$ is monotone and ρ-Lipschitz, , in $\mathcal{H}_K$. From [32, Prop. 2.1 (3)], we obtain that for $\varpi^* \in \mathrm{fix}(\mathcal{T}_\Phi)$ it holds for some $\bar{\gamma} > 0$

$$\|\mathcal{T}_\Phi \varpi - \varpi^*\|_K^2 \leq \|\varpi - \varpi^*\|_K - (1+\rho^2)\|\varpi - x\|_K^2 \tag{3.35}$$

where $x \coloneqq \mathrm{J}_{\mathcal{M}}(\varpi - \mathcal{D}\varpi)$. Hence, we conclude that $\mathcal{T}_\Phi$ is quasi-nonexpansive in $\mathcal{H}_K$.

(ii) If $L_k \leq m_k$, then the result follows directly from [32, Prop. 2.1 (1)], where we considered $A \coloneqq \mathcal{M}$, $B_1 = 0$ and $B_2 \coloneqq \mathcal{D}$. ■

Proof of Theorem 3.12

Consider $\mathcal{T}_\Phi$, as in (3.34), then the following relation always holds

$$\overline{\boldsymbol{Q}} U(\mathrm{Id} - \mathcal{T}_\Phi)(x) = \overline{\boldsymbol{Q}} \Phi(x - \mathrm{J}_{\Phi^{-1}\boldsymbol{\mathcal{A}}}) \,. \tag{3.36}$$

From Lemma 3.15 we know that $\mathcal{T}_\Phi$ is quasi-nonexpansive in $\mathcal{H}_K$, hence $\mathcal{S} \coloneqq (\mathrm{Id} + \mathcal{T}_\Phi)/2$ belongs to the class $\mathfrak{I}$ in $\mathcal{H}_K$, [52, Prop. 2.2(v)]. From [32, Prop. 4.1] and (3.36), we define the operator

$$\begin{aligned} \mathcal{W}_\Phi &\coloneqq \mathrm{Id} - \|K\|^{-1} K(\mathrm{Id} - \mathcal{S}) \\ &= \mathrm{Id} - \frac{1}{2}\|K\|^{-1} K(\mathrm{Id} - \mathcal{T}_\Phi) \,, \end{aligned} \tag{3.37}$$

belonging to $\mathfrak{I}$ in $\mathcal{H}$ and $\mathrm{fix}(\mathcal{W}_\Phi) = \mathrm{fix}(\mathcal{T}_\Phi) = \mathrm{zer}(\boldsymbol{\mathcal{A}})$, where the last equality comes from Lemma 3.15. The update rule in (3.22) can be rewritten as

$$\boldsymbol{\varpi}^+ = \boldsymbol{\varpi} + 2\gamma\|K\|(\mathcal{W}_\Phi \boldsymbol{\varpi} - \boldsymbol{\varpi}) \,, \tag{3.38}$$

where $\gamma\|K\| < 1$ for all k, due to the choice of δ_i and β. Thus, from [52, Th. 4.2(ii) and 4.3], we have that $(\|\boldsymbol{\varpi} - \mathcal{W}_\Phi \boldsymbol{\varpi}\|^2)_{k\in\mathbb{N}}$ is summable and converges in $\mathcal{H}$ to an element $\overline{\boldsymbol{\varpi}} \in \mathcal{E}_c$, hence to a pn-ENWE, if and only if every sequential cluster point of sequence belong to $\mathcal{E}_c$.

Toward this aim, we define $x_\varpi \coloneqq \mathrm{J}_{\Phi^{-1}\boldsymbol{\mathcal{A}}}(\varpi)$ then we prove that $\varpi - x_\varpi \to 0$ and $x_\varpi \to \overline{x}_\varpi \in \mathrm{zer}(\boldsymbol{\mathcal{A}})$, concluding the proof.

First, notice that, due to the choice of the coefficients $\boldsymbol{\delta}$ and β in $\Phi(k)$, it holds

$$\begin{aligned} \|\boldsymbol{\varpi} - \mathcal{T}_\Phi \boldsymbol{\varpi}\|_K^2 &\leq \|K^{-1}\| \|\boldsymbol{\varpi} - \mathcal{T}_\Phi \boldsymbol{\varpi}\|^2 \\ &\leq 4 m_k^{-1} M_k^2 \|\boldsymbol{\varpi} - \mathcal{W}_\Phi \boldsymbol{\varpi}\|^2 \to 0 \,. \end{aligned} \tag{3.39}$$

Let us define $x_\varpi \coloneqq \mathrm{J}_{\bar{\gamma}\mathcal{A}}(\varpi - \bar{\gamma} U^{-1} S \varpi)$, Moreover, from (3.35), it follows

$$\begin{aligned} (1-\rho^2)\|\varpi - x_\varpi\|_K &\leq \|\varpi - \varpi^*\|_K - \|\mathcal{T}_\Phi \varpi - \varpi\|_K \\ &= -\|\mathcal{T}_\Phi \varpi - \varpi\|_K - 2\langle \mathcal{T}_\Phi \varpi - \varpi, \varpi - \varpi^* \rangle_K \\ &\leq -\|\mathcal{T}_\Phi \varpi - \varpi\|_K - 2M_k \|\mathcal{T}_\Phi \varpi - \varpi\|_K \|\varpi - \varpi^*\| \end{aligned}$$

The above inequality leads to

$$(1-\rho^2)m_k q_m\|\varpi - x_\varpi\| \leq -\|\mathcal{T}_\Phi\varpi - \varpi\|_K - 2M_k\|\mathcal{T}_\Phi\varpi - \varpi\|_K\|\varpi - \varpi^*\| \quad (3.40)$$

The sequence $(\|\varpi(k) - \varpi^*\|)_{k\in\mathbb{N}}$ is bounded and from (3.39) and (3.40), we deduce that $\varpi - x_\varpi \to 0$. Notice also that

$$\|\overline{Q}\Phi(\varpi - x_\varpi)\| \leq (M_k + L)\|\varpi - x_\varpi\| \to 0\,.$$

From the definition of x_ϖ, it follows

$$u_k \coloneqq \overline{Q}\Phi(\varpi - x_\varpi) \in \boldsymbol{\mathcal{A}}x_\omega\,.$$

Thus, since $u_k \to 0$, we conclude that $x_\varpi \to \overline{x}_\varpi \in \mathrm{zer}(\boldsymbol{\mathcal{A}})$. ■

4

Asynchronous networked generalized Nash equilibrium seeking

In this chapter, we present three distributed algorithms to solve a class of GNE seeking problems in strongly monotone games. The first one (SD-GENO) is based on synchronous updates of the agents, while the second and the third (AD-GEED and AD-GENO) represent asynchronous solutions that are robust to communication delays. AD-GENO can be seen as a refinement of AD-GEED, since it only requires node auxiliary variables, enhancing the scalability of the algorithm. Our main contribution is to prove convergence to a variational generalized Nash equilibrium (v-GNE) of the game via an operator-theoretic approach. Finally, we apply the algorithms to a network Cournot game and show how different activation sequences and delays affect convergence. We also compare the proposed algorithms to a state-of-the-art algorithm solving a similar problem, and observe that AD-GENO outperforms it.

4.1 Introduction

In modern society, multi-agent network systems arise in several areas, leading to increasing research activities. When self-interested agents interact with each other, one of the best mathematical tools to study the emerging collective behavior is noncooperative game theory over networks. Networked games emerges in several application domains, such as smart grids [65, 46], social networks [99, 43, 95], and distributed robotics [47]. In a game setup, the players (or agents) aim at minimizing a local and private cost function that represents their individual interest, and, at the same time, satisfy local and global constraints, limiting the possible decisions (or strategies/actions). The cost function and constraints of a single player are influenced by the behavior of a fraction of the others, called "neighbors". Thus, each decision is influenced by some local information, which is typically exchanged with the neighbors. One popular notion of solution for these games is the GNE, where no player benefits from unilaterally changing its strategy, see [79].

In [99, 178, 18], e.g., in the algorithms presented in Chapter 3, the authors focused on developing synchronous and distributed equilibrium seeking algorithms for noncooperative games, namely, the case in which all the agents update their strategies at the same time. Even though this assumption is quite common, it may lead to severe limitations in the case of agents with heterogeneous computational capabilities in the game. For example, consider an allocation game between several processors, as in [177], and assume that they are of two types: high and low performances. A synchronous update scheme implies that all the players must complete their current update, before a new one can start. Thus, the low-performance processors create a bottleneck in the overall performance. To overcome this problem, we focus on developing asynchronous update rules. It is known that asynchronicity can speed up the convergence, facilitate the insertion of new agents in the network, and even increase robustness w.r.t. communication faults, see [25] and references therein.

Among the very first works on asynchronous distributed optimization, the one of Bertsekas and Tsitsiklis in [24] stands out. From there onward, several authors elaborated on these ideas and produced novel results for convex optimization [149, 53, 130]. In [177], Yi and Pavel developed an asynchronous algorithm to solve noncooperative generalized games subject to equality coupling constraints. This result was enabled by the framework (ARock), recently introduced by Peng et al. in [147], that provides a wide range of asynchronous variations of the classical fixed point iterative algorithms.

4.1.1 Contributions

In this chapter, we develop an asynchronous algorithm robust to delayed information to solve noncooperative games subject to affine coupling constraints. This work generalizes and extends the current literature on the topic in the following ways.

- We tackle the case of a game subject to inequality coupling constraint (rather than only equality constraint). This drastically broadens the type of problems

that can be solved by the proposed approach. For example, in signal processing [157] and smart grids [65] inequality constraints arise naturally. This generalization would be difficult to achieve extending the results currently available, due to the different control structure considered.

- The algorithms that we develop rely on node variables only, rather than edge variables as in [177]. This, apparently subtle, difference leads to a solution that adopts (almost always) a lower number of variables. So, it is lighter from a computational point of view, requires less memory and involves lighter communication between agents. All these features make the proposed solution achieve overall better performances than [177].

We conclude the chapter comparing the proposed algorithms to that in [177], for the case of a Cournot game, showing that our algorithms achieve faster convergence. All the proofs are reported at the end of the chapter in Appendix 4.8.

4.2 Problem formulation

4.2.1 Mathematical formulation

As a first step, we introduce formally the class of games on which our analysis focuses. As done in Chapters 2 and 3, we consider a noncooperative game Γ between N agents (or players) subject to affine coupling constraints. We define the game as the triplet $\Gamma := (\boldsymbol{\mathcal{X}}, \{f_i\}_{i\in\{1\dots N\}}, \mathcal{G})$, where its elements are respectively: the collective feasible decision set, the players' local cost functions and the graph describing the communication network. In the following subsections, each one of them is introduced.

Feasible strategy set

Every agent $i \in \mathcal{N} := \{1, \dots, N\}$ has a local decision variable (or strategy) x_i belonging to its private decision set $\Omega_i \subset \mathbb{R}^{n_i}$, namely the set of all those strategies that satisfy the local constraints of player i. The collective vector of all the strategies, or strategy profile of the game, is denoted as $\boldsymbol{x} := \text{col}(x_1, \dots, x_N) \in \mathbb{R}^n$, where $n := \sum_{i\in\mathcal{N}} n_i$. Then, all the decision variables of all the players other than i are represented via the compact notation $\boldsymbol{x}_{-i} := \text{col}(x_1, \dots, x_{i-1}, x_{i+1}, \dots, x_N)$. We assume that the agents are subject to m affine coupling constraints described by the affine function $\boldsymbol{x} \mapsto A\boldsymbol{x} + b$, where $A \in \mathbb{R}^{m\times n}$ and $b \in \mathbb{R}^m$. Thus, the collective feasible decision set can be written as

$$\boldsymbol{\mathcal{X}} := \boldsymbol{\Omega} \cap \{\boldsymbol{x} \in \mathbb{R}^n \mid A\boldsymbol{x} \leq b\} \ , \tag{4.1}$$

where $\boldsymbol{\Omega} = \prod_{i\in\mathcal{N}} \Omega_i \subset \mathbb{R}^n$, is the Cartesian product of the local constraints sets Ω_i's. Accordingly, the set of all the feasible strategies of each agent $i \in \mathcal{N}$ reads as

$$\mathcal{X}_i(\boldsymbol{x}_{-i}) := \left\{ y \in \Omega_i \mid A_i y - b_i \leq \textstyle\sum_{j\in\mathcal{N}\setminus\{i\}} (b_j - A_j x_j) \right\} ,$$

where $A = [A_1, \dots, A_N]$, $A_i \in \mathbb{R}^{m \times n_i}$ and $\sum_{j=1}^{N} b_j = b$. The choice of affine coupling constraints is widely spread in the literature of noncooperative games, see e.g., [178, 138, 43]. Moreover, in [99, Remark 3], it is highlighted that separable and convex coupling constraints can always be rewritten in an affine form. Finally, we introduce some blanket assumptions on this set of feasible strategy, standard in the literature [43, 79, 178, 177, 42].

Standing Assumption 4.1 (Convex constraint sets)**.** *For each player $i \in \mathcal{N}$, the set Ω_i is convex, nonempty and compact. The collective feasible set $\boldsymbol{\mathcal{X}}$ satisfies Slater's constraint qualification.* □

Cost functions

Each player $i \in \mathcal{N}$ has a local cost function $f_i(x_i, \boldsymbol{x}_{-i}) : \Omega_i \times \boldsymbol{\Omega}_{-i} \to \mathbb{R}$, where $\boldsymbol{\Omega}_{-i} \coloneqq \prod_{j \in \mathcal{N} \setminus \{i\}} \Omega_j$. The coupling between the players appears not only in the constraints but also in the cost function, due to the dependency on both x_i and $\boldsymbol{x}_{-i}$. Next, we assume some properties for these functions that are extensively used in the literature [79, 178].

Standing Assumption 4.2 (Convex and differentiable cost functions)**.** *For all $i \in \mathcal{N}$, the cost function $f_i(x_i, \boldsymbol{x}_{-i})$ is continuously differentiable and convex in x_i.* □

Communication network

The communication between agents is described by an *undirected and connected* graph $\mathcal{G} = (\mathcal{N}, \mathcal{E})$ where $\mathcal{E} \subseteq \mathcal{N} \times \mathcal{N}$ is the set of edges, as described in Appendix B, as well as the sets $\mathcal{E}_i^{\text{out}}$ and $\mathcal{E}_i^{\text{in}}$ for every $i \in \mathcal{N}$. The number of edges in the graph is denoted by $E \coloneqq |\mathcal{E}|$ and the the *incidence matrix* $V \in \mathbb{R}^{E \times N}$ is as in Definition B.8. The matrix L is the Laplacian matrix of $\mathcal{G}$ and, from [94, Lem. 8.3.2], it holds that $L \coloneqq V^\top V$.

4.2.2 Generalized Nash equilibrium

In summary, the considered generalized game is described by the following set of inter-dependent optimization problems:

$$\forall i \in \mathcal{N} \; : \; \begin{cases} \operatorname{argmin}_{y \in \mathbb{R}^{n_i}} & f_i(y, \boldsymbol{x}_{-i}) \\ \text{s.t.} & y \in \mathcal{X}_i(\boldsymbol{x}_{-i}) \, . \end{cases} \tag{4.2}$$

The most popular equilibrium concept considered for noncooperative games with coupling constraints is the GNE, thus the configuration in which all the relations in (4.2) simultaneously hold.

Definition 4.1 (Generalized Nash Equilibrium)**.** A collective strategy $\boldsymbol{x}^* \in \boldsymbol{\mathcal{X}}$ is a GNE if, for each player i, it holds

$$f_i(x_i^*, \boldsymbol{x}_{-i}^*) \leq \inf\{\, f_i(y, \boldsymbol{x}_{-i}^*) \mid y \in \mathcal{X}_i(\boldsymbol{x}_{-i}^*) \,\}\,.$$

□

In this work, we focus on a subset of GNE, the so called variational GNE (v-GNE), a class of equilibria that is considered in many other works throughout the literature – see [79, 18, 111, 112]. The name of these equilibria derives from the fact that they can be formulated as the solutions to a *variational inequality* (VI). An important property of these equilibria is that each agent faces the same penalty to fulfill the coupling constraints, which is particularly useful to represent a "fair" competition between agents [79]. Variational GNE can be seen as a particular case of the concept of *normalized equilibrium points*, already introduced in Chapter 3.

To properly characterize this set, we define the *pseudo-gradient* mapping (or game mapping) of (4.2), as

$$F(\boldsymbol{x}) = \operatorname{col}\left((\nabla_{x_i} f_i(x_i, \boldsymbol{x}_{-i}))_{i\in\mathcal{N}}\right)\,. \tag{4.3}$$

The pseudo-gradient gathers in a collective vector form the gradients of the cost functions each w.r.t. the local decision variable. Next, recalling the concepts introduced in Definion A.5, we introduce some standard technical assumptions, e.g., [67, 17].

Standing Assumption 4.3. *The mapping F in* (4.3) *is α-strongly monotone and ℓ-Lipschitz continuous, for some $\alpha, \ell > 0$.* □

When Standing assumption 4.2 holds true, the mapping F is single valued and the set of v-GNE of the game in (4.2) corresponds to the solution of $\mathrm{VI}(F, \boldsymbol{\mathcal{X}})$, namely the problem of finding a vector $\boldsymbol{x}^* \in \boldsymbol{\mathcal{X}}$ such that

$$\langle F(\boldsymbol{x}^*), \boldsymbol{x} - \boldsymbol{x}^* \rangle \geq 0\,, \quad \forall \boldsymbol{x} \in \boldsymbol{\mathcal{X}}\,. \tag{4.4}$$

The continuity of F (Assumption 4.2) and compactness of $\boldsymbol{\mathcal{X}}$ (Assumption 4.1) imply the existence of a solution to $\mathrm{VI}(F, \boldsymbol{\mathcal{X}})$, while the strong monotonicity (Assumption 4.3) entails uniqueness, see [80, Th. 2.3.3]. The properties of the cost function assumed above constitute the main differences w.r.t. the setup introduced in Chpater 3.

Next, let us define the KKT conditions associated to the game in (4.2). The strong duality of the problem (Assumptions 4.1, 4.2) implies that, if $\boldsymbol{x}^*$ is a GNE of (4.2), then there exist N dual variables $\lambda_i^* \in \mathbb{R}^m_{\geq 0}$, for all $i \in \mathcal{N}$, such that the following inclusions are satisfied:

$$\forall i \in \mathcal{N} : \begin{cases} \mathbf{0} \in \nabla_{x_i} f_i(x_i^*, x_{-i}^*) + A_i^\top \lambda_i^* + N_{\Omega_i}(x_i^*)\,, \\ \mathbf{0} \in b - A\boldsymbol{x}^* + N_{\mathbb{R}^m_{\geq 0}}(\lambda_i^*)\,. \end{cases} \tag{4.5}$$

Instead of looking for the solution of the general case where $\lambda_1^*, \ldots, \lambda_N^*$ may be different, we examine the special case when $\lambda^* \coloneqq \lambda_1^* = \cdots = \lambda_N^*$, namely

$$\forall i \in \mathcal{N} : \begin{cases} \mathbf{0} \in \nabla_{x_i} f_i(x_i^*, x_{-i}^*) + A_i^\top \lambda^* + N_{\Omega_i}(x_i^*)\,, \\ \mathbf{0} \in b - A\boldsymbol{x}^* + N_{\mathbb{R}^m_{\geq 0}}(\lambda^*)\,. \end{cases} \tag{4.6}$$

It follows from [78, Th. 3.1(ii)], that the KKT inclusions in (4.6) correspond to the solution set to VI$(F, \boldsymbol{\mathcal{X}})$. Thus, every solution $\boldsymbol{x}^*$ to VI$(F, \boldsymbol{\mathcal{X}})$ is also a GNE of the game in (4.2), [78, Th. 3.1(i)]. Since the solution set to VI$(F, \boldsymbol{\mathcal{X}})$ is a singleton, we conclude that there exists a unique v-GNE of the game (4.2).

4.3 Synchronous distributed GNE seeking algorithm

We first introduce the synchronous counterpart of AD-GENO, i.e., the *Synchronous Distributed GNE Seeking Algorithm with Node variables* (SD-GENO). The derivation of the algorithm is based on an operator splitting approach to solve the KKT system in (4.6). A similar approach was also adopted in [178, 18] in the contest of GNE finding problems.

4.3.1 Algorithm design

The KKT conditions of each agent i in (4.5) are satisfied by a couple (x_i, λ_i), where the dual variables λ_i may be different among the players. If we enforce the consensus among the dual variables, then the unique solution of the inclusions is the v-GNE of the game. This is achieved by exploiting the fact that $\ker(V) = \operatorname{span}(\mathbf{1})$ and introducing the auxiliary variables σ_l, $l \in \{1, \dots, E\}$, one for every edge in the graph. Using the notations $\boldsymbol{\lambda} \coloneqq \operatorname{col}((\lambda_i)_{i\in\mathcal{N}}) \in \mathbb{R}^{mN}$, $\Lambda \coloneqq \operatorname{diag}((A_i)_{i\in\mathcal{N}}) \in \mathbb{R}^{mN\times n}$, $\bar{b} \coloneqq \operatorname{col}((b_i)_{i\in\mathcal{N}}) \in \mathbb{R}^{mN}$, $\boldsymbol{\sigma} \coloneqq \operatorname{col}((\sigma_l)_{l\in\{1\dots E\}}) \in \mathbb{R}^{mE}$, $\boldsymbol{V} \coloneqq V \otimes I_m \in \mathbb{R}^{mE\times mN}$ and $\boldsymbol{L} \coloneqq L \otimes I_m \in \mathbb{R}^{mE\times mN}$, we cast the augmented version of the inclusions in (4.5) by

$$\begin{aligned} &\mathbf{0} \in F(\boldsymbol{x}) + \Lambda^\top \boldsymbol{\lambda} + N_{\boldsymbol{\Omega}}(\boldsymbol{x}) \\ &\mathbf{0} \in \bar{b} - \Lambda \boldsymbol{x} + N_{\mathbb{R}^{mN}_{\geq 0}}(\boldsymbol{\lambda}) + \boldsymbol{L}\boldsymbol{\lambda} + \rho \boldsymbol{V}^\top \boldsymbol{\sigma} \\ &\mathbf{0} = -\rho \boldsymbol{V} \boldsymbol{\lambda}\,, \end{aligned} \tag{4.7}$$

where $\rho \in \mathbb{R}_{>0}$. In (4.7), the term $\boldsymbol{L}\boldsymbol{\lambda}$ accelerates the convergence of the dual variables to consensus.

A solution $\varpi = \operatorname{col}(\boldsymbol{x}^*, \boldsymbol{\sigma}^*, \boldsymbol{\lambda}^*)$ of the above inclusions can be equivalently recast as a zero of the sum of two mappings $\mathcal{A}$ and $\mathcal{B}$ defined as

$$\begin{aligned} \mathcal{A} : \varpi \mapsto &\begin{bmatrix} 0 & 0 & \Lambda^\top \\ 0 & 0 & -\rho \boldsymbol{V} \\ -\Lambda & \rho \boldsymbol{V}^\top & 0 \end{bmatrix} \varpi + \begin{bmatrix} N_{\boldsymbol{\Omega}}(\boldsymbol{x}) \\ 0 \\ N_{\mathbb{R}^{mN}_{\geq 0}}(\boldsymbol{\lambda}) \end{bmatrix} \\ \mathcal{B} : \varpi \mapsto &\begin{bmatrix} F(\boldsymbol{x}) \\ 0 \\ \bar{b} + \boldsymbol{L}\boldsymbol{\lambda} \end{bmatrix}. \end{aligned} \tag{4.8}$$

In fact, $\varpi^* \in \operatorname{zer}(\mathcal{A}+\mathcal{B})$ if and only if ϖ^* satisfies (4.7).

Next, we show that the zeros of $\mathcal{A}+\mathcal{B}$ characterize the v-GNE of the original game.

Proposition 4.2. *Let $\mathcal{A}$ and $\mathcal{B}$ be as in* (4.8)*. Then, the following holds:*

(i) $\operatorname{zer}(\mathcal{A}+\mathcal{B}) \neq \varnothing$,

(ii) if $\operatorname{col}(\boldsymbol{x}^*, \boldsymbol{\sigma}^*, \boldsymbol{\lambda}^*) \in \operatorname{zer}(\mathcal{A}+\mathcal{B})$ *then* $(\boldsymbol{x}^*, \boldsymbol{\lambda}^*)$ *satisfies the KKT conditions in* (4.5)*, with* $\lambda_1^* = \cdots = \lambda_N^*$*, hence* $\boldsymbol{x}^*$ *is the unique v-GNE of the game in* (4.2)*.* □

The proof is attained by exploiting the property that $\ker(V) = \ker(L)$, for the graph described in Section 4.2.1. The steps are similar to those in [178, Th. 2].

Several researchers have analyzed the problem of finding a zero of the sum of two monotone operators. In Appendix A we introduce the so called *splitting methods* that are one of the most popular approaches to derive an iterative algorithm solving this class of problem – see [69], [14, Ch. 26].

Lemma 4.3. *The mappings $\mathcal{A}$ and $\mathcal{B}$ in* (4.8) *are maximally monotone. Moreover, $\mathcal{B}$ is χ-cocoercive, where* $\chi \coloneqq \min\left\{\frac{\alpha}{\ell^2}, \lambda_{\max}(L)^{-1}\right\}$. □

The properties of the operators proved above drive us to select the pFB to derive a distributed and iterative algorithm seeking $\operatorname{zer}(\mathcal{A}+\mathcal{B})$. This approach was previously adopted by other researchers, e.g., [178].

The FB splitting operator reads as

$$T \coloneqq \mathrm{J}_{\Phi^{-1}\mathcal{A}} \circ (\mathrm{Id} - \Phi^{-1}\mathcal{B}) \,. \tag{4.9}$$

The so-called preconditioning matrix Φ is defined by

$$\Phi := \begin{bmatrix} \boldsymbol{\tau}^{-1} & 0 & -\Lambda^\top \\ 0 & \delta^{-1} I_{mM} & \rho \boldsymbol{V} \\ -\Lambda & \rho \boldsymbol{V}^\top & \boldsymbol{\varepsilon}^{-1} \end{bmatrix} \tag{4.10}$$

where $\delta \in \mathbb{R}_{>0}$, $\boldsymbol{\varepsilon} = \operatorname{diag}((\varepsilon_i)_{i\in\mathcal{N}}) \otimes I_m$ with $\varepsilon_i > 0$, for all $i \in \mathcal{N}$ and $\boldsymbol{\tau}$ is defined in a similar way.

The update rule of the algorithm is obtained by including a relaxation step, i.e.,

$$\begin{aligned} \tilde{\varpi}(k) &= T\varpi(k) \\ \varpi(k+1) &= \varpi(k) + \eta(\tilde{\varpi}(k) - \varpi(k)) \,. \end{aligned} \tag{4.11}$$

It comes from (4.9) that $\operatorname{fix}(T) = \operatorname{zer}(\mathcal{A}+\mathcal{B})$, in fact $\varpi \in \operatorname{fix}(T) \Leftrightarrow \varpi \in T\varpi \Leftrightarrow 0 \in \Phi^{-1}(\mathcal{A}+\mathcal{B})\varpi \Leftrightarrow \varpi \in \operatorname{zer}(\mathcal{A}+\mathcal{B})$, see [14, Th. 26.14].

In the remainder of this section, we provide the complete derivation of SD-GENO, obtained directly from (4.11). In the following, we denote $\varpi \coloneqq \varpi(k)$, $\varpi^+ \coloneqq$

$\varpi(k+1)$ and $\tilde{\varpi} \coloneqq \tilde{\varpi}(k)$ to simplify the notation. Consider $\tilde{\varpi} = T\varpi$. From (4.9) it holds that $\tilde{\varpi} = \mathrm{J}_{\Phi^{-1}\mathcal{A}} \circ (\mathrm{Id} - \Phi^{-1}\mathcal{B})\varpi \Leftrightarrow \Phi(\varpi - \tilde{\varpi}) \in \mathcal{A}\tilde{\varpi} + \mathcal{B}\varpi$, thus

$$\mathbf{0} \in \mathcal{A}\tilde{\varpi} + \mathcal{B}\varpi + \Phi(\tilde{\varpi} - \varpi)\,. \tag{4.12}$$

The update rule of each components of ϖ is attained by analyzing the row blocks of (4.12). The first reads as $\mathbf{0} \in F(\boldsymbol{x}) + N_{\boldsymbol{\Omega}}(\tilde{\boldsymbol{x}}) + \boldsymbol{\tau}^{-1}(\tilde{\boldsymbol{x}} - \boldsymbol{x}) + \Lambda^\top \boldsymbol{\lambda}$. By solving this inclusion by $\tilde{\boldsymbol{x}}$, we attain the update rule for the primal variables:

$$\tilde{\boldsymbol{x}} = \mathrm{J}_{N_{\boldsymbol{\Omega}}} \circ \big(\boldsymbol{x} - \boldsymbol{\tau}(F(\boldsymbol{x}) + \Lambda^\top \boldsymbol{\lambda})\big)\,. \tag{4.13}$$

Similarly, from the second row block of (4.12), we attain the update for $\tilde{\boldsymbol{\sigma}}$, i.e.,

$$\tilde{\boldsymbol{\sigma}} = \boldsymbol{\sigma} + \delta\rho \boldsymbol{V}\boldsymbol{\lambda}\,. \tag{4.14}$$

Finally, the third row block of (4.12) is $\mathbf{0} \in \bar{b} + \boldsymbol{L}\boldsymbol{\lambda} + N_{\mathbb{R}^{mN}_{\geq 0}}(\tilde{\boldsymbol{\lambda}}) + \Lambda(2\tilde{\boldsymbol{x}} - \boldsymbol{x}) + \rho \boldsymbol{V}^\top(2\tilde{\boldsymbol{\sigma}} - \boldsymbol{\sigma}) + \boldsymbol{\varepsilon}^{-1}(\tilde{\boldsymbol{\lambda}} - \boldsymbol{\lambda})$, from which we obtain

$$\begin{aligned}\tilde{\boldsymbol{\lambda}} &= \mathrm{J}_{N_{\mathbb{R}^{mN}_{\geq 0}}} \circ \big(\boldsymbol{\lambda} + \boldsymbol{\varepsilon}(\Lambda(2\tilde{\boldsymbol{x}} - \boldsymbol{x}) - \bar{b} - \rho \boldsymbol{V}^\top(2\tilde{\boldsymbol{\sigma}} - \boldsymbol{\sigma}) - \boldsymbol{L}\boldsymbol{\lambda})\big) \\ &\overset{(4.14)}{=} \mathrm{proj}_{\mathbb{R}^{mN}_{\geq 0}}\big(\boldsymbol{\lambda} + \boldsymbol{\varepsilon}(\Lambda(2\tilde{\boldsymbol{x}} - \boldsymbol{x}) - \bar{b} \\ &\qquad - \rho \boldsymbol{V}^\top \boldsymbol{\sigma} - (2\delta\rho^2 + 1)\boldsymbol{L}\boldsymbol{\lambda})\big)\,.\end{aligned} \tag{4.15}$$

Note that, the update of $\tilde{\boldsymbol{\lambda}}$ depends only on the aggregate information $\boldsymbol{V}^\top \boldsymbol{\sigma}$. We can exploit this feature to replace the edge auxiliary variables σ_l's, with a single variable for each agent i defined by $z_i \coloneqq \big([V^\top]_i \otimes I_m\big)\boldsymbol{\sigma} \in \mathbb{R}^{mN}$. Recalling that $\boldsymbol{V}^\top \boldsymbol{V} = L \otimes I_m =: \boldsymbol{L}$, we compute the update rule of these new variables and replace (4.14) by

$$\tilde{\boldsymbol{z}} = \boldsymbol{V}^\top \boldsymbol{\sigma} + \delta\rho \boldsymbol{V}^\top \boldsymbol{V}\boldsymbol{\lambda} = \boldsymbol{z} + \delta\rho \boldsymbol{L}\boldsymbol{\lambda}\,. \tag{4.16}$$

Consequently, (4.15) is modified accordingly as

$$\begin{aligned}\tilde{\boldsymbol{\lambda}} = \mathrm{proj}_{\mathbb{R}^{mN}_{\geq 0}}\big(&\boldsymbol{\lambda} + \boldsymbol{\varepsilon}(\Lambda(2\tilde{\boldsymbol{x}} - \boldsymbol{x}) - \bar{b} \\ &- \rho \boldsymbol{z} - (2\delta\rho^2 + 1)\boldsymbol{L}\boldsymbol{\lambda})\big)\,.\end{aligned} \tag{4.17}$$

To ensure that this change of variables does not affect the equilibrium of the game, we introduce the following result proving that an equilibrium point of the new set of equations is indeed a v-GNE of (4.2).

Theorem 4.4. *If* $\mathrm{col}(\boldsymbol{x}^*, \boldsymbol{z}^*, \boldsymbol{\lambda}^*)$ *is a solution to the equations* (4.13), (4.16), (4.17), *with* $\mathbf{1}^\top \boldsymbol{z}^* = 0$, *then* $\boldsymbol{x}^*$ *is a v-GNE of the game in* (4.2). □

Remark 4.1. *In [177], the algorithm SYDNEY achieves convergence to the v-GNE of the game* (4.2), *when this is subject to equality coupling constraints only. This solution relies on edge auxiliary variables to enforce the consensus of the* λ_i*'s.*

Algorithm 4.1: SD-GENO

Input: $k = 0$, for all $i \in \mathcal{N}$, $x_i(0) \in \mathbb{R}^{n_i}$, $\lambda_i(0) \in \mathbb{R}^m$, $z_i(0) = \mathbf{0}_m$.
Choose δ, ε_i, τ_i satisfying (4.19), while $\eta \in (0, 1)$ and $\rho \in (0, 1]$.

Iteration k until convergence

// communication with neighbors
each $i \in \mathcal{N}$ gathers $\lambda_j(k)$ from the neighbors and updates the disagreement vector $d_i(k) \coloneqq \sum_{j \in \mathcal{N}_i} (\lambda_i - \lambda_j)$

// local update
for $i \in \mathcal{N}$ **do**

$$\tilde{x}_i = \mathrm{proj}_{\Omega_i}\big(x_i - \tau_i(\nabla_i f_i(x_i, \boldsymbol{x}_{-i}) + A_i^\top \lambda_i)\big)$$
$$\tilde{z}_i = z_i + \rho\,\delta\, d_i(k)$$
$$\tilde{\lambda}_i = \mathrm{proj}_{\mathbb{R}^m_{\geq 0}}\big(\lambda_i + \varepsilon_i\,\big(A_i(2\tilde{x}_i - x_i) - b_i - \rho z_i - (2\delta\rho^2 + 1)d_i(k)\big)\,\big)$$
$$x_i^+ = x_i + \eta(\tilde{x}_i - x_i)$$
$$z_i^+ = z_i + \eta(\tilde{z}_i - z_i)$$
$$\lambda_i^+ = \lambda_i + \eta(\tilde{\lambda}_i - \lambda_i)$$

$k \leftarrow k + 1$

Therefore, the number of variables that each agent must store is $\mathcal{O}(N)$.
The change of "variables", from $\boldsymbol{\sigma}$ to $\boldsymbol{z}$, is convenient when the edges outnumber the nodes, which is almost always the case. A lower number of variables leads to an overall increment in the algorithmic efficiency and to a fixed memory requirement for each player that does not increase with N. Furthermore, if SYDNEY in [177] is modified to address inequality constraints, it would require an additional round of communication between the agents, making it more demanding and slower than SD-GENO. □

4.3.2 Synchronous, distributed algorithm with node variables (SD-GENO)

The complete formulation of the algorithm is obtained by gathering together all the update rules introduced in the previous section, i.e., (4.13), (4.16), (4.17) and adding a relaxation step. The algorithm in compact form is expressed as

$$\begin{cases} \tilde{\boldsymbol{x}} = \mathrm{proj}_{\boldsymbol{\Omega}}\big(\boldsymbol{x} - \boldsymbol{\tau}(F(\boldsymbol{x}) + \Lambda^\top \boldsymbol{\lambda})\big) \\ \tilde{\boldsymbol{z}} = \boldsymbol{z} + \rho\delta \boldsymbol{L}\boldsymbol{\lambda} \\ \tilde{\boldsymbol{\lambda}} = \mathrm{proj}_{\mathbb{R}^{mN}_{\geq 0}}\big(\boldsymbol{\lambda} + \boldsymbol{\varepsilon}(\Lambda(2\tilde{\boldsymbol{x}} - \boldsymbol{x}) - \bar{b} \\ \qquad\qquad -\rho\boldsymbol{z} - (2\delta\rho^2 + 1)\boldsymbol{L}\boldsymbol{\lambda})\big) \\ \boldsymbol{x}^+ = \boldsymbol{x} + \eta(\tilde{\boldsymbol{x}} - \boldsymbol{x}) \\ \boldsymbol{z}^+ = \boldsymbol{z} + \eta(\tilde{\boldsymbol{z}} - \boldsymbol{z}) \\ \boldsymbol{\lambda}^+ = \boldsymbol{\lambda} + \eta(\tilde{\boldsymbol{\lambda}} - \boldsymbol{\lambda})\,, \end{cases} \tag{4.18}$$

while the local updates and the initial condition of SD-GENO are provided in Algorithm 4.1, where we used the fact that $\mathrm{J}_S = \mathrm{proj}_S$, as shown in Appendix A.

The final formulation of SD-GENO is obtained from (4.18) specifying the local update rule for each player of the game. It is composed of two main phases: the communication with the neighbors and the local update. First, each agent gathers the information about the strategies and the dual variables of the neighbors. Next, the local update is performed, based on a gradient descent and dual ascend structure. It is worth noticing that only one round of communication is required at each iteration of SD-GENO.

The convergence of SD-GENO to the v-GNE of the game in (4.2) is proven in the following theorem.

Theorem 4.5. *Set the step sizes ε_i, δ, τ_i, for all $i \in \mathcal{N}$, and $\vartheta \in \mathbb{R}$ such that*

$$\tau_i \leq (\|A_i\| + \vartheta)^{-1} \tag{4.19a}$$

$$\delta \leq (2\rho + \vartheta)^{-1} \tag{4.19b}$$

$$\varepsilon_i \leq (\rho|\mathcal{N}_i| + \|A_i\| + \vartheta)^{-1}\,, \tag{4.19c}$$

$$\vartheta > \frac{1}{2\chi} \tag{4.19d}$$

with χ as in Lemma 4.3 and $\eta \in \left(0, \frac{4\chi\vartheta - 1}{2\chi\vartheta}\right)$. Then, the sequence $(\boldsymbol{x}(k))_{k\in\mathbb{N}}$ generated by SD-GENO (Algorithm 4.1) converges to the v-GNE of the game in (4.2). □

4.4 Asynchronous, distributed algorithm with edge variables (AD-GEED)

In the case of heterogeneous agents with diverse update rates, SD-GENO can converge slowly, due to its synchronous structure. To overcome this limitation, we introduce here the *Asynchronous Distributed GNE Seeking Algorithm with Edge variables* (AD-GEED). It uses edge auxiliary variables $\{\sigma_l\}_{l\in\{1\dots E\}}$ and an asynchronous update to compute the v-GNE of the game in (4.2). As discussed in the previous section, the use of edge-based auxiliary variables may lead to a limited scalability of the final algorithm. In Section 4.5, we use AD-GEED as a starting point to develop an algorithm relying on node variables only. From a technical point of view, the asynchronicity is achieved by exploiting an asynchronous framework for fixed-point iterations, the so called "ARock" framework, developed in [147].

4.4.1 Algorithm design

The update rule in the asynchronous case, is similar to that in (4.11), with the main difference that, at each iteration, only one agent $i \in \mathcal{N}$ updates its strategy x_i, dual variable λ_i and local auxiliary variables $\{\sigma_l\}_{l\in\mathcal{E}_i^{\text{out}}}$. To mathematically formulate this concept, we introduce N diagonal matrices $\boldsymbol{H}_i$, where $[\boldsymbol{H}_i]_{jj}$ is 1 if the j-th element of $\text{col}(\boldsymbol{x}, \boldsymbol{\sigma}, \boldsymbol{\lambda})$ is an element of $\text{col}(x_i, \{\sigma_l\}_{l\in\mathcal{E}_i^{\text{out}}}, \lambda_i)$ and 0 otherwise. The matrix $\boldsymbol{H}_i$ triggers the update of those elements in ϖ that are associated to agent i. We assume that the choice of which agent performs the update during the iteration k is ruled by an i.i.d. random variable $\zeta(k)$, taking values in $\boldsymbol{H} := \{\boldsymbol{H}_i\}_{i\in\mathcal{N}}$. Given a discrete probability distribution $(p_1, \dots, p_N)$, let $\mathbb{P}[\zeta(k) = \boldsymbol{H}_i] = p_i$, for all $i \in \mathcal{N}$. Therefore, the update rule in the asynchronous case is cast as

$$\varpi(k+1) = \varpi(k) + \eta\zeta(k)(T\varpi(k) - \varpi(k)) \,. \tag{4.20}$$

An illustrative example is now provided to clarify how to construct the set $\boldsymbol{H}$.

Example 4.2. Consider a game with $N = 3$, $E = 2$, $m = 1$, $n_i = 1$, $i = 1, 2, 3$ and ϖ is the collective vector of all the strategies and auxiliary variables in the game. The communication network is described by the undirected graph $\mathcal{G}$, where the arrows describe the convention adopted for the edges.

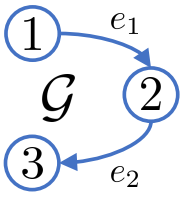

$$\mathcal{E}_1^{\text{out}} = \{e_1\}$$
$$\mathcal{E}_2^{\text{out}} = \{e_2\}$$
$$\mathcal{E}_3^{\text{out}} = \varnothing$$

$$\varpi = \begin{bmatrix} x_1 \\ x_2 \\ x_3 \\ \sigma_1 \\ \sigma_2 \\ \lambda_1 \\ \lambda_2 \\ \lambda_3 \end{bmatrix}$$

In this case, $\boldsymbol{H}$ is a set of three 8×8 matrices, namely

$$\begin{aligned} \boldsymbol{H}_1 &:= \text{diag}((1,0,0,1,0,1,0,0)) \\ \boldsymbol{H}_2 &:= \text{diag}((0,1,0,0,1,0,1,0)) \\ \boldsymbol{H}_3 &:= \text{diag}((0,0,1,0,0,0,0,1)) \,. \end{aligned}$$

If during iteration k agent 2 is updating, (4.20) turns into

$$\varpi(k+1) = \varpi(k) + \eta\boldsymbol{H}_2(T\varpi(k) - \varpi(k)) \,. \tag{4.21}$$

So, the only elements of ϖ that change are $(x_2, \sigma_2, \lambda_2)$, precisely the variables associated to agent 2. □

We assume that each agent i is equipped with public and private memory, the former is used by the neighbors to write their strategies (and dual/auxiliary variables) when they complete an update. The latter instead is used by i to store a copy of the

public memory, when it is performing a local update. This memory is not accessible to the neighbors, so it ensures the consistency of the local updates, refer also to [147]. If an agent $j \in \mathcal{N}_i$ concludes its update during iteration k while agent i is still computing its future strategy, then the value of the strategy of j, which agent i is using, becomes outdated. We denote the vector of (possibly) outdated strategy used for the update during the iteration k by $\hat{\varpi}(k)$. All the variables updated by an agent i, i.e., x_i, λ_i and $\{\sigma_l\}_{l\in\mathcal{E}_i^{\text{out}}}$, share the same delay $\varphi_i(k) \in \mathbb{N}$, since they are written at the same moment in the neighbors' public memories. Technically, the components of $\hat{\varpi}(k)$ associated to agent $j \neq i$ used during the k-th iteration by agent i for the update are $\text{col}(x_j(k-\varphi_j(k)), \{\sigma_\ell(k-\varphi_j(k))\}_{\ell\in\mathcal{E}_j^{\text{out}}}, \lambda_j(k-\varphi_j(k)))$, hence $\hat{\varpi}_j(k) = \varpi_j(k-\varphi_j(k))$.

According to this, the final formulation of the update rule (4.20) becomes

$$\varpi(k+1) = \varpi(k) + \eta\zeta(k)(T - \text{Id})\hat{\varpi}(k)\,. \tag{4.22}$$

The only assumption that we impose over the delay, is boundedness, as formalized next.

Assumption 4.4 (Bounded maximum delay)**.** *The delays are uniformly upper bounded, i.e. there exists* $\bar{\varphi} > 0$ *such that* $\sup_{k\in\mathbb{N}_{\geq 0}} \max_{i\in\mathcal{N}}\{\varphi_i(k)\} \leq \bar{\varphi} < +\infty$. □

The local update rules of AD-GEED are presented in Algorithm 4.2 and they are achieved via steps similar to those introduced in Sec. 4.3.1 for SD-GENO. To ease the notation, for each agent $j \in \mathcal{N}$, we define $\hat{x}_j \coloneqq x_j(k+\varphi_j(k))$, $\hat{\lambda}_j \coloneqq \lambda_j(k-\varphi_j(k))$ and $\hat{\sigma}_l \coloneqq \sigma_l(k-\varphi_j(k))$, for all $l \in \mathcal{E}_j^{\text{out}}$, and furthermore $\hat{\boldsymbol{x}} \coloneqq \text{col}((\hat{x}_j)_{j\in\mathcal{N}})$, $\hat{\boldsymbol{\lambda}} \coloneqq \text{col}((\hat{\lambda}_j)_{j\in\mathcal{N}})$, $\hat{\boldsymbol{\sigma}} \coloneqq \text{col}((\hat{\sigma}_j)_{j\in\mathcal{N}})$. Notice that each agent has always access to the most recent value of its variables, i.e., $\varphi_i(k) = 0$ for every agent $i \in \mathcal{N}$.

The following convergence theorem is achived by exploiting the results in [147] for a Krasnosel'skiĭ asynchronous iteration.

Theorem 4.6. *For every* $i \in \mathcal{N}$*, choose* ε_i*,* δ*,* τ_i *as in* (4.19)*, and let* $\eta \in \left(0, \frac{cNp_{\min}}{2\bar{\varphi}\sqrt{p_{\min}}+1}\left(2 - \frac{1}{2\chi\vartheta}\right)\right]$ *and* $c \in (0,1)$*. Then, the sequence* $(\boldsymbol{x}(k))_{k\in\mathbb{N}}$ *generated by AD-GEED (Algorithm 4.2) converges to the v-GNE of the game in* (4.2) *almost surely.* □

Remark 4.3. *If the probability distribution is uniform, i.e.,* $p_{\min} = \frac{1}{N}$*, and we choose* $\vartheta = \frac{1}{\chi}$*, then the bounds on the relaxation step simplify as* $\eta \in \left(0, \frac{3}{2}\frac{c\sqrt{N}}{2\bar{\varphi}+\sqrt{N}}\right]$*. Moreover, if there is no delay, i.e.,* $\bar{\varphi} = 0$*, or the number of agents is very high, then the bounds may be chosen independently from the number of players, e.g., as* $\eta \in (0,1]$. □

The structure of AD-GEED is similar to that of ADAGNES in [177, Alg. 1], where edge auxiliary variables are used to achieve consensus over the dual variables. However, unlike ADAGNES, our algorithm can handle inequality coupling constraints. Moreover, it has better performances, in terms of convergence time, according to our numerical experience, see Figure 4.5.

Algorithm 4.2: AD-GEED

Input: $k=0$, $\boldsymbol{x}^0 \in \mathbb{R}^n$, $\boldsymbol{\lambda}^0 \in \mathbb{R}^{mN}$, $\boldsymbol{\sigma}^0 = \mathbf{0}_{mM}$, chose δ, ε_i, τ_i satisfying (4.19) and $\eta \in (0,1)$.

Iteration k until convergence

// agent selection

select the agent i_k with probability $\mathbb{P}[\zeta(k) = \boldsymbol{H}_{i_k}] = p_{i_k}$

// reading memory

agent i_k copies in its private memory the current values of the public memory, i.e. $\hat{x}_j$, $\hat{\lambda}_j$, $\forall j \in \mathcal{N}_{i_k}$ and $\hat{\sigma}_l$, $\forall l \in \mathcal{E}^{\text{in}}_{i_k}$ and $l \in \mathcal{E}^{\text{out}}_j$.

// local update of i

$$\tilde{x}_{i_k} = \text{proj}_{\Omega_{i_k}}\left(x_{i_k} - \tau_{i_k}(\nabla_{i_k} f_{i_k}(x_{i_k}, \hat{\boldsymbol{x}}_{-i_k}) + A_{i_k}^\top \lambda_{i_k}\right)$$

$$\tilde{\sigma}_l = \sigma_l + \delta\rho([V]_l \otimes I_m)\hat{\boldsymbol{\lambda}}\,, \quad \forall l \in \mathcal{E}^{\text{out}}_{i^k}$$

$$\tilde{\lambda}_{i_k} = \text{proj}_{\mathbb{R}^m_{\geq 0}}\Bigg(\lambda_{i_k} + \varepsilon_{i_k}\big(A_{i_k}(2\tilde{x}_{i_k} - x_{i_k}) - b_{i_k} - \rho([V^\top]_{i_k} \otimes I_m)\hat{\boldsymbol{\sigma}} - (2\delta\rho^2+1)\textstyle\sum_{j\in\mathcal{N}_{i_k}}(\lambda_i - \hat{\lambda}_j)\big)\Bigg)$$

$$x^+_{i_k} = x_{i_k} + \eta(\tilde{x}_{i_k} - x_{i_k})$$
$$\sigma^+_l = \sigma_l + \eta(\tilde{\sigma}_l - \sigma_l)\,, \quad \forall l \in \mathcal{E}^{\text{out}}_{i^k}$$
$$\lambda^+_i = \lambda_{i_k} + \eta(\tilde{\lambda}_{i_k} - \lambda_{i_k})$$

// write in the public memories of all $j \in \mathcal{N}_{i_k}$

$$(x_{i_k}, \lambda_{i_k}) \leftarrow (x^+_{i_k}, \lambda^+_{i_k})$$
$$\{\sigma_l\}_{l\in\mathcal{E}^{\text{out}}_{i_k}} \leftarrow \{\sigma^+_l\}_{l\in\mathcal{E}^{\text{out}}_{i_k}}$$
$$k \leftarrow k+1$$

4.5 Asynchronous, distributed algorithm with node variables (AD-GENO)

This section presents the main result of the chapter, namely, we use AD-GEED as a backbone to design an algorithm converging in the same number of iterations, but relying on node auxiliary variables only, and therefore it is intrinsically lighter from a computational point of view. We name it *Asynchronous Distributed GNE Seeking Algorithm with Node variables* (AD-GENO). It is based on an idea akin to the one used to develop SD-GENO. In fact, the local update of λ_i in AD-GEED requires only the aggregate quantity $([V^\top]_i \otimes I_m)\boldsymbol{\sigma}$. We introduce a variable z_i to capture the variation of this aggregate quantity and show that it does not affect the dynamics of the pair (x_i, λ_i), thus preserving the convergence proved in Theorem 4.6. Unlike the synchronous case, we cannot directly define $\boldsymbol{z} = \boldsymbol{V}^\top\boldsymbol{\sigma}$, due to the different update frequencies of $\{\sigma_l\}_{l\in\mathcal{E}_i}$ and z_i that would affect the dynamics of $\boldsymbol{\lambda}$. This mismatch is clarified via the following example.

Example 4.4. Consider the communication network in Example 4.2 and assume that in the first three time instances, agent 2 updates twice and then 3 updates once, i.e., $i_0 = i_1 = 2$ and $i_2 = 3$. For $k = 1$, according to Algorithm 4.2 it holds

$$\begin{aligned} \sigma_2(2) &= \sigma_2(1) + \eta\rho\delta(\lambda_2(1) - \lambda_3(0)) \\ \lambda_2(2) &\propto \rho(\sigma_2(1) - \sigma_1(0)) \,, \end{aligned} \tag{4.23}$$

where $\propto$ is used to describe dependency. Next, for $k = 2$ only λ_3 is updated, then

$$\lambda_3(3) \propto -\rho\sigma_2(2) \,. \tag{4.24}$$

If we substitute the edge variables σ_1, σ_2 with $z_i = [V^\top]_i\boldsymbol{\sigma}$ for $i = 1, 2, 3$, and apply the same activation sequence, it leads to

$$\begin{aligned} z_3(3) &= z_3(0) + \eta\rho\delta(\lambda_3(0) - \lambda_2(2)) \\ \lambda_3(3) &\propto \rho z_3(0) \,. \end{aligned} \tag{4.25}$$

From the comparison of (4.24) and (4.25), it is clear that the value of $\lambda_3(3)$ would be different in the two cases. This is explained by the fact that σ_2 is updated twice, while z_3 only once. □

To bridge the gap between $\boldsymbol{\sigma}$ and $\boldsymbol{z}$, we introduce an extra variable $\mu_i \in \mathbb{R}^m$ for each node i. The role of μ_i is to store the changes of the neighbors dual variable λ_j, during the time between the last update of i and the next one.

In Algorithm 4.3, we present the local update rules of AD-GENO.The convergence of AD-GENO is proven by the following theorem. Essentially, we show that introducing $\boldsymbol{z}$ and μ does not affect the dynamics of $(\boldsymbol{x}, \boldsymbol{\lambda})$.

Theorem 4.7. *For every $i \in \mathcal{N}$ choose ε_i, δ, τ_i as in* (4.19)*. Let*

$$\eta \in \left(0, \frac{cNp_{\min}}{2\bar{\varphi}\sqrt{p_{\min}} + 1}\left(2 - \frac{1}{2\chi\vartheta}\right)\right]$$

with $p_{\min} := \min\{p_i\}_{i\in\mathcal{N}}$ and $c \in (0, 1)$. Then, the sequence $(\boldsymbol{x}(k))_{k\in\mathbb{N}}$ generated by AD-GENO (Algorithm 4.3) converges to the v-GNE of the game in (4.2) *almost surely.* □

Remark 4.5. *Only one extra scalar variable μ_i is used for every agent $i \in \mathcal{N}$, and hence the benefits of adopting only node variables, discussed in Remark 4.1, hold also in this asynchronous counterpart. Furthermore, the number of required communication rounds between agents does not increase, since the variable μ_i is updated by the neighbors of agent i during their writing phase.* □

4.6 Simulations

We conclude by proposing two sets of simulations to validate the theoretical results in the previous sections. First, we apply AD-GENO on a network Cournot game and study how delays and different activation sequences affect the convergence. Then, we compare the total computation time required by AD-GENO, AD-GEED and ADAGNES (in [177, Alg. 1]), over different communication graphs.

Algorithm 4.3: AD-GENO

Input: $k = 0$, $\boldsymbol{x}(0) \in \mathbb{R}^n$, $\boldsymbol{\lambda}(0) \in \mathbb{R}^{mN}$, $\boldsymbol{z}(0) = \mathbf{0}_{mN}$. For every $i \in \mathcal{N}$, choose δ, ε_i, τ_i satisfying (4.19), $\eta \in (0,1)$ and set $\mu_i = \mathbf{0}_m$.

Iteration k until convergence

// agent selection

select the agent i_k with probability $\mathbb{P}[\zeta(k) = H_{i_k}] = p_{i_k}$

// reading memory

agent i_k copies its public memory in the private one, i.e., the values $\hat{x}_j$, $\hat{\lambda}_j$, $\forall j \in \mathcal{N}_{i_k}$, and μ_{i_k}.

reset the public values of μ_{i_k} to $\mathbf{0}_m$.

// local update

$$\tilde{x}_{i_k} = \mathrm{proj}_{\Omega_{i_k}}\left(x_{i_k} - \tau_{i_k}(\nabla_{i_k} f_{i_k}(x_{i_k}, \hat{\boldsymbol{x}}_{-i_k}) + A_{i_k}^\top \lambda_{i_k})\right)$$

$$\tilde{z}_{i_k} = z_{i_k} + \delta\eta\mu_{i_k}$$

$$\tilde{\lambda}_{i_k} = \mathrm{proj}_{\mathbb{R}^m_{\geq 0}}\big(\lambda_{i_k} + \varepsilon_{i_k}(A_{i_k}(2\tilde{x}_{i_k} - x_{i_k}) - b_{i_k} - \rho\tilde{z}_{i_k} + (2\delta\rho^2 - 1)\textstyle\sum_{j\in\mathcal{N}_{i_k}\setminus\{i_k\}}(\lambda_{i_k} - \hat{\lambda}_j)\big)\big)$$

$$x_{i_k}^+ = x_{i_k} + \eta(\tilde{x}_{i_k} - x_{i_k})$$

$$z_{i_k}^+ = \tilde{z}_{i_k} + \eta\delta\rho\textstyle\sum_{l\in\mathcal{E}_{i_k}^{\mathrm{out}}}([V]_l \otimes I_m)\hat{\boldsymbol{\lambda}}$$

$$\lambda_{i_k}^+ = \lambda_{i_k} + \eta(\tilde{\lambda}_{i_k} - \lambda_{i_k})$$

// write in the public memory of all $j \in \mathcal{N}_{i_k}$

$$(x_{i_k}, \lambda_{i_k}) \leftarrow (x_{i_k}^+, \lambda_{i_k}^+)$$

$$\mu_j \leftarrow \mu_j + \hat{\lambda}_j - \lambda_{i_k}$$

$$k \leftarrow k + 1$$

4.6.1 AD-GENO convergence

In a network Cournot game, N firms compete over m markets and the coupling constraints model the maximum markets capacities. We propose a smilar formulation to that proposed in [178]. Here, we considered $N = 8$ firms, with the possibility to act over $m = 3$ markets, i.e., $x_i \in \mathbb{R}^3$, for all $i \in \mathcal{N}$. The local production is bounded, i.e., $0 \leq x_i \leq \overline{x}_i$, where each component of $\overline{x}_i \in \mathbb{R}^3$ is randomly drawn from $[10, 45]$. In Figure 4.1a, the interaction of each firm with the markets is shown; an edge is drawn between a firm and a market if one of former's strategies is applied to the latter. Two firms are neighbors if they compete over the same market, therefore the communication network between the firms is the one in Figure 4.1b. The coupling constraints are defined by $\boldsymbol{A}\boldsymbol{x} \leq b$, where $\boldsymbol{A} \coloneqq [A_1, \ldots, A_N] \in \mathbb{R}^{3\times 24}$ while $b \in \mathbb{R}^3$. The element $[A_i]_{jk}$ is nonzero, if $[x_i]_k > 0$ and it is applied to market j. Each nonzero element in $\boldsymbol{A}$ is randomly chosen from $[0.6, 1]$, this value can be seen as the efficiency of a strategy on a market. The components of $b \in \mathbb{R}^3$ are the capacities of the markets, randomly drawn from $[20, 100]$. The local cost function

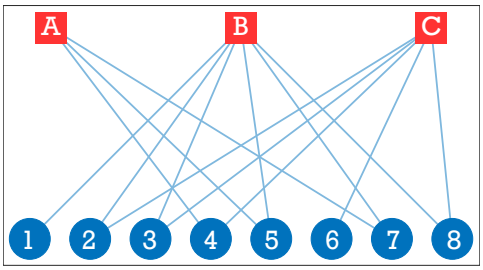

(a)

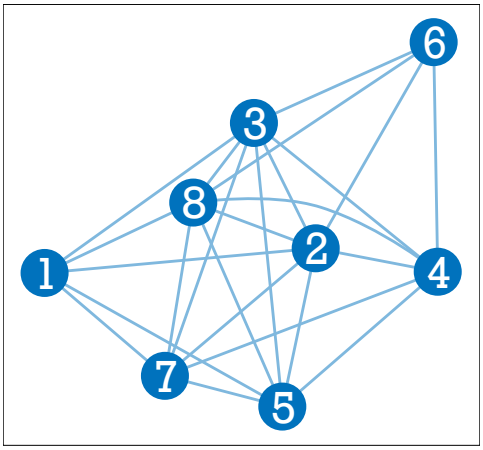

(b)

Figure 4.1: (a) Action of players $\{1, \dots, 8\}$ over the three markets A, B, C, D, (b) Communication network arising from the competition over the markets.

is defined as $f_i(x_i, \boldsymbol{x}_{-i}) := c_i(\boldsymbol{x}) - P(\boldsymbol{A}\boldsymbol{x})^\top A_i x_i$; $c_i(\boldsymbol{x})$ and it describes the cost of opting for a certain strategy, while $P(\boldsymbol{A}\boldsymbol{x})$ is the reward attained. The price is assumed linear in its argument $P(z) = \bar{P} - Dz$, where $\bar{P} \in \mathbb{R}^3$ and $D \in \mathbb{R}^{3\times 3}$ is a diagonal matrix, their non zero components are randomly chosen from $[250, 500]$ and $[1, 5]$ respectively. The function $c_i(\boldsymbol{x}) = x_i^\top Q_i x_i + q_i^\top x_i$ is quadratic, where $Q_i \in \mathbb{R}^{4\times 4}$ is diagonal and $q_i \in \mathbb{R}^4$. Their values are randomly chosen from $[1, 8]$ and $[1, 4]$, respectively.

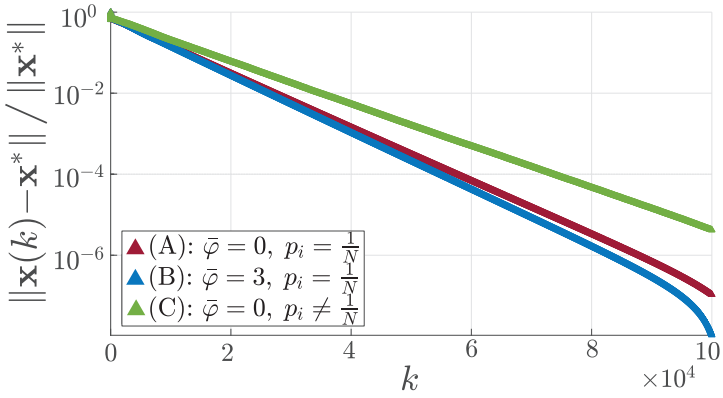

Figure 4.2: Normalized distance from the v-GNE.

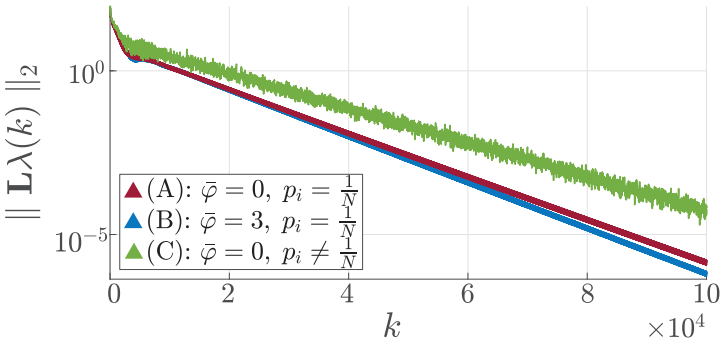

Figure 4.3: Norm of the disagreement between the dual variables.

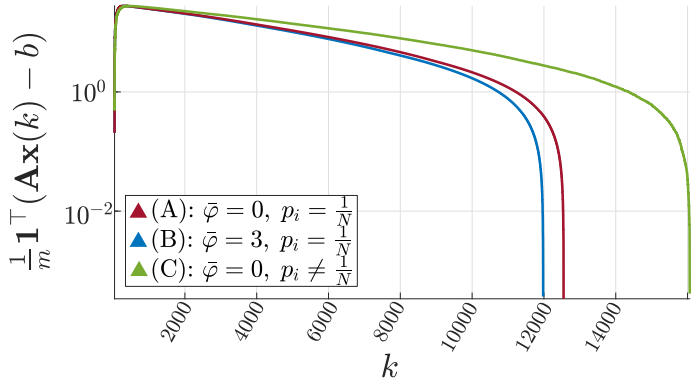

Figure 4.4: Constraints violation.

In order to explore different setups we simulate three different cases:

(A) The communication is delay free, i.e., $\bar{\varphi} = 0$, and the activation sequence is alphabetic, and hence $P[\zeta(k) = \boldsymbol{H}_i] = \frac{1}{N}$, for every $i \in \mathcal{N}$.

(B) The activation sequence is still alphabetic, but the communication may be delayed of 3 time instants at most, i.e., $\bar{\varphi} = 3$.

(C) The communication has no delay, but the probability of update is different between agents, half of them have $p_i = \frac{1}{6}$, while the rest $p_i = \frac{1}{12}$.

The outcomes of these scenarios are now analyzed. More precisely, in Figure 4.2 we show the convergence of the collective strategy $\boldsymbol{x}(k)$ to the v-GNE of the game. It is interesting to notice that the delayed information does not affect the convergence drastically, while a more skewed probability update makes it significantly slower. The same effect can be recognized in the evolution of the consensual disagreement (Figure 4.3). Finally, the coupling constraints are satisfied in all three cases after 16000 iterations (Figure 4.4). From simulations, we noticed that the convergence of the dual variables is often the bottleneck to high convergence performances. In all our algorithms, we mitigated this effect by an appropriate tuning of ρ.

4.6.2 Comparison between algorithms

Next, we compare the performance of AD-GENO with respect to AD-GEED and ADAGNES, from a computational time point of view. For the comparison with ADAGNES, we consider a modified version of the Nash-Cournot game presented in Section 4.6.1 with coupling equality constraints, i.e., only $\boldsymbol{A}\boldsymbol{x} = b$. Here, we consider $N = 40$ firms, each with at most $n_i = 2$ products. To provide an extensive comparison, we considered many instances of this game varying the communication network, from a complete to a sparse graph. The other quantities in the games are chosen as in the previous section. We compared the algorithms over 160 different graphs. The computational time required to obtain convergence is compared in the three cases.[1]

The results of the simulations are presented in Figure 4.5. As expected AD-GENO always outperforms AD-GEED, since it achieves the same dynamics of $(\boldsymbol{x}, \boldsymbol{\lambda})$ with fewer auxiliary variables. As expected, the gap between the two algorithms shrinks for a sparse graph while it increases for a dense one, from $\sim 3\%$ to $\sim 20\%$. A similar behavior arises when AD-GENO is compared to ADAGNES, due to the increment of auxiliary variables for highly connected graphs. In particular, the advantage in using AD-GENO starts from $\sim 20\%$ when the graph has an average degree of 3 and becomes $\sim 60\%$ when the graph is complete.

[1]The computation is performed on a single computer, thus the considered time is due to the local updates only and not the communications between the agents.

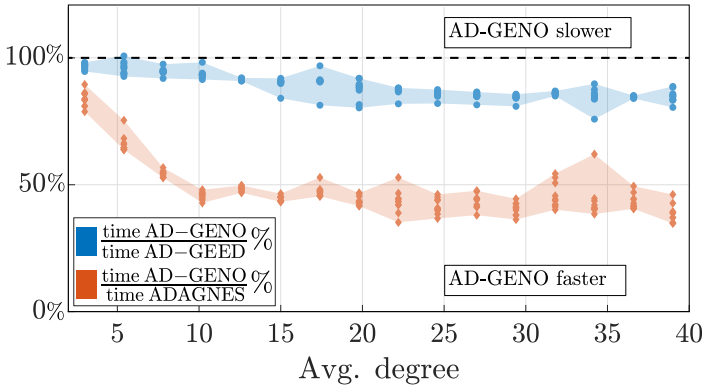

Figure 4.5: Comparison of the computation time of ADAGNES vs AD-GENO (orange diamond) and AD-GEED vs AD-GENO (blue dots), w.r.t. the variation of the communication network connectivity. If a value is lower then 100%, then AD-GENO is faster than the compared algorithm. The smaller the average node degree the more sparse the graph.

4.7 Conclusion

The AD-GENO algorithm developed in this chapter solves GNE seeking problems in strongly monotone games via a fully asynchronous update scheme. It adopts node variables only, and ensures resilience to delayed information. These features allow to increase the scalability of the algorithm and increase the performances. In our numerical experience, AD-GENO outperforms the available solutions in the literature, both in terms of computational time and the number of variables required.

4.8 Appendix

4.8.1 Proofs of Section 4.3

Proof of Lemma 4.3

The operator $\mathcal{A}$ is the sum of two operators $\mathcal{A}_1 + \mathcal{A}_2$, the first is a real skew symmetric matrix, hence maximally monotone by [14, Ex. 20.35]. $\mathcal{A}_2$ is $N_{\boldsymbol{\Omega}} \times 0 \times N_{\mathbb{R}^{mN}_{\geq 0}}$, thus maximally monotone from [14, Ex. 20.26]. By [14, Cor. 25.5(i)], we conclude that $\mathcal{A}$ is maximally monotone, since $\mathrm{dom}(\mathcal{A}_1) = \mathbb{R}^{n+(E+N)m}$.

Notice that the cocoercity of an operator also implies its maximally monotoniticy, see [14, Ex. 20.31].

Next, we prove the cocoercivity of $\mathcal{B}$. For all $\varpi_1, \varpi_2 \in \mathrm{dom}(\mathcal{B})$, it holds

$$
\begin{aligned}
&\langle \mathcal{B}(\varpi_1) - \mathcal{B}(\varpi_2) | x - y \rangle = < \begin{bmatrix} F(\boldsymbol{x}_1) - F(\boldsymbol{x}_2) \\ 0 \\ \boldsymbol{L}(\boldsymbol{\lambda}_1 - \boldsymbol{\lambda}_2) \end{bmatrix} | \varpi_1 - \varpi_2 > \\
&= < F(\boldsymbol{x}_1) - F(\boldsymbol{x}_2) | \boldsymbol{x}_1 - \boldsymbol{x}_2 > + (\boldsymbol{\lambda}_1 - \boldsymbol{\lambda}_2)^\top \boldsymbol{L} (\boldsymbol{\lambda}_1 - \boldsymbol{\lambda}_2) \\
&\geq \tfrac{\alpha}{\ell^2} \| F(\boldsymbol{x}_1) - F(\boldsymbol{x}_2) \|^2 + \lambda_{\max}(\boldsymbol{L})^{-1} \| \boldsymbol{L}(\boldsymbol{\lambda}_1 - \boldsymbol{\lambda}_2) \|^2 \\
&\geq \min \left\{ \tfrac{\alpha}{\ell^2}, \lambda_{\max}(\boldsymbol{L})^{-1} \right\} \| \mathcal{B}(\varpi_1) - \mathcal{B}(\varpi_2) \|^2 \\
&= \chi \, \| \mathcal{B}(\varpi_1) - \mathcal{B}(\varpi_2) \|^2 ,
\end{aligned}
$$

where the first inequality is attained by the α-strong monotonicity and ℓ Lipschitzianity of F and by recalling that for every symmetric real matrix $M \succeq 0$ it holds $y^\top M y \geq \lambda_{max}(M)^{-1} \| My \|^2$, with $\lambda_{\max}(M) \in \mathbb{R}_{>0}$. ■

Proof of Theorem 4.4

Consider the equilibrium point $\mathrm{col}(\boldsymbol{x}^*, \boldsymbol{\lambda}^*, \boldsymbol{z}^*)$ with $\boldsymbol{z}^* = \boldsymbol{V}^\top \boldsymbol{\sigma}^*$. Then, (4.16) at the equilibrium reduces to $\mathbf{0} = -\rho \boldsymbol{L} \boldsymbol{\lambda}^*$, and thus $\boldsymbol{\lambda}^* = \lambda^* \otimes \mathbf{1}$. Moreover, manipulating (4.17) and evaluating it in the equilibrium lead to

$$
\mathbf{0} \in N_{\mathbb{R}^{mN}_{\geq 0}}(\boldsymbol{\lambda}^*) + \bar{b} - \Lambda \boldsymbol{x}^* + \rho \boldsymbol{z}^* + (2\rho\delta + 1) \boldsymbol{L} \boldsymbol{\lambda}^* . \tag{4.26}
$$

Recalling that $\boldsymbol{L}\boldsymbol{\lambda}^* = \mathbf{0}$ and multiplying both sides of (4.26) by $(\mathbf{1}^\top \otimes I_m)$ leads to

$$
\mathbf{0} \in (\mathbf{1}^\top \otimes I_m)(N_{\mathbb{R}^{mN}_{\geq 0}}(\boldsymbol{\lambda}^*) + \bar{b} - \Lambda \boldsymbol{x}^* + \rho \boldsymbol{z}^*) . \tag{4.27}
$$

Using the fact that $\sum_{i \in \mathcal{N}} N_{\mathbb{R}^m_{\geq 0}}(\lambda^*) = N_{\cap_{i \in \mathcal{N}} \mathbb{R}^m_{\geq 0}}(\lambda^*) = N_{\mathbb{R}^m_{\geq 0}}(\lambda^*)$ and the assumption $\mathbf{1}^\top \boldsymbol{z}^* = 0$, (4.27) becomes

$$
\mathbf{0} \in N_{\mathbb{R}^m_{\geq 0}}(\lambda^*) + \bar{b} - A \boldsymbol{x}^* . \tag{4.28}
$$

Finally, (4.15) evaluated in the equilibrium is

$$
\mathbf{0} \in F(\boldsymbol{x}^*) + N_{\boldsymbol{\Omega}}(\boldsymbol{x}^*) + \Lambda^\top \boldsymbol{\lambda}^* , \tag{4.29}
$$

or equivalently

$$\mathbf{0} \in \nabla f_i(x_i^*, \boldsymbol{x}_{-i}^*) + N_{\Omega_i}(x_i^*) + A_i^\top \lambda^* \,, \quad \forall i \in \mathcal{N} \,. \tag{4.30}$$

Inclusions (4.30) and (4.28) are the KKT conditions in (4.6), and hence from [78, Th. 3.1] we conclude that $\operatorname{col}(\boldsymbol{x}^*, \boldsymbol{\lambda}^*, \boldsymbol{z}^*)$ is a v-GNE of the game. ■

Proof of Theorem 4.5

From [84, Th. 2], the choice of ϑ, ε_i, δ and τ_i in (4.19) implies that $\Phi - \vartheta I \succ 0$. Then, from [177, Lem. 2], $\Phi^{-1}\mathcal{B}$ and $\Phi^{-1}\mathcal{A}$ are respectively $\chi\vartheta$-cocoercive and maximally monotone in the Φ induced norm. Furthermore, it also shows that $(\operatorname{Id} - \Phi^{-1}\mathcal{B})$ is $\frac{1}{2\chi\vartheta}$-AVG and $\mathrm{J}_{\Phi^{-1}\mathcal{A}} \coloneqq (\operatorname{Id}+\Phi^{-1}\mathcal{A})$ is FNE. Applying [14, Prop. 4.44], we conclude that T is $\frac{2\chi\vartheta}{4\chi\vartheta-1}$-AVG. So, the iteration in (4.11) converges to $\varpi^* \in \operatorname{fix}(T)$ if $\eta \in \left(0, \frac{4\chi\vartheta-1}{2\chi\vartheta}\right)$, [14, Th. 5.14]. The above argument establishes that $\lim_{k\to+\infty} \boldsymbol{\sigma}^k = \boldsymbol{\sigma}^*$, and hence $\lim_{k\to+\infty} \boldsymbol{V}^\top \boldsymbol{\sigma}^k = \boldsymbol{V}^\top \boldsymbol{\sigma}^* =: \boldsymbol{z}^*$. So, $\boldsymbol{z}$ converges and consequently we conclude that Algorithm 4.1 converges to $\operatorname{col}(\boldsymbol{x}^*, \boldsymbol{\lambda}^*, \boldsymbol{z}^*)$. The choice of $\boldsymbol{z}_0 = \mathbf{0}$, implies that $\mathbf{1}^\top \boldsymbol{z}^k = 0$, for all $k \in \mathbb{N}$ since its values will be in the range of L. Finally, applying Theorem 4.4 we prove that the equilibrium is the v-GNE of the original game. ■

4.8.2 Proof of Theorem 4.6

Since T is $\frac{2\chi\vartheta}{4\chi\vartheta-1}$-AVG, then it can be rewritten as

$$T = \left(1 - \frac{2\chi\vartheta}{4\chi\vartheta - 1}\right) \operatorname{Id} + \frac{2\chi\vartheta}{4\chi\vartheta - 1} P \,,$$

where P is nonexpansive, [14, Prop. 4.35]. By substituting it into (4.22), we obtain

$$\varpi^{k+1} = \varpi^k + \frac{2\eta\chi\vartheta}{4\chi\vartheta - 1} \zeta^k (P - \operatorname{Id}) \hat{\varpi}^k \,. \tag{4.31}$$

For (4.31), we apply [147, Lem. 13 and Lem. 14], to conclude that $(\varpi^k)_{k\in\mathbb{N}}$ is bounded and that it converges almost surely to $\varpi^* \in \operatorname{fix}(P) = \operatorname{fix}(T)$, for $\frac{2\eta\chi\vartheta}{4\chi\vartheta-1} \in \left(0, \frac{cNp_{\min}}{2\bar{\varphi}\sqrt{p_{\min}}+1}\right]$, thus if $\eta \in \left(0, \frac{cNp_{\min}}{2\bar{\varphi}\sqrt{p_{\min}}+1} \left(2 - \frac{1}{2\chi\vartheta}\right)\right]$. Since $\operatorname{fix}(T) = \operatorname{zer}(\mathcal{A} + \mathcal{B})$, we conclude from Proposition 4.2 that $\{\boldsymbol{x}^k\}_{k\in\mathbb{N}_{\geq 0}}$ converges to the v-GNE of (4.2) almost surely. ■

4.8.3 Proof of Theorem 4.7

If we show that the modified update of $\boldsymbol{\lambda}$, with $\boldsymbol{z}$ instead of $\boldsymbol{\sigma}$, is equivalent to the one in Algorithm 4.2, we can infer the convergence from Theorem 4.6.

We prove by induction that, given an agent i, the update of λ_i at time k in Algorithm 4.2 and 4.3 are equivalent. Note that the two update rules are equivalent if it holds that

$$\tilde{z}_i(k) = ([V^\top]_i \otimes I_m)\hat{\boldsymbol{\sigma}}(k)\,, \tag{4.32}$$

for every $k > 0$ and $i \in \mathcal{N}$.

Base case: Iteration k is the first in which agent i updates its variables. If $k = 0$, then in AD-GENO $\mu_i = \mathbf{0}_m$ for every i and $\hat{\boldsymbol{\sigma}}(0) = \mathbf{0}_{mM}$ in AD-GEED, hence (4.32) is trivially verified.

If instead $k > 0$, it holds that $z_i(k) = z_i(0) = \mathbf{0}_m$, while $\hat{\boldsymbol{\sigma}}(k) \neq \mathbf{0}_{mM}$, since the neighbors of i can update more than once before the first update of i (as shown in Example 4.4). We define for each $j \in \mathcal{N}_i$ the set $\mathcal{S}_j(k)$, a $t \in \mathbb{N}$ where $t < k$ belongs to $\mathcal{S}_j(k)$ if, at the iteration t, the agent j completes an update. The maximum time in $\mathcal{S}_j(k)$ is denoted as $m_j(k) := \max\{\mathcal{S}_j(k)\}$ and $\check{\mathcal{S}}_j(k) := \mathcal{S}_j(k) \setminus m_j(k)$. From this definitions, we obtain that

$$([V^\top]_i \otimes I_m)\hat{\boldsymbol{\sigma}}(k) = \sum_{l \in \mathcal{E}_i^{\text{out}}} \sigma_l(0) - \sum_{d \in \mathcal{E}_i^{\text{in}}} \sigma_d(m_j(k))\,, \tag{4.33}$$

where j is the element of e_d different from i. Furthermore, from the update rule of σ_d in Algorithm 4.2, we derive

$$\begin{aligned} \sigma_d(m_j(k)) &= \sigma_d\left(\max\{\check{\mathcal{S}}_j(k)\}\right) + \eta\delta\rho\Big(\lambda_j\left(\max\{\check{\mathcal{S}}_j(k)\}\right) - \lambda_i(0)\Big) \\ &= \eta\delta\rho \sum_{h \in \check{\mathcal{S}}_j(k)} (\lambda_j(h) - \lambda_i(0)) \end{aligned} \tag{4.34}$$

Substituting (4.34) into (4.33) leads to

$$([V^\top]_i \otimes I_m)\hat{\boldsymbol{\sigma}}(k) = \rho\eta\delta \left(\sum_{j \in \mathcal{N}_i \setminus \{i\}} \left|\check{S}_j(k)\right| \lambda_i(0) - \sum_{j \in \mathcal{N}_i \setminus \{i\}} \sum_{h \in \check{\mathcal{S}}_j(k)} \lambda_j(h) \right). \tag{4.35}$$

From the definition given in Algorithm 4.3 of μ_i, we attain that $([V^\top]_i \otimes I_m)\hat{\boldsymbol{\sigma}}(k) = \eta\delta\mu_i = \tilde{z}_i(k)$, therefore (4.32) hold.

Induction step: Suppose that (4.32) holds for some $\bar{k} > 0$ that corresponds to the latest iteration in which agent i performed the update, i.e. $z_i(\bar{k}) \neq \mathbf{0}$.

Consider the next iteration k in which agent i updates, $k > \bar{k}$. Here, $\mathcal{S}_j(k)$ is defined as above, but for time indexes $(\bar{k}, k]$. Following similar reasoning in the previous case, we obtain

$$\begin{aligned} ([V^\top]_i \otimes I_m)\hat{\boldsymbol{\sigma}}(k) = ([V^\top]_i \otimes I_m)\hat{\boldsymbol{\sigma}}(\bar{k}) + \eta\delta\rho \sum_{l \in \mathcal{E}_i^{\text{out}}} ([V]_l \otimes I_m)\hat{\boldsymbol{\lambda}}(\bar{k}) \\ + \eta\delta\rho \left(\sum_{j \in \mathcal{N}_i \setminus \{i\}} \left|\check{S}_j(k)\right| \lambda_i(0) - \sum_{j \in \mathcal{N}_i \setminus \{i\}} \sum_{h \in \check{\mathcal{S}}_j(k)} \lambda_j(h) \right) \end{aligned} \tag{4.36}$$

where we used the fact that $l \in \mathcal{E}_i^{\text{out}}$ is updated at the same time of i. Furthermore, from the induction assumption,

$$\begin{aligned}([V^\top]_i \otimes I_m)\hat{\boldsymbol{\sigma}}(k) &= z_i(\bar{k}) + \eta\delta\rho\left(\sum_{j\in\mathcal{N}_i\setminus\{i\}} \left|\check{S}_j(k)\right| \lambda_i(0) - \sum_{j\in\mathcal{N}_i\setminus\{i\}} \sum_{h\in\check{\mathcal{S}}_j(k)} \lambda_j(h)\right) \\ &= z_i(\bar{k}) + \eta\delta\rho\mu_i = \tilde{z}_i(k)\,,\end{aligned} \tag{4.37}$$

where the last step holds because in the reading phase of Algorithm 4.3, we reset to zero the values of μ_i, every time that i starts an update. Therefore, (4.32) holds for k.

Finally, the convergence of $(\boldsymbol{x}(k))_{k\in\mathbb{N}}$ to the v-GNE of the game (4.2) follows from Theorem 4.6. ■

Part II

Decision making via potential game theory

5

Relative Best Response dynamics

The role of human decision making is becoming increasingly important for complex engineering systems. More often than not, the social behavior of large groups of humans is modeled on the basis of *rationality*. However, behavioral and experimental economics suggest that humans are not always rational and our decisions are likely to be influenced by a form of *social learning* in which new behaviors result from imitation. We propose novel evolutionary dynamics for games over networks, called h-RBR dynamics, that result from an intuitive mixture of rational BR and social learning by imitation. Under such a class of dynamics, the players optimize their payoffs over the set of actions employed by relatively successful neighbors. As such, the h-RBR dynamics share the defining non-innovative characteristic of imitation-based dynamics and may lead to equilibria that differ from classic NE. We study the asymptotic behavior of the h-RBR dynamics for both finite and convex games in which the action spaces are finite discrete and infinite compact sets, respectively, and provide preliminary sufficient conditions for finite-time convergence to a (approximate) GNE. We then couple our results to those obtained for classic BR dynamics and show how a mixture of rational best responding individuals and h-relative best responders can affect the equilibria.

5.1 Introduction

Game theoretic scenarios in which players interact exclusively with a fixed group of neighbors trace back to the early 1990s when economists and biologists started to explore the effect of simple spatial structures in (probabilistic) decision-making processes driven by rational best response processes and more biologically inspired imitation processes [29, 70, 136]. Later, the simple spatial structures were extended to arbitrary topologies defined by graphs [181, 118, 162]. The long-run collective behavior of non-cooperative games over networks have been extensively studied for myopic best response dynamics in which the players, given the last plays of their neighbors, select an action that maximizes their own payoff. These extended research efforts resulted in the identification of several classes of games that converge to a pure Nash equilibrium under a variety of such best response processes [127, 68, 171, 180] and brought forth a number of algorithms that ensure convergence to an equilibrium [99, 145, 178]. Best response dynamics are "*innovative*" in the sense that, in order to optimize their payoffs, players are always able to select new actions that are not played in the current action profile. They are in line with classic economic theories that support the idea that absolute optimization (or rational behavior) is a natural result of evolutionary forces [88]. Recently, the systems and control community has been interested in the analysis of dynamical systems driven by *imitation* [182, 57, 10, 11, 96]. Such dynamics are "*non–innovative*": players can only select actions that already exist in the networked population. Therefore, non–innovative dynamics can lead to equilibrium concepts that differ from traditional Nash equilibria. In [115, 169], the authors studied an evolutionary process where the players, most of the time, choose a best response from the set of actions that exist in the entire population. In [169], this process was simply referred to as imitation. Perhaps a more suitable name was proposed in [115], where such a revision process was called a Relative Best Response (RBR). In fact, RBR combines the non–innovative nature of pure imitation with the rationality of best response. Such dynamics match classic economic studies in which rather than absolute performance, the players opt for *relative performance*, that prove decisive in the long run [6]. Experimental evidences of such behaviour are documented in [60, 168]. Another motivation for studying such dynamics is that they can take into account the effect of *word-of-mouth communication* and social learning in decision-making processes [71]. For example, when considering alternative technologies an individual may ask friends or family about their current choice and benefits. This local spread of information in turn is likely to affect the individual's decision, and may very well lead to a complete disregard of technology that is not used by her peers. Traditional best response dynamics do not capture such a process of information exchange and social learning, rather they reflect situations in which an individual adopts some technology solely on the basis of her *own* expectation, regardless of how others have perceived it. In many real-world decision-making processes it is likely that both types of learning processes occur [126], but from a theoretical point of view the effects of social learning is often overlooked.

In this chapter, we propose novel social learning dynamics for finite and convex games over networks that result from an intuitive combination of rational behavior and imitation. We start on the basis of a spatial version of RBR dynamics under

which the players choose a best response from (a convex combination of) the current set of actions in their neighborhood. In this case, the players interact and relate their success exclusively with a *fixed* group of neighbours. Even though this process contains an element of social learning, namely that the players *conform* themselves to observed actions, it does not take into account the relative performance of these actions. To this end, we generalize RBR dynamics to the h-RBR, where players relate their future strategy to the h-top performing neighbors. This process relies on local information exchange of both decisions and benefits, that are fundamental to social learning and imitation. Even though under h-RBR dynamics the feasible action sets of the players are state dependent and the overall problem is non-jointly convex, we show that for a general class of games such dynamics converge to a (approximate) generalized Nash equilibrium in finite time. We relate our results to classes of games for which best response dynamics converge to a (approximate) Nash equilibrium. Our results suggest that for these general classes of games, that cover many real-world applications, having both best responses and h-relative best responses in the population does not compromise finite-time convergence. Hence, our proposed dynamics can be used to study the effects of social learning on the equilibria of many models in the literature of games over networks.

5.1.1 Games over networks

Let us introduce the three main ingredients that we use to define a non-cooperative game Γ over a network.

1. *The network structure:* the interdependence between the players is described by an undirected graph $\mathcal{G} = (\mathcal{I}, \mathcal{E})$, see Appendix B denotes a graph whose node set $\mathcal{I} = \{1, \dots, N\}$ represents the players (or agents) involved in the game, and $\mathcal{E} \subseteq \mathcal{I} \times \mathcal{I}$ the set of edges, i.e., the interactions between players. For each $i \in \mathcal{I}$, the set of its neighbors is defined as $\mathcal{N}_i := \{j \in \mathcal{I} : (i,j) \in \mathcal{E}\} \setminus \{i\}$.
2. *The action space:* the set of local actions (or strategies) that a player $i \in \mathcal{I}$ can implement is denoted by $\mathcal{S}_i$. Thus, the action space of the game is $\boldsymbol{\mathcal{S}} = \prod_{i \in \mathcal{I}} \mathcal{S}_i$. An *action profile* (or collective strategy) s is an element of this set, hence $\boldsymbol{s} := \mathrm{col}((s_i)_{i \in \mathcal{I}}) \in \boldsymbol{\mathcal{S}}$.
3. *The combined payoff function:* $\pi_i : \boldsymbol{\mathcal{S}} \to \mathbb{R}$ denotes the local payoff function of player $i \in \mathcal{I}$. The combined payoff function $\pi : \boldsymbol{\mathcal{S}} \to \mathbb{R}^N$ maps each action profile $\boldsymbol{s} \in \boldsymbol{\mathcal{S}}$ to a payoff vector $\pi(\boldsymbol{s}) := \mathrm{col}(\{\pi_i(s)\}_{i \in \mathcal{I}})$ who's elements correspond to the payoffs that the players receive for adopting the corresponding action. Here, the spatial structure is incorporated into the payoff function π.

The network structure determined by the graph $\mathcal{G}$, the action space $\boldsymbol{\mathcal{S}}$, and combined payoff function π completely describe a game over the network as the triplet $\Gamma := (\mathcal{G}, \boldsymbol{\mathcal{S}}, \pi)$.

Throughout the chapter, we consider the following assumption on the action sets, that naturally allows players to imitate each other and is in fact common in imitation–like dynamics [11, 182, 136].

Standing Assumption 5.1 (Identical action sets)**.** *All players have the same action set $\mathcal{S}$, i.e., $\mathcal{S}_i = \mathcal{S}$ for all $i \in \mathcal{I}$.* □

The dynamics we propose in this chapter aspire at bridge the gap between imitation dynamics and BR dynamics. For this reason, the above assumption is necessary in order to allow the players in the game to "imitate" the action of the others.

5.1.2 Finite and convex games over networks

We say that a game Γ is *finite* if the action set of each player is a finite set that can be represented by a subset of the integer numbers, that is, $\mathcal{S} \subset \mathbb{Z}$ and therefore a profile action belongs to $\boldsymbol{\mathcal{S}} \subset \mathbb{Z}^N$. We denote a generic finite game as Γ^{f}. On the other hand, we say that Γ is a *convex* game, and we denote it by Γ^{c}, if the action set of each player is described by a non-empty, convex subset of $\mathbb{R}^n$, i.e., $\mathcal{S} \subset \mathbb{R}^n$ and $\boldsymbol{\mathcal{S}} \subset \mathbb{R}^{Nn}$. The convexity assumption over the action set for convex games is common in the literature of monotone games, as highlighted in the previous chapters. Hereafter, we use the superscripts "f" and "c" if the variable or result introduced is referred to finite or convex games respectively. If the introduced quantity has the same definition for both class of games no superscript is used.

5.2 h-Relative Best Response dynamics

Before defining the h-RBR dynamics, for the purpose of comparison, we give the definition of the best response mapping.

Definition 5.1 (Best response mapping)**.** The best response mapping of player $i \in \mathcal{I}$ is defined as

$$\mathcal{BR}_i(\boldsymbol{s}_{-i}) \coloneqq \operatorname*{argmax}_{y \in \mathcal{S}} \pi_i(y, \boldsymbol{s}_{-i}). \tag{5.1}$$

where $\mathcal{BR}_i(\boldsymbol{s}_{-i}) \subseteq \mathcal{S}$ might be a set. □

The defining distinction of a *relative* best response is that, instead of optimizing over a fixed action set $\mathcal{S}$, each player $i \in \mathcal{I}$ optimizes her payoff over some *feasible* subset of $\mathcal{S}$ that depends on the actions of the neighbors of i and s_i itself. For a game Γ and an action profile $\boldsymbol{s} \in \boldsymbol{\mathcal{S}}$, we denote the feasible action set for player $i \in \mathcal{I}$ by $\mathcal{F}_i(\boldsymbol{s}) \subseteq \mathcal{S}$. For a finite game Γ^{f}, the feasible action set of player $i \in \mathcal{I}$ is simply determined as the local set of actions, i.e.,

$$\mathcal{F}_i^{\mathrm{f}}(\boldsymbol{s}) \coloneqq \{s_j \in \boldsymbol{s} \mid j \in \mathcal{N}_i \cup \{i\}\} \subseteq \mathcal{S}^{\mathrm{f}}, \tag{5.2}$$

where $\mathcal{S}^{\mathrm{f}}$ is the action set of game Γ^{f}. Instead, for a convex game Γ^{c}, the action sets are convex and compact subsets of $\mathbb{R}^n$, hence the feasible action set for player $i \in \mathcal{I}$ is determined as

$$\mathcal{F}_i^{\mathrm{c}}(\boldsymbol{s}) = \operatorname{conv}\left(\{s_j \in \boldsymbol{s} \mid j \in \mathcal{N}_i \cup \{i\}\}\right) \subseteq \mathcal{S}^{\mathrm{c}}, \tag{5.3}$$

where $\mathcal{S}^{\mathrm{c}}$ is the action set of game Γ^{c}.

We are now ready to formalize the idea of RBR for both finite and convex games.

Definition 5.2 (Relative Best Response mappings)**.** Given a game Γ, the relative best response mapping for every player $i \in \mathcal{I}$ is defined as

$$\mathcal{RBR}_i(\boldsymbol{s}_{-i}) \coloneqq \underset{y \in \mathcal{F}_i(\boldsymbol{s})}{\operatorname{argmax}} \ \pi_i(y, \boldsymbol{s}_{-i}), \tag{5.4}$$

where $\mathcal{RBR}_i(\boldsymbol{s}_{-i}) \subseteq \mathcal{S}$ might be a set. □

The definition above can be specialized for convex and finite games using the feasible action sets $\mathcal{F}_i^{\mathrm{f}}(\boldsymbol{s})$ in (5.2) and $\mathcal{F}_i^{\mathrm{c}}(\boldsymbol{s})$ in (5.3), respectively.

Imitation dynamics are often associated with *social learning*, in which new behaviors are acquired by observing and mimicking others [8]. In the context of a game, in order to choose which neighbor's action to imitate, the players must thus have information about the actions and the current payoffs of their neighbors. It is this local exchange of information — absent in BR dynamics — that can lead to surprising "non-rational" behaviors. As BR, the RBR dynamics are based only on the neighbors actions, and thus do not to take into account the *payoffs* of others. An interesting and natural generalization of RBR is a decision process in which the feasible action set of player $i \in \mathcal{I}$ depends on a subset of the neighbors that receive the h_i highest payoffs. Rouglhy speaking, only those actions that are taken by succesfull neighbors are considered in the action update. In this case, the *relative success* of the neighbors of i will have an influence on the future action of player i, and $h_i \in \mathbb{N}$ is a measure for how restricting this relative success is for player $i's$ feasible action set.

We dedicate the remainder of this section to formalize this novel decision process and illustrate some applications with examples that are likely to be affected by relative performance considerations and social influence. Before formally defining the decision-making process, it is necessary to introduce some additional auxiliary sets, that will prove themselves useful in the proceeding of the analysis. For some action profile $\boldsymbol{s} \in \boldsymbol{\mathcal{S}}$, let us define the set of *distinct* payoffs obtained by the neighbors of i as $\mathcal{R}_i(\boldsymbol{s}) \coloneqq \{\pi_j(\boldsymbol{s}) \mid j \in \mathcal{N}_i\}$, and define the set of neighbors that receive at least the h_i highest payoff as

$$\mathcal{H}_i(\boldsymbol{s}_{-i}, h_i) \coloneqq \{j \in \mathcal{N}_i \mid \pi_j(\boldsymbol{s}) \geq \max{}^{h_i}(\mathcal{R}_i(\boldsymbol{s}))\}\,.$$

Note that it always holds true that $|\mathcal{N}_i| \geq |\mathcal{H}_i(\boldsymbol{s}_{-i}, h_i)| \geq h_i$. Then, the set of actions of these successful players is given by

$$\mathcal{M}_i(\boldsymbol{s}_{-i}, h_i) \coloneqq \{s_j \in \boldsymbol{s} \mid j \in \mathcal{H}_i(\boldsymbol{s}_{-i}, h_i)\}. \tag{5.5}$$

For a finite game Γ^{f}, the feasible set of actions is determined by

$$\forall i \in \mathcal{I} : \mathcal{F}_i^{\mathrm{f}}(\boldsymbol{s}, h_i) \coloneqq \{\mathcal{M}_i(\boldsymbol{s}_{-i}, h_i)\} \cup \{s_i\} \subseteq \mathcal{S}, \tag{5.6}$$

while for a convex game Γ^{c}, it is

$$\forall i \in \mathcal{I} : \mathcal{F}_i^{\mathrm{c}}(\boldsymbol{s}, h_i) \coloneqq \operatorname{conv}\big(\{\mathcal{M}_i(\boldsymbol{s}_{-i}, h_i)\} \cup \{s_i\}\big). \tag{5.7}$$

An illustrative example of how these sets are defined for a convex game among 5 agents is depicted Figure 5.1.

Let $\boldsymbol{h} = \operatorname{col}((h_i)_{i \in \mathcal{I}}) \in \mathbb{N}^N$. An h-RBR can now be formalized as follows.

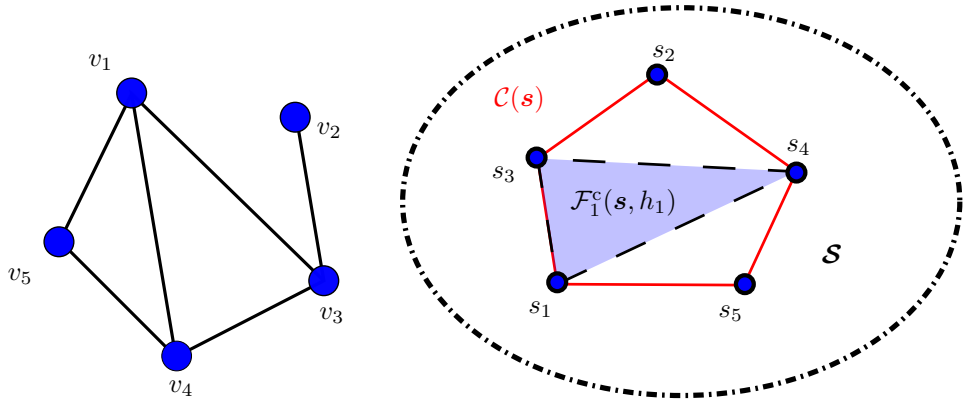

(a) **(b)**

Figure 5.1: Suppose $\mathcal{G}$ as in (a), so $n = 5$. Thus, $\mathcal{M}_1(\boldsymbol{s}, |\mathcal{N}_1|) = \{s_3, s_4, s_5\}$. Moreover, if $\pi_4(\boldsymbol{s}) > \pi_3(\boldsymbol{s}) > \pi_2(\boldsymbol{s}) > \pi_5(\boldsymbol{s})$ and $h_1 = 2$, then, $\mathcal{M}_1(\boldsymbol{s}_{-i}, 2) = \{s_4, s_5\}$, $\mathcal{F}_1^{\mathrm{c}}(\boldsymbol{s}, 2) = \mathrm{conv}(\{s_4, s_5, s_1\})$, i.e., the shaded area with the dashed border in (b), while $\mathcal{C}(\boldsymbol{s}) \coloneqq \mathrm{conv}(\boldsymbol{s})$ is indicated by the region enclosed by the red solid border.

Definition 5.3 (h-Relative Best Response mappings)**.** Given a game Γ, the h–relative best response mappings is defined, for all players $i \in \mathcal{I}$, as

$$\mathcal{RBR}_i(\boldsymbol{s}_{-i}, h_i) \coloneqq \underset{y \in \mathcal{F}_i(\boldsymbol{s}, h_i)}{\operatorname{argmax}} \ \pi_i(y, \boldsymbol{s}_{-i}). \tag{5.8}$$

□

It is worth mentioning that, if $h_i = |\mathcal{N}_i|$ for every $i \in \mathcal{I}$, then the h-RBR mappings in Definition 5.3 boils down to RBR mappings. In contrast, for finite games, when $h_i = 1$, player i can only choose between their own action and the action of their most successful neighbors. Therefore, if for all $i \in \mathcal{I}$, $h_i = 1$ the feasible actions of the h-RBR dynamics for finite games are exactly the feasible set of actions in an unconditional imitation process. This relation between the three dynamics is summed up in the following scheme

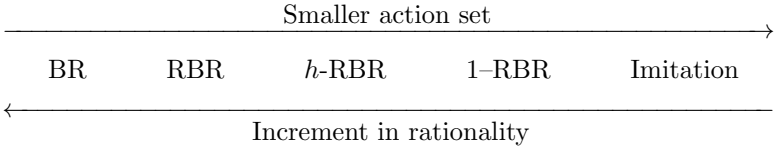

5.2.1 Examples of h-RBR applications

Example 5.1 (Adoption of competing products)**.** Let us elaborate on the role of h_i in the context of the technology adoption that can be described as a finite

game. Suppose an individual i is considering to purchase a new product and that she can choose between models X, Y and Z, to replace her current product C, i.e., $\mathcal{S}^{\mathrm{f}} = \{X, Y, Z, C\}$. She values her current product with a 3 on a scale from 0 to 5, hence $\pi_i(C) = 3$. To perform a decision about which product to adopt, she gathers information from three peers, labeled as $\mathcal{N}_i = \{a, b, c\}$, who she believes value the product in a similar manner as herself. Suppose model X is used by peer a that values the model with a full score 5 out of five. In this case, $s_a = X$ and $\pi_a(X) = 5$. Model Y is used by peer b who values it with 2 (i.e., $s_b = Y$, $\pi_b(Y) = 2$) and model Z is used by peer c who values it with 4 (i.e., $s_c = Z, \pi_c(Z) = 4$). The distinct payoffs obtained by the neighbors are organized in the set $\mathcal{R}_i(\boldsymbol{s}) = \{5, 2, 4\}$. If $h_i = 1$, then i considers to keep her current phone or buy model X, because she believes models Y and Z are worse than X. In our notation, the set of action chosen by her most successful peer are $\mathcal{M}_i^{\mathrm{f}}(\boldsymbol{s}, 1) = \{s_a\} = \{X\}$, and the set of feasible actions is $\mathcal{F}_i^{\mathrm{f}}(\boldsymbol{s}, 1) = \{C, X\}$. However, if $h_i = 2$, she would also consider buying model Z that may be an overall better choice for her. In this case, $\mathcal{M}_i^{\mathrm{f}}(\boldsymbol{s}, 2) = \{s_a, s_c\} = \{X, Z\}$ and $\mathcal{F}_i^{\mathrm{f}}(\boldsymbol{s}, 2) = \{C, Z, X\}$. In this example, h_i influences how the information from peers reflect her own valuation of a product. If $h_i = 3$, then she would take into account every product because she could be uncertain if the low score of model Y reflects her own preferences accurately. □

Example 5.2 (Adoption of renewable energy)**.** Suppose that a household faces the possibility to determine the source of the energy used, either fossil fuel of renewable. In particular it is allowed to select the fraction of the total energy obtained from renewable sources, so $\mathcal{S}^{\mathrm{c}} = [0, 1]$. This problem can be modeled as a convex game Γ^{c}. To obtain an idea on how costly and sustainable the usage of renewable energy is compared to fossil fuel, they gather information from neighboring households with similar energy demands. If none of the neighbors are using renewable energy sources, then the household may be inclined to refrain from using renewable energy, due to a lack of incentive to deviate from the overall *status quo*, in this case $\mathcal{F}_i^{\mathrm{c}}(\boldsymbol{s}, h_i) = \{0\}$. However, if neighboring households are already using renewable energy and have informed the household that they are satisfied with the supply and costs, an appealing option is to choose some fraction of sustainable energy based on the fraction chosen by the neighbors. This decision is plausible because of two reasons: first, the information gathered from similar households suggest that renewable energy is a good alternative source of energy and second, conformity forces that result peer pressures may lead the household to decide to try renewable energy sources [122].

In some contexts it makes sense to apply a transformation to the action profile and payoffs before applying an h-relative best response.

Example 5.3 (Opinion dynamics)**.** Consider an opinion dynamics model in which $s_i \in [0, 1]$ represents an *opinion* on a topic, where 1 (0) means complete agreement (disagreement). In these settings, it is well-established that social learning plays a crucial role in the evolution of opinions as individuals tend to adjust their opinion to a local weighted average [62, 87]. Such a process can be represented via a game

over network subject to BR dynamics. Now, let us define a simple auxiliary "payoff function" that player i observes from neighbor j as

$$\epsilon_{ij}(\boldsymbol{s}) \coloneqq 1 - |s_i - s_j|,$$

and let $\epsilon_i(\boldsymbol{s}) \in \mathbb{R}^{|\mathcal{N}_i|+1}$ be the vector of these opinion errors. Now suppose the player applies the principle of selecting the h_i highest valued neighbors. Then the opinion dynamics would result in a bounded-confidence like model in which the player only takes into account those neighbors that have an opinion similar to the player's own opinion. □

Now that we have defined the h-RBR mappings, let us introduce the *asynchronous*, or sequential, game dynamics that are associated with the h-RBR mapping. Specifically, at each time step $t \in \mathbb{N}$ for which $\boldsymbol{s}(t+1) \neq \boldsymbol{s}(t)$, there exists a unique player $i_t \in \mathcal{I}$ such that the collective dynamics satisfy

$$\boldsymbol{s}(t+1) = (s_{i_t}(t+1)), \boldsymbol{s}_{-i_t}(t+1)) \in (\mathcal{RBR}_{i_t}(\boldsymbol{s}_{-i_t}(t), h_{i_t}), \boldsymbol{s}_{-i}(t)). \tag{5.9}$$

For the asynchronous dynamics in (5.9), we assume that the activation sequence ensures that, each player updates over a sufficiently long period of time.

Standing Assumption 5.2 (Persistent activation sequence)**.** *Every sequence of activated players $(i_t)_{t\in\mathbb{N}}$ driving the asynchronous dynamics* (5.9) *is persistent, i.e., for all player $j \in \mathcal{I}$ and time $t \in \mathbb{N}$, there exists $\bar{t} \geq t$ such that $i_{\bar{t}} = j$.* □

5.2.2 Equilibrium concept

We are interested to characterize the conditions under which the dynamics in (5.9) converge to an equilibrium action profile, i.e., when all players cannot increase their payoff by unilaterraly deviate from the current selected strategy. For the h-RBR dynamics, the local feasible action set for each player is constrained by the actions of the other players and hence the equilibrium of these dynamics correspond to a GNE, [61].

Definition 5.4 (Generalized Nash Equilibrium)**.** The action profile $\boldsymbol{s}^* \in \boldsymbol{\mathcal{S}}$ is a GNE for Γ, if for all $i \in \mathcal{I}$

$$s_i^* \in \mathcal{RBR}_i(\boldsymbol{s}_{-i}^*, h_i), \tag{5.10}$$

where the feasible action set $\mathcal{F}_i(\boldsymbol{s}^*, h_i)$ of a finite game and convex game are given by (5.6) and (5.7), respectively. □

It is worth mentioniong that, in the convex game case, our GNEP is not jointly convex [79], differently from the problems presented in the previous chapters. In Sections 5.3 and 5.4, we will study the convergence properties of (5.9) for finite and convex games under the assumption that players switch to another action if they have an incentive to deviate from their current strategy.

Standing Assumption 5.3 (Incentive to deviate)**.** *If in a game* Γ*, player* i *updates at time* $t \in \mathbb{N}$*, then* $s_i(t+1) \neq s_i(t)$ *only if there exists* $y \in \mathcal{F}_i(\boldsymbol{s}, h_i)$ *such that*

$$\pi_i(y, \boldsymbol{s}_{-i}(t)) - \pi_i(s_i(t), \boldsymbol{s}_{-i}(t)) > 0.$$

□

5.3 Convergence for finite games

In this section, we study the convergence of the asynchronous h-RBR dynamics (5.9) when all players choose h-relative best responses and they can have a finite set of actions that they can choose from. First, we define two sets that will prove useful in the analysis of the h-RBR dynamics in finite and convex games. For an initial action profile $\boldsymbol{s}(0)$, let us denote the set that contains all actions that are employed by at least one player in the initial action profile by $\mathcal{S}_0 \coloneqq \cup_{i\in\mathcal{I}}\{s_i(0)\}$, and let $\boldsymbol{\mathcal{S}}_0 \coloneqq \mathcal{S}_0^N$. The set $\mathcal{S}_0$ is called the *support* of $\boldsymbol{s}(0)$ in [115]. The key property of $\boldsymbol{\mathcal{S}}_0$ is that it is positively invariant with respect to the h-RBR dynamics (5.9), due to their non–innovative nature. To study the convergence properties of finite games under the asynchronous h-RBR dynamics we use the theory of potential games [127]. Next, we elaborate on Definition C.2 of potential function, and define a potential like function useful for games subject to RBR.

Definition 5.5 (Generalized $\mathcal{S}_0$–potential function)**.** A function $P : \boldsymbol{\mathcal{S}} \to \mathbb{R}$ is a $\mathcal{S}_0$-potential function for Γ^{f} and some $\boldsymbol{s}(0) \in \boldsymbol{\mathcal{S}}$, if for every $i \in \mathcal{I}$, $s_i, s_i' \in \mathcal{S}_0$ and $\boldsymbol{s}_{-i} \in \mathcal{S}_0^{N-1}$, it holds

$$\pi_i(s_i', \boldsymbol{s}_{-i}) - \pi_i(s_i, \boldsymbol{s}_{-i}) > 0, P(s_i', \boldsymbol{s}_{-i}) - P(s_i, \boldsymbol{s}_{-i}) > 0. \tag{5.11}$$

□

If a such $\mathcal{S}_0$-potential function exists, then we call Γ^{f} a generalized *relative* potential game with respect to $\mathcal{S}_0$.

Remark 5.4. *When the initial action profile* $\boldsymbol{s}(0) \in \boldsymbol{\mathcal{S}}$ *is such that* $\boldsymbol{\mathcal{S}}_0 \equiv \boldsymbol{\mathcal{S}}$*, then Definition 5.5 is equivalent to the definition of generalized ordinal potential function and of a generalized ordinal potential game, see Appendix C. In its classic definition, the implication in* (5.11) *needs to be satisfied on the entire action space* $\boldsymbol{\mathcal{S}}$ *to ensure convergence of the innovative BR dynamics to a pure NE.* □

We are now ready to present the main result for finite games that relies on the existence of a $\mathcal{S}_0$-potential function.

Theorem 5.6. *Suppose that* Γ^{f} *is a generalized relative potential game with respect to* $\mathcal{S}_0$*. Then, for all* $\boldsymbol{s}(0) \in \boldsymbol{\mathcal{S}}_0$*, the asynchronous h-RBR dynamics defined in* (5.9) *converge to a GNE in finite time.* □

Proof. Let us consider a generic initial condition $\boldsymbol{s}(0) \in \boldsymbol{\mathcal{S}}_0$. Because the h-RBR dynamics are non–innovative, it follows that $\forall t \geq 0 : \boldsymbol{s}(t) \in \boldsymbol{\mathcal{S}}_0$. Γ^{f} is a relative potential game with respect to $\mathcal{S}_0$, hence there exists a function $P : \boldsymbol{\mathcal{S}} \to \mathbb{R}$ such that for every $i \in \mathcal{I}$, for every $s_i, s_i' \in \mathcal{S}_0 \cap \mathcal{S}_i$ and every $\boldsymbol{s}_{-i} \in \prod_{j \in \mathcal{I} \setminus \{i\}} \mathcal{S}_0$, the following implication holds:

$$\pi_i(s_i', \boldsymbol{s}_{-i}) - \pi_i(s_i, \boldsymbol{s}_{-i}) > 0 \Rightarrow P(s_i', \boldsymbol{s}_{-i}) - P(s_i, \boldsymbol{s}_{-i}) > 0. \tag{5.12}$$

By Definition 5.3, equation (5.6), and dynamics in (5.9), it follows that after a player switches, its payoff is at least as high as it was before. That is, for all $t \geq 1$:

$$\exists\, i_t \in \mathcal{I} :\ \pi_{i_t}(t) \geq \pi_{i_t}(t-1). \tag{5.13}$$

By Standing Assumption 5.3, if a player switches, then inequality (5.13) holds *strictly* and hence the trajectory of relative best response dynamics generates an improvement path γ. Since for all $t \geq 0$, we have $\mathcal{F}_i^{\mathrm{f}}(\boldsymbol{s}(t), h_i) \subseteq \mathcal{S}_0$. From implication (5.12), it follows that the $\mathcal{S}_0$-potential function P is strictly increasing along γ. Since the action space is finite, P is a bounded function. This implies that the h-RBR dynamics converge to a GNE in finite time. ■

It may happen that there exist generalized $\mathcal{S}_0$-potential functions only for a subset of initial action profiles. To guarantee finite-time convergence from any initial condition, it is required the existence of a generalized potential function, *not necessarily the same*, for every initial action profile. This is formalized in the following definition.

Definition 5.7 (Generalized relative potential game)**.** If for Γ^{f} there exist generalized $\mathcal{S}_0$-potential functions for every $s(0) \in \boldsymbol{\mathcal{S}}$, then Γ^{f} is called a generalized relative potential game. □

An example of a generalized relative potential game can be found in Example 5.5. An immediate consequence of Theorem 5.6 is stated in the following corollary.

Corollary 5.8. *For every finite generalized relative potential game, the asynchronous h-RBR dynamics converge globally to a GNE in finite time.* □

5.3.1 Relation to generalized ordinal potential games

From Definition 5.5 and Definition C.2, it can be easily seen that every generalized ordinal potential game is a generalized *relative* potential game. In particular, a generalized ordinal potential game has a *common* generalized ordinal potential function that holds for every initial condition. By means of the following illustrative counter-example, we show that the converse is not always true.

Example 5.5. Consider the symmetric rock-scissors-paper (RSP) game with payoff matrix

$$\boldsymbol{M} = \begin{bmatrix} a & b & c \\ c & a & b \\ b & c & a \end{bmatrix}, \quad b > a \geq c. \tag{5.14}$$

Because each improvement path in the RSP game converges to the improvement cycle: $(R,S) \to (R,P) \to (P,S) \to (S,R) \to (P,R) \to (P,S) \to (R,S)$, the RSP game is not a generalized ordinal potential game. However, for every initial action profile $\boldsymbol{s}(0) \in \boldsymbol{\mathcal{S}} \coloneqq \{R,S,P\}^2$ there exists a generalized $\mathcal{S}_0$–potential and thus the RSP game is a generalized relative potential game. □

Proposition 5.9. *Let G,R denote the class of generalized ordinal potential games and generalized relative potential games, respectively. Then, $G \subset R$.* □

Proof. The inclusion $G \subseteq R$ follows from Definition 5.5 and strictness follows from Example 5.5. ■

Corollary 5.10. *For every finite generalized ordinal potential game, the asynchronous h-RBR dynamics converge globally to a GNE in finite time.* □

5.4 Convergence of convex games

In this section, we use the concepts of *bounded* games and ϵ-improvement paths, introduced in Appendix C, to study the convergence in finite time of convex games to an approximate GNE.

Definition 5.11 (ϵ-Generalized Nash equilibrium)**.** The action profile $\boldsymbol{s} \in \boldsymbol{\mathcal{S}}$ is an ε Generalized Nash equilibrium (ε-GNE) for Γ, if for all $i \in \mathcal{I}$, $s_i \in \boldsymbol{s}$ there exists $\varepsilon > 0$ such that

$$\pi_i(s_i, \boldsymbol{s}_{-i}) - \pi_i(s_i', \boldsymbol{s}_{-i}) > \epsilon, \quad \forall s_i' \in \mathcal{F}_i^{\mathrm{c}}(\boldsymbol{s}_{-i}, h_i)\,. \qquad \square$$

Consider the following class of games inspired by the definition of weighted potential games in [127].

Definition 5.12 (Weighted $\mathcal{S}_0$–potential function)**.** A function $P : \boldsymbol{\mathcal{S}} \to \mathbb{R}$ is a weighted $\mathcal{S}_0$-potential function for Γ^{c} and some $\boldsymbol{s}(0) \in \boldsymbol{\mathcal{S}}$, if for every $i \in \mathcal{I}$, $s_i, s_i' \in \mathcal{S}_0$ and $\boldsymbol{s}_{-i} \in \mathcal{S}_0^{N-1}$, the following implication holds

$$\pi_i(s_i', \boldsymbol{s}_{-i}) - \pi_i(s_i, \boldsymbol{s}_{-i}) = w_i \left[P(s_i', \boldsymbol{s}_{-i}) - P(s_i, \boldsymbol{s}_{-i})\right],$$

for some $w_i > 0$. □

If such a function satisfying the above definition exists, then we call Γ^{c} a weighted relative potential game with respect to $\mathcal{S}_0$. Moreover, if $w_i = 1$ for all $i \in \mathcal{I}$, then Γ^{c} is called an exact relative potential game with respect to $\mathcal{S}_0$.

The following lemma proves that for every weighted relative potential game one can design an equivalent exact relative potential game by scaling the payoff functions of the players.

Lemma 5.13 (Equivalence of weighted and exact $\mathcal{S}_0$–potential function)**.** Γ^{c} *is a weighted relative potential game with respect to* $\mathcal{S}_0$ *if and only if* Γ'^{c}*,with payoff functions* $\frac{1}{w_i}\pi_i$*, is an exact relative potential game with respect to* $\mathcal{S}_0$ □

Proof. The sufficient condition is trivial. For the necessary condition, we recall that from the definition of a weighted potential game Γ^{c} we have $\pi_i(s_i, s_{-i}) - \pi_i(s'_i, s_{-i}) = w_i\left(P(s_i, \boldsymbol{s}_{-i}) - P(s'_i, \boldsymbol{s}_{-i})\right)$. On the other hand, from the definition of a potential game Γ'^{c} it holds $\frac{1}{w_i}\pi_i(s_i, s_{-i}) - \frac{1}{w_i}\pi_i(s'_i, s_{-i}) = P(s_i, \boldsymbol{s}_{-i}) - P(s_i, \boldsymbol{s}'_{-i})$ Clearly these are equivalent. ■

We are now ready to prove that convex weighted relative potential games subject to h-RBR dynamics globally converge to an ε-GNE of the game.

Theorem 5.14. *Suppose that* Γ^{c} *is a bounded weighted relative potential game with respect to* $\mathcal{S}_0$*. Then for every* $\epsilon > 0$*, and initial action profile* $s(0) \in \boldsymbol{\mathcal{S}}_0$*, every* $\epsilon-$*improvement path generated by* (5.9)*, converges to an* ε*-GNE in finite time.* □

Proof. If we prove that the above statement holds true in the case of an bounded exact relative potential game, then Lemma 5.13 ensures convergence also in the case of a bounded weighted relative potential game. Thus, we can consider Γ^{c} as an exact relative potential game with respect to $\mathcal{S}_0$. By the definition of $\mathcal{F}_i^{\mathrm{c}}(\boldsymbol{s}_{-i}, h_i)$ in (5.7), it follows that the dynamics (5.9) are positively invariant w.r.t $\boldsymbol{\mathcal{S}}_0$. That is,

$$\forall t \geq 0: \quad \boldsymbol{s}(t) \in \boldsymbol{\mathcal{S}}_0. \tag{5.15}$$

Because Γ^{c} is a bounded game, it follows from Definition 5.12 that P must be bounded as well. That is,

$$\exists M > 0: \quad |P(\boldsymbol{s})| \leq M, \ \forall \boldsymbol{s} \in \boldsymbol{\mathcal{S}}_0\,. \tag{5.16}$$

To prove that the game has the Approximate Finite Improvement Property (AFIP), we use contradiction. Suppose γ is an infinite ϵ–improvement path. Denote the unique deviator at time t as i_t. By definition, if $i = i_t$ then

$$\pi_i(t+1) - \pi_i(t) > \epsilon, P(s_i(t+1), \boldsymbol{s}_{-i}(t+1)) - P(s_i(t), \boldsymbol{s}_{-i}(t)) > \epsilon. \tag{5.17}$$

This implies that

$$P(t) - P(0) > t\epsilon \Leftrightarrow P(t) > t\epsilon + P(0)\,. \tag{5.18}$$

Then, for every $\epsilon > 0$

$$\lim_{t\to\infty} P(t) = \infty. \tag{5.19}$$

On the other hand, by assumption P is a bounded function, hence a contradiction arises. Hence, every ϵ–improvement path terminates after a finite number of time steps T, i.e., the game has the AFIP. Hence, it holds that

$$P(\boldsymbol{s}(T)) \leq M < P(\boldsymbol{s}(T)) + \epsilon \Rightarrow P(\boldsymbol{s}(T)) > M - \epsilon,$$

which completes the proof. ■

For generalized ordinal potential games, bounded payoff functions do not imply that the generalized ordinal potential function is bounded, and consequently convergence is not guaranteed. However, if one assumes that the generalized potential function is bounded for every $\boldsymbol{s} \in \boldsymbol{\mathcal{S}}_0$, then the result in Theorem 5.14 carries over to this more general class of convex games.

5.5 Networks of best and h-relative best responders

We have showed that the dynamics of games over network in which all players adopt h-RBR converge to a GNE. Due to their non-innovative nature, the h-RBR dynamics converge for a more general class of games than BR dynamics do. Moreover, any homogeneous action profile, in which all players choose the same strategy, is a trivial GNE of the game; h-RBR dynamics share this property with imitation dynamics. Adding *noise* in the decision-making process will destabilize most of these trivial equilibrium profiles; a characterization of the stochastically stable states is an interesting development for this theory. Instead, we investigate an interesting scenario in which both best responses and relative best responses occur in the network game. In this case, it is not guaranteed that a homogeneous action profile is an equilibrium and the behavior may be closer to real-world scenarios in which decision makers value social information in different ways. For simplicity, we assume that players always best respond or always relative best respond, and thus do not switch between the two decision rules. Although this is a simplification, it is reasonable in accordance to the empirical findings in [126] suggesting that humans tend to *consistently* apply a decision rule under a variety of contexts. The following results follow immediately from the proofs of Theorem 5.6 and Theorem 5.14 for finite and convex games respectively.

Corollary 5.15. *Consider a generalized ordinal potential game Γ^{f}, in which players consistently adopts BR or consistently h-RBR dynamics. For all initial condition, every improvement path generated by* (5.9)*, converges to a ε-GNE in finite time* □

Corollary 5.16. *Consider a weighted potential game Γ^{c}, in which players consistently adopts BR or consistently h-RBR dynamics. For every $\epsilon > 0$, and initial condition, every ϵ–improvement path generated by* (5.9)*, converges to a ε-GNE in finite time. The same holds for generalized ordinal potential games Γ^{f}, with $\epsilon = 0$.* □

Having a mixture of best responders and h-relative best responders in a game over network can lead to significantly different behaviors and equilibrium profiles, that have not yet been studied. As more and more engineering systems take into account the complex behavior of humans, one may be interested in how different levels of social learning or different topologies of local information flows, and how they affect the long run behavior of economic decision-making models. In the remainder of the chapter, we investigate the various effects that social learning through h-RBR have in economic models related to technology adoption and energy scheduling.

5.6 Competing products with network effects

Suppose there are two competing substitute products X and Y on a market with N players using one of the two. Each product has an associated price $\gamma > 0$ and $\lambda > 0$ and individuals decide which product to use. We are not modeling how a certain initial product adoption came to be, but we are interested in if, in the long run, one of the technologies dominates the other or not. However, it is worth mentioning that the adoption of a new product can be modeled in a very similar manner. Let $s_i = 1$ and $s_i = 0$ denote that player i uses product X or Y, respectively. Due to *network effects* [158], the utility that individuals experience from these products partially depends on the number of individuals that are using it. Agents may perceive this network effect differently, but, in general, a growing number of users increases the utility of the product. To this end, let $S = \sum_{i \in \mathcal{I}} s_i$ denote the number of players in the network using product X. The network effect associated to the product X is modeled with an affine function, that is for all $i \in \mathcal{I}$

$$G_i(S) \coloneqq aS + b_i, \quad a > 0,\ b_i \geq 0.$$

Because Y and X are substitutes, their network effects have a negative correlation. Such that, for all $i \in \mathcal{I}$

$$H_i(N - S) \coloneqq d(N - S) + f_i, \quad d > 0,\ f_i \geq 0\,.$$

The individual network effect parameters b_i and f_i reflect the incidence on the decision of player i. If b_i is large, the player is eager to use product X even though the network effect is small. In a simplified model in which $d_i = 0$ and the player simply needs to choose to adopt a new product, the players with high b_i represent "early adopters" and those with low b_i "laggards", see [13]. The utility that player $i \in \mathcal{I}$ obtains from using X or Y is given by

$$G_i(S) - \gamma, \text{ and } H_i(N - S) - \lambda.$$

Hence, the payoff of a player i is

$$\pi_i(s_i, \boldsymbol{s}_{-i}) = [G_i(S) - \gamma]\, s_i + (1 - s_i)\, [H_i(N - S) - \lambda]\,.$$

The following function is an exact potential function for the competing product game

$$P(\boldsymbol{s}) \coloneqq \sum_{i=1}^{N} (b_i + \lambda - dN - \gamma - f_i) s_i - d \sum_{i=1}^{N} s_i + (a + d) \left[\sum_{i=1}^{N} s_i^2 + \frac{1}{2} \sum_{i=1}^{N} \sum_{j \neq i}^{N} s_i s_j \right].$$

In fact, the difference in the payoff of $i \in \mathcal{I}$ is

$$\begin{aligned} \pi_i(0, \boldsymbol{s}_{-i}) - \pi_i(1, \boldsymbol{s}_{-i}) &= H_i(N - S) - \lambda - G_i(S + 1) + \gamma \\ &= d(N - S) + f_i - \lambda - a(S + 1) - b_i + \gamma \end{aligned}$$

and the difference in the potential is

$$P(0, \boldsymbol{s}_{-i}) - P(1, \boldsymbol{s}_{-i}) = -(b_i + \lambda - dN - \gamma - f_i) + d - (a + d)(S + 1),$$

which equals the payoff difference.

Because this competing product game is an exact potential game, our results for finite games apply. In particular, for every mixture of best responders and h-relative best responders, the fraction of the population using product X and Y will converge to a GNE in finite time.

Remark 5.6 (Mixed strategy extension)**.** *Because the competing products model is an exact potential game, it follows that its mixed-strategy extension, in which the players choose the fraction of time to use product X or Y, is also a potential game [127, Lemma 2.10]. Hence, the convergence results for h-RBR dynamics in convex games are valid in this game. Such a setting can represent the dynamics of Example 5.2, in which the network effect of renewable energy may capture an increasingly cleaner environment.* □

The addition of h-RBR players is of particular interest in this model because they add a social influence to the competing product game that is not captured by best responses in which decisions of a player are solely based on the aggregate network effects and the cost and benefit parameters of the player. For relative best responses, the local information exchanges in the underlying social network of the players will affect their decisions.

Figure 5.2 shows that, when $h = 1$, the variation in the fraction of X adopters in the network is significantly larger than in myopic BR dynamics. These simulation results were obtained for 100 random initial conditions with $\approx 50\%$ adopters of product X. The slopes of the network effects are: $a = 0.15$ and $b = 0.12$. To introduce variation in the individual payoffs, the offsets b_i and f_i were randomly chosen between 0 and 10. The costs associated with the products are $\gamma = 3$ and $\lambda = 2$. The large variation in the standard deviation of the X adopters in the network is also typical for imitation dynamics and can be attributed to the variation in the initial action profiles, the stochasticity of the activation sequence and the large variety of GNE in the product adoption game. From the blue line in Figure 5.2 it can also be seen that, on average, the relative performance considerations in the 1-RBR dynamics allow for significantly higher adoption rates of product X that has a higher cost ($\gamma > \lambda$), but also a larger slope of the network effect ($a > b$). Naturally, these social effects are rather sensitive to the payoffs. In particular, for large networks, the network effect in the payoff can become dominant and an obvious best choice may arise that dominates under both types of dynamics. Figure 5.3 shows another simulation on a similar network under the same conditions as in Figure 5.2. One can observe that the 1-RBR dynamics have very similar qualitative behavior as imitation dynamics in which players imitate the strategy of their best performing neighbor.

A peculiar feature of h-RBR dynamics is shown in Figure 5.4. As h increases up to the point that all players employ RBR, the standard deviation in the fraction of X adopters tends to decrease. Interestingly, even for random initial conditions, the network structure causes significant differences in the behavior between BR and h-RBR dynamics (shown in Figure 5.2). However, these differences decrease when the connectivity in the network increases. In Figure 5.5, the extreme case

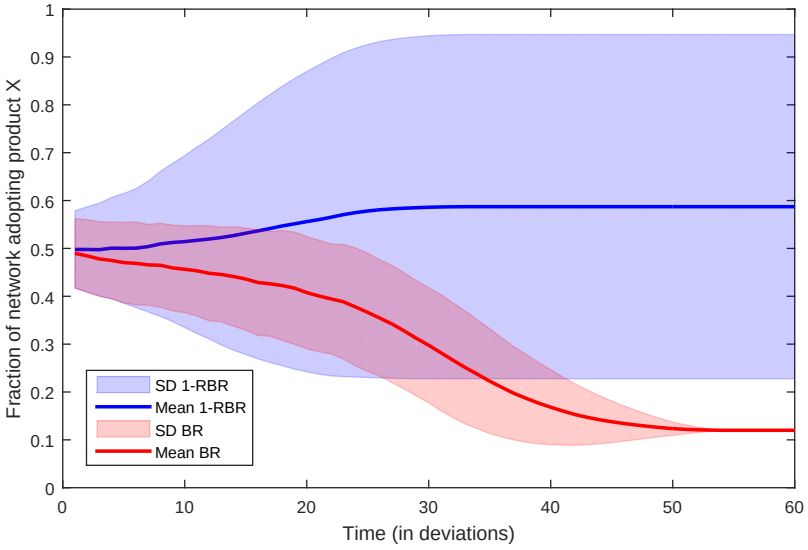

Figure 5.2: Fraction of players adopting product X in a product adoption game with a *preferential attachment* network [9] with 50 players. The solid lines and shaded areas represent the mean and standard deviation of 100 iterations with random initial conditions. Comparison between BR (in red) and 1–RBR (in blue) dynamics.

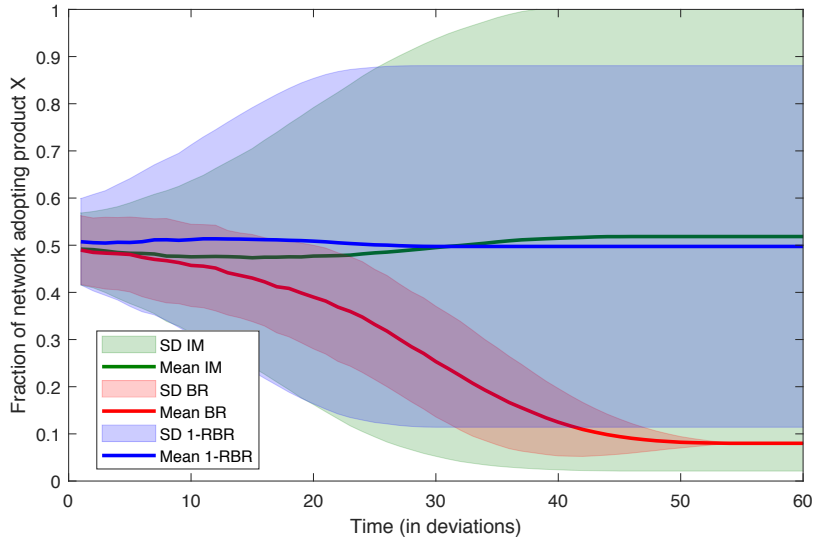

Figure 5.3: Fraction of players adopting product X in a product adoption game. Comparison of BR (in red), imitate-the-best (indicated by IM) and 1-RBR dynamics on a preferential attachment network of size 50.

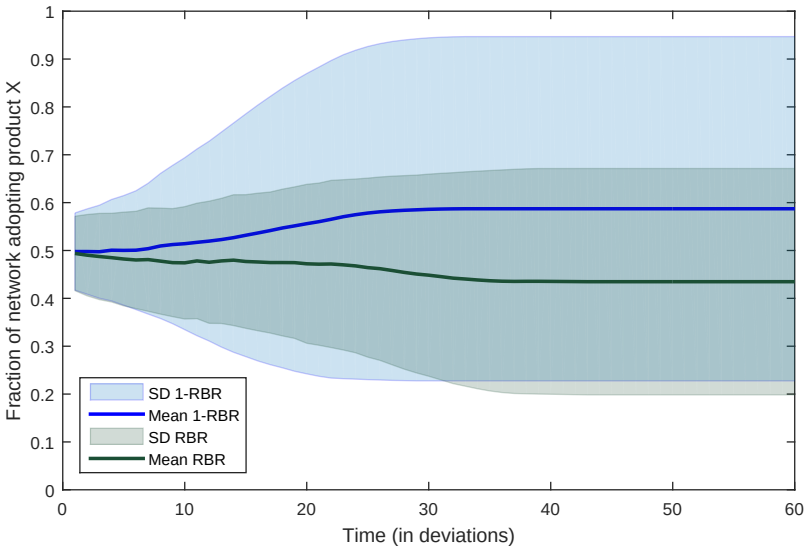

Figure 5.4: Fraction of players adopting product X in a product adoption game. Comparison of 1–RBR (in blue) and RBR (in green).

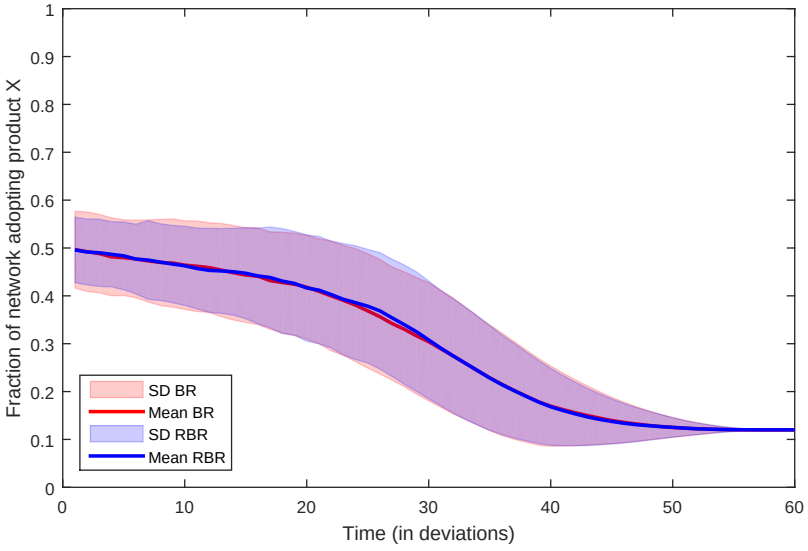

Figure 5.5: Fraction of players adopting product X in a product adoption game over a complete network with 50 players.

of a well-mixed network is shown and it can be seen that the behavior of the two types of dynamics are very similar.

5.7 Conclusion and final remarks

The h-RBR dynamics model partial rationality of the players in the game and are defined for both finite and convex games. These dynamics converge for a general class of games to a GNE. These novel dynamics are "compatible" with BR dynamics, since convergence still holds for games in which there is a mixture of relative and myopic best responders. By varying the coefficient h, different levels of rationality can be mimicked. We showed via simulations that the game evolution is close to the one obtained via imitation dynamics, if $h = 1$, and to the one achieved via BR dynamics, if h is high. Finally, we simulated the problem of product adoptions under different configuration to validate our theoretical findings.

6

Charging coordination for plug-in electric vehicles

In this chapter, we consider the charge scheduling coordination of a fleet of plug-in electric vehicles, developing a hybrid decision-making framework for efficient and profitable usage of the distribution grid. Each vehicle's charging dynamics are affected by the aggregate behavior of the whole fleet, and they are modeled as an inter-dependent, mixed-logical-dynamical system. The coordination problem is formalized as a generalized mixed-integer aggregative potential game, and solved via semi-decentralized implementation of a sequential best-response algorithm that leads to an approximated equilibrium of the game.

6.1 Introduction

PEVs represent a promising alternative to the conventional fuel-based transportation [103]. However, they require a "smart" charge/discharge coordination to prevent undesired electricity demand peaks and congestion in the low-voltage distribution grid [26, 49]. Indeed, a fleet of PEVs can serve as a *mobile extension* of the grid, mitigating the intermittent behavior of renewable energy sources by storing (or providing) energy when the generation is higher (or lower) than the load demand. These capabilities are known as grid-to-vehicle (g2v) and vehicle-to-grid (v2g), respectively [161]. In this context, a key role is played by the "fleet manager" or "aggregator", which is partially responsible for providing charging services to the PEVs, coordinating the charge/discharge schedule to fulfill the needs of the PEVs owners and (desirably) providing ancillary services to the distribution system operator [103, 26]. For all these reasons, the charge and discharge scheduling of a PEV fleet is attracting high research interest [119, 91, 139, 120, 98, 184].

An attracting framework, that suitably condenses both individual interests and intrinsic limitations related with the shared facilities, is represented by noncooperative game theory. The game's equilibrium, for instance in [119], allows to design a scheduling to coordinate the charging of a population of PEVs in a decentralized fashion with the aim of filling the night-time valley, while each PEV minimizes its individual charging cost. A similar non-cooperative equilibrium problem is addressed in [139] using mean field game theory, introducing general, convex, local charging constraints. In [91], the authors generalize the notion of valley-filling and study a social welfare optimization problem associated with the charging scheduling, proposing an asynchronous optimization algorithm. The PEV charging coordination game is further developed in [120] by including the battery degradation cost within the cost function of each vehicle. More generally, a semi-decentralized coordination algorithm based on fixed-point operator theory is proposed in [98], which achieves global exponential convergence to an aggregative equilibrium, even for large population size, while a distributed approach based on the progressive second price auction mechanism has been recently proposed in [184]. Most of these works allows each PEV to only purchase energy, preventing the provision for instance of ancillary services to the distribution system operator.

However, most of the models adopted in the literature do not describe the intrinsic discrete operations of each PEV, e.g., being plugged-in or plugged-out from one of the available charging points, in g2v or in v2g mode [179, 173, 151]. The selfish nature of each PEV, which pursues an economic, possibly profitable, usage of the charging station, together with the presence of both continuous (amount of energy charged/discharged) and discrete decision variables (operating mode) over a certain prediction horizon, motivates us to model the charge scheduling coordination of the PEVs as a collection of inter-dependent mixed-integer optimization problems, where the coupling constraints arise in aggregative form (Section 6.2). In fact, the common electricity price, as well as the operational limitations of the charging station, e.g., the number of charging points, directly depend on the overall behavior of the fleet. We then formulate the coordination problem as a mixed-integer aggregative game (Section 6.3), proving that it corresponds to a

Mixed-Integer Generalized Potential Game (MI-GPG) [81]. To the best of authors knowledge, this is the first work that models the PEV charging/discharging problem as a mixed-integer aggregative game. Furthermore, we assume the presence of an aggregator, i.e., the charging station, that provides the aggregate information to the fleet and allows to compute an (approximated) equilibrium of the game by means of a semi-decentralized implementation of a sequential best-response algorithm (Section 6.4). Finally, we define the game setup and the solution algorithm via numerical simulations on an illustrative scenario (Section 6.5).

6.2 PEVs scheduling and charge as a system of mixed-logical-dynamical systems

We start by modeling the charge scheduling of a PEV over a certain prediction horizon by first introducing the dynamics of the State of Charge (SoC) and the related control variables, both discrete and continuous. Then, we define the cost function that each PEV aims to minimize and, by means of logical implications, the interactions arising both among the set of PEVs itself and with the charging station.

6.2.1 Decision variables and the SoC dynamics

Let $\mathcal{I} \coloneqq \{1, \dots, N\}$ be the set indexing a population of PEVs that share the charging resources on a single charging station with a finite number of charging points, over a prediction horizon $\mathcal{T} \coloneqq \{1, \dots, T\}$. For each vehicle $i \in \mathcal{I}$, the SoC of its battery at time $t \in \mathcal{T}$ is denoted by $x_i(t) \in [0, 1]$, where $x_i(t) = 1$ represents a fully charged battery, while $x_i(t) = 0$ a completely discharged one. The amount of energy exchanged between each vehicle and the charging station, during the time period t, is denoted by $u_i(t) \in \mathcal{U} \coloneqq [\underline{u}, \overline{u}]$, $\underline{u} < 0$, $\overline{u} > 0$. Specifically, $u_i(t)$ takes positive values if vehicle i absorbs power during the time period t, while negative values if it gives energy back. For all $t \in \mathcal{T}$, we assume the dynamics of the SoC described by

$$x_i(t+1) = x_i(t) + b_i \delta_i(t) u_i(t) - (1 - \delta_i(t)) \mu_i(t), \tag{6.1}$$

where $b_i = \frac{\eta_i}{C_i}$ is a positive parameter which depends on the efficiency $\eta_i > 0$ of the i-th battery and the corresponding capacity $C_i > 0$. In (6.1), $\delta_i(t) \in \mathbb{B}$ is a scheduling variable of each vehicle, i.e., $\delta_i(t) = 1$ if the i-th PEV is connected to the charging station at time t, 0 otherwise. Within the dynamics (6.1), we consider that the SoC of the battery decreases when the vehicle is actively driving. In fact, if $\delta_i(t) = 0$, the SoC decreases according to $\mu_i(t) > 0$, which represents the discharge due to the energy consumed while driving during the time period $t \in \mathcal{T}$. Therefore, $\mu_i(t) > 0$ (driving vehicle) can only affects the SoC when the PEV is not connected to the grid, i.e., $\delta_i(t) = 0$. If the vehicle is not driving during the time period t, then $\mu_i(t) = 0$. Thus, over the whole horizon $\mathcal{T}$, each PEV $i \in \mathcal{I}$ has decision variables $u_i \coloneqq \mathrm{col}((u_i(t))_{t \in \mathcal{T}})$, $\delta_i \coloneqq \mathrm{col}((\delta_i(t))_{t \in \mathcal{T}})$ and controls the SoC, $x_i \coloneqq \mathrm{col}((x_i(t))_{t \in \mathcal{T}})$.

6.2.2 Cost function

In the previous section, we introduced both, the model of the SoC and the constraints that the PEVs have to satisfies while the interact with the grid. Now, we proceed to present the last component that defines the game, the local cost function J_i of each PEV $i \in \mathcal{I}$. We assume that when a PEV is connected to the charging station it can either acquire energy from the charging station, or give it back. In the first scenario, the value of the required power $u_i(t)$ is positive and in the second negative. If the i-th PEV at time $t \in \mathcal{T}$ requires power from the charging station, i.e., $u_i > 0$, then it faces a cost associated to the purchase and to the battery degradation. We model the first term as $c(d(t) + \sum_{j \in \mathcal{I} \setminus \{i\}} u_j^+(t))u_i(t)$, where we assume a fair electricity market with the cost per energy unit $c > 0$, the same for all the PEVs, and $u_j^+(t) \coloneqq u_j(t)$ if $u_j(t) \geq 0$, 0 otherwise. The values $(d(t))_{t \in \mathbb{N}}$ represent the non-PEV loads of the network, which is assumed to be a-priori known, while $\sum_{i \in \mathcal{I} \setminus \{i\}} u_i^+(t) =: a_i(\boldsymbol{u}(t))$ is the *aggregate* demand of energy associated with the set of PEVs at time t. Then, we assume that the degradation cost associated to the charging of the battery is proportional to the variation of the energy exchanged between the PEV and the charging station, i.e., $\rho_i^+(u_i(t) - u_i(t-1))^2$, with $\rho_i^+ > 0$ depending on each single battery. Therefore, for all $t \in \mathcal{T}$ and for all $i \in \mathcal{I}$, the cost function associated to the charging phase (g2v) is

$$J_i^{\text{g2v}}(u_i(t), \boldsymbol{u}_{-i}(t)) \coloneqq c(d(t) + a_i(\boldsymbol{u}(t)))u_i(t) + \rho_i^+(u_i(t) - u_i(t-1))^2.$$

Similarly, when the PEV gives energy to the charging station, i.e., $u_i(t) < 0$, the v2g interaction implies a degradation cost due to the battery discharge, i.e., $\rho_i^-(u_i(t) - u_i(t-1))^2$, $\rho_i^- > 0$. However, this cost is generally compensated by a reward $r_i(t)u_i(t)$, for some given values $(r_i(t))_{t \in \mathbb{N}}$, that a PEV receives from the charging station for actively participating in the scheduling. Thus, the cost function related with the v2g mode reads as

$$J_i^{\text{v2g}}(u_i(t)) \coloneqq r_i(t)u_i(t) + \rho_i^-(u_i(t) - u_i(t-1))^2,$$

for all $t \in \mathcal{T}$ and $i \in \mathcal{I}$.

Now, we introduce two binary decision variables, i.e., δ_i^{c}, $\delta_i^{\text{d}} \in \mathbb{B}$, which allow to model the mutual actions of charging/discharging and guarantee that the local cost function is equal to 0 when $u_i = 0$. They shall satisfy the next logical implications, for all $t \in \mathcal{T}$ and for all $i \in \mathcal{I}$:

$$[\delta_i^{\text{c}}(t) = 1] \iff [u_i(t) \geq 0], \tag{6.2}$$

$$[\delta_i^{\text{d}}(t) = 1] \iff [u_i(t) \leq 0]. \tag{6.3}$$

Namely, $\delta_i^{\text{c}}(t)$ (or, equivalently, $\delta_i^{\text{d}}(t)$) is equal to 1 if the PEV is not discharging (not charging), and 0 otherwise. Finally, for all $i \in \mathcal{I}$, the complete cost function reads as follows

$$\begin{aligned} J_i(u_i, \delta_i^{\text{d}}, \delta_i^{\text{c}}, \boldsymbol{u}_{-i}) \coloneqq \textstyle\sum_{t \in \mathcal{T}} & J_i^{\text{g2v}}(u_i(t), \boldsymbol{u}_{-i}(t)) \left(1 - \delta_i^{\text{d}}(t)\right) \\ & + J_i^{\text{v2g}}(u_i(t))(1 - \delta_i^{\text{c}}(t)), \end{aligned} \tag{6.4}$$

where $\delta_i^{\text{c}} \coloneqq \text{col}((\delta_i^{\text{c}}(t))_{t \in \mathcal{T}})$ and $\delta_i^{\text{d}} \coloneqq \text{col}((\delta_i^{\text{d}}(t))_{t \in \mathcal{T}})$.

6.2.3 Local and global constraints

The possible interactions between each PEV and the grid are of two different natures. Local interactions regard each PEV as a single entity, while global interactions consider the overall behavior of the population of PEVs and impose constraints, e.g., due the limited capacity of the grid. By considering a generic PEV $i \in \mathcal{I}$, first we assume that, for all $t \in \mathcal{T}$, it is desired that the corresponding level of SoC is at least equal to a reference level $x_i^{\text{ref}}(t) \in [0, 1]$, i.e.,

$$x_i^{\text{ref}}(t) \leq x_i(t)\,. \tag{6.5}$$

The driving pattern of each PEV, that is usually assumed to be known *a priori*, limits the possible values of $\delta_i(t)$. Namely, if $\mu_i(t) > 0$ then feasible set of $\delta_i(t)$ is $\mathcal{B}(t) = 0$; otherwise $\mathcal{B}(t) = \mathbb{B}$. Thus, the feasible set $\mathcal{B}(t)$ of $\delta_i(t)$ becomes time varying.

If $\delta_i(t)$ is left free, then it may force a vehicle to persistently switch between being connected and unconnected during consecutive time intervals. This behaviour is not only unnatural, but could also acceleragte the battery's degradation [125]. To exclude this potential source of damage, we impose that, if a PEV is plugged-in at a certain time $t \in \mathcal{T}$, i.e., $\delta_i(t-1) = 0$ and $\delta_i(t) = 1$, then it has to remain connected to the charging station for at least $h_i \in \mathbb{N}$ consecutive time intervals, where $h_i \leq T$. Thus, for all $i \in \mathcal{I}$ and $t \in \mathcal{T}$, this constraint is cast using the following logical implication

$$[\delta_i(t-1) = 0] \wedge [\delta_i(t) = 1] \Rightarrow [\delta_i(t+h) = 1,\, \forall h \leq h_i]. \tag{6.6}$$

Next, to exclude that a PEV charges or discharges when it is plugged-out (i.e., $\delta_i(t) = 0$), we impose that $u_i(t) \in \mathcal{U}(t) \coloneqq [\underline{u}\delta_i(t), \overline{u}\delta_i(t)]$. Thus, $u_i(t) = 0$ if $\delta_i(t) = 0$, otherwise u_i takes values in $[\underline{u}, \overline{u}]$. Moreover, to exclude that a vehicle is plugged-in without being neither charged nor discharged, we impose that $\delta_i(t) = 0$, if $u_i(t) = 0$. Thus, the next logical implication needs to be satisfied for all $t \in \mathcal{T}$ and $i \in \mathcal{I}$:

$$[u_i(t) = 0] \iff [\delta_i(t) = 0]. \tag{6.7}$$

Successively, due to the intrinsic limitations of the grid capacity $\overline{d} > 0$, we assume that the amount of energy required in a single time period by both the PEVs and non-PEV loads cannot be greater than $\overline{d}$. This translates into a constraint on the PEVs total demand, i.e.,

$$d(t) + \textstyle\sum_{j \in \mathcal{I}} u_j(t) \in \left[0, \overline{d}\right]. \tag{6.8}$$

Finally, it is natural to assume that the charging station has a finite number of charging spots, i.e., the number of vehicles that can charge/discharge at the same time cannot exceed a finite value $\overline{v} \in \mathbb{N}$. Thus, we impose, for all $t \in \mathcal{T}$,

$$\textstyle\sum_{j \in \mathcal{I}} \delta_j(t) \leq \overline{v}\,. \tag{6.9}$$

6.2.4 Mixed-integer game formulation

We conclude this section by summarizing a preliminary formulation of the optimization problem for the scheduling and charging/discharging of each PEV as follows:

$$\forall i \in \mathcal{I} : \begin{cases} \min\limits_{u_i, x_i, \delta_i, \delta_i^{\mathrm{d}}, \delta_i^{\mathrm{c}}} & J_i(u_i, \delta_i^{\mathrm{d}}, \delta_i^{\mathrm{c}}, \boldsymbol{u}_{-i}) \\ \text{s.t.} & (6.1), x_i(t) \in [0,1], \\ & u_i(t) \in \mathcal{U}(t), \delta_i(t) \in \mathcal{B}(t), \\ & \delta_i^{\mathrm{c}}(t), \delta_i^{\mathrm{d}}(t) \in \mathbb{B}, \\ & (6.2), (6.3), \ (6.5)\text{–}(6.9), \ \forall t \in \mathcal{T}. \end{cases} \tag{$\mathcal{G}$}$$

We emphasize that several constraints in ($\mathcal{P}$), as well as the cost function, are either expressed as logical implications, or directly depend on the evaluation of a logical proposition. In the next section, we translate all these logical implications into mixed-integer-linear inequalities, hence the problem in ($\mathcal{P}$) as a (parametric) mixed integer quadratic problem.

6.3 Translating the logical implications into mixed-integer linear constraints

In this section, we show how to translate the logical implications (6.2), (6.6) and (6.7) in ($\mathcal{P}$) into mixed-integer linear constraints suitable for for a standard formulation of a Mixed-Integer Programming (MIP). Note that also the SoC dynamics in (6.1) and the cost function in (6.4) contain a binary variable. At the end of the procedure, such functions will not depend directly from the binary variables anymore, at the price of satisfying a set of additional linear constraints. Thus, by referring to the vehicle i, we introduce the constraints to be designed for each time interval $t \in \mathcal{T}$.

6.3.1 Preliminaries

For the sake of clarity, we adopt the same notation used in [76, 77], i.e., we define several patterns of inequalities that allow to handle all the constraints. Specifically, given a linear function $f : \mathbb{R} \to \mathbb{R}$, let us define $M \coloneqq \max_{x \in \mathcal{X}} f(x)$, $m \coloneqq \min_{x \in \mathcal{X}} f(x)$ with $\mathcal{X}$ being a compact set. Then, with $c \in \mathbb{R}$ and $\delta \in \mathbb{B}$, a first system $\mathcal{S}_{\geq}$ of mixed-integer inequalities correspond to $[\delta = 1] \iff [f(x) \geq c]$, i.e.,

$$\mathcal{S}_{\geq}(\delta, f(x), c) \coloneqq \begin{cases} (c - m)\delta \leq f(x) - m \\ (M - c + \epsilon)\delta \geq f(x) - c + \epsilon, \end{cases}$$

Here $\epsilon > 0$ is a small tolerance beyond which the constraint is regarded as violated. With the same idea, the following set of inequalities corresponds to $[\delta = 1] \iff$

$[f(x) \leq c]$:

$$\mathcal{S}_{\leq}(\delta, f(x), c) \coloneqq \begin{cases} (M-c)\delta \leq M - f(x) \\ (c+\epsilon-m)\delta \geq \epsilon + c - f(x). \end{cases}$$

Successively, we define the next block of inequalities, involving binary variables only, which allow to solve propositions with logical AND, i.e., $[\delta = 1] \iff [\sigma = 1] \wedge [\gamma = 1]$:

$$\mathcal{S}_{\wedge}(\delta, \sigma, \gamma) \coloneqq \begin{cases} -\sigma + \delta \leq 0 \\ -\gamma + \delta \leq 0 \\ \sigma + \gamma - \delta \leq 1, \end{cases}$$

Finally, to recast bilinear terms, i.e., products of binary and continuous variables, into a mixed-integer linear formulation, we introduce the following pattern of inequalities.

$$\mathcal{S}_{\Rightarrow}(g, f(x), \delta) \coloneqq \begin{cases} m\delta \leq g \leq M\delta \\ -M(1-\delta) \leq g - f(x) \leq -m(1-\delta) \end{cases}$$

The latter is equivalent to: $[\delta = 0] \implies [g = 0]$, while $[\delta = 1] \implies [g = f(x)]$.

6.3.2 The mixed-integer-linear constraints

The logical implications in (6.2) and (6.3) translate into:

$$\mathcal{S}_{\geq}(\delta_i^{\mathrm{c}}(t), u_i(t), 0), \tag{6.10}$$

$$\mathcal{S}_{\leq}(\delta_i^{\mathrm{d}}(t), u_i(t), 0). \tag{6.11}$$

By referring to the SoC dynamics in (6.1), the bilinear term $u_i\delta_i$ can be handled by following the procedure in [21], which allows to rewrite it as mixed-integer-linear inequalities by means of additional auxiliary variables (both real and binary, [172]). Specifically, we define the auxiliary variable $f_i \coloneqq u_i\delta_i \in \mathbb{R}$ that shall satisfy the pattern of inequalities:

$$\mathcal{S}_{\Rightarrow}(f_i(t), u_i(t), \delta_i(t)). \tag{6.12}$$

Thus, the SoC dynamics at the generic time $t \in \mathcal{T}$ reads as

$$x_i(t+1) = x_i(t) + b_i f_i(t) - (1 - \delta_i(t))\mu_i(t), \tag{6.13}$$

The same approach allows to manage the bilinear terms that appear in the cost function (6.4). Hence, by defining $g_i(t) \coloneqq u_i(t)(1-\delta_i^{\mathrm{c}}(t)) \in \mathbb{R}$, $s_i(t) \coloneqq u_i(t-1)(1-\delta_i^{\mathrm{c}}(t)) \in \mathbb{R}$, $\ell_i(t) \coloneqq u_i(t)(1-\delta_i^{\mathrm{d}}(t)) \in \mathbb{R}$ and $\kappa_i(t) \coloneqq u_i(t-1)(1-\delta_i^{\mathrm{d}}(t)) \in \mathbb{R}$, subjected to inequalities, for all $i \in \mathcal{I}$ and $t \in \mathcal{T}$,

$$\mathcal{S}_{\Rightarrow}(g_i(t), u_i(t), 1-\delta_i^{\mathrm{c}}(t)), \tag{6.14}$$

$$\mathcal{S}_{\Rightarrow}(s_i(t), u_i(t-1), 1-\delta_i^{\mathrm{c}}(t)), \tag{6.15}$$

$$\mathcal{S}_{\Rightarrow}(\ell_i(t), u_i(t), 1-\delta_i^{\mathrm{d}}(t)), \tag{6.16}$$

$$\mathcal{S}_{\Rightarrow}(\kappa_i(t), u_i(t-1), 1-\delta_i^{\mathrm{d}}(t)), \tag{6.17}$$

the cost function (6.4) reads as (omitting the dependencies),

$$J_i = c(d(t) + a_i(\boldsymbol{u}(t)))\ell_i(t) + r_i(t)g_i(t) + \rho_i^- \left(g_i(t) - s_i(t)\right)^2 + \rho_i^+(\ell_i(t) - \kappa_i(t))^2 \,. \tag{6.18}$$

Notice that via these variables we can rewrite also $a(\boldsymbol{u}(t)) = \sum_{j\in\mathcal{I}\setminus\{i\}} \ell_j(t)$. Let us consider proposition (6.7), equivalently rewritten as $[u_i(t) \leq 0] \wedge [u_i(t) \geq 0] \implies [(1-\delta_i(t)) = 1]$. Since δ_i^{c} and δ_i^{d} already satisfy the inequalities in (6.10) and (6.11), for all $t \in \mathcal{T}$, the constraint in (6.7) reads as

$$\mathcal{S}_\wedge(1 - \delta_i(t), \delta_i^{\mathrm{c}}(t), \delta_i^{\mathrm{d}}(t)). \tag{6.19}$$

Next, by referring to (6.6), we introduce a binary auxiliary variable α_i, which is equal to 1 when both $\delta_i(t-1) = 0$ and $\delta_i(t) = 1$, 0 otherwise. Hence, α_i shall satisfy, for all $t \in \mathcal{T}$, $[\alpha_i(t) = 1] \iff [(1 - \delta_i(t-1)) = 1] \wedge [\delta_i(t) = 1]$, which translates into the pattern of integer linear inequalities

$$\mathcal{S}_\wedge(\alpha_i(t), 1 - \delta_i(t-1), \delta_i(t)). \tag{6.20}$$

Thus, (6.6) can be rewritten as a nonlinear equality constraint

$$\alpha_i(t)\left(\sum_{h=1}^{h_i} \delta_i(t+h) - h_i\right) = 0.$$

Successively, we introduce a set of variables $\beta_i^{(h)} \in \mathbb{B}$ such that, for all $t \in \mathcal{T}$, $[\beta_i^{(h)}(t) = 1] \iff [\alpha_i(t) = 1] \wedge [\delta_i(t+h) = 1, \forall h \leq h_i]$, which corresponds to the following patterns of inequalities

$$\mathcal{S}_\wedge(\beta_i^{(h)}(t), \alpha_i(t), \delta_i(t+h)),\ \forall h \leq h_i. \tag{6.21}$$

This allows to rewrite the equality constraint in linear form

$$\textstyle\sum_{h=1}^{h_i} \beta_i^{(h)}(t) - \alpha_i(t)h_i = 0. \tag{6.22}$$

6.3.3 Final mixed-integer-linear model

By rearranging all the inequalities, we obtain the following mixed-integer aggregative game

$$\forall i \in \mathcal{I} : \begin{cases} \min\limits_{u_i, x_i, \ldots, \beta_i} & J_i(u_i, g_i, s_i, \ell_i, \kappa_i, \boldsymbol{u}_{-i}) \\ \text{s.t.} & (6.5), x_i(t) \in [0,1], \\ & (6.8)\text{–}(6.17), (6.19)\text{–}(6.22), \\ & u_i(t), f_i(t), g_i(t), s_i(t) \in \mathcal{U}(t), \\ & \ell_i(t), \kappa_i(t) \in \mathcal{U}(t),\ \delta_i(t) \in \mathcal{B}(t), \\ & \delta_i^{\mathrm{c}}(t), \alpha_i(t), \delta_i^{\mathrm{d}}(t) \in \mathbb{B},\ \forall t \in \mathcal{T}, \\ & \beta_i^{(h)}(t) \in \mathbb{B},\ \forall h \leq h_i, \forall t \in \mathcal{T}. \end{cases} \tag{6.23}$$

The coupling constraints in (6.8)–(6.9), as well as the cost function, depend on the aggregate behavior of the fleet of PEVs. By defining $z_i \coloneqq \mathrm{col}(u_i, x_i, \dots, \beta_i) \in \mathbb{R}^{n_i}$ and $\boldsymbol{z} \coloneqq \mathrm{col}((z_i)_{i\in\mathcal{I}}) \in \mathbb{R}^n$, $n \coloneqq \sum_{i\in\mathcal{I}} n_i$, as the vectors stacking local and collective mixed-integer variables, respectively, we have, for some suitable matrix A and vector b,

$$\forall i \in \mathcal{I} : \min_{z_i} J_i(z_i, \boldsymbol{z}_{-i}) \ \text{ s.t. } \ A\boldsymbol{z} \leq b. \tag{6.24}$$

6.4 PEVs charge coordination as a generalized mixed-integer potential game

Our aim is now to design suitable sequences of decisions that guarantee to each PEV an effective, economic, possibly profitable, usage of the electrical distribution network, while satisfying both the intrinsic limitations of the charging station itself, and by the presence of the other vehicles. We propose to achieve such a trade-off by formalizing the charge coordination of the set of PEVs as a MI-GPG [81], an instance of the GNEPs [79].

6.4.1 Potential game setup

First, we identify the player set with $\mathcal{I}$, and we define the feasible set of each player, i.e., $\mathcal{Z}_i(\boldsymbol{z}_{-i}) \coloneqq \{z_i \in \mathbb{R}^{n_i} \mid A(z_i, \boldsymbol{z}_{-i}) \leq b\}$, and $\boldsymbol{\mathcal{Z}} \coloneqq \{\boldsymbol{z} \in \mathbb{R}^n \mid A\boldsymbol{z} \leq b\}$. Next, we introduce the mixed-integer best response mapping for player i, given the strategies of the other players $\boldsymbol{z}_{-i}$:

$$z_i^\star(\boldsymbol{z}_{-i}) \coloneqq \operatorname*{argmin}_{z_i} J_i(z_i, \boldsymbol{z}_{-i}) \ \text{ s.t. } \ (z_i, \boldsymbol{z}_{-i}) \in \boldsymbol{\mathcal{Z}}. \tag{6.25}$$

Hence, in the proposed game $\Gamma \coloneqq (\mathcal{I}, \{J_i\}_{i\in\mathcal{I}}, \{\mathcal{Z}_i\}_{i\in\mathcal{I}})$, we are interested in the following notion of equilibrium.

Definition 6.1 (ε-Mixed-Integer Nash equilibrium)**.** Let $\varepsilon > 0$. $\boldsymbol{z}^* \in \boldsymbol{\mathcal{Z}}$ is an MINE of the game Γ in (6.25) if, for all $i \in \mathcal{I}$,

$$J_i(z_i^*, \boldsymbol{z}_{-i}^*) \leq \inf_{z_i \in \mathcal{Z}_i(\boldsymbol{z}_{-i}^*)} J_i(z_i, \boldsymbol{z}_{-i}^*) + \varepsilon. \qquad \square$$

In the following, we derive an exact potential function for the game at hand, i.e., a function that satisfies in Definition C.2(i). Consider the cost function in (6.18) defined for all $t \in \mathcal{T}$. Due to the particular structure of the cost of the acquired energy, it can be written in compact form as

$$J_i(z_i, \boldsymbol{z}_{-i}) = \phi_i(z_i) + \textstyle\sum_{j\in\mathcal{I}\setminus\{i\}} \omega_{ij}(z_i, z_j), \tag{6.26}$$

where $\phi_i(z_i) \coloneqq z_i^\top Q_i z_i + q_i^\top z_i$, for some suitable positive semi-definite matrix $Q_i \in \mathbb{R}^{n_i \times n_i}$ and vector $q_i \in \mathbb{R}^{n_i}$, while

$$\omega_{ij}(z_i, z_j) \coloneqq z_j^\top \begin{bmatrix} \mathbf{0} & \mathbf{0} & \mathbf{0} \\ \mathbf{0} & c\,I & \mathbf{0} \\ \mathbf{0} & \mathbf{0} & \mathbf{0} \end{bmatrix} z_i = c\,\ell_j^\top \ell_i. \tag{6.27}$$

Algorithm 6.1: Sequential best-response

Initialization: Choose $\boldsymbol{z}(0) \in \boldsymbol{\mathcal{Z}}$, set $k \coloneqq 0$
while $\boldsymbol{z}(k)$ is not an MINE **do**
  //choice of the agent to update
  $\mathcal{AG}$ **do**
    Chooses $i \coloneqq i(k) \in \mathcal{I}$
    Sets $p_i(\boldsymbol{u}(k))$ as in (6.29), $e(\boldsymbol{\delta}(k))$ as in (6.30)
    Sends $p_i(\boldsymbol{u}(k))$, $e(\boldsymbol{\delta}(k))$ to i
  end
  //computation of the local update
  Player i **do**
    Compute $z_i^*(k) \in z_i^\star(k)$ as in (6.25)
    if $J_i(z_i(k), p_i(\boldsymbol{u}(k))) - J_i(z_i^*(k), p_i(\boldsymbol{u}(k))) \geq \varepsilon$
      $z_i(k+1) \coloneqq z_i^*(k)$
    else
      $z_i(k+1) \coloneqq z_i(k)$
  end
  $\mathcal{AG}$ collects $z_i(k+1)$
  Set $z_j(k+1) \coloneqq z_j(k)\ \forall j \neq i$, $k \coloneqq k+1$

The following theorem proves that the games at hand is a MI-GPG and introduces the associated potential function, the proof can be found in Appendix 6.7.

Theorem 6.2. *The game* Γ *in* (6.25) *is an MI-GPG with exact potential function*

$$P(\boldsymbol{z}) \coloneqq \sum_{i\in\mathcal{I}} \left(\phi_i(z_i) + \sum_{j\in\mathcal{I}, j<i} \omega_{ij}(z_i, z_j) \right). \tag{6.28}$$

□

Proof. The proof replicates the one in [75, Prop. 2]. ■

To conclude, we recall that the set of ε-approximated minimum over $\boldsymbol{\mathcal{Z}}$ of P corresponds to a subset of the MINE of the game [154, Th. 2].

6.4.2 Semi-decentralized solution algorithm

To compute a solution of (6.24), each player requires the aggregate information over the whole horizon $\mathcal{T}$, i.e., the PEVs demand of energy $a_i(\boldsymbol{u}) \coloneqq \mathrm{col}((a_i(\boldsymbol{u}(t)))_{t\in\mathcal{T}})$, or, equivalently, the price associated to such demand

$$p_i(\boldsymbol{u}) \coloneqq c(d + a_i(\boldsymbol{u})), \tag{6.29}$$

with $d \coloneqq \mathrm{col}((d(t))_{t\in\mathcal{T}})$, and the number of available charging points at the charging station, i.e.,

$$e(\boldsymbol{\delta}) \coloneqq \overline{v}\mathbf{1}_T - \left(\mathbf{1}_N^\top \otimes I_T\right)\boldsymbol{\delta}, \tag{6.30}$$

where $\boldsymbol{\delta} \coloneqq \mathrm{col}((\delta_i)_{i\in\mathcal{I}})$. Specifically, while the number of available charging points $e(\boldsymbol{\delta})$ reflects the coupling constraint in (6.9), the price of energy $p_i(\boldsymbol{u})$ affects both the constraints and the cost function in (6.26), which can be equivalently expressed as function of z_i and $p_i(\boldsymbol{u})$.

In this context, it seems unrealistic or, at least, impractical to assume full communication among all the potential users of the same charging station, over the same horizon $\mathcal{T}$. Therefore, to compute an MINE, we propose a semi-decentralized implementation of the sequential best-response method, summarized in Algorithm 6.1, that includes an aggregator $\mathcal{AG}$, whose role is played by the charging station, within the communication pattern. According to [103], we assume the driving patterns of each PEV to be known by the $\mathcal{AG}$. As shown in the scheme in Fig. 6.1, at each iteration k, the aggregator $\mathcal{AG}$ chooses the next agent taking part in the game, communicating the price of energy and the number of available charging points. With this information, the selected agent computes a best response and decides to change strategy only if it leads to an (at least) ε-improvement in terms of minimization of its cost function. Finally, $\mathcal{AG}$ collects the decision of such agent, while the remaining part of players keeps its strategy unchanged.

Corollary 6.3. *Choose arbitrarily $\varepsilon > 0$ and assume that, in Algorithm 6.1, there exists $K > 0$ such that $j \in \{i(k), i(k+1), \dots, i(k+K)\}$ for all $j \in \mathcal{I}$ and $k \geq 0$. Algorithm 6.1 computes an MINE, $\boldsymbol{z}^* \in \boldsymbol{\mathcal{Z}}$, of the game Γ in* (6.25) *in finite time.* □

Proof. In view of Theorem 6.2, the game Γ in (6.25) is an MI-GPG. Therefore, by [154, Th. 5], the sequential best-response based Algorithm 6.1 converges to an MINE in finite time. ■

Remark 6.1 (Accuracy of the approximited solution)**.** *In Algorithm 6.1, the value of ε can be chosen arbitrarily small. From [154, Th. 5], it follows that the convergence is achieved in finite time and that the number of iterations is inversely proportional to ε. Therefore, it is possible to achieve an arbitrarily high level of accuracy at the cost of losing the convergence in finite time, i.e., only asymptotic*

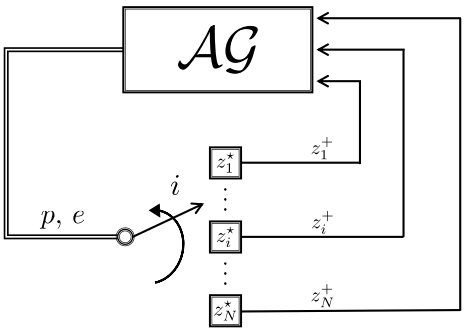

Figure 6.1: Semi-decentralized implementation of Algorithm 6.1, where $z_i^+ \coloneqq z_i(k+1)$.

Table 6.1: Values of the parameters used in the numerical simulations.

Name	[ ]	Description	Values
N		PEVs number	6
T		Time intervals in $24h$	48
u	[kWh]	Energy exchanged per interval	$[-7.5, 7.5]$
η		Battery efficiency	0.85
C_i	[kWh]	Battery capacity	[40, 75]
x_0		Initial SoC of battery	0.23
x^{ref}		Ref. battery SoC	[0.2, 0.85]
c	[€/kWh]	Energy cost	1.09×10^{-3}
$\bar{r}$	[€/kWh]	Constant reward	1.23×10^{-3}
ρ^+ (ρ^-)	[€/kWh^2]	Degradation cost	$1(0.5) \times 10^{-3}$
$\overline{d}$	[kWh]	Grid power capacity	45
h		Min. consecutive v2g slots	5
$\overline{v}$		Max. connected PEVs	5

convergence is guaranteed. Moreover, it is possible to rely on the procedure described in [154, Th. 6] to compute a 0*-MINE at the price of significantly increase computational burden. It is interesting to notice that this type of equilibria have the characteristic of being Pareto optimal, see [154, Th. 3]. So, the choice of* ε *should reflect the preference of the policy-maker on whether he prefers and accurate or fast equilibrium.* □

6.5 Numerical simulations

In this section, we show numerical results obtained by solving the MI-GPG in (6.25) with parameter values specified in Tab. 6.1 (see [119, 151]) and reward function $r(t)$ chosen proportional to the nominal demand and the energy generated by the vehicles, i.e., $r(t) \coloneqq \overline{r}(\sum_{j \in \mathcal{I} \setminus \{i\}} u_j^-(t) + d(t))$, where $d(t)$ corresponds to a typical daily demand curve [151], and $u_j^-(t)$ defined analogously to $u_j^+(t)$.

For a subset of PEVs, we show in Fig. 6.2 that the SoC $x_i(t)$, as well as the scheduling variable $\delta_i(t)$, satisfies the constraints on the required SoC $x_i^{\text{ref}}(t)$ (6.5) and on the number h_i of plugged-in consecutive intervals (6.6).

In Fig. 6.3, note that the peak value of $d(t)$ exceeds the maximum capacity $\overline{d}$ at $t =$ 19 h. Consequently, the constraint (6.8) forces some of the vehicles to discharge during this time period, showing the so-called "valley filling" phenomenon.

Finally, Fig. 6.4 shows the value of the potential function $P(\boldsymbol{z})$ and the convergence of the algorithm after approximately 25 iterations.

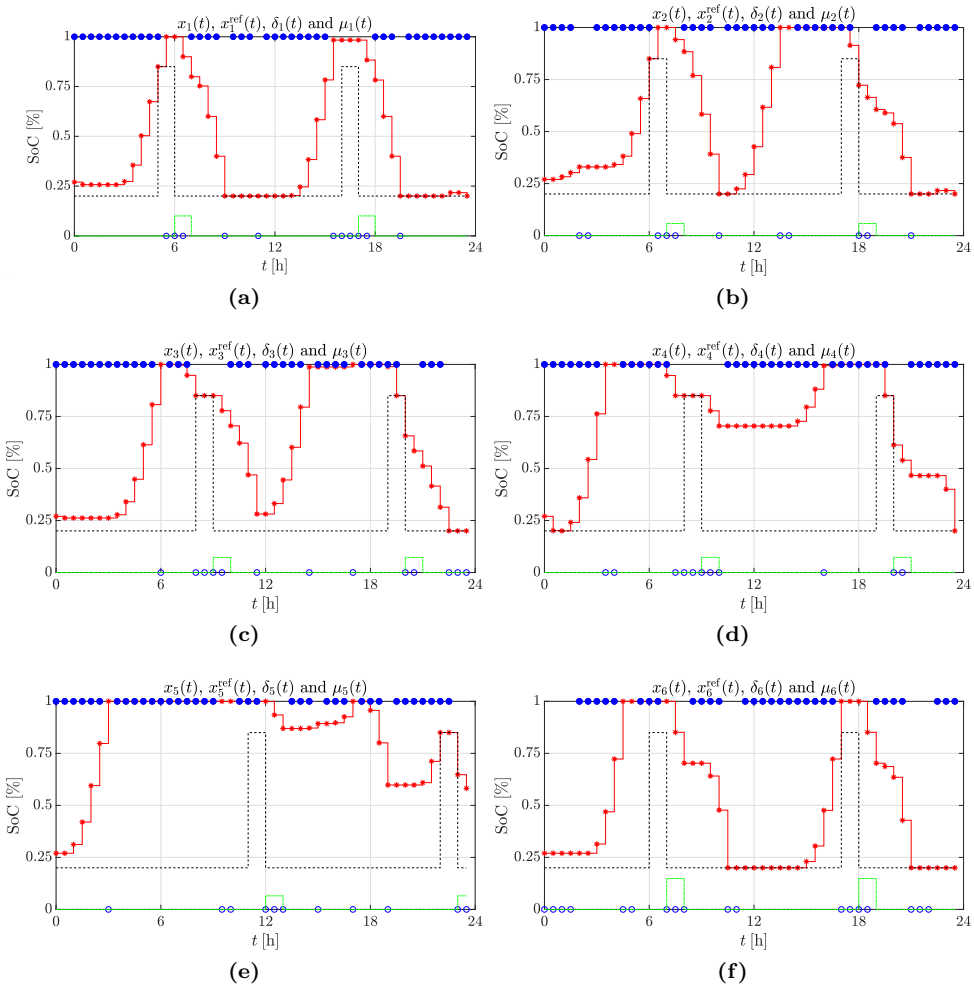

Figure 6.2: For each PEV $i \in \mathcal{I}$, the SoC $x_i(t)$ (solid red line), the desired lower bound of the SoC $x_i^{\mathrm{ref}}(t)$ (dashed black line), the value of the binary sheduling variable $\delta_i(t)$ (empty and filled blue circles) and $\mu_i(t)$ (dashed green line), over the horizon $\mathcal{T}$.

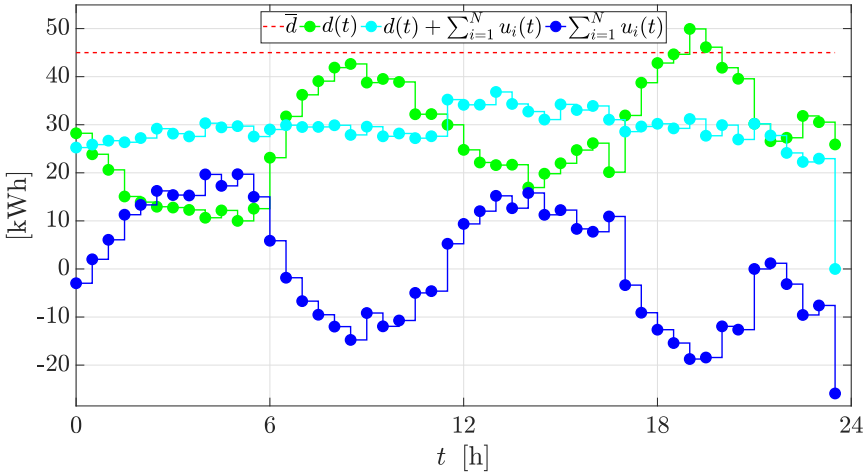

Figure 6.3: Power required by the load in the grid $d(t)$ (green), the one exchanged with the fleet, $\sum_{i=1}^{N} u_i(t)$ (blue) and the maximum capacity of the charging station, $\overline{d}$ (red dashed).

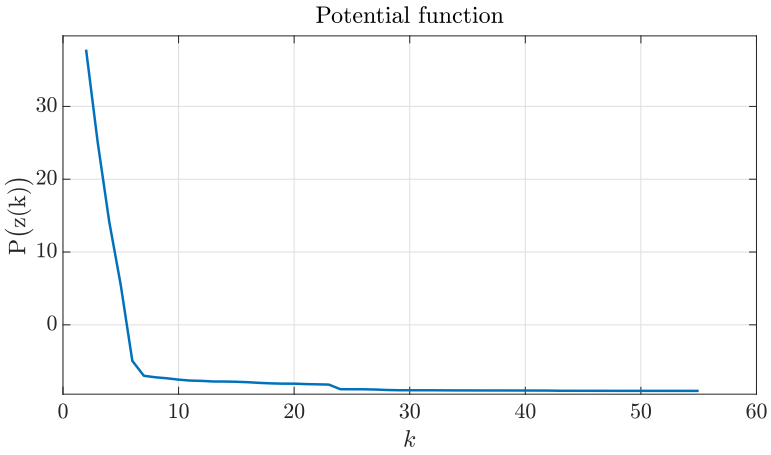

Figure 6.4: The values of the potential function $P(\boldsymbol{z})$ associated to the updating PEV in Algorithm 6.1.

6.6 Conclusion and outlook

A mixed-integer aggregative game can efficiently solve the charge scheduling coordination of a fleet of PEVs, each one modeled as a system of mixed-logical-dynamical systems. Discrete decision variables, as well as logical propositions, allow to describe the different interests of each PEV and the heterogeneous interactions between the set of vehicles and the charging station. By playing the role of central aggregator, the charging station is key in computing an (approximated) equilibrium of the associated generalized potential game in a semi-decentralized fashion. In fact, the specific sequence of activation of the PEVs highly influences both the outcome of the game and the speed of convergence. The analysis of this phenomenon is left to future works, as well as the generalization in the case of multiple charging stations, i.e., possible multiple central aggregators.

6.7 Appendix

Proof of Theorem 6.2:

Let us consider an arbitrary player $i \in \mathcal{I}$, a strategy $\boldsymbol{z}_{-i}$ such that $\mathcal{Z}_i(\boldsymbol{z}_{-i}) \neq \varnothing$ and two feasible strategies $z_i,\ y_i \in \mathcal{Z}_i(\boldsymbol{z}_{-i})$. Then, the cost variation of the i-th player that results by adopting the two strategies is:

$$J_i(z_i, \boldsymbol{z}_{-i}) - J_i(y_i, \boldsymbol{z}_{-i}) = h_i(z_i) - h_i(y_i) + \sum_{j \in \mathcal{I} \setminus \{i\}} w_{ij}(z_i, z_j) - \sum_{j \in \mathcal{I} \setminus \{i\}} w_{ij}(y_i, z_j).$$

Successively, let us consider the variation of the potential function in (6.28) due to the deviation of strategy of the i-th player, while the others keep the same strategies, i.e.,

$$P(z_i, \boldsymbol{z}_{-i}) - P(y_i, \boldsymbol{z}_{-i}) = h_i(z_i) - h_i(y_i) + \sum_{k \in \mathcal{I}} \sum_{h \in \mathcal{I}, h<k} w_{kh}(z_k, z_h) - \sum_{k \in \mathcal{I}} \sum_{h \in \mathcal{I}, h<k} w_{kh}(z_k, z_h).$$

Here, the only non-null elements resulting from the difference of the two summations are those that couple player i, the only one that changes strategy, with all the other players in $\mathcal{I}$. Specifically, for all $k < i$,

$$\sum_{h \in \mathcal{I}, h<k} w_{kh}(z_k, z_h) - \sum_{h \in \mathcal{I}, h<k} w_{kh}(z_k, z_h) = 0,$$

while, for all $k > i$,

$$\sum_{h \in \mathcal{I}, h<k} w_{kh}(z_k, z_h) - \sum_{h \in \mathcal{I}, h<k} w_{kh}(z_k, z_h) = w_{ki}(z_k, z_i) - w_{ki}(z_k, y_i).$$

On the other hand, when $k = i$, we have that the difference of the summations corresponds to $w_{ih}(z_i, z_h) - w_{kh}(y_i, z_h)$, for all $h < i$. Therefore, given the particular structure of each term in (6.27), characterized by the symmetric block $c\,I$ that makes $w_{ki}(z_k, z_i) = w_{ik}(z_i, z_k)$ for all $k \in \mathcal{I} \setminus \{i\}$ and for all $z_i \in \mathcal{Z}_i(\boldsymbol{z}_{-i})$, we have $J_i(z_i, \boldsymbol{z}_{-i}) - J_i(y_i, \boldsymbol{z}_{-i}) = P(z_i, \boldsymbol{z}_{-i}) - P(y_i, \boldsymbol{z}_{-i})$ and then the function P in (6.28) is an exact potential function for the game Γ. ■

7

Highway congestion control via smart electric mobility

In this chapter, we study how to alleviate highway traffic congestion by encouraging plug-in hybrid and electric vehicles to stop at a charging station around peak congestion times. Specifically, we design a pricing policy to make the charging price dynamic and dependent on the traffic congestion, predicted via the cell transmission model, and the availability of charging spots. Furthermore, we develop a novel framework to model how this policy affects the drivers' decisions by formulating a mixed-integer potential game. Technically, we introduce the concept of "road-to-station" (r2s) and "station-to-road" (s2r) flows, and show that the selfish actions of the drivers converge to charging schedules that are individually optimal in the sense of Nash. Then, we propose a case study and simulate the adoption of a dynamic charging price depending on the traffic congestion. We use real traffic data of the A13 highway stretch between The Hague and Rotterdam, in The Netherlands, to identify the Cell Transmission Model. Then, we show the benefits of our strategy in terms of traffic congestion alleviation. Finally, we carry out a sensitivity analysis of the proposed algorithm and discuss how to optimize its performance.

7.1 Introduction

7.1.1 Motivation

In the recent years, urban mobility in highly populated cities is becoming a central issue in many countries. Some alarming statistics show a pressing need for change, as the cost of congestion to the EU society is no less than €267 billion per year [156]. In fact, an inefficient transportation system deteriorates not only the citizens' well-being, but also the environment, since traffic jams heavily increase the emission of CO_2 [12]. The classical solution to the Traffic Demand Management (TDM) problem is to increase the roads' capacity or to build alternative routes. Although this approach produces tangible benefits [92], policymakers and researchers are exploring alternatives that may be sensibly faster and cheaper to implement, and provide dynamic solutions that adapt to the traffic evolution.

7.1.2 "Hard" and "soft" policies

In the past years, there has been a growing interest from the research community in the problem of ATDM, i.e., a dynamic or even real-time solution to the traffic control problem. The literature on the topic can be divided into the design of "hard" and "soft" policies to address the problem [36]. The hard type of measures tries to enforce changes in the drivers' behavior by imposing some constraints or penalizing undesired actions. For example, several works studied the use of dynamic traffic signaling or traffic lights to influence the current traffic flow [134, 101]. In [148], the authors impose an artificial bottleneck to decrease the flow in strategic part of the road and achieve an alleviation of the congestion. Another approach is to increase the transit price of the most congested roads in order to boost the use of alternative routes [66].

On the other hand, the so-called soft measures are designed to incentivize virtuous driver behaviors, and have their roots in behavioural economics and psychology. The word *soft* refers to the possibility of the drivers to ignore the incentives and stick to their regular conduct [36]. Usually, these policies do not imply any physical change of the infrastructure. In fact, they rely on economic incentives or leverage psychological phenomena to change the drivers' habits. Most of the solutions based on this approach lack strong theoretical fundations, and an *a posteriori* analysis is performed to study their consequences. In [150], the author explores the effectiveness of: monetary incentives, gifts and social nudges tapping into altruistic values. A personalized set of incentives (mostly monetary) is proposed in [104], where a platform is introduced that enables the commuters to receive incentives if they change their departure time to off-peak hours or use an alternative. Several other pilot studies have been performed and they have experimentally validated the benefits of soft policies, see [22] among others. It is important to stress that these two classes of measures are not always mutually exclusive but they can be used in combination to amplify the final effect of congestion alleviation, as we advocate in this chapter.

7.1.3 Smart charging of PEVs

The continuous growth of the number of PEVs is also due to the improvements in the smart charging, allowing the vehicles to charge up to 150 kW. This technology increases the appeal of short stops for the users, making the PEVs more similar to fuel vehicles. This motivates several studies on how the PEV drivers may optimize their charging schedules and how they affect the distribution network. The results in [119] and Chapter 6, tackle the problem of high peaks in the energy demand by proposing a dynamic energy price that leads to a change in the charging habits of the PEV owners, and consequently to the so-called "valley filling" effect [140]. Some recent works considered smart charging coupled with mobility. In [174], the smart charging problem is enhanced by considering also the travel habits. However, the goal is solely to decrease the energy peak demand rather than the traffic congestion level. Other works focus on optimizing the charging of the PEVs to decrease their travel time [109, 63]. However, in these works the overall congestion level is not taken into account in the decision process. For this reason, we cannot consider these solutions as a form of ATDM. To the best of the authors' knowledge, it is still an open, yet appealing, problem to develop ATDM strategies based on smart-charging of PEVs whose main goal is traffic congestion alleviation.

7.1.4 Main contribution

Inspired by the conventional ramp metering control and motivated by the rising number of PEVs, we propose for the first time a novel ATDM based on soft measures (via monetary incentives) that leverages smart fast charging of PEVs in the road to alleviate traffic congestion during rush hours. Specifically, we propose a dynamic energy price discounted proportionally to the (predicted) congestion level. This approach encourages the PEV owners to stop for charging when the congestion level is (going to be) high, thus aligning the goal of the traffic control with the drivers' self-interest. In the following, we emphasize our main contributions:

- We use for the first time the electricity price as control input for the ATDM. While historically, traffic control had suffered from a lack of control means, this additional control input may prove itself essential to achieve the desired results by acting in synergy with the classical TDM.
- We enrich the CTM with the introduction of road-to-station (r2s) and station-to-road (s2r) flows, newly defined to model the entering and leaving of the PEVs in and out of a CS.
- We carry out a formal analysis of the effects of the presented soft policy by describing the decision process of the PEV drivers as a generalized exact potential game.
- We propose a semi-decentralized control scheme ensuring that the PEVs involved in the decision reach an optimal charging schedule that represents their individual best trade-off between monetary saving and travel time.

- We validate our theoretical framework by means of real traffic data extracted in from the A13 highway stretch between The Hague and Rotterdam, in The Netherlands.
- We show by simulation that a dynamic charging price policy can alleviate highway traffic congestion and significantly reduce the peak traffic congestions.
- We perform an extensive sensitivity analysis on the system parameters, which allows us to identify the "best" setup that maximizes the performance of the proposed strategy

7.1.5 Structure of the chapter

The chapter is divided into two parts, the first formalizes and introduces the theoretical framework developed to tackle the problem (Sections 7.2–7.5) and the second validates the strategy proposed by analyzing a case study (Sections 7.6–7.10). Specifically, in Section 7.2 we introduce the traffic model considered and in Section 7.3 we model the decision making carried out by the PEVs owners. Then, we describe the algorithm solving this problem in Section 7.5. The case study begins with the identification of the traffic model via real data, in Section 7.6. In Section 7.8, the parameters are chosen such that they reflect the current market scenario and the performance of the algorithm are analyzed in detail. Then, a sensitivity analysis is carried out in Section 7.9 for the most relevant decision parameters. To conclude, we discuss the policies that emerge from the simulation results as the most effective in Section 7.10.

7.2 Cell Transmission Model with Charging Station

We consider a freeway stretch without ramps and only one CS where PEVs may stop. In the literature, the most used model for traffic control is the CTM, see [58].

7.2.1 Cell Transmission Model with charging station

Here, we explicitly introduce a revised version of the CTM described in [85, Sec. 3.3.1] adapted to our problem. We consider the discretized version of the model where each time interval $[kT, (k+1)T)$ of length T is denoted by an integer $k \in \mathbb{N}$. The highway stretch is modeled as a chain of N subsequent *cells* (Figure 7.1). The vehicles in each cell $\ell \in \mathcal{N} \coloneqq \{1, \dots, N\}$ are a mixture of PEVs and non-PEVs moving at a constant speed. Two subsequent cells are connected via an *interface* that models a certain flow of vehicles, whose value depends on the cells' demand

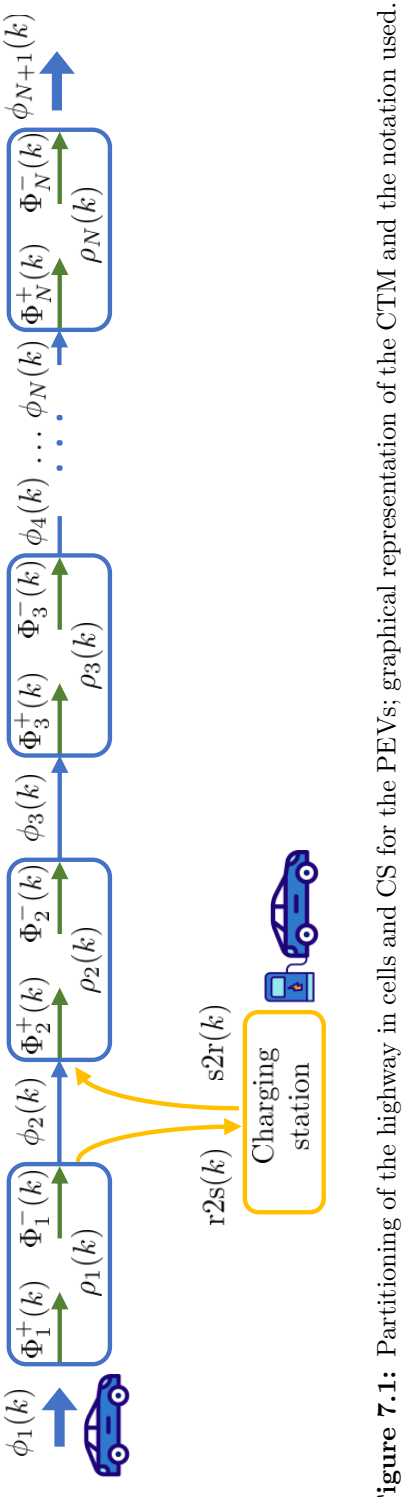

Figure 7.1: Partitioning of the highway in cells and CS for the PEVs; graphical representation of the CTM and the notation used.

and supply capabilities. Without loss of generality, we assume that the CS is located between the first two cells. To formalize the CTM, for every cell $\ell \in \mathcal{N}$ and interval $k \in \mathbb{N}$, we introduce the following set of variables:

- $\rho_\ell(k)$ [veh/km]: traffic density of cell ℓ during k;
- $\Phi_\ell^+(k)$ [veh/h] (resp. $\Phi_\ell^-(k)$): total flow entering (exiting) the cell ℓ during k;
- $\phi_\ell(k)$ [veh/h]: flow entering cell ℓ from cell $\ell - 1$ during k; $\phi_1(k)$ (resp. $\phi_{N+1}(k)$) is the flow entering (exiting) the highway during the same interval;

We enrich the conventional CTM introducing two flows:

- r2s(k) [veh/h]: flow of PEVs entering the CS during k;
- s2r(k) [veh/h]: flow of PEVs exiting the CS during k.

Then, we associate a set of fixed parameter to each cell ℓ:

- L_ℓ [km]: cell length;
- $\overline{v}_\ell$ [km/h]: free-flow speed;
- w_ℓ [km/h]: congestion wave speed;
- $q_\ell^{\max}$ [veh/h]: maximum cell capacity;
- $\rho_\ell^{\max}$ [veh/km]: maximum jam density.

Each cell can be seen as an input-output system where the inflow is the input and the outflow the output. The dynamics of the density ρ_ℓ of cell $\ell \in \mathcal{N}$ read as

$$\rho_\ell(k+1) = \rho_\ell(k) + \frac{T}{L_\ell}\left(\Phi_\ell^+(k) - \Phi_\ell^-(k)\right) , \tag{7.1}$$

where the inflow and outflow are defined as

$$\Phi_\ell^-(k) \coloneqq \begin{cases} \phi_{\ell+1}(k) + \text{r2s}(k) & \text{if } \ell = 1 \\ \phi_{\ell+1}(k) & \text{otherwise} \end{cases} \tag{7.2a}$$

$$\Phi_\ell^+(k) \coloneqq \begin{cases} \phi_\ell(k) + \text{s2r}(k) & \text{if } \ell = 2 \\ \phi_\ell(k) & \text{otherwise.} \end{cases} \tag{7.2b}$$

Thus, the flows entering and exiting the CS modify only the definition of the in-flow of cell 2 and out-flow from cell 1.

Remark 7.1 (r2s and s2r flows)**.** *The concepts of* r2s *and* s2r *flows are inspired by the "off-ramp" and "on-ramp" flows [58], respectively, and used to model the temporary stop of some PEVs at the CS, which leads, differently from the off- and on-ramp flows, to a mutual dependency between* r2s *and* s2r*. We investigate this further in Sections 7.3 and 7.5. In the literature, only the on-ramp flow can be controlled, e.g. via a toll, while our control action influences the off-ramp flow as well.* □

The *demand* $D_{\ell-1}(k)$ of cell $\ell-1$ and the *supply* $S_\ell(k)$ of cell ℓ directly influence the admissible flow between the two cells, see Figure 7.2. The former is the flow that cell $\ell-1$ can send to cell ℓ in the time interval k, while $S_\ell(k)$ describes the flow that cell ℓ can receive in the same interval:

$$D_{\ell-1}(k) \coloneqq \min\left\{\overline{v}_{\ell-1}\rho_{\ell-1}(k)\,,\, q_{\ell-1}^{\max}\right\}\,, \tag{7.3a}$$

$$S_\ell(k) \coloneqq \min\left\{w_\ell\big(\rho_\ell^{\max}-\rho_\ell(k)\big)\,,\, q_\ell^{\max}\right\}\,. \tag{7.3b}$$

The relations in (7.3) directly define $\phi_\ell(k)$ in (7.2). In fact, if $\ell \in \{3,\dots,N\}$, then the flow between the cells reads as $\phi_\ell \coloneqq \min\{D_{\ell-1}(k),\, S_\ell(k)\}$. On the other hand, the flow ϕ_2 between cell 1 and 2 is described by a more complex relation, due to the presence of the CS:

$$\begin{cases} \phi_2 \coloneqq D_1 - \mathrm{r2s} & \text{if } D_1 - \mathrm{r2s} \le S_2 - \mathrm{s2r} \\ \phi_2 \coloneqq S_2 - \mathrm{s2r} & \text{otherwise}\,, \end{cases} \tag{7.4}$$

where the time dependency is omitted. The first case in (7.4) reflects the free-flow scenario, while the second reflects the presence of a congestion, as the supply of cell 2 is saturated by $\phi_2(k)$ and $\mathrm{s2r}(k)$. Finally, $\phi_1(k)$ and $\phi_{N+1}(k)$ are the input and output flows of the CTM, respectively.

Throughout this section, we have defined the whole CTM except for $\mathrm{r2s}(k)$ and $\mathrm{s2r}(k)$. The remainder of this theoretical part of the chapter is devoted to design the decision process that the PEVs carry out to choose whether or not it is worth stopping at the CS. In turn, this determines $\mathrm{r2s}(k)$ and $\mathrm{s2r}(k)$, as we show in Section 7.5.

7.3 Decision making process

We assume the presence of a Highway Operator (HO) that aims at minimizing the congestion. It does that by discounting the energy price if the level of congestion grows (or is expected to grow). In this setup, the HO would have the role of the so-called *choice architect*, by designing the price at all time intervals. Our solution leverages two main aspects: first, if the road is congested, the benefit of keep driving decreases, due to a longer travel time, and, at the same time, stopping at a CS to charge becomes more profitable due to an energy price discount. Secondly, we take advantage of the *range anxiety*, which is a well-known cognitive bias affecting PEV drivers making them impatient to stop at a CS even if they do not strictly need it [133].

We model the multi-agent decision process of the PEVs exiting cell 1, at every time interval k, by defining a set of interdependent local optimization problems. Each PEV (or agent/player) aims at minimizing its own local cost function subject to a set of constraints, where couplings between the agents arise in both the cost functions and the constraints. From a mathematical point of view, specific in our problem setup, the collection of all these optimization problems determines a *mixed-integer potential game* subject to best-response dynamics. The output of

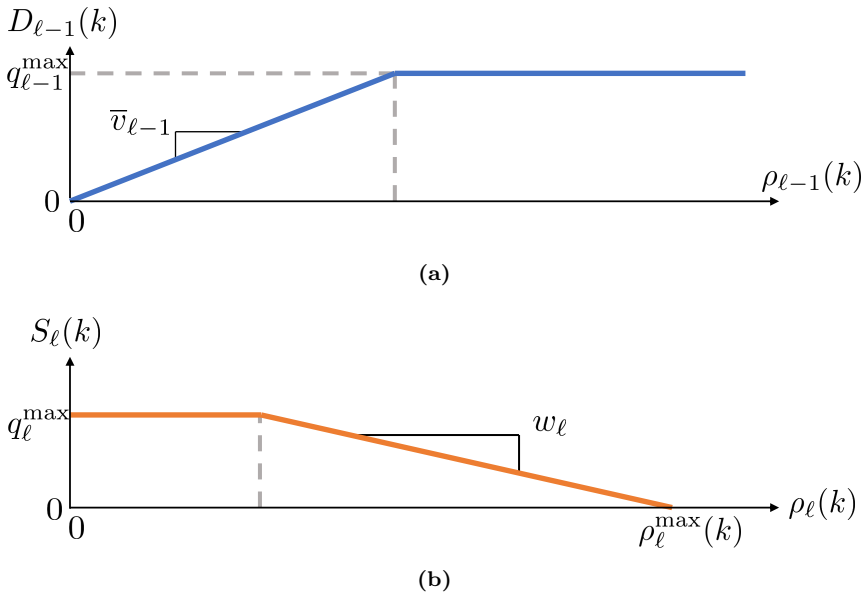

Figure 7.2: (a) Demand function of the cell $\ell - 1$, (b) Supply function of the cell ℓ.

the decision making process (or game) is the set of all the choices (or strategies) of the PEVs to stop or not at the CS, which affects the r2s flow. The s2r flow is instead a consequence of how long the agents decide to linger at the CS.

7.3.1 Cost function

Next, we design the cost function of the PEVs exiting cell 1 that are involved in the decision making process. We postulate that the interest of each driver is twofold: he is interested in minimizing the travel time, while he is also willing to save money for charging his PEV. Between the two, in most cases, the primary concern will be the travel time, especially in normal traffic conditions, when no discount is present. Nevertheless, the travel time aspect becomes less relevant if a heavy congestion arises; in this situation, the relative impact of the travel time spent at the CS decreases, and at the same time, the discounted energy price may steer the decision of the agent towards the choice of stopping to charge the PEV.

Number of vehicles

During each time interval $k \in \mathbb{N}$, the number of vehicles involved in the decision process is $n_{\text{EV}}(k)$, which may vary due to the traffic conditions. From (7.2), we show that the total number of vehicles exiting cell 1 during k is $\Phi_1^-(k)\,T$. Between those, the fraction of PEVs is denoted by $p_{\text{EV}} \in [0, 1]$. By relying on (7.2a) and

(7.4), we attain

$$\begin{cases} n_{\mathrm{EV}} = \lfloor p_{\mathrm{EV}} D_1 \, T \rfloor \,, & \text{if } D_1 - \mathrm{r2s} \leq S_2 - \mathrm{s2r} \\ n_{\mathrm{EV}} = \lfloor p_{\mathrm{EV}} (S_2 - \mathrm{s2r} + \mathrm{r2s}) T \rfloor \,, & \text{otherwise} \end{cases} \tag{7.5}$$

where the time dependency is omitted and $\lfloor x \rfloor \in \mathbb{N}$ denotes the floor of $x \in \mathbb{R}$.

To compute $n_{\mathrm{EV}}(k)$ via (7.5), the value of $\mathrm{r2s}(k)$ is necessary, even though it is the solution of the decision process that we are defining. Thus, it is not possible to exactly define $n_{\mathrm{EV}}(k)$. At the same time, $\mathrm{s2r}(k)$ does not affect the computation of $n_{\mathrm{EV}}(k)$, since it is due to PEVs already at the CS, so not involved in the decision process arising at time k. To overcome this impasse, we compute the number of agents $n(k)$ involved in the game under the assumption of maximum congestion, namely if no agent stops at the charging station ($\mathrm{r2s}(k) = 0$). Then the number of agents taking part in the decision process is obtained as

$$\begin{cases} n(k) = \lfloor p_{\mathrm{EV}} \, D_1(k) T \rfloor \,, & \text{if } D_1(k) + \mathrm{s2r}(k) \leq S_2(k) \\ n(k) = \lfloor p_{\mathrm{EV}} (S_2(k) - \mathrm{s2r}(k)) T \rfloor \,, & \text{otherwise} \,. \end{cases}$$

This assumption not only implies that $n(k)$ can be computed for every k, but also that all the vehicles involved in the game manage to exit cell 1 during the time interval k, and therefore being able to implement their strategies.

Decision variables and the SoC dynamics

The time-varying set indexing the $n(k)$ PEVs taking part in the game during the k-th time interval is denoted by $\mathcal{I}(k) \coloneqq \{1, \ldots, n(k)\}$. The decisions of the agents are performed over a prediction horizon $\mathcal{T}(k)$ of T_{h} time intervals. The length of the time intervals in the decision making process may be longer than the one used in the CTM. Specifically, we assume intervals of length lT, with $l \in \mathbb{N}$. Thus, the PEVs should plan their behavior over the set of intervals $\mathcal{T}(k) \coloneqq \{k, k+1, \ldots, k+T_{\mathrm{h}}\}$, where each index denotes an interval of length lT, e.g., $k \in \mathcal{T}(k)$ represents here $[kT, kT + lT)$ and similarly $k+1 \in \mathcal{T}(k)$ denotes $[kT + lT, kT + 2lT)$.

The SoC of the battery of every PEV $i \in \mathcal{I}(k)$ at time $t \in \mathcal{T}(k)$ is denoted by $x_i(t) \in [0, 1]$, where $x_i(t) = 1$ represents a fully charged battery, while $x_i(t) = 0$ a completely discharged one. The amount of energy purchased by agent $i \in \mathcal{I}(k)$ during the time period $t \in \mathcal{T}(k)$ is $u_i(t) \geq 0$. For every interval $t \in \mathcal{T}(k)$, the SoC reads as

$$x_i(t+1) = x_i(t) + b_i u_i(t) \,, \tag{7.6}$$

where $b_i = \frac{\eta_i}{C_i} > 0$ is a coefficient associated to the battery efficiency $\eta_i \in (0, 1]$ and capacity $C_i > 0$. Let us introduce the variable $\delta_i(t) \in \mathbb{B} \coloneqq \{0, 1\}$ as a binary decision variable, which takes value $\delta_i(t) = 1$ if the vehicle is actively charging at the CS and $\delta_i(t) = 0$ otherwise:

$$[\delta_i(t) = 1] \iff [u_i(t) > 0], \quad \forall t \in \mathcal{T}(k), \, \forall i \in \mathcal{I}(k). \tag{7.7}$$

The logical implication above entails that the energy purchased by PEV i is positive if and only if $\delta_i(t) = 1$, therefore we define $u_i(t) \in \mathcal{U}(t) \coloneqq [\underline{u}\delta_i(t), \overline{u}\delta_i(t)]$, with $\overline{u} > 0$

(respectively $\underline{u} > 0$) being the maximum (minimum) energy that the vehicle can receive from the CS in a single time interval. We define a first collection of decision variables associated with each PEV $i \in \mathcal{I}(k)$, over the whole horizon $\mathcal{T}(k)$, as the collective vectors $u_i \coloneqq \mathrm{col}((u_i(t))_{t\in\mathcal{T}})$, $\delta_i \coloneqq \mathrm{col}((\delta_i(t))_{t\in\mathcal{T}})$ and the evolution of the SoC, $x_i \coloneqq \mathrm{col}((x_i(t))_{t\in\mathcal{T}})$.

Travel time and congestion

An important quantity influencing the PEV decisions is the additional time $\xi(t) \geq 0$ that a PEV would experience due to the presence of congestion. Specifically, $\xi(t)$ denotes the difference between the travel time that a PEV experiences to actually travel throughout the cells $\{2, \dots, N\}$ and the one it would spend in conditions of free flow. It provides insightful information on the traffic evolution, allowing the PEVs to discern whether or not they prefer to stop at the CS. If agent $i \in \mathcal{I}(k)$ decides to stop for charging, the congestion it will experience, when it merges back in the mainstream during the time interval $t_i \in \mathcal{T}(k)$, depends also on those that were behind it at the time of the decision $k < t_i$. Among all the vehicles exiting cell 1 in the time interval $(k, t_i]$, the PEVs have the possibility to stop for charging, deciding via a process akin to the one that agent i is currently carrying out. For this reason, the exact value of $\xi(t)$ cannot be computed in advance by agent i for the whole prediction horizon. We work around this difficulty by adopting a conservative approximation of $\xi(t)$, computed assuming that all the PEVs in $\mathcal{I}(k)$ and the ones following them do not stop at the CS. This leads to a value of $\xi(t)$ that over-estimates the actual experienced travel time. This approximation allows the agents to cope with the worst-case scenario, hence being able to meet possible time constraints. Moreover, it can be computed at every time interval and provides insightful information on the potential traffic evolution.

For a cell $\ell \in \mathcal{N}$, the vehicles' speed is attained as $v_\ell(k) = \Phi_\ell^-(k)/\rho_\ell(k)$. If an agent i enters cell ℓ during the time interval k and it takes $\bar{t} \in \mathbb{N}$ intervals to travel through it, then the velocity at which it will move when it enters the next cell is $v_{\ell+1}(k+\bar{t})$. This observation motivates the following recursive, but implementable, definition

$$\xi(t) \coloneqq \xi_N(t)\,,\ \forall t \in \mathcal{T}(k) \tag{7.8}$$

where

$$\begin{cases} \xi_1(t) = 0 \\ \xi_\ell(t) = \xi_{\ell-1}(t) + \dfrac{L_\ell}{\hat{v}_\ell(t+\xi_{\ell-1}(t))} - \dfrac{L_\ell}{\overline{v}_\ell}\,,\ \forall \ell\{2,\dots,N\}. \end{cases}$$

Here, $\hat{v}_\ell$ denotes the vehicles' speed computed in the worst-case scenario described above. The value $L_\ell/\overline{v}_\ell$ represents the travel time in the case of no congestion in the cell ℓ. Under the assumption above, $\xi_\ell(t)$ can be always computed by letting the CTM evolve freely. It is worth noticing that, if the PEVs will experience no congestion along the whole freeway, i.e., $\hat{v}_\ell(t) = \overline{v}_\ell$ for all $\ell \in \mathcal{N}$, then $\xi(t) = 0$.

Another important quantity related to the congestion is the number of vehicles that leave the CS at every time instant. In fact, if an agent leaves the CS when

many others are also merging back into the mainstream, it may experience high levels of congestion. To model this phenomenon, we introduce a binary variable $\vartheta_i \in \mathbb{B}$ for every $i \in \mathcal{I}(k)$.

For every PEV $i \in \mathcal{I}(k)$ entering cell 2 at time $t_i \in \mathcal{T}(k)$, and for every $t \in \mathcal{T}(k)$, we define $\vartheta_i(t) = 1$ if $t \in \{t_i - W, \dots, t_i + W\}$, and 0 otherwise. Thus, ϑ_i is a rectangular function of width at most $2W + 1$ intervals and at least $W + 1$ (Figure 7.3). This variable is used to capture the influence of the PEVs entering cell 2 around the same time as agent i. The value of $W \in \mathbb{N}$ depends on lT. In fact, if lT is large, then PEV i will not experience the congestion due to the PEVs that precede or follow him, so $W = 0$. On the other hand, if lT is small, the value of W has to be high to model correctly the possible congestion due to those agents that enter cell 2 around the same time as agent i. We elaborate further on this in the next section. Also in this case, we denote the collective vector over the whole $\mathcal{T}(k)$ as $\vartheta_i \coloneqq \mathrm{col}((\vartheta_i(t))_{t\in\mathcal{T}(k)})$. Therefore, for every $t \in \mathcal{T}(k)$ and $i \in \mathcal{I}(k)$, $\xi_i^{\mathrm{CS}}(t)$ approximates the extra time that agent i would experience due to those PEVs entering cell 2 around time t and it reads as

$$\xi_i^{\mathrm{CS}}(t) \coloneqq \gamma \left(\sum_{\bar{k}<k} \sum_{j\in\mathcal{I}(\bar{k})} \vartheta_j(t) + \sum_{j\in\mathcal{I}(k)\setminus\{i\}} \vartheta_j(t) \right) . \tag{7.9}$$

The first double summation, denoted by $\vartheta^{\mathrm{old}}(t)$ for all $t \in \mathcal{T}(k)$, represents the number of PEVs, that already completed the decision process, entering cell 2 during one of the intervals $\{\max(k, t-W), \dots, t+W\}$. The coefficient $\gamma > 0$ is proportional to the average amount of time agent i spends for every PEV entering cell 2 during the intervals $\{\max(k, t - W), \dots, t + W\}$. This coefficient may be estimated via historical data and engineering understanding or based on the worst-case scenario.

Energy price

In our model the dynamic energy price $p(k)$ is discounted by the HO in conjunction with a traffic congestion. On the other hand, it is also linked to the local energy demand required in the distribution network, i.e., $d(k)+u^{\mathrm{PEV}}(k)$, where $u^{\mathrm{PEV}}(k) \coloneqq \sum_{\bar{k}\in\mathbb{N}} \sum_{i\in\mathcal{I}(\bar{k})} u_i(k)$ is the total energy purchased by the PEVs and $d(k)$ denotes the base energy demand of the local network. During the time interval k, we can study the congestion by looking at how much the travel time increases with respect to the free-flow case, for each cell $\ell \in \mathcal{N}$. This quantity is defined by $\Delta_\ell(k) \coloneqq \frac{L_\ell}{v_\ell(k)} - \frac{L_\ell}{\overline{v}_\ell}$, and $\Delta_\ell(k) \geq 0$. Here we assume it is used by the HO to link the price to the congestion level, namely the higher $\Delta_\ell(k)$ the lower the price. Thus, the energy price that the HO imposes for every unit of energy purchased reads as

$$p(k) \coloneqq c_1\, d(k) + c_2 u^{\mathrm{PEV}}(k) - c_3 \sum_{\ell=2}^{N} \Delta_\ell(k)\,, \tag{7.10}$$

where $c_1, c_2, c_3 > 0$ are scaling parameters tuned by the HO. This is one of the key parameters analyzed in the sensitivity analysis carried out in Section 7.9.

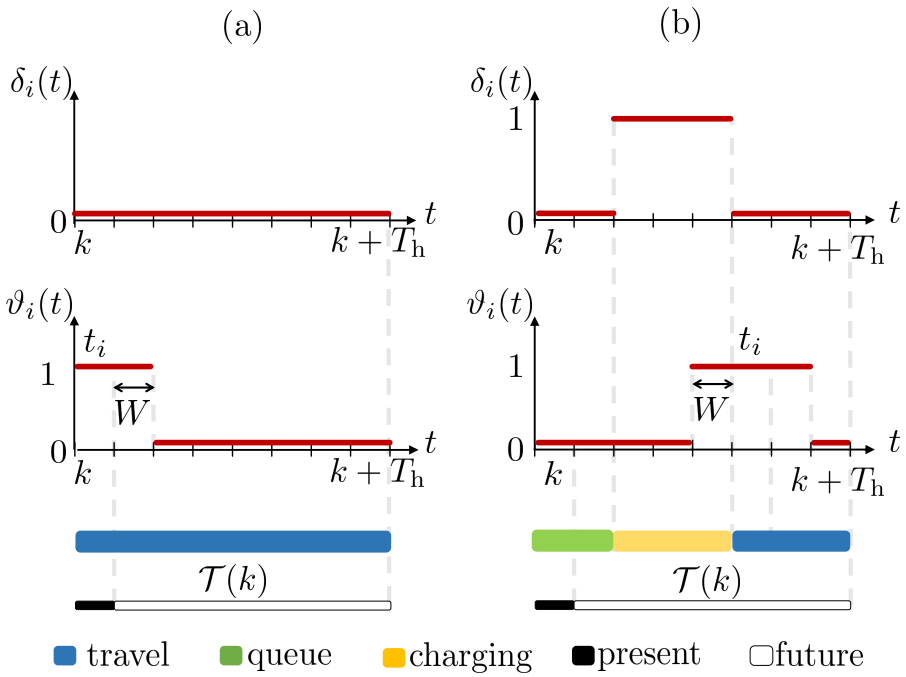

Figure 7.3: Feasible choices of δ_i and ϑ_i for $i \in \mathcal{I}$ when $l = 1$ and $W = 1$. The two illustrations show when: (a) the PEV does not stop at the CS; (b) the PEV decides to stop.

We note that the exact energy price applied in the future time intervals $t \in \mathcal{T}(k)$ cannot be computed in advance by the HO, since it depends on the traffic evolution, which is not completely known due to the arbitrary future choices of the drivers. Nevertheless, to allow the PEVs to perform an informed choice, we let the HO compute an estimation $\hat{p}(t)$ of the real $p(t)$ for the whole prediction horizon $\mathcal{T}(k)$. Then, this value is broadcast to the PEVs in $\mathcal{I}(k)$ and it is used by them to execute the decision process. If the congestion grows, then the price should drop, even though, intuitively, the discounted price leads to a larger number of PEVs stopping, and consequently an increment of $u^{\mathrm{PEV}}(k)$. We define $\hat{\Delta}_\ell(k)$ as an approximate value of $\Delta_\ell(k)$, which is computed by assuming that no agent exiting cell 1 during the prediction horizon $\mathcal{T}(k)$ stops at the CS. This assumption translates into $\mathrm{r2s}(t) = 0$ for all $t \in \mathcal{T}(k)$. The density and the flow during the time interval $t \in \mathcal{T}(k)$ are attained by letting the CTM evolve freely. Therefore, the approximation of the additional time spent by the agent, due to the congestion in the cell ℓ, reads as

$$\hat{\Delta}_\ell(t) := \frac{L_\ell}{\hat{v}_\ell(t)} - \frac{L_\ell}{\overline{v}_\ell}\,. \tag{7.11}$$

The value of $\hat{\Delta}_\ell(t)$ overestimates the additional travel time spent due to the congestion level on the road during the interval t. We introduce two time-varying vectors

of offsets and coefficients, $\boldsymbol{\beta}_0(k) \coloneqq \mathrm{col}((\beta_0(t))_{t\in\mathcal{T}(k)})$ and $\boldsymbol{\beta}_1(k) \coloneqq \mathrm{col}((\beta_1(t))_{t\in\mathcal{T}(k)})$ respectively, and define the estimated price, for every time interval $t \in \mathcal{T}(k)$, by

$$\hat{p}(t) \coloneqq c_1\, d(t) - \left[\beta_0(t) + \beta_1(t) \sum_{\ell=2}^{N} \hat{\Delta}_\ell(t)\right] . \tag{7.12}$$

At every time instant $k \in \mathbb{N}$, the HO may use historical data on the traffic flow to compute the values of $\boldsymbol{\beta}_0(k)$ and $\boldsymbol{\beta}_1(k)$ that are supposed to minimize the error between the real and estimated price. This may be done with several techniques (e.g. linear regression or Bayesian estimation).

Remark 7.2. *The definition in* (7.12) *implies that the estimated price is not affected by the strategies of the other agents in the game. Nevertheless, the strategies implemented by the PEVs involved during k, directly influence the estimated price used by the PEVs that will play the game during $k+1$. Therefore, the price dynamically changes over time and is assumed to be fixed only inside the single decision process.* □

Cost function formulation

The goal of each PEV is to find the best trade-off between saving money, and travel time. These two cost terms are described for every PEV $i \in \mathcal{I}(k)$ by the functions J_i^{price} and J_i^{time}, respectively. The amount agent i saves by charging at a discounted price depends on the total energy it purchases:

$$J_i^{\mathrm{price}}(u_i|k) \coloneqq \sum_{t\in\mathcal{T}(k)} (\hat{p}(t) - \bar{p}_i) u_i(t) \,,$$

where $\bar{p}_i > 0$ represents the average cost agent i would experience via standard fast charging, and it might vary between PEVs. Next, we define the cost associated to the total travel time experienced by vehicle i by

$$J_i^{\mathrm{time}}(\vartheta_i, \boldsymbol{\vartheta}_{-i}|k) \coloneqq \sum_{t\in\mathcal{T}(k)} \chi(t)\big[(t-k)\upsilon + \xi(t) + \xi_i^{\mathrm{CS}}(t)\big]\vartheta_i(t) \,.$$

The quantity $(t-k)$ weights the time spent at the charging station, while the rest approximates the additional time spent if the agent enters cell 2 during the time interval t. The parameter $\upsilon > 0$ weights the different perception that the agent has in spending time at the CS or in a congestion. The time-varying factor $\chi(t)$ normalizes the cost function with respect to the width of the rectangular function ϑ_i. Note that the presence of $\xi_i^{\mathrm{CS}}(t)$ creates a coupling between all the decisions of the PEVs in the game. In J_i^{time}, the presence of ϑ_i entails that only some elements of the summation are not zero. Furthermore, its rectangular shape implies that the decision of agent i depends also on those agents that enter cell 2 during an interval distant at most $2W$ intervals from the one in which i will enter cell 2, see Figure 7.3. As anticipated, this feature models the different speeds of the vehicles in a cell.

Each agent may weight differently the two objectives thus we model the final cost as a convex combination of the two:

$$J_i(u_i, \vartheta_i, \boldsymbol{\vartheta}_{-i}|k) \coloneqq \alpha_i J_i^{\text{price}} + (1-\alpha_i) J_i^{\text{time}}\,, \tag{7.13}$$

for some $\alpha_i \in (0,1)$. We study the effects of this parameter on the performance in Section 7.9. Finally, we highlight that the nature of the approximation of ξ_i^{CS} and the estimation $\hat{p}$ are intrinsically different. In fact, despite both uncertainties are due to the presence of the human in the loop, the second is part of the policy designed by the HO to reduce the congestion, while the first is used to model the drivers' local decision. Consequently, the complete policy includes the actual price applied and its estimation over the prediction horizon, that are broadcast by the HO to the PEVs and used to influence their decision.

7.3.2 Local and coupling constraints

We model the constraints on the drivers' possible choices as a collection of logical implications. First, we impose that the $2W+1$ intervals in which $\vartheta_i = 1$ are consecutive. To do so, we require that, for all $i \in \mathcal{I}(k)$, ϑ_i changes its value from 0 to 1 and back to 0 only once:

$$\sum_{p \in \mathcal{T}(k)} (1 - \vartheta_i(p-1))\vartheta_i(p) = 1 \tag{7.14a}$$

$$\sum_{p \in \mathcal{T}(k)} \vartheta_i(p-1)(1 - \vartheta_i(p)) = 1\,, \tag{7.14b}$$

where $\vartheta_i(k-1) = 0$, so the raising edge must precede the falling one. Then, we force the intervals in which $\vartheta_i(k) = 1$ to be consecutive, and hence for all $i \in \mathcal{I}(k)$ and $t \in \mathcal{T}(k)$ it must hold that

$$\begin{gathered} \vartheta_i(t)(1 - \vartheta_i(t+1))\Bigg(\sum_{p \in \mathcal{T}(k)} \vartheta_i(p) - \mathfrak{P}\Bigg) = 0 \\ \mathfrak{P} \coloneqq \min\{t - k + W + 1, 2W + 1\}\,. \end{gathered} \tag{7.15}$$

Clearly, if a PEV enters cell 2 at time t_i, it cannot charge in the remaining time intervals (Figure 7.3), and thus we obtain the following relation, for all $t \in \mathcal{T}(k)$ and $i \in \mathcal{I}(k)$:

$$\begin{gathered} [\vartheta_i(t-1)(1- \vartheta_i(t)) = 1] \implies [\delta_i(r) = 0]\,, \\ \forall r \in \{t - W - 1, \dots, k + T_{\text{h}}\}\,. \end{gathered} \tag{7.16}$$

This condition models also the case in which a PEV is not stopping, so $\vartheta_i(k) = \cdots = \vartheta_i(k+W) = 1$ and (7.16) implies that the PEV is never charging, i.e., $\delta_i(t) = 0$ for all $t \in \mathcal{T}(k)$. Furthermore, (7.14) and (7.15) imply that the PEVs disconnect at least $W+1$ time intervals before the end of the prediction horizon.

Next, we impose that, when an agent is done with charging, it exits the CS, and hence, for all $t \in \mathcal{T}(k)$, agent $i \in \mathcal{I}(k)$ has to satisfy

$$\begin{aligned}[\delta_i(t-1)=1] \wedge [\delta_i(t)=0] \implies [\vartheta_i(r)=1] \\ \forall r \in \{\max(k, t-W), \ldots, t+W\}\,.\end{aligned} \tag{7.17}$$

We impose that each PEV charges for at least $\overline{h} \in \mathbb{N}$ consecutive time intervals. In fact, the value lT may be small and it is unreasonable to allow a PEV to stop for charging for only one time interval (e.g. 2 minutes). This translates into

$$[\delta_i(t-1)=0] \wedge [\delta_i(t)=1] \Rightarrow [\delta_i(t+h)=1,\ \forall h \leq \overline{h}]\,. \tag{7.18}$$

Similarly, if a PEV decides to stop, then we assume it remains at the CS for at least $2W+1$ time intervals, and hence

$$\sum_{t \in \mathcal{T}(k)} \vartheta_i(t) > W+1 \Leftrightarrow \vartheta_i(k) = \cdots = \vartheta_i(k+W) = 0\,. \tag{7.19}$$

For each PEV, the minimum level of SoC necessary to reach the final destination from cell 2 is denoted by $x_i^{\mathrm{ref}} \in (0,1]$. Thus, we assume that a PEV can enter cell 2 if $x_i(t) > x_i^{\mathrm{ref}}$, otherwise it must stop (or remain) at the CS for charging, so for all $t \in \mathcal{T}(k)$,

$$[x_i(t) < x_i^{\mathrm{ref}}] \implies [\vartheta_i(\max(k, t-W)) = 0]\,, \tag{7.20}$$

where $\vartheta_i(\max(k,t-W))=0$ implies that PEV i cannot leave the charging station during the time interval t. The next constraint limits the maximum amount of energy that the CS can supply during each time interval by $u^{\max} > 0$. Thus, for all $t \in \mathcal{T}(k)$, we have the following coupling constraint on the connected PEVs:

$$u^{\mathrm{old}}(t) + \sum_{i \in \mathcal{I}(k)} u_i(t) \leq u^{\max}\,, \tag{7.21}$$

where $u^{\mathrm{old}}(t) \coloneqq \sum_{\bar{k}<k} \sum_{j \in \mathcal{I}(\bar{k})} u_j(t)$ is the total energy that the agents, that already completed the decision process, planned to purchase during the time interval t.

Finally, we consider that if several PEVs stop at the CS simultaneously there can be a scarcity of charging plugs. Let $\overline{\delta}$ denote the total number of plugs at the CS. Then, we have

$$\delta^{\mathrm{old}}(t) - \sum_{i \in \mathcal{I}(k)} \delta_i(t) + \leq \overline{\delta}\,,\ \forall t \in \mathcal{T}(k) \tag{7.22}$$

where $\delta^{\mathrm{old}}(t)$ is defined analogously to $u^{\mathrm{old}}(t)$.

The above constraints allow the PEVs to stop at the CS and do not start charging immediately (for example due to a lack of free plugs), and this may lead to the formation of a queue. We model the queue as a *First-In-First-Out* (FIFO), i.e., the vehicles already waiting have the priority over the PEVs entering it afterwards.

This aspect is important to realistically model the PEV behaviors, which would be hard to formalize without the use of mixed-integer variables.

In Figure 7.3, we qualitatively represent a feasible choice of δ_i and ϑ_i for PEV i and how it is reflected in the driver's behavior. In Figure 7.3a, agent i does not stop at the CS. In comparison, in Figure 7.3b, the PEV enters the CS, but, since all the plugs are busy, it waits for the first two time intervals before connecting to the CS. Once it finishes the charging phase, i.e., $\delta_i(t) = 0$, it merges back into the mainstream, according to (7.17).

We conclude this section by introducing a preliminary formulation of the set of inter-dependent mixed-integer optimization problems that model the decision process performed by the $n(k)$ PEVs during every time interval $k \in \mathbb{N}$:

$$\forall i \in \mathcal{I}(k) : \begin{cases} \min\limits_{u_i, x_i, \delta_i, \vartheta_i} & J_i(u_i, \vartheta_i, \boldsymbol{\vartheta}_{-i} | \, k) \\ \text{s.t.} & (7.6), x_i(t) \in [0,1], \delta_i(t) \in \mathbb{B}, \\ & u_i(t) \in \mathcal{U}(t), \vartheta_i(t) \in \mathbb{B}, \\ & (7.7), (7.14)\text{–}(7.22), \ \forall t \in \mathcal{T}(k). \end{cases} \tag{$\mathcal{P}$}$$

Several constraints in $(\mathcal{P})$ are expressed via logical implications, thus this problem should be mathematically reformulated to be solved. Specifically, in the Appendix 7.12 we adopt a process akin to the one used in Chapter 6 and [77] to transform the logical implications into mixed-integer affine coupling constraints by additional auxiliary variables.

7.4 Formulation of the mixed-integer game

As a result of translating the logical implications into affine constraints, we recast $(\mathcal{P})$ as the following mixed-integer aggregative game, subject only to linear mixed-integer inequalities:

$$\forall i \in \mathcal{I}(k) : \begin{cases} \min\limits_{u_i, \ldots, \nu_i} & J_i(u_i, \vartheta_i, \vartheta_i, \boldsymbol{\vartheta}_{-i} | \, k) \\ \text{s.t.} & x_i(t) \in [0,1], u_i(t) \in \mathcal{U}(t), \\ & \delta_i(t), \vartheta_i(t), \psi_i(t) \in \mathbb{B} \\ & \sigma_i(t), \omega_i(t) \in \mathbb{B} \\ & \varphi_i^{\mathrm{LH}}(t), \varphi_i^{\mathrm{HL}}(t), \nu_i \in \mathbb{B} \\ & \mu_i^{(h)}(t) \in \mathbb{B} \ \forall h \leq \overline{h} \\ & g_i(t), q_i(t) \in \mathbb{N} \\ & (7.21)\text{–}(7.44), \ \forall t \in \mathcal{T}(k). \end{cases} \tag{$\mathcal{G}(k)$}$$

The vector of all the decision variables in $(\mathcal{G}(k))$ is defined as

$$z_i \coloneqq \mathrm{col}(u_i, x_i, \delta_i, \vartheta_i, \psi_i, \sigma_i, \varpi_i, \varphi_i^{\mathrm{LH}}, \varphi_i^{\mathrm{HL}}, \mu_i^{(1)} \ldots, \mu_i^{(\overline{h})}, g_i, q_i, \nu_i) \in \mathbb{R}^{n_i},$$

and $\boldsymbol{z} \coloneqq \mathrm{col}((z_i)_{i\in\mathcal{I}(k)})$, we obtain a compact form of $\mathcal{G}(k)$:

$$\forall i \in \mathcal{I}(k) \ : \quad \min_{z_i\in\mathcal{Z}_i(k)} J_i(z_i, \boldsymbol{z}_{-i}|k) \quad \text{s.t. } A\boldsymbol{z} \leq b \tag{7.23}$$

where $\mathcal{Z}_i(k)$ is the set of strategy that satisfy the local constraints of i, while A and b are of suitable dimensions and are used to describe all the coupling constraints between the agents. We denote the set of all feasible strategies of player $i \in \mathcal{I}(k)$ as

$$\mathcal{Z}_i(\boldsymbol{z}_{-i}|k) \coloneqq \{y \in \mathcal{Z}_i(k) \subset \mathbb{R}^{n_i} \mid A(y, \boldsymbol{z}_{-i}) \leq b\}\,. \tag{7.24}$$

Then, the set of all the feasible collective strategies is

$$\boldsymbol{\mathcal{Z}}(k) \coloneqq \left\{\boldsymbol{z} \in \textstyle\prod_{i\in\mathcal{I}(k)}\mathcal{Z}_i(k) \subset \mathbb{R}^n \mid A\boldsymbol{z} \leq b\right\},$$

where $n \coloneqq \sum_{i\in\mathcal{I}(k)} n_i$.

Perhaps, the most popular notion of equilibrium for games like $\mathcal{G}(k)$ is the Generalized Nash Equilibrium (GNE), where no agent can reduce its cost by unilaterally changing its strategy to another feasible one. Here, we are interested in an approximate solution for mixed-integer games, i.e., MINE.

Definition 7.1 (ε-Mixed-Integer Nash equilibrium)**.** A set of strategies $\boldsymbol{z}^* \in \boldsymbol{\mathcal{Z}}$ is an MINE, with $\varepsilon > 0$, of the game $\mathcal{G}(k)$ if, for all $i \in \mathcal{I}$,

$$J_i(z_i^*, \boldsymbol{z}_{-i}^*|k) \leq \inf_{z_i\in\mathcal{Z}_i(\boldsymbol{z}_{-i}^*|k)} J_i(z_i, \boldsymbol{z}_{-i}^*|k) + \varepsilon.$$

with $\mathcal{Z}_i$ as in (7.24). □

7.4.1 Potential game structure

In this subsection, we prove that the game $\mathcal{G}(k)$ is an *exact potential game* with potential function P, see Appendix C for an introduction on potential games.

To find the potential function P, we first reorganize the local cost function $J_i(z_i, \boldsymbol{z}_{-i}|k)$ as:

$$J_i(z_i, \boldsymbol{z}_{-i}|k) = \zeta_i(z_i) + \textstyle\sum_{j\in\mathcal{I}(k)\setminus\{i\}}\lambda_{i,j}(z_i, z_j)\,, \tag{7.25}$$

where ζ_i depends on the local variables only, and $\lambda_{i,j}$ incorporates the cross terms depending on the other players' strategy z_j. From (7.9), we derive that

$$\lambda_{i,j}(z_i, z_j) \coloneqq \sum_{t\in\mathcal{T}(k)} \chi(t)\gamma\,\vartheta_j(t)\vartheta_i(t). \tag{7.26}$$

Thus, $\lambda_{i,j}(z_i, z_j) = \lambda_{j,i}(z_j, z_i)$ meaning that the agents influence each other in a symmetric way. In the next statement, we introduce the exact potential function for the game in $\mathcal{G}(k)$.

Theorem 7.2. *For each $k \in \mathbb{N}$, the game $\mathcal{G}(k)$ is an exact potential game with*

$$P(\boldsymbol{z}|k) \coloneqq \sum_{i\in\mathcal{I}(k)} \left(\zeta_i(z_i) + \sum_{j\in\mathcal{I}(k),\, j<i} \lambda_{i,j}(z_i, z_j) \right),$$

as an exact potential function, where $\lambda_{i,j}$ is as in (7.26). □

Proof. The proof is akin to the one in [75]. ■

The pivotal result that highlights the importance of the above theorem is that an ε-approximated minimum of the potential function is also an MINE of the game $\mathcal{G}(k)$, see [154, Th. 2]. Thus, it is sufficient to show that the proposed algorithm converges to a minimum of the potential function in order to achieve the sought convergence result.

7.5 CTM traffic control scheme

We can now focus on the connection between the traffic dynamics and the decision process of the PEVs. Then, we describe in details our proposed algorithm that the agents can use to seek an equilibrium of the game.

7.5.1 Iterative semi-decentralized algorithm

We propose here a semi-decentralized iterative algorithm (Algorithm 7.1) that the agents in $\mathcal{I}(k)$ can adopt to solve the MI-GPG $\mathcal{G}(k)$. The notation $z_i(\tau)$ denotes the strategy of agent i at the τ-th iteration of the algorithm.

After the initialization step, where the players receive the information broadcast by the HO, each PEV decides to update its strategy independently from the others. If an agent wants to update, it sends a request to the HO. If no other player is currently updating, then agent i starts its local update given the aggregate quantities $\sum_{j\in\mathcal{I}(k)\setminus\{i\}} \vartheta_j(t)$, $\sum_{j\in\mathcal{I}(k)\setminus\{i\}} u_i(t)$ and $\sum_{j\in\mathcal{I}(k)\setminus\{i\}} \delta_i(t)$, used to compute the cost J_i^{time} and the coupling constraints (7.21), (7.22). On the other hand, if another agent is performing the update, agent i enters a FIFO queue from which the HO extracts sequentially the future agents that are allowed to update. At the moment of the update, agent i computes a best-response strategy z_i^* with respect to the strategies of the others. We define the *mixed-integer best-response* mapping for agent $i \in \mathcal{I}(k)$, as

$$\mathcal{BR}_i(\boldsymbol{z}_{-i}) \coloneqq \begin{cases} \operatorname{argmin}_{z_i} J_i(z_i, \boldsymbol{z}_{-i}|k)\,, \\ \quad \text{s.t. } (z_i, \boldsymbol{z}_{-i}|k) \in \boldsymbol{\mathcal{Z}}(k) \end{cases} \tag{7.27}$$

where $\mathcal{BR}_i$ may be a set, thus $z_i^* \in \mathcal{BR}_i(\boldsymbol{z}_{-i})$.

Agent i updates its current strategy only if z_i^* leads to an (at least) ε-improvement in terms of minimization of its cost.

The iteration is completed after the PEV communicates to the HO its (possibly) new strategy and the HO uses it to revise all the quantities in the game that depend on z_i.

In the following result, we show that Algorithm 7.1 converges to an MINE of the game $\mathcal{G}(k)$, under the assumption that all the players manage to update their strategies over a sufficiently large number of iterations.

Proposition 7.3. *Let $\varepsilon > 0$ and $k \in \mathbb{N}$, and assume that for every $j \in \mathcal{I}(k)$ and $\tau \in \mathbb{N}$ there exists a $\bar{\tau} > \tau$ such that $j \in \{i(\tau), \dots, i(\bar{\tau})\}$. Then, Algorithm 7.1 computes an MINE of the game $\mathcal{G}(k)$ in* (7.23). □

Proof. From Theorem 7.2, $\mathcal{G}(k)$ is an MI-GPG with an exact potential function for all $k \in \mathbb{N}$. Therefore, the result in [154, Th. 4] applies to show that the sequential best-response based algorithm proposed in Algorithm 7.1 converges to an MINE of the game. ■

Remark 7.3 (Privacy and scalability)**.** *In Algorithm 7.1, the HO shares with each PEV only aggregate information on the choices of the others. This feature allows to preserve the privacy of the agents in the game, since an agent cannot retrieve the local decision strategy of another PEV based on the data received from the HO. Moreover, using aggregate information is also important to preserve the scalability of Algorithm 7.1. In fact, the amount of data shared between each PEV and the HO does not grow with $n(k)$. This is crucial to obtain an implementable solution, due to the (possibly) large number of vehicles involved.* □

Algorithm 7.1 shares the update structure with Algorithm 6.1. So, Remark 6.1 on the accuracy and optimality of the attained approximated equilibrium holds also in this case. Moreover, it is important to stress that Algorithm 7.1 has to operate in real-time, so ε must be chosen accordingly. Notice that, thanks to the asynchronous update structure proposed, $\boldsymbol{z}(\tau)$ is a collective strategy that satisfies all the constraints of the game for all $\tau \in \mathbb{N}$. This differentiate Algorithm 7.1 from the ones proposed in Chapters 2–4 in which the constraints are satisfied only at the equilibrium. Furthermore, this feature allows the HO to end the algorithm at any iteration and still achieve a result that has physical meaning and can be directly adopted by the PEVs, with the only drawback of a loss in optimality.

7.5.2 Complete CTM control loop

The HO, introduced in Section 7.3, plays a crucial role in collecting and broadcasting information from and to the vehicles on the highway stretch. We propose the following decision process which takes place at the beginning of every time interval $k \in \mathbb{N}$ via the following four steps.

S.1) HO collects information

The HO collects information, from the sensors on the highway (placed at the interfaces between cells), on the cells' density, i.e., $\rho_\ell(k)$ for all $\ell \in \mathcal{N}$. The HO

Algorithm 7.1: Sequential best-response

Initialization: For $k \in \mathbb{N}$, HO sends to every $i \in \mathcal{I}(k)$ the coefficients $\bar{h}, u^{\max}, \bar{\delta}, \gamma \in \mathbb{R}$ and $\xi(t)$, $\vartheta^{\text{old}}(t)$,$u^{\text{old}}(t)$,$\delta^{\text{old}}(t)$, $\hat{p}(t)$, $\forall t \in \mathcal{T}(k)$.

Update: Choose $\boldsymbol{z}(0) \in \boldsymbol{\mathcal{Z}}(k)$, set $\tau \coloneqq 0$

while $\boldsymbol{z}(\tau)$ is not an MINE **do**

  HO **do**

    Extracts from the waiting queue $i \coloneqq i(\tau) \in \mathcal{I}(k)$.

    Sends $\sum_{j \in \mathcal{I}(k)\setminus\{i\}} \vartheta_j(t)$, $\sum_{j \in \mathcal{I}(k)\setminus\{i\}} u_i(t)$ and $\sum_{j \in \mathcal{I}(k)\setminus\{i\}} \delta_i(t)$ to i.

  end

  Player i **do**

    Computes $z_i^*(\tau) \in \mathcal{BR}_i(\boldsymbol{z}_{-i}(\tau))$ as in (7.27)

    if $J_i(z_i(\tau), \boldsymbol{z}_{-i}(\tau))) - J_i(z_i^*(\tau), \boldsymbol{z}_{-i}(\tau))) \geq \varepsilon$

      $z_i(\tau+1) \coloneqq z_i^*(\tau)$

    else

      $z_i(\tau+1) \coloneqq z_i(\tau)$

    Sends $z_i(\tau+1)$ to HO

  end

  Set $z_j(\tau+1) \coloneqq z_j(\tau)\ \forall j \neq i$, $\tau \coloneqq \tau + 1$

computes the following set of variables: $\xi(t)$ via (7.8), $\vartheta^{\text{old}}(t)$, $\delta^{\text{old}}(t)$, $u^{\text{old}}(t)$, $\Delta_\ell(k)$, $\hat{\Delta}_\ell(t)$ via (7.11), $p(k)$ via (7.10) and $\hat{p}(t)$ via (7.12), by exploiting the CTM and the strategies of the PEVs that performed the process during the previous time intervals.

S.2) HO broadcasts information

Those PEVs that have the possibility to stop during the time interval k, i.e., the ones leaving cell 1, connect with the HO, forming the set $\mathcal{I}(k)$ of players involved in the game. The HO broadcasts to all of them the quantities they need to initialize the game $\mathcal{G}(k)$, i.e., the initialization phase in Algorithm 7.1. Moreover, the HO applies the price $p(k)$ in (7.10) to the energy purchased by the PEVs currently charging at the CS.

S.3) Iterative solution of the decision process

After the initialization, the agents update their strategy as shown in Algorithm 7.1, and described in Section 7.5.1. The PEVs keep updating until they converge to an MINE of the game $\mathcal{G}(k)$, hence a feasible set of strategies $\boldsymbol{z} \in \boldsymbol{\mathcal{Z}}(k)$, which is convenient to each of the PEVs. We stress that the iterations $\tau \in \mathbb{N}$ to solve the game are unrelated to the intervals of the CTM or the intervals in $\mathcal{T}(k)$, and in fact they are all completed within the interval k.

S.4) Strategy implementation

The agents in $\mathcal{I}(k)$ implement their final strategies (i.e., stop at the CS or continue driving) and the process will start again from *(S.1)* at the beginning of the interval $k+1$.

The presence of the human in the loop imposes a bi-level implementation of step (S.4). We envision that every PEV performs the computations in (S.3) via a dedicated software, then the final strategy is translated into a simple message that is prompted to the human user advising whether it is convenient or not to stop at the CS. In the end, the driver implements the suggested behavior.

Finally, we want to elaborate on how to compute, starting from $\boldsymbol{z}$, the in and out flow of the CS, i.e., r2s and s2r respectively. From the constrains in Sec. 7.3.2, agent $i \in \mathcal{I}(k)$ does not stop at the CS if and only if $\vartheta_i(k) = 1$, thus the flow entering the CS is defined by

$$\mathrm{r2s}(k) \coloneqq \frac{1}{T}\left(n(k) - \sum_{i \in \mathcal{I}(k)} \vartheta_i(k)\right) . \tag{7.28}$$

The flow exiting the CS is

$$\mathrm{s2r}(k) \coloneqq \frac{1}{lT} \sum_{\bar{k}<k} \sum_{j \in \mathcal{I}(\bar{k})} \vartheta_j(k-W)\vartheta_j(k+W) , \tag{7.29}$$

where the double summation selects only those agents exiting the CS during the time interval k. In fact, for those PEVs that do not stop, we have $\sum_{t\in\mathbb{N}} \vartheta_j(t) = W+1$, thus they never contribute to (7.28). Conversely, if PEV i stops, $\vartheta_j(k-W)\vartheta_j(k+W) = 1$ if i exists the CS during k. The PEVs that contribute to $\mathrm{s2r}(k)$ decide to exit during an interval m long lT time instants that encloses k, so the contribution to the flow is $1/l$. The definitions above represent the actual connections between the CTM and the decision process, thus we have arrived at the goal stipulated at the beginning of the chapter.

This concludes the theoretical framework introduced to describe the ATDM strategy developed. The remainder of the chapter is dedicated to the study of this policy's effectiveness and performance when it is applied to a case study with real traffic data.

7.6 CTM identification

Let us introduce the examined case study and identify the parameters of the associated CTM, introduced in Section 7.2, starting from real-world data and following the schematic procedure depicted in Figure 7.5. We consider a stretch of the A13 highway in The Netherlands connecting the cities of The Hague and Rotterdam. The Dutch government embraces the policy of making traffic data accessible via



Figure 7.4: Location along the A13 highway of the 8 sensors selected for the simulations; [129] indicates how to access this info.

the Nationaal Dataportaal Wegverkeer (NDW) [3]. In particular, the NDW-Dexter portal [129] allows us to access the sensors placed along the highway and extract the traffic data related to a particular date and time. Here, we select 8 sensors, denoted in the following by $s_1, \dots, s_8$, on the roadway that from The Hague enters Rotterdam (Figure 7.4). The sensors are placed approximately at 500 m from each other and measure the number of vehicles and their average speed during a period of 1 minute. We consider the data of the 15/10/2019 from 07:00 to 20:00, since there is no traffic congestion during the remaining hours.

Remark 7.4 (Minimum sample frequency)**.** *The frequency of the data samples has to be high enough to allow the CTM to evolve correctly. In fact, if for some $\ell \in \mathcal{N}$ the inequality*

$$\frac{T\bar{v}_\ell}{L_\ell} < 1$$

is not satisfied, then the associated cell's density ρ_ℓ can take negative values. This is a consequence of the density definition in (7.1) *and the lower bound for the sampling frequency is obtained from the worst-case scenario. One can solve this issue by considering longer cells or by interpolating the data obtained from the sensors to decrease the sampling time. For the problem at hand, we show that the free flow speed is approximately* 120 km/h*, therefore we interpolated the data to obtain a sampling time of $T = 10$*s*, so $T\bar{v}_\ell/L_\ell \simeq 0.66 < 1$.* □

We construct a CTM composed of $N = 7$ cells, in which the flows $\phi_1, \dots, \phi_8$ between cells are obtained directly from the raw data provided by the sensors, i.e., for all $j \in \{1, \dots, 8\}$

$$\phi_j := \frac{\#\text{ veh. from } s_j}{T}.$$

The the average speed of the vehicles is also measured by each sensor, thus for each

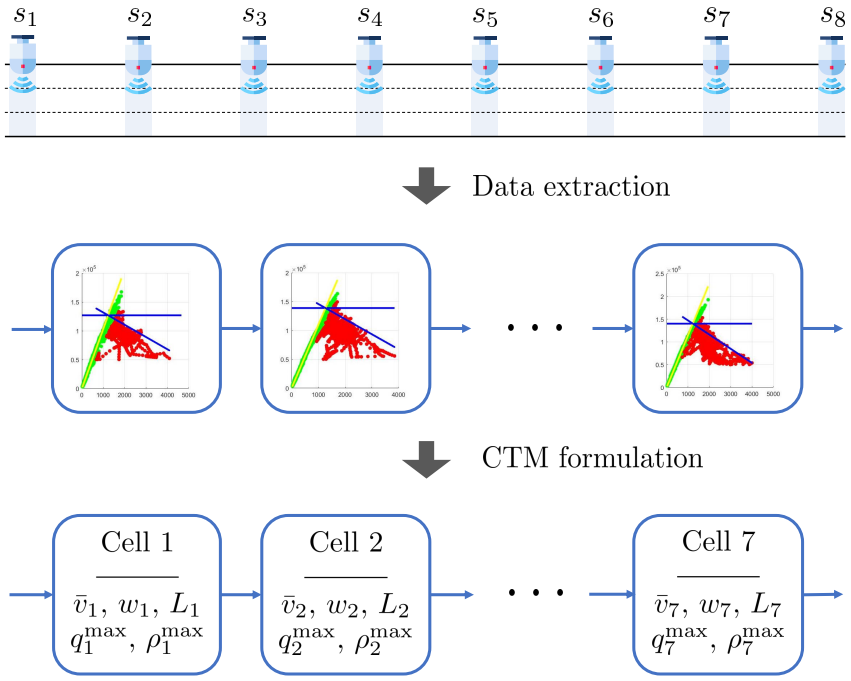

Figure 7.5: Schematic structure of the procedure adopted to identify the parameters of the CTM.

cell $\ell \in \{1, \dots, 7\}$ the density is

$$\rho_\ell := \frac{\phi_\ell}{\text{avg. speed from } s_\ell}.$$

The relation between the flow and the density is represented for cell 1 in the *fundamental diagram* depicted in Figure 7.6a, where we used a threshold on the average vehicles' velocity to distinguish between the data associated with the free flow and those measured during a traffic congestion. As in [85] and more in details in [116, Sec. 3.2], we identified the parameters of each cell of the CTM by using linear regression. For a cell ℓ, the free flow speed $\bar{v}_\ell$ is the slope of the linear regression applied to the data measured during the free flow (the yellow line in Figure 7.6a). Similarly, the congestion wave speed w_ℓ is the slope of the quantile regression applied to the leftover data. The result of the regression is illustrated via the blue line in Figure 7.6a, and the density at which it intersects the horizontal axis represents the (theoretical) cell's maximum density $\rho_\ell^{\max}$. Finally, the intersection of the two regression lines (i.e., the blue and the yellow) defines the maximum cell capacity $q_\ell^{\max}$. Therefore, by applying these steps, sketched in Figure 7.5 for all the cells, we identify the parameters that, together with ϕ_1 and ϕ_8, fully describe the CTM. Their final values are reported in Table 7.1 and the code used is available at [39].

Table 7.1: The variables and parameters (respectively in the upper and bottom part of each table) related to the CTM and the charging scheduling decision problem.

Parameters		Identified values of the CTM						
ℓ	–	1	2	3	4	5	6	7
L_ℓ	[km]	0.39	0.41	0.365	0.365	0.365	0.5	0.5
T	[s]	10	10	10	10	10	10	10
$\bar{v}_\ell$	[km/h]	103.15	109.34	111.67	112.77	113.07	114.12	114.18
w_ℓ	[km/h]	21.23	26.19	19.91	26.13	27.73	26.62	31.11
$q_\ell^{\max}$	[veh/h]	$1.26 \cdot 10^5$	$1.38 \cdot 10^5$	$1.28 \cdot 10^5$	$1.40 \cdot 10^5$	$1.40 \cdot 10^5$	$1.38 \cdot 10^5$	$1.40 \cdot 10^5$
$\rho_\ell^{\max}$	[veh/km]	$7.2 \cdot 10^3$	$6.56 \cdot 10^3$	$7.58 \cdot 10^3$	$6.62 \cdot 10^3$	$6.29 \cdot 10^3$	$6.41 \cdot 10^3$	$5.73 \cdot 10^3$

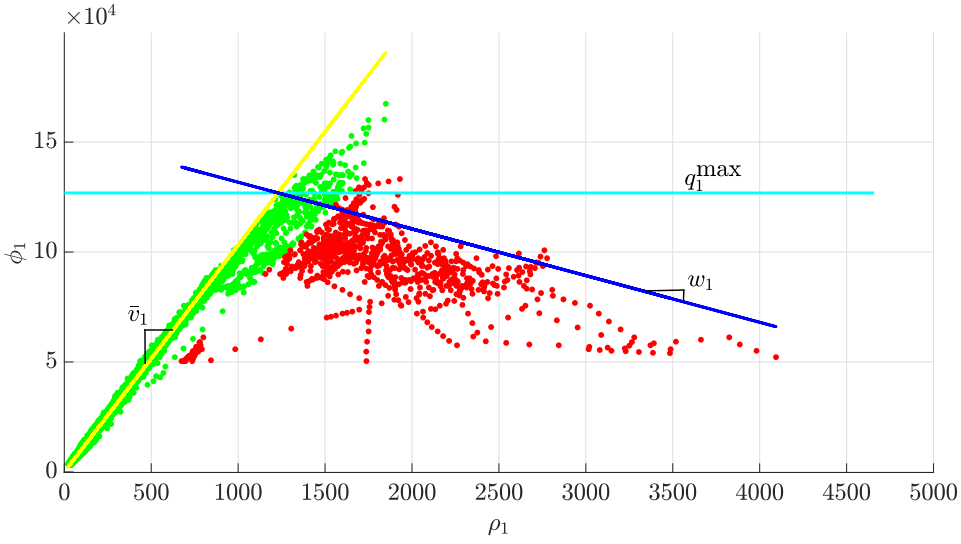

(a)

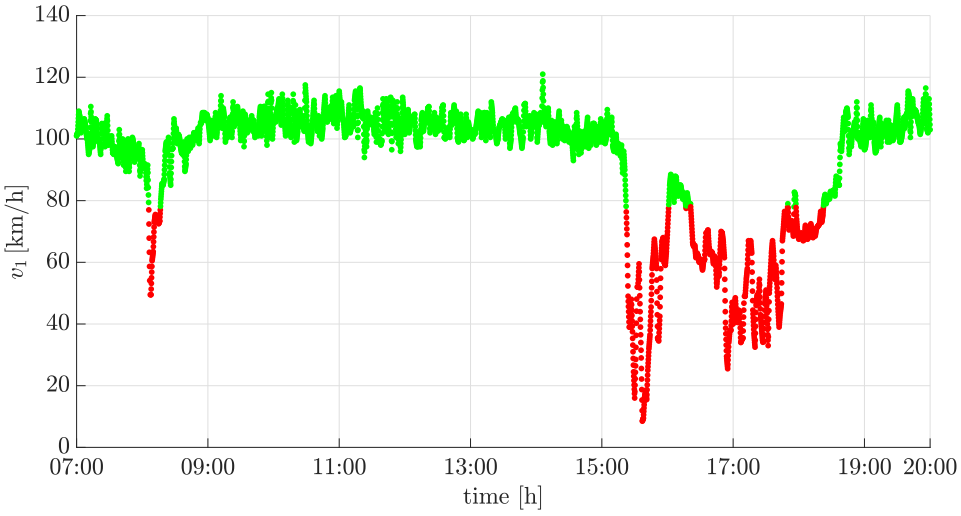

(b)

Figure 7.6: (a) The fundamental diagram of cell 1 obtained from the data of s_1. The data points are green if the cell is in a free-flow condition and red otherwise. (b) Average vehicles speed in cell 1 during the day (the color legend is as in (a)).

Table 7.2: The most important variables involved in the charging scheduling decision problem.

Decision making process of agent $i \in \mathcal{I}$		
x_i	–	battery SoC of PEV i
u_i	[kWh]	energy purchased by PEV i
δ_i	–	binary var. 1 iff PEV i is charging
u^{PEV}	[kWh]	total energy purchased by PEVs
p	[€/kWh]	price for 1kWh at CS
$\hat{p}$	[€/kWh]	predicted future price at CS
t_i	[h]	interval in which PEV i enters cell 2
ϑ_i	–	rectangular function centered in t_i
ξ	[h]	(over)estimation of the extra travel time due to congestion
ξ_i^{CS}	[h]	estimation of the extra travel time due to PEVs exiting the CS
x_i^{ref}	–	min. SoC of PEV i before leaving the CS
p_{EV}	–	percentage of PEVs in the market
lT	[h]	length of the time interval
T_{h}	–	number of intervals composing the horizon
C_i	[kWh]	battery capacity
η_i	[1/kWh]	scaling associated to battery efficiency
α_i	–	interest of PEV i in saving money
$\bar{\delta}$	–	number of charging spots at the CS
$u^{\max}$	[kWh]	CS max. energy providable in an interval
$\overline{u}(\underline{u})$	[kWh]	upper(lower) bound on purchasable energy
d	[kWh]	base energy demand in the grid
c_1, c_2	[€/kWh^2]	price scaling factors
c_3	[€/(h · kWh)]	price scaling factor
$\overline{p}_i$	[€/kWh]	fixed avg. price for 1kWh not at CS
β_0	[€/kWh]	estimated price scaling factor
β_1	[€/(h · kWh)]	estimated price scaling factor
W	–	half width of ϑ_i
γ	[h]	scaling used to compute in ξ_i^{CS}
χ	[h]	time-varying scaling of the travel time
υ	–	weight over the time spent at the CS

7.7 Decision process' parameters selection

In this section, we focus on the parameters describing the decision making process (or game) in which the PEVs are involved during every time interval. A short list and description of the most important parameters involved in the decision making process is conveniently proposed in Table 7.2. The chosen values are reported in Table 7.3 and characterize what we call the *base case* in the remaining of the paper. Now, we list the motivations behind the choice of the values of the most significant parameters in the game.

- p_{EV}: the current market share of PEVs in the Netherlands is around 2%. However, PEVs are expected to constitute more than 7% of total vehicles in the market by 2030 [105]. For this reason, we choose $p_{\text{EV}} = 5\%$.
- l: it is natural to consider the interval during which each player does not vary its strategy (namely if/when and for how long to stop at the CS) longer than T. Then, we choose $lT = 100$s.
- T_{h}: in [73] a group of commuters traveling via the A12 in the Netherlands participated in a test, whose results indicate that 60% of the involved commuters could start their work within 30 min later than usual. Therefore, we considered $T_{\text{h}} = 15$, implying that the maximum time PEVs can spend at the CS (i.e., the length of the prediction horizon) is equal to 25 min.
- $\bar{\delta}$: in The Netherlands, the government is putting a lot of effort in increasing the number of available charging points, doubling it between 2015 and 2019 [5]. Thus, we choose $\bar{\delta} = 100$ to model the foreseeable increment in charging spots.
- C_i: the battery capacity of each PEV is randomly chosen from a pool of the most common PEV models. Specifically, $C_i \in [12, 100]$, where 12 kWh represents the capacity of a Mitsubishi Outlander and 100 kWh the one of a Tesla Model S.
- α_i: for the realization of this Gaussian variable we choose mean and variance equal to $\mu_\alpha = 0.05$ and $\sigma_\alpha = 0.03$, respectively. This choice reflects the assumption that agents are more keen to save time rather than money. The small variance mimics an homogeneous interest among the PEVs owners. The case of a more heterogeneous population is analyzed in Section 7.9.
- $\bar{u}$: the charging spots are able to fast charge the PEVs and the maximum energy that can be delivered by each spot in an hour is 150 kWh. Thus, during a single time interval we have $\bar{u} = 150 \cdot lT = 4.16$ kWh.
- $u^{\max}$: the CS is assumed to be able to deliver the maximum power to all the charging spots simultaneously.
- $\bar{p}_i$: this energy price is chosen equal to 0.205 €/kWh and represents the average between the price for fast charging (see [163, 83]) and the one for charging at home (see [106]).

Table 7.3: The values of the parameters in the decision making process for the base case.

Base case: Game parameters		
x_i^{ref}	–	$[0.25, 0.35]$
p_{EV}	–	5%
lT	$[h]$	0.0278
T_{h}	–	15
C_i	[kWh]	$\{12, \cdots, 93.4, 100\}$
η_i	[1/kWh]	$[0.85, 0.99]$
$\bar{\delta}$	–	100
α_i	–	$(0, 1)$
$u^{\max}$	[kWh]	416.6
$\overline{u}(\underline{u})$	[kWh]	4.16
d	[MWh]	$[3.94, 4.16]$
c_1, c_2	[€/kWh^2]	$5.07 \cdot 10^{-5}$
c_3	[€/(h · kWh)]	0.33
$\overline{p}_i$	[€/kWh]	0.205
β_0	[€/kWh]	0
β_1	[€/(h · kWh)]	0.3315
W	–	3
γ	[s]	1.79
χ	[h]	$\{0.143, 0.25\}$
υ	–	1

- d: the base demand profile of the grid is obtained from [167] and scaled to match the average demand of a regional grid in the Netherlands, so $d(k) \in [3.94, 4.16]$ MWh.
- c_1, c_2, c_3: these values must be chosen simultaneously to make the average value of $p(t)$ equal to $\bar{p}_i$ and normalize the three components in the price. Furthermore, c_3 is particularly important, since it defines the discount due to the traffic congestion. We introduce here what we refer to as *incentive* in the remainder of the chapter. We say that we apply an incentive of y% if the term in the price function directly associated to the traffic congestion makes p decrease of y% during the intervals of peak traffic congestion.
- χ: this normalizing factor takes different values along the prediction horizon. Specifically, $\chi(t) = 1/(W+1)$ for the first $W+1$ time intervals in $\mathcal{T}(k)$ and $\chi(t) = 1/(2W+1)$ for the others. This is due to the definition of and constraints on ϑ_i (see [44] for more details).

Finally, let us suppose that the percentage of the PEV users that are traveling with an insufficient SoC is very low, since we focus on drivers commuting during the rush hours so that the optimization problem is always feasible. From a theoretical point of view, one can prevent feasibility problems by increasing the length of the

prediction horizon T_{h} or by translating the hard constraint on the minimum SoC into a soft one. In a real scenario, this would not be an issue, since these users will simply extend their staying at the CS.

7.8 Numerical results

In this section, we present and discuss the simulation results for the base case introduced in the previous section (see Table 7.3), focusing on the benefit of the ATDM strategy in terms of the average total travel time for all the drivers.

7.8.1 Performance index

The goal of the proposed policy is to alleviate traffic congestion during the rush hours for *all* the drivers on the highway, not only for the PEV owners. To quantify the benefit (and performance) of the proposed policy, we first define the quantity $\Delta_0 \coloneqq \sum_{\ell=1}^{N} \Delta_{0,\ell}$, which denotes the sum of the extra travel times $\Delta_{0,\ell}$ of the drivers in the absence of the CS. Furthermore, we define $\Delta \coloneqq \sum_{\ell=1}^{N} \Delta_{\ell}$ as the extra travel time in the presence of the CS and supposing that PEVs subscribe the proposed policy. We then introduce the following performance index:

$$\pi(\Delta_0, \Delta) \coloneqq \frac{\sum_{k\in\mathbb{N}} \Delta_0(k) - \Delta(k)}{\sum_{k\in\mathbb{N}} \Delta_0(k)} \cdot 100. \tag{7.30}$$

The larger π, the greater the benefit emerging from the behavior of PEV owners. The index (7.30) is a good yardstick to evaluate the performance of the policy over the whole day and whether or not its adoption achieves the desired traffic congestion alleviation.

7.8.2 Simulation base case

We are now ready to discuss the effects of the ATDM strategy proposed in the first theoretical part of the chapter. Figure 7.7 highlights that there are two time intervals during which a traffic congestion occurs and they are centered around 08:00 and 18:00, respectively, and reflect the real data in Figure 7.6b, where the velocity drops exactly in those time intervals. The traffic jam in the morning lasts fro almost one hour while the one in the afternoon for three hours, with a particularly high peak (in terms of travel time) at 18:00. Remarkably, despite the percentage of PEVs on the highway is modest, our algorithm manages to decrease the afternoon peak of more than 5.4% in terms of Δ. If there is no congestion all the cells are traveled by a vehicle in 1.62 min. During peak traffic congestion this time becomes 12.54 min, the proposed ATDM strategy reduces it to 12.06 min. The overall achievement in terms of travel time is $\pi = 1.05$. In Figure 7.8, we highlight the difference between the travel time with vs without our ATDM strategy. The ATDM manages to decrease the peaks and redistribute the vehicles in the "valleys", i.e., the parts in which the curve takes lower values with respect to the closest peaks.

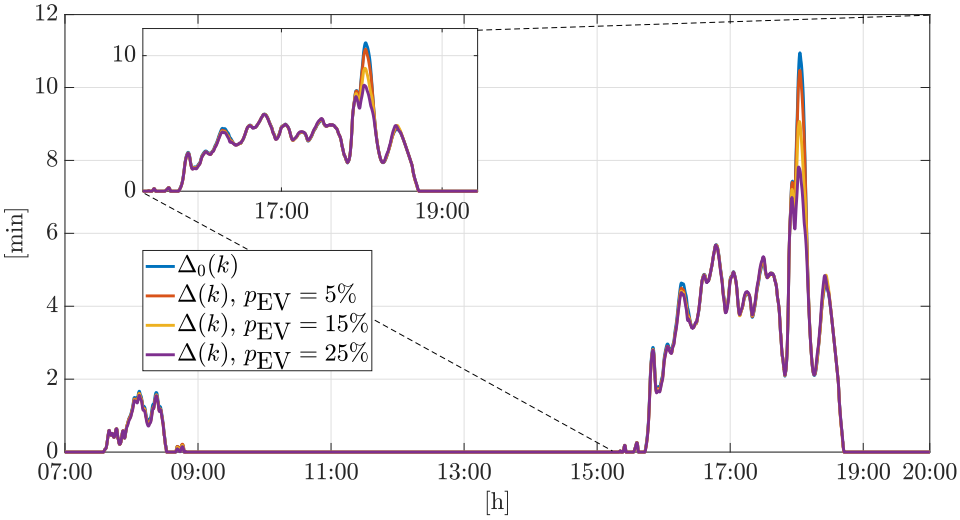

Figure 7.7: Comparison of the extra travel time due to the congestion in the presence (Δ) and absence (Δ_0) of the CS, respectively. The simulations are carried out for different values of p_{EV}.

This emerging behavior matches the expectation: in fact, it relates to the "valley filling" phenomenon, well known in the electricity market, where the energy price depends on the energy demand, see [119] and Chapter 6. The redistribution of the vehicles creates a global reduction of the travel time. This effect of the ATDM on the PEVs is confirmed by the flows shown in Figure 7.9, where r2s increases before the two peaks of Δ, while s2r peaks immediately after the reduction of Δ after the rush hours.

The dynamic energy price p designed by the HO is reported in Figure 7.10. It shows a slow variation due to the base energy demand d and a fast one associated with the traffic congestion on the highway stretch. Interestingly, these two quantities act in opposite directions since the major traffic congestions happen during the rush hours, which are notoriously those during which the demand of energy is at its highest. The parameters c_1, c_2 and c_3 are chosen such that the incentive provided is the 25%, i.e., the maximum discount is equal to 0.05€/kWh with respect to the average price $\bar{p}_i = 0.205$€/kWh. Finally, in Figures 7.11 and 7.12, we illustrate the number of PEVs simultaneously connected to the grid, i.e., $\sum_{\bar{k}<k} \sum_{i \in \mathcal{I}(\bar{k})} \delta_i(\bar{k})$, and the amount of energy purchased u^{PEV}. These two quantities are closely related and for this reason their profiles are almost identical. In both cases, the strategies implemented satisfy the upper bound constraints. As expected, during the period of high traffic congestion all the charging spots at the CS are busy. This highlights a key difference between longer and shorter traffic congestion; in the latter, there are only brief periods during which no charging spot is available, i.e., $\sum_{\bar{k}<k} \sum_{i \in \mathcal{I}(\bar{k})} \delta_i(\bar{k}) = \bar{\delta}$. Therefore, if a PEV decides to enter the CS, then it is almost sure to connect immediately. On the other hand, a traffic congestion that lasts for a substantial amount of time creates a queue of PEVs

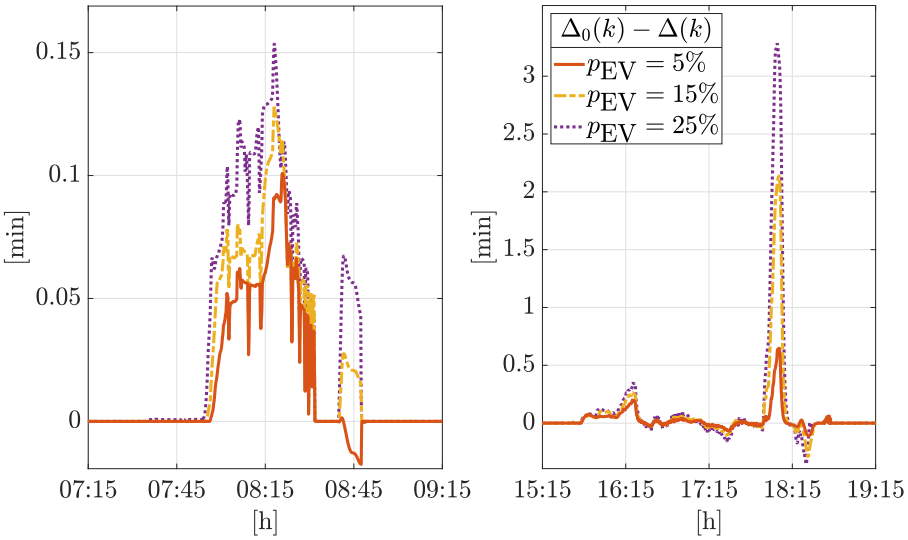

Figure 7.8: Comparison of the difference $\Delta_0 - \Delta$ computed with different values of p_{EV}. The two figures show the detail related to the morning and afternoon congestion, respectively.

at the CS waiting for charging. This idle waiting time creates an extra cost for the PEVs stopping. Moreover, this phenomenon generates detrimental effects in the concurrence of high traffic congestion peaks surrounded by an overall elevated traffic congestion level. In fact, if we consider PEVs exiting cell 1 at 18:10, then it should be beneficial for them to stop and charge for a short period, waiting for the traffic congestion to disappear. Unfortunately, all the charging spots are occupied, so the PEV cannot stop, hence contributing to increase the traffic congestion. In fact, Figure 7.9 shows that in concurrence with the highest congestion peak, the r2s flow decreases.

This first example highlighted the overall benefit of adopting a dynamic energy price to enforce an ATDM. The most important macroscopic effect is the redistribution of the vehicles that creates a valley filling like phenomenon in the travel time.

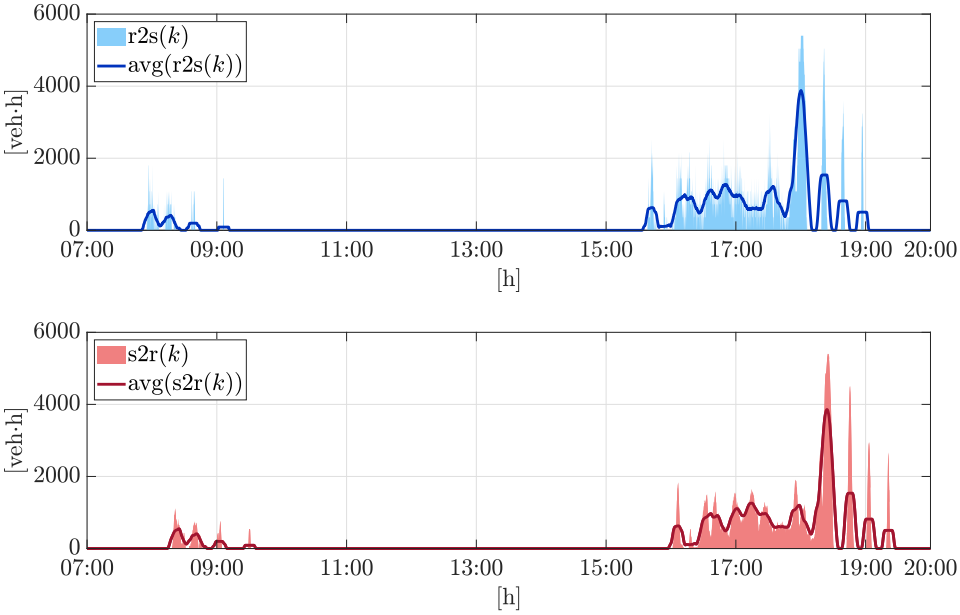

Figure 7.9: The flows entering and exiting the CS, i.e., r2s and s2r respectively. The shaded area represents the actual flow, while the solid line a moving average with a window of 10 min.

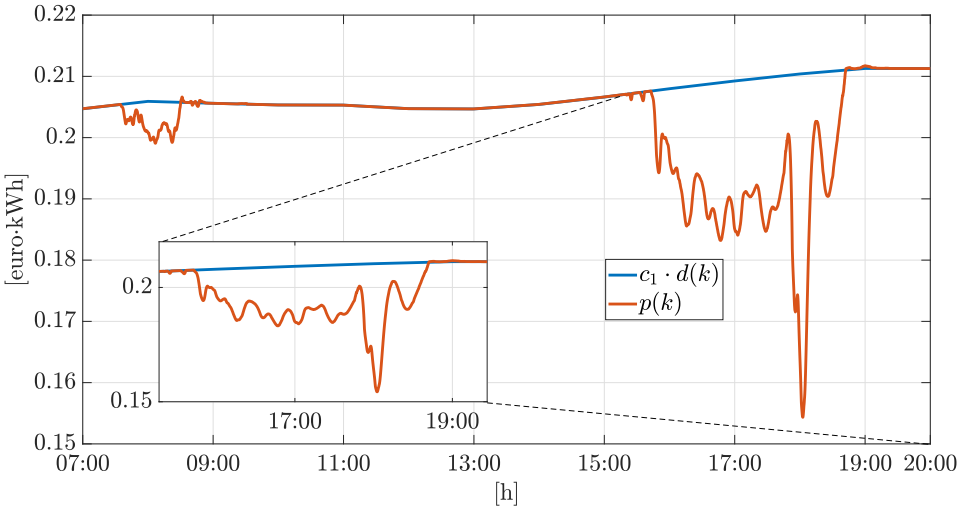

Figure 7.10: The energy price p adopted by the CS and the base demand d scaled by the factor c_1.

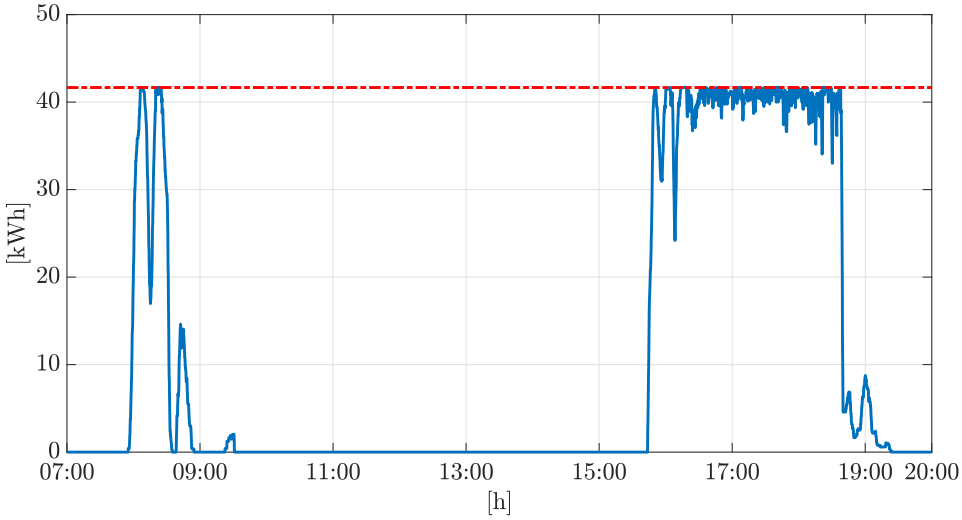

Figure 7.11: The total energy purchased by the PEVs, u^{PEV}. The red dashed line denotes $u^{\max}$.

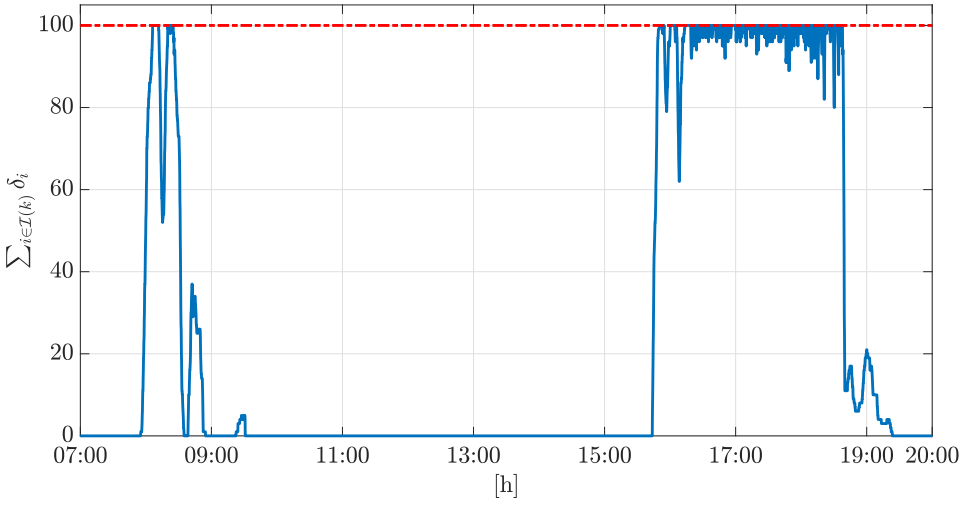

Figure 7.12: The number of busy charging spots at the CS. The red dashed line is set equal to $\bar{\delta} = 100$, the capacity of the CS.

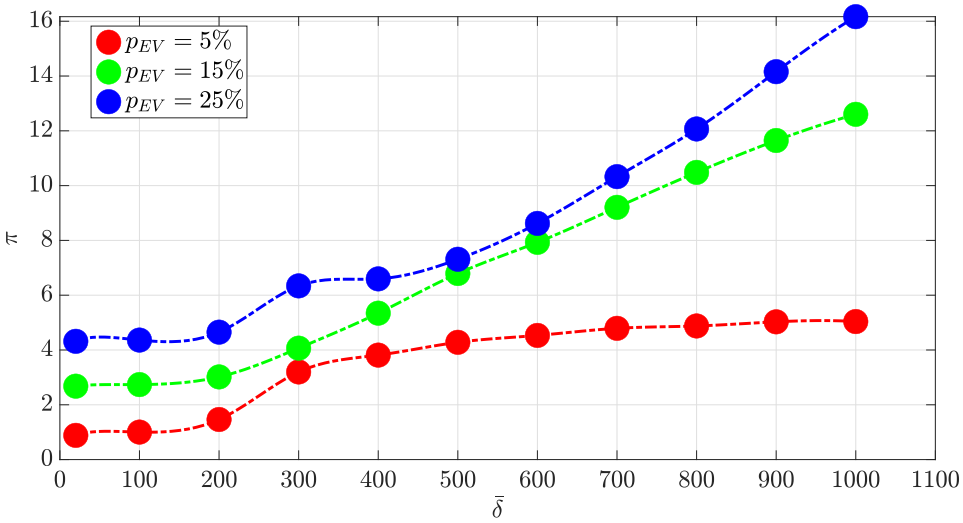

Figure 7.13: Effect of the increment $\bar{\delta}$ on the performance index π in (7.30). The simulations are carried out for different values of p_{EV}.

7.9 Sensitivity analysis

Next, we investigate the effects that a single parameter has on Δ. They are difficult to extrapolate directly from the base case due to the complexity of the decision making process and the multitude of variables involved. In this section, we propose a sensitivity analysis that focuses on the most compelling features of the proposed ATDM. Specifically, we start from the parameter configuration in Table 7.3 and vary one parameter (or at most two) to highlight how it affects the travel time. Note that the values used for this variation may deviate from what one can reasonably expect in a real-world scenario, e.g. a CS with $\bar{\delta} = 1000$, but they are meant to investigate the performance in extreme configurations or approximations of possible future configurations, e.g. one CS that approximates the charging capacity of two or more nearby CSs.

7.9.1 Number of available charging spots

Intuitively, a larger number of charging spots $\bar{\delta}$ mitigates the effects of prolonged traffic congestion; in fact, the PEVs take more time to saturate the available spots at the CS, and, as a consequence, the congestion alleviation during the rush hours can be more effective. The variation of π with respect to the increment of charging spots is presented in Figure 7.13 for different PEV shares, i.e., p_{EV}. The curve profile for $p_{\text{EV}} = 5\%$ shows two plateaus, one for small values of $\bar{\delta}$ and the other for values greater than 400. The transit between the two happens between $\bar{\delta} = 200$ and $\bar{\delta} = 300$. It represents the setting in which an investment to increase the number of charging spots is the most profitable in terms of performance. In fact, going from $\bar{\delta} = 100$ to $\bar{\delta} = 300$ triples the value of π, which rises from 1.05 to 3.19.

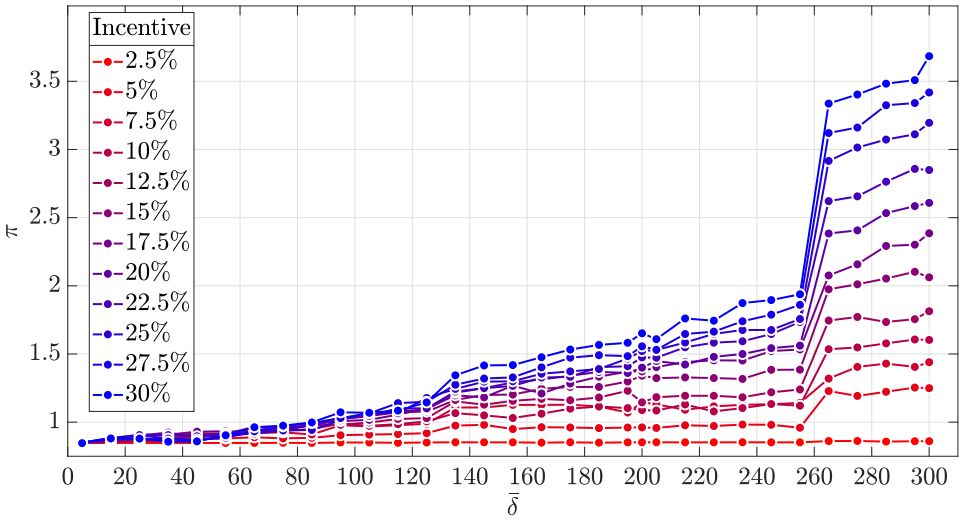

Figure 7.14: The performance π as a function of the number of charging spots, i.e., $\bar{\delta}$, computed for different incentives.

Assuming a higher number of PEVs on the highway does not avoid the initial plateau, but, surprisingly, it prevents the occurrence of an analogous plateau for greater values of $\bar{\delta}$. This implies that investing in more charging spots creates a high return in terms of performance, after a certain "critical" value, i.e., the value of $\bar{\delta}$ after which the initial plateau ends. Interestingly, even if p_{EV} varies, the critical value of $\bar{\delta}$ remains between 200 and 300. In Figures 7.7 and 7.8, we note that the beneficial effect of an increment of the PEVs number. In fact, the more PEVs subscribe the higher the traffic alleviation is. Figure 7.8, clearly shows the valley filling effect, namely a higher peak reduction implies a subsequent increment of travel time during the less-congested period.

7.9.2 Charging spots and incentive

Starting from the parameters in Table 7.3, we analyze the performance obtained by varying simultaneously the number of available charging spots, i.e., $\bar{\delta}$, and the incentive on the energy price. Figure 7.14 depicts the different curves resulting by increasing the number of available charging spots, i.e., $\bar{\delta} \in [5, 295]$, when the incentive ranges between 2.5% and 30%. An increment in the number of plugs generates, in general, an higher performance increment compared to a greater incentive. Surprisingly, the value of $\bar{\delta}$ at which the initial plateau of performance stops is not affected by the incentive. In fact, the consequent steep increment in π settles between $\bar{\delta} = 255$ and 265; this can be considered the critical value for this configuration. On the other hand, an increment in the incentive creates a smaller effect on the performance yet it is more predictable especially if the number of plugs is high. This result suggests that an investment in increasing $\bar{\delta}$ leads to a high return only if the additional charging spots allow to surpass the critical level.

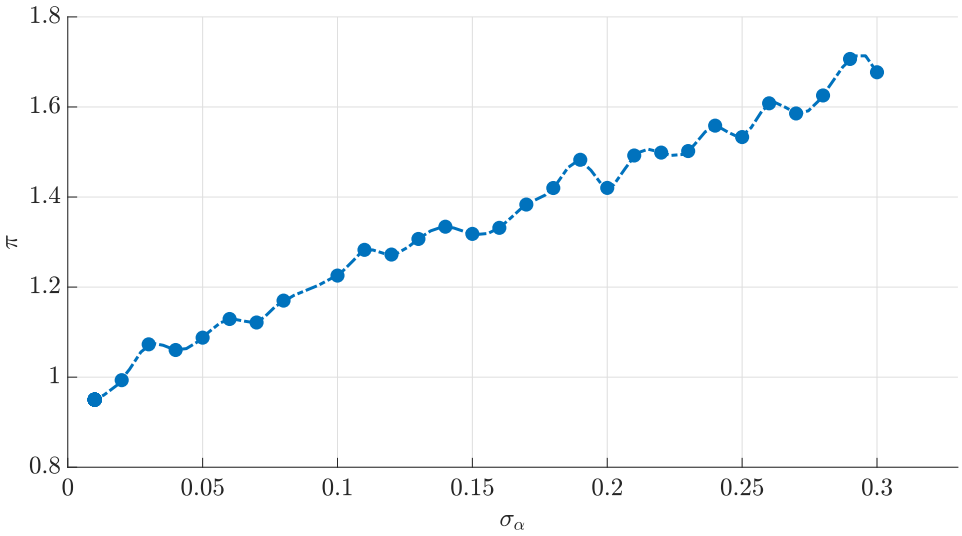

Figure 7.15: Performance π as a function of σ_α, the heterogeneity in drivers interests.

If this is not possible, then increasing the incentive is a more profitable strategy.

7.9.3 Heterogeneous population of PEVs

In the simulations performed for the base case in Section 7.8.2, we have considered a fairly homogeneous population of PEV owners, i.e., drivers that value similarly their interest of saving time or money. The probability distribution, from which all the α_i are drawn, has variance $\sigma_\alpha = 0.03$. Next, we consider a collection of heterogeneous PEVs, in which some are more interested in maintaining the travel time at its minimum and others in saving money. In Figure 7.15, we show the performance increment attained by assuming a population of agents with increasingly diverse interests (all the other parameters are set as in Table 7.3). Interestingly, the value of π increases from 0.95, when $\sigma_\alpha = 0.01$, all the way to 1.71, if $\sigma_\alpha = 0.29$. The trend of the increment is almost linear and does not seem to slow down for higher values of σ_α. From [73], it seems reasonable to assume that the commuters involved in the decision making process form a heterogeneous set; nevertheless, the fact that we focus only on PEV owners may reduce this variability. The value of α that describes the best a real-world scenario is for these reasons an open problem that requires further investigation. The increment in the performance can be explained by looking at Figure 7.12. In fact, a more heterogeneous population leads to fewer PEVs stopping at the CS during the long afternoon congestion peak. This alleviates the problem of overcrowding the CS where all the charging spots are generally busy during the largest traffic congestion peaks.

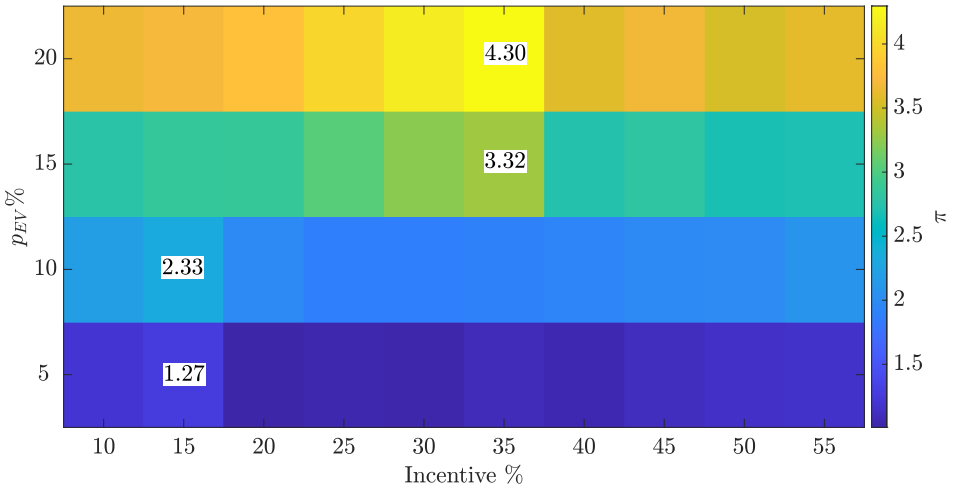

Figure 7.16: The performance π in (7.30) for different combinations of p_{EV} and percentage of incentive. We explicitly reported the value of π only for the best performer of each row.

7.9.4 Incentive

Based on our numerical study, we have chosen the incentive used in the base case heuristically. In this subsection, we study the effect of different incentives if p_{EV} varies. In Figure 7.16, we report the performance π computed for all the combinations of the incentive $[10, 55]$ and $p_{\text{EV}} \in \{5, 10, 15, 20\}$. If $p_{\text{EV}} = 5\%$ the value of π is almost constant with fluctuations of ± 0.1. In the other cases, an interesting trend arises: the optimal incentive that maximizes the performance is not the highest one. In fact, if $p_{\text{EV}} = 10\%$ the optimal incentive is 15% while for $p_{\text{EV}} = 15\%$ and $p_{\text{EV}} = 20\%$ it is 35%. This relates to the phenomena described at the end of Section 7.8.2. Inflating the incentive makes the number of PEVs willing to stop grow. This has a beneficial effect on the morning peak, but a detrimental one on the afternoon rush hour, since it exacerbates the problem of the overly crowded CS and the lack of available charging spots. To mitigate this issue, we propose in the next simulation a discount that varies over time and, in particular, takes a higher value during the morning traffic congestion peak and a lower value during the afternoon one. Specifically, if we say we apply an incentive of $y\%$, then it means that we apply a $y\%$ incentive from 7:00 to 16:00, and $0.2\,y\%$ for the remainder of the day. Implementing this smarter type of incentive leads to striking results. In Figure 7.17, for $p_{\text{EV}} = 5\%$ the travel time significantly decreases with the increment of the incentive, i.e., π goes from 1.27 (see Figure 7.16) to 1.96. This trend holds also for higher values of p_{EV}, increasing the overall maximum performance π from 4.3 to 5.09. This suggests that the problem of over incentivizing the PEVs to stop during the afternoon should be solvable with incentives decreased for the afternoon peak only. Finally, the fact that the maximum value of π always coincides with the maximum incentive suggests that there is still room for improving the performance

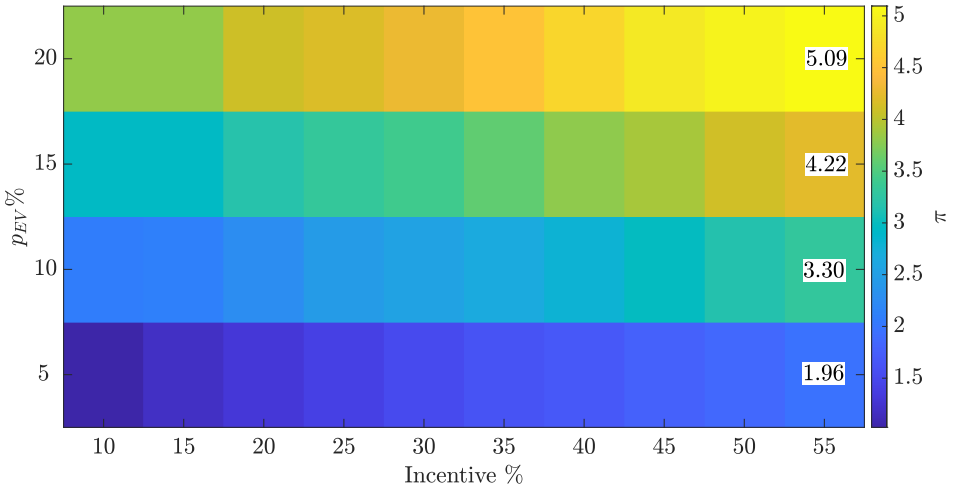

Figure 7.17: The performance π in (7.30) for different combinations of p_{EV} and percentage of incentive. The incentive takes the nominal value during the morning peak and 1/5 of it during the afternoon peak. We explicitly reported the value of π only for the best performer of each row.

by increasing the incentive even further. Nevertheless, one should be careful in implementing a very large incentive, because it might be overly costly for the HO that has to take care of the economical burden associated with the energy price discount.

7.10 Policy recommendation

Let us now extrapolate the key messages based on the numerical analysis and results of the previous sections, and then elaborate on possible policies that can improve the performance of the ATDM.

As illustrated in the previous section, tuning the parameters involved in the decision making process translates into *infrastructural* or *sociological* actions. The former are related to tangible features of the infrastructure, e.g., the number of available charging spots $\bar{\delta}$ or the maximum power that fast charging can deliver $\bar{u}$; the latter instead are intrinsically linked to the behaviors and decisions of the drivers, e.g., the interests of each agent α_i or the incentive applied to steer the drivers' behavior. As expected, the infrastructural improvements create greater outcomes in terms of performance, as shown in Figure 7.14 where the performance improvement by increasing the number of available charging spots overcomes that due to a higher monetary discount. This type of interventions is expensive and produces inelastic changes with respect to the demand. As an illustrative example, let us focus on $\bar{\delta}$: increasing it leads to a CS that has a low percentage of charging spots occupied throughout most of the day, and thus the return of the investment is limited. This

economic point of view and the existence of a critical value of $\bar{\delta}$ (see Section 7.9.1) suggest that the HO should carefully decide whether it is convenient to invest in this direction. Infrastructural actions should be rare and performed when a substantial leap forward can be achieved, while small incremental improvement should be avoided.

Enforcing a change in the drivers' behavior is not as straightforward as changing some physical features. Nevertheless, our formal analysis and modeling of the decision making process help us to infer some possible policies to achieve an improvement in the traffic congestion alleviation. The energy price discount generates remarkable performance, if it is designed by the HO based on the severity of the traffic congestions, see Figures 7.16 and 7.17. This policy does not require massive investment to be implemented and it is elastic with respect to the current traffic situation. Thus, from an economic perspective, a dynamic energy price currently seems the safest and the most remunerative option for the HO. The growing trend of incentivizing smart working and flexible working hours has a beneficial effect on the proposed policy for ATDM. In fact, it will increase the variety of interests among the PEV owners and consequently the performance should also increase, see Figure 7.15. Moreover, flexible schedules may shift the overall interest of the drivers towards saving money rather than time. This variation will allow the HO to attain the same performance even with lower incentives.

To summarize, the theoretical framework developed and the numerical simulations carried out in this chapter have convinced us that a solid policy to maximize the efficacy of the ATDM over time should be composed of *short term* and *long term* actions following two broad guidelines:

- *Short term:* a dynamic energy price should be implemented where the incentive varies with respect to the intensity and (estimated) duration of the traffic congestion.
- *Long term:* consider a major infrastructural investment to increase the CS capabilities, e.g., increase the number of charging spots, and consequently achieve a performance boost. In the A13 case study analyzed here, the long term actions should be introduced, in addition to the short term ones, when the HO can increase the charging plugs above 100. This ensures a substantial improvement in performance that motivates the monetary investment.

7.11 Conclusion

On a highway stretch with one charging station, the adoption of a dynamic energy price, discounted proportionally to the traffic level, can contribute to alleviate the traffic congestion. It incentivizes the plug-in electric vehicles' owners to stop for charging during, or close to, the rush hours. Under the assumption of a rational self-interested behavior, a multi-agent game arises between the plug-in electric vehicles that have to choose whether or not it is convenient to stop at the charging station. The decision process can be formalized as a mixed-integer generalized potential

game, and solved via a semi-decentralized iterative scheme, where the highway operator acts as an aggregator. This control scheme converges to a mixed-integer Nash equilibrium of the game, i.e., an approximated optimal charging strategy for the electric vehicles. The ATDM strategy proposed has been validated by simulation in a highly congested highway stretch, achieving a reduction of the peak traffic congestion of about 5.4% in terms of travel time. This result is obtained with the current value of PEV market shares that is around the 5%. This method creates a redistribution of the vehicles throughout the day, achieving a travel time that is on average 1% lower for all the vehicles (not only PEVs) traveling on the highway. The foreseeable increment of the PEVs and the strengthening of the charging infrastructure, together with the increasing popularity of flexible working schedules, will enhance the benefits of applying the proposed policy, making it even more effective over the upcoming years.

7.12 Appendix

In the following, we adopt the same notation and definitions as in Appendix 6.7 to describe how to translate basic logical implications to sets of inequalities by means of auxiliary variables.

The expression in (7.7) can be directly transformed into the set of linear inequalities

$$\mathcal{S}_{\geq}(\delta_i(t), u_i(t), \underline{u}) \,. \tag{7.31}$$

The two conditions in (7.14) can be recast using the two auxiliary variables $\varphi_i^{\mathrm{LH}}, \varphi_i^{\mathrm{HL}} \in \mathbb{B}$ denoting the rising and falling edge of ϑ_i respectively, so, for every $t \in \mathcal{T}(k)$, they have to satisfy

$$\mathcal{S}_{\wedge}(\varphi_i^{\mathrm{LH}}(t), (1 - \vartheta_i(t-1)), \vartheta_i(t)) \,, \tag{7.32a}$$

$$\mathcal{S}_{\wedge}(\varphi_i^{\mathrm{HL}}(t), \vartheta_i(t-1), (1 - \vartheta_i(t))) \,. \tag{7.32b}$$

Using the variable introduced above for all $t \in \mathcal{T}(k)$, the condition in (7.15) becomes

$$\begin{aligned} &\varphi_i^{\mathrm{HL}}(t+1) g_i(t) = 0 \,, \\ &g_i(t) \coloneqq \sum_{p \in \mathcal{T}(k)} \vartheta_i(p) - \min\{t - k + W + 1, 2W + 1\} \,. \end{aligned} \tag{7.33}$$

The nonlinearity in (7.33) can be converted using the auxiliary variable $q_i(t)$ for every $t \in \mathcal{T}(k)$ as

$$\mathcal{S}_{\Rightarrow}(q_i(t), g_i(t), \varphi_i^{\mathrm{HL}}(t+1)) \,. \tag{7.34}$$

Finally, (7.33) becomes

$$q_i(t) = 0 \,. \tag{7.35}$$

The constraint in (7.16) is equivalent to the linear inequality

$$\sum_{p=k}^{t+W+1} \varphi_i^{\mathrm{HL}}(p) + \delta_i(t) \leq 1 \,, \; \forall t \in \mathcal{T}(k) \,. \tag{7.36}$$

The logical implication (7.17) requires the introduction of an auxiliary binary variable $\psi_i(t) \in \mathbb{B}$ defined for every $t \in \mathcal{T}(k)$ as $[\psi_i(t) = 1] \iff [\delta_i(t-1) = 1] \wedge [\delta_i(t) = 0]$. This implication can be transformed to the set of inequalities

$$\mathcal{S}_{\wedge}(\psi_i(t), \delta_i(t-1), (1 - \delta_i(t))) \,. \tag{7.37}$$

Then, (7.17) translates into $[\psi_i(t) = 1] \implies [\vartheta_i(r) = 1]$ that can be rephrased, for all $t \in \mathcal{T}(k)$ and $r \in \{\max(k, t - W), \ldots, t + W\}$, as

$$\vartheta_i(r) - \psi_i(t) \geq 0 \,. \tag{7.38}$$

The constraint in (7.18) requires an additional step. First, we introduce the binary auxiliary variable $[\sigma_i(t) = 1] \iff [\delta_i(t-1) = 0] \wedge [\delta_i(t) = 1]$, for every $t \in \mathcal{T}(k)$. By exploiting σ_i, (7.18) can be equivalently written as

$$\sigma_i(t) \left(\sum_{h=1}^{\overline{h}} \delta_i(t+h) - \overline{h} \right) = 0 \,. \tag{7.39}$$

Next, to eliminate the nonlinearity in (7.39), we define $\overline{h}$ auxiliary binary variables $\mu_i^{(1)}(t), \ldots, \mu_i^{(\overline{h})}(t) \in \mathbb{B}$ for every t as

$$\mathcal{S}_\wedge(\mu_i^{(h)}(t), \sigma_i(t), \delta_i(t+h)) \,, \; \forall h \in \{1, \ldots, \overline{h}\}. \tag{7.40}$$

Thus, (7.39) reduces to the linear equation

$$\sum_{h=1}^{\overline{h}} \mu_i^{(h)}(t) - \sigma_i(t)\overline{h} = 0 \,. \tag{7.41}$$

We transform (7.19) into the following set of linear constraints by introducing the auxiliary variable $\nu_i \in \mathbb{B}$, and hence for every $i \in \mathcal{I}(k)$ it must be true that

$$\begin{gathered} 0 < \nu_i + \tfrac{1}{W+1} \sum_{p=0}^{W} \vartheta_i(k+p) \leq 1 \\ \mathcal{S}_\geq(\nu_i, \textstyle\sum_{t \in \mathcal{T}(k)} \vartheta_i(t), W+2) \end{gathered} \tag{7.42}$$

The last logical implication to be transformed into a linear inequality is (7.20). The variable $\omega_i(t) \in \mathbb{B}$ is defined as $[x_i(t) < x_i^{\text{ref}}] \iff [\omega(t) = 1]$, so it satisfies the pattern of inequalities

$$\mathcal{S}_\leq(\omega_i(t), x_i(t), x_i^{\text{ref}}) \,. \tag{7.43}$$

Finally, (7.20) is equivalent to the linear inequality

$$\omega_i(t) + \vartheta_i((\max(k, t-W))) \leq 1 \,. \tag{7.44}$$

8

Conclusion and Outlook

We live in a society that is more and more connected in which the interactions are not anymore only among people but also among intelligent machines. In this thesis, we studied from both a theoretical and applied perspective multi-agent network games that model a wide range of decision making processes in complex highly connected systems. They can be used to model decisions among machines (as in Chapter 3 with the distributed model-fitting algorithm), a mixture of machines and humans (as done in Chapters 6 and 7 with a policy design problem) and humans only (via opinion dynamics models, as in Chapter 2). This final chapter is dedicated to summarizing the main contributions achieved in the previous chapters. We discuss possible developments and future research directions that may expand and improve the analysis we carried out. For some problems, we also discuss some inherent limitations and challenges.

8.1 Part I: Multi-agent network games via operator theory

8.1.1 Chapter 2

In this chapter, we proved global convergence for multi-agent network games with proximal type dynamics in which the communication network is described by a strongly connected weighted digraph. In the case of asynchronous dynamics with possibly delayed information, we computed a theoretical upper bound on the delay that ensures convergence. Moreover, we also considered games with a time-varying communication network. In this case, we established convergence to a persistent network equilibrium of the game, if the players can select the weight they give to their self-loops. Finally, we have highlighted the relevance of the achieved results applying them to classical opinion dynamics models.

Outlook

Although we have analyzed several different setups, this topic still presents challenging open problems that can be explored in future research.

(i) In the case of a time-varying graph, see Section 2.3.3, we have assumed that at every time instant the communication networks satisfy Standing Assumption 2.3. It can be interesting to weaken this assumption by considering repeatedly jointly connected communication networks, as done in [89].

(ii) An interesting extension of this work is to replace the communication network with a signed graph. This structure arises in several applications, e.g., the Altafini opinion dynamics model [7].

8.1.2 Chapter 3

Starting from the results developed in Chapter 2, we considered in this chapter the more general case of multi-agent network games with the proximal type dynamics subject to, not only local constraints but also affine coupling constraints. We showed that these additional constraints create non-converging dynamics, therefore we rephrased them as pseudo-collaborative ones. A central coordinator sends to the agents a global variable used to meet the constraint. For these new dynamics, we developed Prox-GNWE, a semi-decentralized iterative algorithm globally converging to a generalized network equilibrium of the game. Then, we generalized the setup by allowing the communication network and the constraints to be time-varying. The assumptions required to ensure the existence of an equilibrium point were discussed and the previous algorithm was modified, obtaining TV-Prox-GNWE, to ensure global convergence to a persistent generalized network equilibrium. We conclude the chapter by applying the developed algorithms to solve the problems of distributed model fitting and constrained consensus.

Outlook

Even though the problem of multi-agent network games has been studied extensively, we propose some possible extensions and challenging open problems that may spark interesting new results.

(i) The existence of an equilibrium point, for the time-varying case, has to be assumed or implied by restrictive technical assumptions. To weak these assumptions or provide others that are easier to check, would constitute an important leap forward to improve the theoretical results developed and make them easier to apply for specific problems.

(ii) The implementation of the asynchronous version of Prox-GNWE presents several technical issues. In fact, the operator in (3.22), describing the synchronous dynamics, is *quasi*-NEX. This is a weaker property than NEX, and thus it does not allow us to extend the approach used in Section 2.3.2 to create the asynchronous version of the constrained dynamics, see [147, Th. 1]. In the literature, there are no asynchronous algorithms providing convergence for the *quasi*-NEX operators that lead to an implementable iterative algorithm, and thus an *ad hoc* solution has to be developed.

8.1.3 Chapter 4

In this chapter, we have steered our focus towards strongly monotone games over networks. In particular, we developed two asynchronous GNE seeking algorithms that are robust to delayed information, i.e., SD-GENO and AD-GENO. The two differ in the auxiliary variables used. In fact, in SD-GENO one auxiliary variable was imposed for every edge in the network; on the other hand, AD-GENO uses node variables only. This difference makes AD-GENO faster and more scalable, without increasing the number of communication required. We validated the improvement in performances by comparing AD-GENO with other algorithms available and showed that, in our simulations, it always outperformed the others in terms of computational time.

Outlook

The results presented allow for several extensions.

(i) The "ARock" framework does not ensure robustness to lossy communication. This is currently an open problem that can increase the adaptability of AD-GENO to real-world scenarios.

(ii) Another interesting topic is the generalization of the algorithm to the case of time-varying communication networks. The use of node variables only seems to be suitable to deal with the technical difficulties arising from the varying network topology.

(iii) It can be interesting to extend AD-GENO to games in which the agents have access only to *partial information* about their neighbors' strategies and must estimate the missing parts.

8.2 Part II: Decision making via potential game theory

8.2.1 Chapter 5

Motivated from theoretical and behavioral economics, we proposed the h-RBR dynamics for finite and convex games to model partial rationality among decision makers. We have shown that for a general class of games these dynamics converge to a GNE, and that the corresponding decision making process is "compatible" with BR dynamics. That is, a mix of best responders and h-relative best responders will eventually reach an equilibrium action profile. These results make it possible to rigorously study how relative performance considerations of irrational (or conforming) decision makers affect the behavior and equilibrium profiles of complex socio-technical and socio-economic processes. These dynamics create a new framework to analyze these problems and can act as a cornerstone for future developments. As an illustrative example, we simulated the product adoption game, in which the agents' decisions are influenced by some network effect.

Outlook

Since this work introduces the h-RBR, the possible extensions and applications are virtually countless. Nevertheless, we list the ones we think are the most relevant.

(i) A trivial extension is the development of an h-relative *better* response. Notice that our convergence results would hold also for these new dynamics.

(ii) The h-RBR dynamics can be enriched by adding coupling constraints between the agents. This extension is not trivial since these constraints will modify the feasible set of the agents, thus they may not be able to adopt the strategy of some of the best performers.

(iii) An open problem is the convergence of h-RBR subject to a synchronous update. The use of a state-dependent feasible decision set creates several technical challenges in establishing convergence.

(iv) From an application point of view, it is interesting to validate with real experiments the modeling power of these dynamics, and this would corroborate our theoretical results.

8.2.2 Chapter 6

Motivated by the increment of PEVs in the market, and the consequent rising in energy demand, we tackled in this chapter the charging scheduling problem for a fleet of electric vehicles. The problem was modeled as a mixed-integer aggregative game in which the mixed-integer affine constraints captured the limitation and preferences in the scheduling of each PEV. The energy price was linked to the total energy demand, making it unfavorable for most users to charge during periods of peaks in demand. The price of the energy is established by an aggregator that takes the role of the grid operator, and this naturally leads to a semi-decentralized algorithm in which the PEVs communicate with the operator and not between each other. Moreover, we have proven that the charging schedule resulting from the proposed control scheme is an MINE of the game. We completed the chapter by showing via simulations that this policy reduces the energy demand peaks by achieving valley filling, i.e., a more homogeneous energy demand throughout the day.

Outlooks

In this chapter, we studied a specific problem configuration; in future research, several modifications or generalizations can be considered to expand and/or generalize the problem studied here.

(i) The specific sequence of activation, which selects among the PEVs the one that has to update, highly influences both the outcome of the game and the speed of convergence. A deep understanding of this phenomenon may lead to interesting reasoning on how to provide a premium subscription to the service by giving priority to some of the PEVs.

(ii) In the setup considered, there is only one charging station at which the PEV may park. Even though this can model a small neighborhood, it is logical to extend it to the case of multiple charging stations placed in different locations.

(iii) An interesting generalization of this approach is a bi-level optimization problem in which, on top of the mixed integer game, the grid operator aims at maximizing its benefit. Therefore, the resulting game would be a mixed-integer Stackelberg game. The development of an iterative algorithm solving this class of games would create an important contribution to this problem.

8.2.3 Chapter 7

In this chapter, we designed an ATDM based on smart charging of PEVs. We considered a highway stretch and propose a control action based on incentivizing the owners of PEVs to stop at a charging station during the period of high traffic congestion. We proposed a monetary incentive in which the energy price is inversely proportional to the level of congestion. This approach was akin to the one proposed in Chapter 6, indeed at every time instant the problem arising was modeled as a

mixed-integer game, in which we exploited the integer variables to describe the possible actions of the PEVs. Different from the charging schedule problem, in this case for every time interval a new game arises and has to be solved before the starting of a new interval. A semi-decentralized control scheme was proposed and we proved the convergence of the decisions of the agents to an MINE, for every instance of the game. The final part of the chapter was devoted to an extensive case study, in which we considered real traffic data from the A13 highway in The Netherlands that connects The Hague and Rotterdam. We identified the charging station and used the model to simulate the effect of the proposed policy in a realistic scenario. Furthermore, we carried out the sensitivity analysis focused on understanding the role of the parameters in the game of the performance. This allows us to extrapolate the most efficient short and long-term policies to maximize traffic alleviation via effective interventions.

Outlook

The novel proposed policy opens many different scenarios that can be studied, we itemize in the following some future research directions.

(i) One can notice that the traffic model considered is used as an oracle by the highway operator to obtain certain information on the future traffic evolution. For this reason, the framework developed in this work can be adapted to accommodate more complex traffic dynamics.

(ii) Since the emerging game is an exact potential game, the myopic best response dynamics adopted by the PEVs might be (partially) replaced by the h-RBR dynamics, introduced in Chapter 6. This would introduce some of the irrational behavior that decision makers usually exhibit in situations like traffic jams.

(iii) A natural generalization of the problem considered is the extension to the case of multiple charging stations placed along the highway stretch. This is not straightforward because every game arising at one charging station influences the ones carried out by the other charging stations.

(iv) The use of soft policy does not prevent the highway operator to implement other classical policies to alleviate the traffic jams. To model how soft and hard policies work in synergy is an important extension to define the most effective collection of ATDM strategies that might be implemented.

(v) In the literature, other ATDM strategies have been proposed, e.g. [1]. It can be of great value to carry out a comprehensive study that analyzes if and how well they work in combination to improve traffic congestion alleviation.

A

Monotone operators and fixed point theory

Developed in the early 1960s, monotone operator theory, convex analysis and fixed point theory are three mayor research areas in the field of nonlinear analysis, and their popularity raised constantly thereafter. Nowadays, these methods are used in a plethora of diverse fields and helped mathematicians and engineers to study highly nonlinear problems. In the past four decades, the literature on these topics thrived and sparked many different results. For this reason, we propose in the following a selection of results that focus mostly on single valued operators on finite dimensional Hilbert spaces. Notice that many of the following theorems still hold in infinite dimensional spaces or might be generalized to other topological spaces.

A.1 Operators

Let the sets $\mathcal{X} \subseteq \mathcal{H}$ and $\mathcal{Y} \subseteq \mathcal{H}$ be nonempty and $\mathcal{H}$ be a finite dimensional Hilbert space. An operator (or mapping) T maps every point $x \in \mathcal{X}$ to a point (or set) $T(x) \subseteq \mathcal{Y}$. If $T(x)$ may contain more than one element, then we call T a *set-valued* operator and denote it by $T : \mathcal{X} \rightrightarrows \mathcal{Y}$. Instead, if $T(x)$ is a singleton for all $x \in \mathcal{X}$, then we call it a *single-valued* operator and we denote it by $T : \mathcal{X} \to \mathcal{Y}$. The domain of an operator is defined as

$$\operatorname{dom} T \coloneqq \{x \in \mathcal{X} \,|\, T(x) \neq \varnothing\} .$$

A special case of single-valued operator $f : \mathcal{X} \to \overline{\mathbb{R}}$ is a *function* and its domain is defined as $\operatorname{dom} f \coloneqq \{x \in \mathcal{X} \,|\, f(x) < +\infty\}$ (this definition slightly differs from the domain definition introduced above, for this reason some authors refer at it as *effective domain*).

Given an operator $T : \mathcal{X} \to \mathcal{X}$, all the points in $\mathcal{X}$ that are mapped in themselves are called *fixed points* of T, and they compose the following set

$$\text{fix}(T) \coloneqq \{x \in \mathcal{X} | T(x) = x\} . \tag{A.1}$$

It is easy to understand why this class of points, i.e., those invariant w.r.t. the transformation applied by T, is of particular interest in many problems.

Given a set valued operator $A : \mathcal{X} \rightrightarrows \mathcal{X}$, the set of all its zeros is defined as

$$\text{zer}(A) = A^{-1} = \{x \in \mathcal{X} \,|\, 0 \in Ax\} .$$

This set of points plays a crucial role in many different research areas. For examples, if A characterizes the dynamics of a systems the set of its zeros describes the stationary points. From the definition above, one can notice that there exists a tight connection between fixed points and zeros of an operator, namely

$$x^* \in \text{fix}(A) \iff x^* \in \text{zer}(\text{Id} - A) ,$$

In the remainder of the chapter, we indicate by $\mathcal{H}_\Phi$ a finite dimensional Hilbert space with $\langle \cdot, \cdot \rangle_\Phi$ and $\Phi = \Phi^\top \succ 0$, while with $\mathcal{H}$ a general finite dimensional Hilbert space.

A.2 Nonexpansive operators

Useful information on the fixed points of T can be obtained by investigating the nonexpansiveness property of the operator at hand. Roughly speaking, these property measure if two points in $\mathcal{X}$ get closer or further apart after the transformation applied by T. This concept is closely related to the one of Lipschitz continuity.

Definition A.1 (Lipschitz's continuity, [14, Def. 1.47])**.** The operator $T : \mathcal{X} \to \mathcal{Y}$ is Lipschitz continuous with constant $\ell > 0$ if

$$(\forall x, y \in \mathcal{X}) , \quad \|T(x) - T(y)\| \leq \ell \|x - y\| . \qquad \square$$

Next, we list different kinds of nonexpansiveness that will prove themselves useful in the next chapters.

Definition A.2 ([14, Def. 4.1])**.** Given D be a nonempty subset of a Hilbert space $\mathcal{H}_\Phi$, the operator $T : D \to \mathcal{H}_\Phi$ is:

(i) *Contractive* (CON) in $\mathcal{H}_\Phi$ if it is ℓ-Lipschitz with $\ell \in (0, 1)$, i.e.,

$$(\forall x, y \in D) , \quad \|T(x) - T(y)\|_\Phi < \ell \|x - y\|_\Phi .$$

(ii) *Firmly nonexpansive* (FNE) in $\mathcal{H}_\Phi$ if it is $\frac{1}{2}$-AVG, i.e.,

$$(\forall x, y \in D) , \quad \|T(x) - T(y)\|_\Phi^2 \leq \|x - y\|_\Phi^2 - \|(\text{Id} - T)(x) - (\text{Id} - T)(y)\|_\Phi^2 .$$

(iii) *η-Averaged* (η-AVG), with $\eta \in (0,1)$, in $\mathcal{H}_\Phi$ if

$$(\forall x, y \in D)\,, \quad \|T(x) - T(y)\|_\Phi^2 \leq \|x - y\|_\Phi^2 - \tfrac{1-\alpha}{\alpha}\|(\mathrm{Id} - T)(x) - (\mathrm{Id} - T)(y)\|_\Phi^2.$$

(iv) *Nonexpansive* (NEX) in $\mathcal{H}_\Phi$ if it is 1-Lipschitz, i.e.,

$$(\forall x, y \in D)\,, \quad \|T(x) - T(y)\|_\Phi \leq \|x - y\|_\Phi.$$

(v) *Quasi-nonexpansive* (Q-NE) in $\mathcal{H}_\Phi$ if it is 1-Lipschitz w.r.t. $\mathrm{fix}(T)$, i.e.,

$$(\forall x \in D)(\forall y^* \in \mathrm{fix}(T))\,, \quad \|T(x) - T(y^*)\|_\Phi \leq \|x - y^*\|_\Phi. \qquad \square$$

It is worth it to highlight that, from the relation above, the following two chains of implication hold:

$$\text{FNE} \implies \text{AVG} \implies \text{NE} \implies \text{Q-NE}$$

$$\text{CON} \implies \text{AVG} \implies \text{NE} \implies \text{Q-NE}\,.$$

As anticipated, we can retrieve insights on the fixed points of T relying on the regularity properties above. Specifically, the following theorem provides a sufficient condition for the existence of at least one fixed point of the operator.

Theorem A.3 (Browder-Göhde-Kirk, [14, Th. 4.29])**.** *Let D be a nonempty bounded closed convex subset of $\mathcal{H}_\Phi$ and let $T : D \to D$ be a NEX operator. Then,* $\mathrm{fix}(T) \neq \varnothing$. $\square$

If the operator is a CON, that is a stronger property than NEX, it is possible to prove that the set of fixed points is a singleton, as done in the following.

Theorem A.4 (Banach–Picard, [14, Th. 1.50])**.** *Let D be a nonempty bounded closed convex subset of $\mathcal{H}_\Phi$ and let $T : D \to D$ be a CON operator. Then,* $\mathrm{fix}(T) = \{x^*\}$*, i.e., the operator possesses a unique fixed point.* $\square$

A.3 Monotone Operators

Similarly to the nonexpansiveness for the fixed points, analyzing the *monotonicity* of an operator provides information on the existence and uniqueness of its zeros. Also in this case, we introduce in the following different types of monotone operators

Definition A.5 ([14, Def. 22.1])**.** Let D be a nonempty subset of $\mathcal{H}_\Phi$, then set valued mapping $A : D \rightrightarrows D$ is:

(i) *Monotone* (MON) if

$$((x,u) \in \mathrm{gra}(A))((y,v) \in \mathrm{gra}(A))\,, \quad \langle x - y,\ u - v\rangle_\Phi \geq 0.$$

(ii) *Strictly monotone* (sMON) if

$$((x,u) \in \mathrm{gra}(A))((y,v) \in \mathrm{gra}(A)), \quad \langle x-y,\ u-v\rangle_\Phi > 0.$$

(iii) *Strongly monotone* (SMON) with constant $\beta > 0$, if

$$((x,u) \in \mathrm{gra}(A))((y,v) \in \mathrm{gra}(A)), \quad \langle x-y,\ u-v\rangle_\Phi \geq \beta\|x-y\|_\Phi^2. \qquad \square$$

Moreover, we define the concepts of *maximally monotone* and *cocoercive* operators.

Definition A.6 ([14, Def. 20.20])**.** Consider D be a nonempty subset of $\mathcal{H}_\Phi$. If the set valued operator $A : D \rightrightarrows D$ is monotone and for every $(x,u) \in D \times D$, it holds

$$(x,u) \in \mathrm{gra}(A) \iff (\forall (y,v) \in \mathrm{gra}(A))\langle x-y|u-v\rangle_\Phi \geq 0, \tag{A.2}$$

then, A is *maximally monotone* (or *maximal monotone*). $\square$

Definition A.7 ([14, Def. 4.10])**.** Let D be a nonempty subset of $\mathcal{H}_\Phi$, and $A : D \rightrightarrows D$, then T is β-*cocoercive* with $\beta > 0$ if βA is FNE. $\square$

As anticipated, one can exploit the properties described above to prove the existence and uniqueness of the zero of the operator.

Proposition A.8 ([14, Prop. 23.35])**.** *Let $D \subset \mathcal{H}_\Phi$ be nonempty, and $A : D \rightrightarrows D$ be a sMON operator. Then, the set* $\mathrm{zer}(A)$ *is at most a singleton.* $\square$

If the operator is maximally monotone and it satisfied some additional assumption, then the existence of at least one zero can be established.

Proposition A.9 ([14, Prop. 23.36])**.** *Let $D \subset \mathcal{H}_\Phi$ be nonempty, and $A : D \rightrightarrows D$ be a maximally monotone operator. Assume that at least one of the following holds:*

(i) A^{-1} *is locally bounded everywhere*

(ii) $\lim_{\|x\|\to+\infty} \inf\|Ax\| = +\infty$

(iii) $\mathrm{dom}(A)$ *is bounded*

Then, $\mathrm{zer}(A) \neq \varnothing$. $\square$

Finally, if A is both maximally monotone and SMON, then one can ensure both the existence and uniqueness of a zero.

Corollary A.10 ([14, Cor. 23.37])**.** *If $D \subset \mathcal{H}_\Phi$ is nonempty, and $A : D \rightrightarrows D$ is a maximally monotone and SMON operator, then* $\mathrm{zer}(A)$ *is a singleton.* $\square$

A.3.1 Monotonicity and firmly nonexpansiveness

The monotonicity properties can be related to the nonexpansiveness one by exploiting the characteristic of the so called the resolvent operator that is defined next.

Definition A.11 ([14, Def. 23.1])**.** Let D is a nonempty subset of $\mathcal{H}_\Phi$, and $A : D \rightrightarrows D$ and $\gamma > 0$, then the *resolvent* of A is

$$\mathrm{J}_A \coloneqq (\mathrm{Id} + A)^{-1} \tag{A.3}$$

□

The resolvent operator is arguably one of the most important concept introduced by operator theory. In fact, it allows us to establish an equivalence between FNE and MON.

Proposition A.12 ([14, Prop. 23.10])**.** *Let D be a nonempty subset of $\mathcal{H}_\Phi$, $T : D \to D$ and set $A \coloneqq T^{-1} - \mathrm{Id}$. Then, it holds:*

(i) $T = \mathrm{J}_A$

(ii) T *is FNE if and only if* A *is MON*

(iii) T *is FNE with* $D = \mathcal{H}_\Phi$ *if and only if* A *is maximally monotone.* □

Corollary A.13 ([14, Ex. 20.30])**.** *Let $T : \mathcal{H}_\Phi \to \mathcal{H}_\Phi$ be β-AVG with $\alpha \in (0, 1/2]$, then T is maximally monotone.* □

Furthermore, the stronger assumption of a SMON operator A translates to the cocoercivity of the associated resolvent.

Proposition A.14 ([14, Prop. 23.13])**.** *Consider a nonempty set $D \subset \mathcal{H}_\Phi$, $A : D \rightrightarrows D$ a MON operator and $\beta > 0$. Then, A is β-SMON if and only if J_A is $(\beta - 1)$-cocoercive, hence J_A is $1/(\beta + 1)$-Lipschitz continuous.* □

A.4 Nonexpansiveness and monotonicity of relevant operators

Next, we describe some examples of very well known operators that posses some of the properties aforementioned.

A.4.1 Linear operators

This is the most common class of operators, they have the interesting characteristic that the regularity properties described above can be completely characterized by the spectrum of the operator. In fact, a linear operator $T : \mathbb{R}^n \to \mathbb{R}^n$ is NEX if

and only if all its eigenvalues lay inside the unitary disc and those on the boundary are semi-simple, see [16, Lem. 3]. Furthermore, T is η-AVG with $\eta \in (0,1)$ if and only if all its eigenvalues lay in the disc centered in η and radius $(1-\eta)$, also in this case, those on the disc boundary have to be semi-simple, see [16, Lem. 4].

Concerning the monotonicity, a matrix $T \succeq 0$ is $\|T\|^{-1}$-cocoercive, as shown in [14, Cor. 18.18]. Moreover, if matrix T is monotone, then it is also maximally monotone, as shown in [14, Ex. 20.34].

A.4.2 Subdifferential

The subdifferential of a function f is a fundamental tool to analyze nondifferentiable convex functions and it finds many interesting applications in the context of optimization.

Definition A.15 ([14, Def. 16.1])**.** Let $f : \mathcal{H} \to]-\infty, +\infty]$ be proper. The *subdifferential* of f is the set-valued operator

$$\partial f : \mathcal{H} \rightrightarrows \mathcal{H} : x \mapsto \{u \in \mathcal{H} \,|\, (\forall y \in \mathcal{H})\, \langle y - x | u \rangle + f(x) \leq f(y)\}\,. \tag{A.4}$$

The function f is said to be *subdifferentiable* at $x \in \mathcal{H}$ if $\partial f(x) \neq \varnothing$; and a vector $z \in \partial f(x)$ is called a *subgradient* of f at x. □

The most important property of this operator was discovered by Fermat back in 1637 and takes the name of *Fermat rule*. The global minimizers of a proper function f are characterized by the zeros of the subdifferential operator ∂f.

Theorem A.16 (Fermat's rule, [14, Th. 16.3])**.** *If $f : \mathcal{H} \to]-\infty, +\infty]$ is proper, then it holds*

$$\operatorname{argmin} f = \operatorname{zer}(\partial f) = \{x \in \mathcal{H} \,|\, 0 \in \partial f(x)\}\,. \tag{A.5}$$

□

Moreover, one can show that the subdifferential of a proper function f is monotone operator, as done in [14, Ex 20.3]. If the funciton is proper and lower semicontinous, i.e. $f \in \Gamma_0$, the subdifferential results maximally monotone.

Theorem A.17 (Moreau, [14, Th. 20.25])**.** *If $f \in \Gamma_0(\mathcal{H})$, then ∂f is maximally monotone.* □

A.4.3 Projection

Given a nonempty convex set $\Omega \subset \mathcal{H}$, the subdifferential of the indicator funciton ι_Ω is equal to the *normal cone* of Ω, i.e., $N_\Omega = \partial \iota_\Omega$, see [14, Ex 16.13]. Interestingly, from [14, Ex 23.4], the projection over the set Ω corresponds to the resolvent of $N_\Omega = \partial \iota_\Omega$, thus

$$\operatorname{proj}_\Omega = (\mathrm{Id} + N_\Omega)^{-1} = \mathrm{J}_\Omega \tag{A.6}$$

Invoking Theorem A.17 one can notice that, N_Ω is maximally monotone. So, the projection is the resolvent of a maximally monotone operator and, from Proposition A.12, it is an FNE operator.

A.4.4 Proximal operator

A useful generalization of the projection operator is the *proximal operator* that is defined as for a function $f \in \Gamma_0$ as

$$\operatorname{prox}_f : \mathcal{H} \to \mathcal{H} : x \mapsto \operatorname{argmin}_{y \in \mathcal{H}} \left(f(y) + \tfrac{1}{2}\|x - y\|^2 \right) . \tag{A.7}$$

From [14, Prop. 16.44], the proximal operator can be equivalently rewritten as the resolvent of ∂f, hence

$$\operatorname{prox}_f = (\mathrm{Id} + \partial f)^{-1} = \mathrm{J}_{\partial f} . \tag{A.8}$$

It is clear from (A.6) that if one chooses $f = \iota_\Omega$ then the projection operator is retrieved.

Invoking Proposition A.12 and Theorem A.17, it follows that prox_f is an FNE operator.

For a lower semicontinuous function $f \in \Gamma_0$ the proximal operator creates a link between zeros and fixed points.

Proposition A.18 ([14, Prop. 27.1])**.** *Let $f \in \Gamma_0$. Then, the following chain of equivalences holds true*

$$\operatorname{zer}(\partial f) = \operatorname{argmin} f = \operatorname{fix}(\operatorname{prox}_f) = \operatorname{fix}(\mathrm{J}_{\partial f}) . \tag{A.9}$$

□

Therefore, in order to find the minimizers of a lower semicontinous function, one can equivalently study the zeros of the function's subdifferential or the fixed points of the associated proximal operator.

These operators and the property described above represent the cornerstone to develop iterative algorithm converging to a zero or a fixed point of an operator.

A.5 Fixed point iterations

In this section, we review the Banch–Picard and the Krasnosel'skii–Mann iterations. For an operator T, that possesses some suitable property from Definiton A.2, these iterations generate a sequence that converges to a point in $\operatorname{fix}(T)$. In most of the cases, the set of fixed points cannot be characterized in closed form and these sequences are used to develop a algorithms that learn the fixed points of T.

The most simple iteration that can be considered to construct an update rule is the Banch–Picard iteration. It consists in applying the operator without any modification, thus given an operator T, it is defined as

$$(\forall k \in \mathbb{N}) \quad x(k+1) = T\big(x(k)\big) . \tag{A.10}$$

To ensure convergence of the sequence $(x(k))_{k \in \mathbb{N}}$ generated by (A.10), the operator T has to be AVG as shown in the following theorem.

Theorem A.19 ([14, Th.1.69 and Prop. 5.16])**.** *Let $D \subset \mathcal{H}_\Phi$ be nonempty, closed and convex and $T : D \to D$ be an operator and $\alpha \in (0,1)$ and $\ell \in (0,1)$. Then*

(i) if T is α-AVG and $\mathrm{fix}(T) \neq \varnothing$, then the sequence $(x(k))_{k\in\mathbb{N}}$ generated by (A.10) *converges globally to a fixed point of T, i.e., $x^* \in \mathrm{fix}(T)$*

(ii) if T is ℓ-CON, then the sequence $(x(k))_{k\in\mathbb{N}}$ generated by (A.10) *converges linearly for every initial condition $x(0)$ to the unique fixed point $x^* \in \mathrm{fix}(T)$, hence $\|x(k) - x^*\|_\Phi \leq \ell^k \|x(0) - x^*\|_\Phi$.* □

The case considered above requires the two strongest regularity properties introduced in Definition A.2. If the operator is merely NEX, the Banach–Picard iteration may fail to converge. As toy example, consider the matrix $M = \left[\begin{smallmatrix} 0 & -1 \\ 1 & 0 \end{smallmatrix}\right]$ that is NEX but not AVG, then the iteration in (A.10) does not converge for every initial condition. A convergent sequence can be attained via the, so called, Krasnosel'skii–Mann iteration that introduces a relaxation term to the Banach–Picard iteration.

Theorem A.20 ([14, Prop. 5.16])**.** *Let $D \subset \mathcal{H}_\Phi$ be nonempty, closed and convex and $T : D \to D$ be a NEX operator, with $\mathrm{fix}(T) \neq \varnothing$, and $\lambda_k \in (0,1)$ such that $\sum_{k\in\mathbb{N}} \lambda_k(1-\lambda_k) = +\infty$, and choose $x(0) \in D$. Then, the sequence $(x(k))_{k\in\mathbb{N}}$ generated via the iteration*

$$(\forall k \in \mathbb{N}) \quad x(k+1) = x(k) + \lambda_k (T(x(k)) - x(k)) \,, \tag{A.11}$$

gloablly converges to a fixed point x^* of T, i.e., $x^* \in \mathrm{fix}(T)$. □

A.6 Zero finding algorithms

As highlighted in the previous sections, finding the zeros of an operator is a very interesting problem. The set of zeros can be difficult to characterize, but throughout the years several zero findings algorithms were proposed. For operators that enjoy some of the monotonicity property in Definition A.5, these algorithms are able to generate a sequence that converges globally to a zero.

Also in this case, we start with the most simple exponent of this type of algorithms. Consider a β-cocoercive operator A, then, to seek the operator's zeros, one can study the Banach–Picard iteration of $\mathrm{Id} - \gamma A$ with $\gamma > 0$, since $\mathrm{zer}(A) = \mathrm{fix}(\mathrm{Id} - \gamma A)$. This update rule takes the name of *forward step*, or forward algorithm and the iteration obtained reads as

$$(\forall k \in \mathbb{N}) \quad x(k+1) = x(k) - \gamma A(x(k)) \,. \tag{A.12}$$

By [14, Prop. 5.16], it follows that if $\gamma \in (0, 2\beta)$, the sequence $(x(k))_{k\in\mathbb{N}}$ generated by (A.12) converges to a point x^* in $\mathrm{zer}(A)$, i.e., $x^* \in \mathrm{zer}(A)$. In fact, the operator $\mathrm{Id} - \gamma A$ is AVG for the chosen γ.

If the assumption over the monotonicity property of the operator is relaxed by assuming A maximally monotone (but not cocoercive), then the above iteration

may fail to generate a converging sequence. To solve this conundrum the PPA was developed, its derivation is based on the following chain of implications

$$\begin{aligned} x^* \in \operatorname{zer}(A) &\Leftrightarrow 0 \in A(x^*) \Leftrightarrow x^* \in x^* + \gamma A(x^*) \Leftrightarrow x^* \in (\mathrm{Id} + \gamma A)(x^*) \\ &\Leftrightarrow x^* \in \operatorname{fix}(\mathrm{J}_{\gamma A}) \,, \end{aligned} \tag{A.13}$$

where $\gamma > 0$. The operator A is assumed maximally monotone, hence J_A is FNE from Proposition A.12. Thanks to the relation in (A.13), we translated the problem into the one of finding a fixed point of J_A. Therefore, from Theorem A.19, a convergent sequence can be generated via a Banach–Picard iteration of J_A.

Theorem A.21 (PPA, [14, Th. 23.41])**.** *Let $A : \mathcal{H} \rightrightarrows \mathcal{H}$ be a maximally monotone operator such that $\operatorname{zer}(A) \neq \varnothing$, set $\gamma_n > 0$ such that $\sum_{n\in\mathbb{N}} \gamma_n^2 = +\infty$. Set,*

$$(\forall k \in \mathbb{N}) \quad x(k+1) = \mathrm{J}_{\gamma_n A}(x(k)) \,. \tag{A.14}$$

then the sequence $(x(k))_{k\in\mathbb{N}}$ converges globally to a point x^* in $\operatorname{zer}(A)$, i.e., $x^* \in \operatorname{zer}(A) = \operatorname{fix}(\mathrm{J}_{\gamma_n A})$. □

The algorithm presented above is very powerful and, in theory, it can be applied to a large class of problems. Unfortunately, the computation of the resolvent operator is not straightforward in most cases. In fact, the resolvent can be efficiently computed only for some classes of operators, e.g., the normal cone or the subdifferential of some lower semicontinous functions. In other cases, the solution obtained might be not suitable for the problem at hand. For example, if the problem presented in Chapter 4 is solved by means of the PPA, then final update rule could not implemented in a distributed fashion.

To overcome these shortcomings of the PPA, the *splitting methods* were introduced. The reader can find a comprehensive discussion of the topic in [14, Ch. 26]. The main idea is to take advantage of the structure of an operator A and split it in the sum of two suitable operators B and C with different monotonicity properties, i.e., $A = B + C$. Even though the reason might seems unclear, it is sometimes possible to isolate a part that has a resolvent that is easy to compute and exploit this feature to construct an efficient zero finding algorithm. In the following, we focus only on the FB algorithm, that can be applied when C is single valued and β-cocoercive, while B is merely maximally monotone. As done for the PPA, we propose a sequence of implications that transform the initial zero finding problem in a fixed point problem. Namely,

$$\begin{aligned} x^* \in \operatorname{zer}(B + C) &\Leftrightarrow 0 \in \gamma(B + C)(x^*) \Leftrightarrow -\gamma C(x^*) \in \gamma B(x^*) \\ &\Leftrightarrow (\mathrm{Id} - \gamma C)(x^*) \in (\mathrm{Id} + \gamma B)(x^*) \\ &\Leftrightarrow x^* = (\mathrm{Id} + \gamma C)^{-1} \circ (\mathrm{Id} - \gamma B)(x^*) \\ &\Leftrightarrow x^* \in \operatorname{fix}\big(\mathrm{J}_{\gamma C} \circ (\mathrm{Id} - \gamma B)\big) \,, \quad \text{with } \gamma > 0. \end{aligned} \tag{A.15}$$

The operator $T_{\gamma B,\gamma C} \coloneqq \mathrm{J}_{\gamma C} \circ (\mathrm{Id} - \gamma B)$ is called forward backward operator, if $\gamma \in (0, 2\beta)$ then $T_{\gamma B,\gamma C}$ is AVG, see [14, Prop. 26.1(iv)(d)]. The FB algorithm, presented in the next theorem, is a Krasnosel'skii–Mann iteration of $T_{\gamma B,\gamma C}$. Therefore, the convergence of the sequence generated to a point in $\operatorname{fix}(T_{\gamma B,\gamma C})$ follows from Theorem A.20.

Theorem A.22 (FB, [14, Th. 26.14]). *Let $B : \mathcal{H} \rightrightarrows \mathcal{H}$ be maximally monotone and $C : \mathcal{H} \to \mathcal{H}$ be β-cocoercive, and set $\gamma \in (0, 2\beta)$ and $\delta = 2 - \gamma/(2\beta)$. Consider $\lambda_k > 0$ such that $\sum_{k\in\mathbb{N}} \lambda_k(\delta - \lambda_k) = +\infty$, and assume $\operatorname{zer}(B + C) \neq \varnothing$. Set*

$$\begin{aligned} (\forall k \in \mathbb{N}) \ : \quad & y(k) = x(k) - \gamma B(x(k)) \\ & x(k+1) = x(k) + \lambda_k \big(\mathrm{J}_{\gamma C}(y(k)) - x(k) \big) \end{aligned} \tag{A.16}$$

then the sequence $(x(k))_{k\in\mathbb{N}}$ generated by (A.16) *globally converges to a point $x^* \in \operatorname{zer}(B + C) = \operatorname{fix}(T_{\gamma B, \gamma C})$.* □

B

Graph theory

Graph theory was introduced by the mathematician Leonhard Euler in 1736 as a tool used to solve and generalize the problem of the seven "bridges of Königsberg". In [74], he proposed some key concepts that set the basis for the future development of graph theory. The interested reader can find a complete discussion in [27], where the authors discuss several classical and fascinating problems associated to graph theory. In the following, we provide some basic definitions and results that are recalled several times during the whole dissertation.

B.1 Graphs

Let us start by introducing the concepts of undirected and directed graphs.

Definition B.1 (Graph)**.** A *graph* is a pair, $\mathcal{G} = (\mathcal{N}, \mathcal{E})$, where $\mathcal{N} = \{1, \dots, n\}$ is a set of n elements called *vertices*, or *nodes*, and $\mathcal{E} \subseteq \mathcal{N} \times \mathcal{N}$ is a set of pairs of vertices, called edges, or arcs. A graph is called *undirected*, if the edges in $\mathcal{E}$ are unordered pairs; a graph is called *directed*, or *digraph*, if the edges in $\mathcal{E}$ are ordered pairs. □

When a weight is associated to each edge of the graph, then the resulting graph is called weighted.

Definition B.2 (Weighted graph)**.** A *weighted digraph* is a triplet, $\mathcal{G} = (\mathcal{N}, \mathcal{E}, A)$, where the pair $(\mathcal{N}, \mathcal{E})$ is a digraph, and $A = [a_{i,j}] \in \mathbb{R}_{\geq 0}^{n \times n}$ is a set of non-negative *weights* such that $a_{i,j} > 0 \Leftrightarrow (i, j) \in \mathcal{E}$. □

From the above definition, one can notice that, given the $\mathcal{N}$ and the matrix of weights A, the set of edges can be extracted by examining the rows of A. For this reason, we sometime define a graph as $\mathcal{G} = (\mathcal{N}, A)$, where the set $\mathcal{E}$ is implicitly defined.

Definition B.3 (Weighted degrees)**.** Let $\mathcal{G}$ be a weighted digraph. The weighted out-degree, d_{out}, and the weighted in-degree, d_{in}, of a vertex $i \in \mathcal{N}$ are defined by $d_{\text{out}}(i) := \sum_{j=1}^{n} a_{i,j}$ and $d_{\text{in}}(i) := \sum_{j=1}^{n} a_{j,i}$. □

Definition B.4 (Weight-balanced graph)**.** A weighted graph is called *weight-balanced* if the weighted degrees are all equal, i.e., $d_{\text{out}}(i) = d_{\text{in}}(i)$ for all $i \in \mathcal{N}$. □

B.2 Relevant matrices

The first important matrix that describe the connections between the nodes in the graph is called adjacency matrix.

Definition B.5 (Adjacency matrix)**.** Given a weighted digraph $\mathcal{G} = (\mathcal{N}, \mathcal{E}, A)$, the matrix $A \in \mathbb{R}_{\geq 0}^{n \times n}$ is called *weighted adjacency matrix*. Given a digraph $\mathcal{G} = (\mathcal{N}, \mathcal{E})$, the binary adjacency matrix $B = [b_{i,j}] \in \{0,1\}^{n \times n}$ is defined by

$$b_{i,j} := \begin{cases} 1 & \text{if } (i,j) \in E \\ 0 & \text{otherwise.} \end{cases}$$

□

The concepts of weighted in and out degree for a weighted digraphs spawn the following definition.

Definition B.6 (Degree matrix)**.** Given a weighted digraph $\mathcal{G} = (\mathcal{N}, \mathcal{E}, A)$, the *weighted out-degree matrix*, D_{out}, and the *weighted in-degree matrix*, D_{in}, are defined by

$$\begin{aligned} D_{\text{out}} &= \operatorname{diag}(A\mathbf{1}_n) = \operatorname{diag}\left((d_{\text{out}}(i))_{i \in V}\right) = \begin{bmatrix} d_{\text{out}}(1) & & \\ & \ddots & \\ & & d_{\text{out}}(n) \end{bmatrix}, \\ D_{\text{in}} &= \operatorname{diag}\left(A^\top \mathbf{1}_n\right) = \begin{bmatrix} d_{\text{in}}(1) & & \\ & \ddots & \\ & & d_{\text{in}}(n) \end{bmatrix}. \end{aligned} \tag{B.1}$$

□

The following lemma allows us to verify whether or not the graph is undirected.

Lemma B.7. *Let $\mathcal{G} = (\mathcal{N}, \mathcal{E}, A)$ be a weighted digraph. The graph $\mathcal{G}$ is undirected if and only if $A = A^\top$ and $a_{i,i} = 0$ for all $i \in V$.* □

A node $i \in \mathcal{N}$ with $d_{\text{in}}(i) = 0$ is called *sink* node; a node i with $d_{\text{out}}(i) = 0$ is called *source* node.

The incidence matrix describes the relation between the edges in the graph and the nodes at it is defined for both directed and undirected graphs.

Definition B.8 (Incidence matrix)**.** Let $\mathcal{G} = (\mathcal{N}, \mathcal{E})$ be a graph with the number of edges in the graph is denoted by $E := |\mathcal{E}|$, and label the edges in $\mathcal{E}$ as e_l, for $l \in \{1, \dots, E\}$. The *incidence matrix* $V \in \mathbb{R}^{E \times N}$ associated to $\mathcal{G}$, is defined as

$$[V]_{li} := \begin{cases} 1 & \text{if } e_l = (i, \cdot) \\ -1 & \text{if } e_l = (\cdot, i) \\ 0 & \text{otherwise .} \end{cases} \tag{B.2}$$

□

In the case of an undirected network, the decision of which of the two nodes composing an edge is the sink and which the source is arbitrary. By construction, $V\mathbf{1}_N = \mathbf{0}_N$. Then, we define $\mathcal{E}_i^{\text{out}}$ (resp. $\mathcal{E}_i^{\text{in}}$) as the set of all the indexes l of the edges e_l that start from (resp. end in) node i, and hence $\mathcal{E}_i = \mathcal{E}_i^{\text{out}} \cup \mathcal{E}_i^{\text{in}}$.

Arguably the most important associated to a graph is the Laplacian matrix that is defined next.

Definition B.9 (Laplacian matrix)**.** Let $\mathcal{G} = (\mathcal{N}, \mathcal{E}, A)$ be a weighted digraph. The *Laplacian matrix* is defined by $L := D_{\text{out}} - A$. □

The elements of a Laplacian matrix $L = [l_{i,j}] \in \mathbb{R}^{n \times n}$ are such that:

$$l_{i,j} = \begin{cases} -a_{i,j} & \text{if } i \neq j \\ \sum_{k \neq i}^{n} a_{i,k} & \text{if } i = j. \end{cases}$$

A graph is undirected if and only if its Laplacian matrix is symmetric. Moreover, due to its structure this matrix enjoys many interesting properties.

Proposition B.10 (Row-sum of the Laplacian)**.** *Let $\mathcal{G}$ be a weighted digraph with n nodes and Laplacian matrix L. Then $L\mathbf{1}_n = \mathbf{0}_n$.* □

Proposition B.11 (Column-sum of the Laplacian)**.** *Let $\mathcal{G}$ be a weighted digraph with n nodes and Laplacian matrix L. The following statements are equivalent:*

(i) $\mathcal{G}$ is weight-balanced;

(ii) $\mathbf{1}_n^\top L = \mathbf{0}_n^\top$. □

For a weighted digraph $\mathcal{G} = (\mathcal{N}, \mathcal{E}, A)$: A is row-stochastic if and only if $d_{\text{out}}(i) = 1$ for all $i \in \mathcal{N}$, hence $D_{\text{out}} = I$; A is doubly-stochastic if and only if $d_{\text{out}}(i) = d_{\text{in}}(i) = 1$ for all $i \in V$, hence $D_{\text{out}} = D_{\text{in}} = I$.

Theorem B.12 (Gersgorin). *For any matrix $A = [a_{i,j}] \in \mathbb{R}^{n\times n}$,*

$$\Lambda(A) \subset \bigcup_{i\in\{1,\dots,n\}} \left\{ z \in \mathbb{C} \mid |z - a_{i,i}| \leq \sum_{j\neq i}^{n} |a_{i,j}| \right\}.$$

□

B.3 Perron–Frobenious theory

In linear algebra the theory developed by Oskar Perron and Georg Frobenius provides several fundamental results for non-negative square matrices. Specifically, it focuses on primitive matrices.

Definition B.13 (Primitive matrix). A non-negative matrix $A \in \mathbb{R}^n$ is primitive if there exists $k \in \mathbb{N}$ such that the matrix A^k is positive. □

The following theorem, together with the associated corollary, manage to characterize several aspects of the primitive matrices, and introduces the Perron–Frobenius eigenvector of a primitive matrix.

Theorem B.14 (Perron–Frobenious). *If a matrix A is primitive, then:*

(i) $\rho(A) =: \lambda_{\mathrm{PF}} \in \Lambda(A) \cap \mathbb{R}_{>0}$*;*

(ii) λ_{PF} *is a simple eigenvalue;*

(iii) $\lambda_{\mathrm{PF}} > \max_{\lambda\in\Lambda(A)\setminus\{\lambda_{\mathrm{PF}}\}} |\lambda|$*;*

(iv) the unique (up to positive scaling) left and right eigenvectors associated with the eigenvalue λ_{PF} *are positive;*

(v) $\lim_{k\to\infty} \frac{1}{\lambda_{\mathrm{PF}}^k} A^k = v_{\mathrm{PF}}\, w_{\mathrm{PF}}^\top$*, where* v_{PF} *and* w_{PF} *are, respectively, the right and left eigenvalues of A associated with the eigenvalue* λ_{PF}*, normalized so that* $v_{\mathrm{PF}}^\top w_{\mathrm{PF}} = 1$*.* □

Corollary B.15. *If a matrix $A \in \mathbb{R}^{n\times n}$ is primitive and row-stochastic matrix, i.e., $A\mathbf{1}_n = \mathbf{1}_n$, then:*

(i) the Perron-Frobenious eigenvalue $\lambda_{\mathrm{PF}} = \rho(A) = 1$ *is simple, hence A is semi-convergent;*

(ii) $\lim_{k\to\infty} A^k = \mathbf{1}_n w^\top$*, where w is the left positive eigenvector of A associated with the eigenvalue* $\lambda_{\mathrm{PF}} = 1$*, normalized so that* $\mathbf{1}_n^\top w = 1$*;*

(iii) the solution to $x(k+1) = Ax(k)$ *satisfies* $\lim_{k\to\infty} x(k) = \lim_{k\to\infty} A^k x(0) = \big(w^\top x(0)\big)\,\mathbf{1}_n$*.*

If, in addition, A is doubly-stochastic,i.e., $A\mathbf{1}_n = A^\top \mathbf{1}_n = \mathbf{1}_n$, then:

(iv) the left eigenvector can be selected as $w = \frac{1}{n}\mathbf{1}_n$, so that $\lim_{k\to\infty} x(k) = \frac{1}{n}\mathbf{1}_n^\top x(0)\mathbf{1}_n$.

□

C

Potential game theory

The use of a potential function in the context of strategic games is attributed to Rosenthal back in 1973, see [153]. The existence of such a function highly simplifies the analysis of the evolution of the game at hand. In fact, it provides some sort of bound on the payoff variation between two iterations of the game. The existence of such a bound is exploited in the literature to prove convergence to an equilibrium, in some cases even in finite time.

In this section, we consider a general formulation of a game Γ. Notice that in the following chapters, this broad definition will be declined to more convenient formulation for the particular problem considered. A game between N players can be defined by the couple $\Gamma \coloneqq \left(\prod_{i=1}^{N} \mathcal{S}_i, \pi\right)$, where $\mathcal{S}_i$ is the set of feasible strategies of agent i, and $\pi \coloneqq \mathrm{col}((\pi_i)_{i\in\mathbb{N}}) : \prod_{i=1}^{N} \mathcal{S}_i \to \mathbb{R}^N$ is the game payoff function[1]. If $S_i \subset \mathbb{R}^n$ then the game is called *convex* (or infinite), while if $S_i \subset \mathbb{Z}^n$ then the game is *finite*.

Definition C.1 (Bounded game)**.** Γ is a *bounded* game if for all $\boldsymbol{s} \in \prod_{i=1}^{N} \mathcal{S}_i$ there exists $M \in \mathbb{R}$ such that, for all $i \in \{1, \dots, N\}$, it holds that $|\pi_i(\boldsymbol{s})| \leq M$. □

C.1 Potential functions

Next, we introduce the different types of potential functions that differ for how tight they manage to describe the variation of the players' payoff.

[1] Equivalently, one can define Γ using a cost function $J \coloneqq -\pi$, instead of a payoff. This approach was adopted in Chapters 6 and 7.

Definition C.2 (Potential function, [127, Sec. 2])**.** Let Γ be a game and $P : \prod_{i=1}^{N} \mathcal{S}_i \to \mathbb{R}$ a continuous function. If, for all $i \in \{1, \ldots, N\}$ and all $(x, \boldsymbol{s}_{-i}), (y, \boldsymbol{s}_{-i}) \in \prod_{i=1}^{N} \mathcal{S}_i$,

(i) P satisfies

$$\pi_i(x, \boldsymbol{s}_{-i}) - \pi_i(y, \boldsymbol{s}_{-i}) = P(x, \boldsymbol{s}_{-i}) - P(y, \boldsymbol{s}_{-i}), \tag{C.1}$$

then it is an *exact potential function* for Γ

(ii) P satisfies

$$\pi_i(x, \boldsymbol{s}_{-i}) - \pi_i(y, \boldsymbol{s}_{-i}) = w_i \left[P(x, \boldsymbol{s}_{-i}) - P(y, \boldsymbol{s}_{-i})\right] \tag{C.2}$$

with $w_i \in \mathbb{R}$, then it is a *weighted potential function* for Γ

(iii) P satisfies

$$\pi_i(x, \boldsymbol{s}_{-i}) - \pi_i(y, \boldsymbol{s}_{-i}) > 0 \Leftrightarrow P(x, \boldsymbol{s}_{-i}) - P(y, \boldsymbol{s}_{-i}) > 0, \tag{C.3}$$

then it is a *ordinal potential function* for Γ

(iv) P satisfies

$$\pi_i(x, \boldsymbol{s}_{-i}) - \pi_i(y, \boldsymbol{s}_{-i}) > 0 \Rightarrow P(x, \boldsymbol{s}_{-i}) - P(y, \boldsymbol{s}_{-i}) > 0, \tag{C.4}$$

then it is a *generalized ordinal potential function* for Γ. □

A game Γ is called an *exact*, *weighted*, *ordinal* or *generalized ordinal potential game* if there exist an *exact*, *weighted*, *ordinal* or *generalized ordinal potential function* respectively. From the relation above, it is clear that if P satisfies (C.1) then it also satisfies (C.2)–(C.4). Similarly, an ordinal potential game is also a generalized ordinal potential game, while the converse is not always true.

C.2 Improvement paths

A path in the context of games is a sequence of strategy profiles in which each element differs from the successive for the strategy of exactly one agent.

Definition C.3. Let $\gamma = (\boldsymbol{s}(k))_{k \in \mathbb{N}}$ denote an action profile sequence for a game Γ. If, for every $k \in \mathbb{N}$, there exists a unique player $i_k \in \{1, \ldots, N\}$, such that

$$\boldsymbol{s}(k) \coloneqq (s_{i_k}(k), \boldsymbol{s}_{-i_k}(k-1)) \text{ for some } s_{i_k}(t) \neq s_{i_k}(k-1),$$

then γ is called a *path* in the action profile of Γ. □

In *finite* potential games, the concept of finite improvement is a very useful tool. In fact, this property is crucial to demonstrate that these games converge in a finite number of iterations to an equilibrium of the game.

Definition C.4. Let γ be a path for the game Γ, with $i_k \in \{1, \dots, N\}$ being the unique deviator between $\boldsymbol{s}(k-1)$ and $\boldsymbol{s}(k)$. If, for all $k \in \mathbb{N}$, it holds

$$\pi_{i_k}(\boldsymbol{s}(k)) > \pi_{i_k}(\boldsymbol{s}(k-1))\,,$$

then γ is called an *improvement path*. Furthermore, if every improvement path is finite then the game Γ has the Finite Improvement Property (FIP). □

Lemma C.5 ([127, Lem. 2.3])**.** *Every finite ordinal potential game* Γ *has the FIP.* □

In the context of convex games, the definitions above have to be adapted due to the infinite number of possible strategies that each player can select. First, we introduce the concept of approximated improvement path and AFIP, that is the counterpart of FIP for convex games.

Definition C.6. Let γ be a path for the convex game Γ, with $i_k \in \{1, \dots, N\}$ being the unique deviator between $\boldsymbol{s}(k-1)$ and $\boldsymbol{s}(k)$, and $\epsilon > 0$. If, for all $k \in \mathbb{N}$, it holds

$$\pi_{i_k}(\boldsymbol{s}(k)) > \pi_{i_k}(\boldsymbol{s}(k-1)) + \epsilon\,,$$

then γ is called an ϵ-*improvement path*. Furthermore, if every ϵ-improvement path is finite, then the game Γ has the AFIP. □

In the case of a convex potential game, the fact that the payoff function is bounded implies that the game posses the AFIP.

Definition C.7 ([127, Lem. 4.2])**.** Every bounded convex potential game Γ has the AFIP. □

Bibliography

[1] BART Perks 2 Program.

[2] In T. Ichiishi, editor, *Game Theory for Economic Analysis*, Economic Theory, Econometrics, and Mathematical Economics, page iv. Academic Press, San Diego, 1983.

[3] Nationaal Dataportaal Wegverkeer, 2009.

[4] D. Acemoglu and A. Ozdaglar. Opinion dynamics and learning in social networks. *Dynamic Games and Applications*, 1(1):3–49, 2011.

[5] N. E. Agency. Statistics Electric Vehicles in the Netherlands (up to and including february 2019). Technology report, March 2019.

[6] A. A. Alchian. Uncertainty, evolution, and economic theory. *Journal of Political Economy*, 58(3):211–221, 1950.

[7] C. Altafini. Consensus problems on networks with antagonistic interactions. *IEEE Transactions on Automatic Control*, 58(4):935–946, 2013.

[8] A. Bandura and R. H. Walters. *Social learning theory*, volume 1. Prentice-hall Englewood Cliffs, NJ, 1977.

[9] A.-L. Barabási and R. Albert. Emergence of scaling in random networks. *science*, 286(5439):509–512, 1999.

[10] J. Barreiro-Gomez, G. Obando, and N. Quijano. Distributed population dynamics: Optimization and control applications. *IEEE Transactions on Systems, Man, and Cybernetics: Systems*, 47(2):304–314, 2017.

[11] J. Barreiro-Gomez and H. Tembine. Constrained evolutionary games by using a mixture of imitation dynamics. *Automatica*, 97:254–262, 2018.

[12] M. Barth and K. Boriboonsomsin. Traffic congestion and greenhouse gases. *Access Magazine*, 1(35):2–9, 2009.

[13] F. M. Bass. A new product growth for model consumer durables. *Management science*, 15(5):215–227, 1969.

[14] H. H. Bauschke, P. L. Combettes, et al. *Convex Analysis and Monotone Operator Theory in Hilbert Spaces*, volume 2011. (2nd Edition) Springer International Publishing, 2017.

[15] H. H. Bauschke, V. Martín-Márquez, S. M. Moffat, and X. Wang. Compositions and convex combinations of asymptotically regular firmly nonexpansive mappings are also asymptotically regular. *Fixed Point Theory and Applications*, 53:1–11, 2012.

[16] G. Belgioioso, F. Fabiani, F. Blanchini, and S. Grammatico. On the convergence of discrete-time linear systems: A linear time-varying Mann iteration converges iff the operator is strictly pseudocontractive. *IEEE Control Systems Letters*, 2018.

[17] G. Belgioioso and S. Grammatico. On convexity and monotonicity in generalized aggregative games. *IFAC-PapersOnLine*, 50(1):14338 – 14343, 2017. 20th IFAC World Congress.

[18] G. Belgioioso and S. Grammatico. Semi-decentralized Nash equilibrium seeking in aggregative games with coupling constraints and non-differentiable cost functions. *IEEE Control Systems Letters*, 1(2):400–405, 2017.

[19] G. Belgioioso and S. Grammatico. A Douglas–Rachford splitting for semi-decentralized equilibrium seeking in generalized aggregative games. In *Proceedings of the IEEE Conference on Decision and Control (CDC)*, pages 3541–3546, Miami, USA, 2018.

[20] G. Belgioioso and S. Grammatico. Projected-gradient algorithms for generalized equilibrium seeking in aggregative games arepreconditioned forward-backward methods. pages 2188–2193, June 2018.

[21] A. Bemporad and M. Morari. Control of systems integrating logic, dynamics, and constraints. *Automatica*, 35(3):407–427, 1999.

[22] E. Ben-Elia and D. Ettema. Changing commuters' behavior using rewards: A study of rush-hour avoidance. *Transportation Research Part F: Traffic Psychology and Behaviour*, 14(5):354 – 368, 2011.

[23] C. Benevolo, R. P. Dameri, and B. D'auria. Smart mobility in smart city. In *Empowering Organizations*, pages 13–28. Springer, 2016.

[24] D. P. Bertsekas and J. N. Tsitsiklis. *Parallel and distributed computation: numerical methods*, volume 23. Prentice hall Englewood Cliffs, NJ, 1989.

[25] D. P. Bertsekas and J. N. Tsitsiklis. Some aspects of parallel and distributed iterative algorithms: A survey. *Automatica*, 27(1):3 – 21, 1991.

[26] R. J. Bessa and M. A. Matos. Economic and technical management of an aggregation agent for electric vehicles: A literature survey. *European Transactions on Electrical Power*, 22(3):334–350, 2012.

[27] N. Biggs, E. K. Lloyd, and R. J. Wilson. *Graph Theory, 1736-1936*. Clarendon Press, USA, 1986.

[28] V. D. Blondel, J. M. Hendrickx, A. Olshevsky, and J. N. Tsitsiklis. Convergence in multiagent coordination, consensus, and flocking. In *Proceedings of the 44th IEEE Conference on Decision and Control*, pages 2996–3000, Dec 2005.

[29] L. E. Blume. The statistical mechanics of strategic interaction. *Games and Economic Behavior*, 5(3):387–424, 1993.

[30] S. Boyd, A. Ghosh, B. Prabhakar, and D. Shah. Randomized gossip algorithms. *IEEE Transactions on Information Theory*, 52(6):2508–2530, 2006.

[31] S. Boyd, N. Parikh, E. Chu, B. Peleato, and J. Eckstein. Distributed optimization and statistical learning via the alternating direction method of multipliers. *Foundations and Trends in Machine Learning*, 3(1):1–122, 2011.

[32] L. Briceno-Arias and D. Davis. Forward-backward-half forward algorithm for solving monotone inclusions. *SIAM Journal on Optimization*, 28(4):2839–2871, 2018.

[33] M. Bruschetta, C. Cenedese, and A. Beghi. A real-time, mpc-based motion cueing algorithm with look-ahead and driver characterization. *Transportation Research Part F: Traffic Psychology and Behaviour*, 61:38–52, 2019. Special TRF issue: Driving simulation.

[34] M. Bruschetta, C. Cenedese, A. Beghi, and F. Maran. A motion cueing algorithm with look-ahead and driver characterization: Application to vertical car dynamics. *IEEE Transactions on Human-Machine Systems*, 48(1):6–16, 2018.

[35] F. Bullo, J. Cortes, and S. Martinez. *Distributed control of robotic networks: a mathematical approach to motion coordination algorithms*, volume 27. Princeton University Press, 2009.

[36] S. Cairns, L. Sloman, C. Newson, J. Anable, A. Kirkbride, and P. Goodwin. Smarter choices: Assessing the potential to achieve traffic reduction using soft measures. *Transport Reviews*, 28(5):593–618, 2008.

[37] M. B. Canzoneri and J. A. Gray. Monetary policy games and the consequences of non-cooperative behavior. *International Economic Review*, 26(3):547–564, 1985.

[38] Y. Cao, W. Yu, W. Ren, and G. Chen. An overview of recent progress in the study of distributed multi-agent coordination. *IEEE Transactions on Industrial Informatics*, 9(1):427–438, Feb 2013.

[39] C. Cenedese. Github repository : Ctm identification, 2021.

[40] C. Cenedese, G. Belgioioso, S. Grammatico, and M. Cao. An asynchronous, forward-backward, distributed generalized Nash equilibrium seeking algorithm. In *2019 18th European Control Conference (ECC)*, pages 3508–3513, June 2019.

[41] C. Cenedese, G. Belgioioso, S. Grammatico, and M. Cao. An asynchronous distributed and scalable generalized Nash equilibrium seeking algorithm for strongly monotone games. *European Journal of Control*, 2020.

[42] C. Cenedese, G. Belgioioso, S. Grammatico, and M. Cao. Time-varying constrained proximal type dynamics in multi-agent network games. May 2020.

[43] C. Cenedese, G. Belgioioso, Y. Kawano, S. Grammatico, and M. Cao. Asynchronous and time-varying proximal type dynamics multi-agent network games. *IEEE Transaction on Automatic Control (in press)*, 2020.

[44] C. Cenedese, M. Cucuzzella, J. Scherpen, S. Grammatico, and M. Cao. Highway Traffic Control via Smart e-Mobility – Part I: Theory. *IEEE-Transaction on intelligent transportation systems (submitted)*, 2020.

[45] C. Cenedese, M. Cucuzzella, J. Scherpen, S. Grammatico, and M. Cao. Highway traffic control via smart e-mobility – part ii: Case study. *IEEE-Transaction on intelligent transportation systems (submitted)*, 2020.

[46] C. Cenedese, F. Fabiani, M. Cucuzzella, J. M. A. Scherpen, M. Cao, and S. Grammatico. Charging plug-in electric vehicles as a mixed-integer aggregative game. In *2019 IEEE 58th Conference on Decision and Control (CDC)*, pages 4904–4909, 2019.

[47] C. Cenedese, Y. Kawano, S. Grammatico, and M. Cao. Towards time-varying proximal dynamics in multi-agent network games. In *2018 IEEE Conference on Decision and Control (CDC)*, pages 4378–4383, Dec 2018.

[48] C. Cenedese, L. Zino, M. Cucuzzella, and M. Cao. Optimal policy design to mitigate epidemics on networks using an sis model. In *2021 IEEE 60th Annual Conference on Decision and Control Austin (CDC) (under review)*, 2021.

[49] K. Clement-Nyns, E. Haesen, and J. Driesen. The impact of charging plug-in hybrid electric vehicles on a residential distribution grid. *IEEE Transactions on Power Systems*, 25(1):371–380, 2010.

[50] N. M. Coe and H. W.-C. Yeung. *Global production networks: Theorizing economic development in an interconnected world*. Oxford University Press, 2015.

[51] A. M. Colman. Cooperation, psychological game theory, and limitations of rationality in social interaction. *Behavioral and Brain Sciences*, 26(2):139–153, 2003.

[52] P. Combettes. Quasi-Fejérian analysis of some optimization algorithms. In *Studies in Computational Mathematics, Inherently parallel algorithms in feasibility and optimization and their applications*, pages 115–152. Elsevier, 2001.

[53] P. Combettes and J. Pesquet. Stochastic quasi-fejér block-coordinate fixed point iterations with random sweeping. *SIAM Journal on Optimization*, 25(2):1221–1248, 2015.

[54] P. L. Combettes and J.-C. Pesquet. Proximal splitting methods in signal processing. In *Fixed-point algorithms for inverse problems in science and engineering*, pages 185–212. Springer, 2011.

[55] P. L. Combettes and I. Yamada. Compositions and convex combinations of averaged nonexpansive operators. *Journal of Mathematical Analysis and Applications*, pages 55–70, 2015.

[56] R. Cominetti, F. Facchinei, and J. Lasserre. *Modern optimization modelling techniques*. Birkhäuser, 2010.

[57] G. Como, F. Fagnani, and L. Zino. Imitation dynamics in population games on community networks. *IEEE Transactions on Control of Network Systems*, pages 1–1, 2020.

[58] C. F. Daganzo. The cell transmission model, part ii: Network traffic. *Transportation Research Part B: Methodological*, 29(2):79 – 93, 1995.

[59] A. Das, S. Gollapudi, and K. Munagala. Modeling opinion dynamics in social networks. In *Proceedings of the 7th ACM International Conference on Web Search and Data Mining*, WSDM '14, pages 403–412, New York, NY, USA, 2014. Association for Computing Machinery.

[60] D. D. Davis. Advance production and Cournot outcomes: an experimental investigation. *Journal of Economic Behavior & Organization*, 40(1):59–79, 1999.

[61] G. Debreu. A social equilibrium existence theorem. *Proceedings of the National Academy of Sciences*, 38(10):886–893, 1952.

[62] M. H. DeGroot. Reaching a consensus. *Journal of the American Statistical Association*, 69(345):118–121, 1974.

[63] V. del Razo and H. Jacobsen. Smart charging schedules for highway travel with electric vehicles. *IEEE Transactions on Transportation Electrification*, 2(2):160–173, 2016.

[64] I. Docherty, G. Marsden, and J. Anable. The governance of smart mobility. *Transportation Research Part A: Policy and Practice*, 115:114 – 125, 2018. Smart urban mobility.

[65] F. Dörfler, J. Simpson-Porco, and F. Bullo. Breaking the hierarchy: Distributed control and economic optimality in microgrids. *IEEE Trans. on Control of Network Systems*, 3(3):241–253, 2016.

[66] A. Downs. *Still stuck in traffic: coping with peak-hour traffic congestion*. Brookings Institution Press, 2005.

[67] A. Dreves, F. Facchinei, C. Kanzow, and S. Sagratella. On the solution of the KKT conditions of generalized Nash equilibrium problems. *SIAM Journal on Optimization*, 21(3):1082–1108, 2011.

[68] P. Dubey, O. Haimanko, and A. Zapechelnyuk. Strategic complements and substitutes, and potential games. *Games and Economic Behavior*, 54(1):77–94, 2006.

[69] J. Eckstein. *Splitting methods for monotone operators with applications to parallel optimization*. PhD thesis, Massachusetts Institute of Technology, 1989.

[70] G. Ellison. Learning, local interaction, and coordination. *Econometrica: Journal of the Econometric Society*, pages 1047–1071, 1993.

[71] G. Ellison and D. Fudenberg. Word-of-mouth communication and social learning. *The Quarterly Journal of Economics*, 110(1):93–125, 1995.

[72] S. R. Etesami and T. Başar. Game-theoretic analysis of the Hegselmann–Krause model for opinion dynamics in finite dimensions. *IEEE Trans. on Automatic Control*, 60(7):1886–1897, 2015.

[73] D. Ettema, J. Knockaert, and E. Verhoef. Using incentives as traffic management tool: empirical results of the "peak avoidance" experiment. *Transportation Letters*, 2(1):39–51, 2010.

[74] L. Euler. Solutio problematis ad geometriam situs pertinentis. *Commentarii academiae scientiarum Petropolitanae*, pages 128–140, 1736.

[75] F. Fabiani and A. Caiti. Nash equilibrium seeking in potential games with double-integrator agents. In *2019 18th European Control Conference (ECC)*, pages 548–553. IEEE, 2019.

[76] F. Fabiani and S. Grammatico. A mixed-logical-dynamical model for automated driving on highways. In *2018 IEEE 57th Conference on Decision and Control (CDC)*, pages 1011–1015. IEEE, 2018.

[77] F. Fabiani and S. Grammatico. Multi-vehicle automated driving as a generalized mixed-integer potential game. *IEEE Transactions on Intelligent Transportation Systems*, 2019. (In press).

[78] F. Facchinei, A. Fischer, and V. Piccialli. On generalized Nash games and variational inequalities. *Operations Research Letters*, 35:159–164, 2007.

[79] F. Facchinei and C. Kanzow. Generalized Nash equilibrium problems. *A Quarterly Journal of Operations Research, Springer*, 5:173–210, 2007.

[80] F. Facchinei and J. Pang. *Finite-dimensional variational inequalities and complementarity problems*. Springer Verlag, 2003.

[81] F. Facchinei, V. Piccialli, and M. Sciandrone. Decomposition algorithms for generalized potential games. *Computational Optimization and Applications*, 50(2):237–262, 2011.

[82] A. Falsone, K. Margellos, S. Garatti, and M. Prandini. Dual decomposition for multi-agent distributed optimization with coupling constraints. *Automatica*, 84:149–158, 2017.

[83] Fastned. Fastned Pricing, 2020.

[84] D. G. Feingold, R. S. Varga, et al. Block diagonally dominant matrices and generalizations of the Gerschgorin circle theorem. *Pacific Journal of Mathematics*, 12(4):1241–1250, 1962.

[85] A. Ferrara, S. Sacone, and S. Siri. *Freeway traffic modelling and control*. Springer, 2018.

[86] G. Fournier and M. Scarsini. Location games on networks: Existence and efficiency of equilibria. *Mathematics of Operations Research*, 44(1):212–235, 2019.

[87] N. E. Friedkin and E. C. Johnsen. Social influence and opinions. *Journal of Mathematical Sociology*, 15(3-4):193–206, 1990.

[88] M. Friedman and M. Friedman. *Essays in positive economics*. University of Chicago Press, 1953.

[89] D. Fullmer and A. S. Morse. A distributed algorithm for computing a common fixed point of a finite family of paracontractions. *IEEE Transactions on Automatic Control*, 63(9):2833–2843, Sep. 2018.

[90] A. Galeotti, S. Goyal, M. O. Jackson, F. Vega-Redondo, and L. Yariv. Network Games. *The Review of Economic Studies*, 77(1):218–244, 01 2010.

[91] L. Gan, U. Topcu, and S. H. Low. Optimal decentralized protocol for electric vehicle charging. *IEEE Transactions on Power Systems*, 28(2):940–951, 2013.

[92] A. A. Ganin, M. Kitsak, D. Marchese, J. M. Keisler, T. Seager, and I. Linkov. Resilience and efficiency in transportation networks. *Science Advances*, 3(12), 2017.

[93] J. Ghaderi and R. Srikant. Opinion dynamics in social networks with stubborn agents: Equilibrium and convergence rate. *Automatica*, 50:3209–3215, 2014.

[94] C. Godsil and G. Royle. *Algebraic Graph Theory*, volume 207 of *Graduate Texts in Mathematics*. Springer Science & Business Media, 2013.

[95] A. Govaert, C. Cenedese, S. Grammatico, and M. Cao. Relative best response dynamics in finite and convex network games. In *2019 IEEE 58th Conference on Decision and Control (CDC)*, pages 3134–3139, 2019.

[96] A. Govaert, P. Ramazi, and M. Cao. Convergence of imitation dynamics for public goods games on networks. In *2017 IEEE 56th Annual Conference on Decision and Control (CDC)*, pages 4982–4987. IEEE, 2017.

[97] S. Goyal. *Connections: an introduction to the economics of networks*. Princeton University Press, 2012.

[98] S. Grammatico. Exponentially convergent decentralized charging control for large populations of plug-in electric vehicles. In *2016 IEEE 55th Conference on Decision and Control (CDC)*, pages 5775–5780, 2016.

[99] S. Grammatico. Proximal dynamics in multi-agent network games. *IEEE Trans. on Control of Network Systems*, 5(4):1707–1716, Dec 2018.

[100] S. Grammatico, F. Parise, M. Colombino, and J. Lygeros. Decentralized convergence to Nash equilibria in constrained deterministic mean field control. *IEEE Trans. on Automatic Control*, 61(11):3315–3329, 2016.

[101] Q. Guo, L. Li, and X. J. Ban. Urban traffic signal control with connected and automated vehicles: A survey. *Transportation Research Part C: Emerging Technologies*, 101:313 – 334, 2019.

[102] Y. Y. Haimes and P. Jiang. Leontief-based model of risk in complex interconnected infrastructures. *Journal of Infrastructure Systems*, 7(1):1–12, 2001.

[103] J. Hu, H. Morais, T. Sousa, and M. Lind. Electric vehicle fleet management in smart grids: A review of services, optimization and control aspects. *Renewable and Sustainable Energy Reviews*, 56:1207–1226, 2016.

[104] X. Hu, Y.-C. Chiu, and L. Zhu. Behavior insights for an incentive-based active demand management platform. *International Journal of Transportation Science and Technology*, 4(2):119 – 133, 2015.

[105] International Energy Agency (IEA). Global EV Outlook: entering the decade of electric drive? Technology report, International Energy Agency (IEA), June 220.

[106] International Energy Agency (IEA). The Netherlands 2020: energy policy review. Technology report, International Energy Agency (IEA), Sept. 220.

[107] M. O. Jackson and L. Yariv. Diffusion of behavior and equilibrium properties in network games. *American Economic Review*, 97(2):92–98, May 2007.

[108] R. Jaina and J. Walrand. An efficient Nash-implementation mechanism for network resource allocation. *Automatica*, 46:1276–1283, 2010.

[109] W. Jing, M. Ramezani, K. An, and I. Kim. Congestion patterns of electric vehicles with limited battery capacity. *PLOS ONE*, 13(3):1–18, 03 2018.

[110] J. Koshal, A. Nedić, and U. Shanbhag. Distributed algorithms for aggregative games on graphs. *Operations Research*, 64(3):680–704, 2016.

[111] A. A. Kulkarni and U. Shanbhag. On the variational equilibrium as a refinement of the generalized Nash equilibrium. *Automatica*, 48:45–55, 2012.

[112] A. A. Kulkarni and U. V. Shanbhag. Revisiting generalized Nash games and variational inequalities. *Journal of Optimization Theory and Applications*, 154(1):175–186, 2012.

[113] J.-J. Laffont. Game theory and empirical economics: The case of auction data 1editors' note: This paper was presented as the marshall lecture at the 10th annual congress of the european economic association in 1995 in prague. for technical reasons, it could not be published in the congress issue (40/3?5).1. *European Economic Review*, 41(1):1–35, 1997.

[114] S. Lee and A. Nedić. Distributed random projection algorithm for convex optimization. *IEEE Journal of Selected Topics in Signal Processing*, 7(2):221–229, 2013.

[115] D. K. Levine and W. Pesendorfer. The evolution of cooperation through imitation. *Games and Economic Behavior*, 58(2):293–315, 2007.

[116] H. Li. Automatically generating empirical speed-flow traffic parameters from archived sensor data. *Procedia - Social and Behavioral Sciences*, 138:54 – 66, 2014. The 9th International Conference on Traffic and Transportation Studies (ICTTS 2014).

[117] N. Li and J. R. Marden. Designing games for distributed optimization with a time varying communication graph. pages 7764–7769, Dec 2012.

[118] E. Lieberman, C. Hauert, and M. A. Nowak. Evolutionary dynamics on graphs. *Nature*, 433(7023):312, 2005.

[119] Z. Ma, D. S. Callaway, and I. A. Hiskens. Decentralized charging control of large populations of plug-in electric vehicles. *IEEE Transactions on Control Systems Technology*, 21(1):67–78, 2013.

[120] Z. Ma, S. Zou, L. Ran, X. Shi, and I. A. Hiskens. Efficient decentralized coordination of large-scale plug-in electric vehicle charging. *Automatica*, 69:35–47, 2016.

[121] S. Martínez, F. Bullo, J. Cortés, and E. Frazzoli. On synchronous robotic networks – Part i: Models, tasks, and complexity. *IEEE Trans. on Automatic Control*, 52:2199–2213, 2007.

[122] A. Masini and E. Menichetti. Investment decisions in the renewable energy sector: An analysis of non-financial drivers. *Technological Forecasting and Social Change*, 80(3):510–524, 2013.

[123] G. Mateos, J. A. Bazerque, and G. B. Giannakis. Distributed sparse linear regression. *IEEE Transactions on Signal Processing*, 58(10):5262–5276, Oct 2010.

[124] E. Melo. A Variational Approach to Network Games. Working Papers 2018.05, Fondazione Eni Enrico Mattei, Feb. 2018.

[125] A. Millner. Modeling lithium ion battery degradation in electric vehicles. In *2010 IEEE Conference on Innovative Technologies for an Efficient and Reliable Electricity Supply*, pages 349–356, 2010.

[126] L. Molleman, P. Van den Berg, and F. J. Weissing. Consistent individual differences in human social learning strategies. *Nature Communications*, 5:3570, 2014.

[127] D. Monderer and L. S. Shapley. Potential games. *Games and Economic Behavior*, 14(1):124–143, 1996.

[128] P. Naghizadeh and M. Liu. On the uniqueness and stability of equilibria of network games. In *2017 55th Annual Allerton Conference on Communication, Control, and Computing (Allerton)*, pages 280–286, 2017.

[129] Nationaal Dataportaal Wegverkeer. NDW-Dexter : Data EXploration + exporTER, 2020.

[130] A. Nedić. Asynchronous broadcast-based convex optimization over a network. *IEEE Transactions on Automatic Control*, 56(6):1337–1351, 2011.

[131] A. Nedić and A. Olshevsky. Distributed optimization over time-varying directed graphs. *IEEE Transactions on Automatic Control*, 60(3):601–615, March 2015.

[132] A. Nedić, A. Olshevsky, and W. Shi. Achieving geometric convergence for distributed optimization over time-varying graphs. *SIAM Journal on Optimization*, 27(4):2597–2633, 2017.

[133] J. Neubauer and E. Wood. The impact of range anxiety and home, workplace, and public charging infrastructure on simulated battery electric vehicle lifetime utility. *Journal of Power Sources*, 257:12 – 20, 2014.

[134] G. Nilsson, P. Hosseini, G. Como, and K. Savla. Entropy-like lyapunov functions for the stability analysis of adaptive traffic signal controls. In *54th IEEE Conference on Decision and Control*, pages 2193–2198, 2015.

[135] Z. Ning, F. Xia, N. Ullah, X. Kong, and X. Hu. Vehicular social networks: Enabling smart mobility. *IEEE Communications Magazine*, 55(5):16–55, 2017.

[136] M. A. Nowak and R. M. May. The spatial dilemmas of evolution. *International Journal of Bifurcation and Chaos*, 3(01):35–78, 1993.

[137] A. N. A. Ozdaglar and P. Parrillo. Constrained consensus and optimization in multi-agent networks. *IEEE Trans. on Automatic Control*, 55(4):922–938, 2010.

[138] D. Paccagnan, B. Gentile, F. Parise, M. Kamgarpour, and J. Lygeros. Distributed computation of generalized Nash equilibria in quadratic aggregative games with affine coupling constraints. In *2016 IEEE 55th Conference on Decision and Control (CDC)*, pages 6123–6128, Dec 2016.

[139] F. Parise, M. Colombino, S. Grammatico, and J. Lygeros. Mean field constrained charging policy for large populations of plug-in electric vehicles. In *53rd IEEE Conference on Decision and Control*, pages 5101–5106, 2014.

[140] F. Parise, M. Colombino, S. Grammatico, and J. Lygeros. Mean field constrained charging policy for large populations of plug-in electric vehicles. In *53rd IEEE Conference on Decision and Control*, pages 5101–5106, 2014.

[141] F. Parise, B. Gentile, S. Grammatico, and J. Lygeros. Network aggregative games: Distributed convergence to Nash equilibria. In *Proc. of the IEEE Conference on Decision and Control*, pages 2295–2300, Osaka, Japan, 2015.

[142] F. Parise and A. Ozdaglar. A variational inequality framework for network games: Existence, uniqueness, convergence and sensitivity analysis. *Games and Economic Behavior*, 114:47–82, 2019.

[143] F. Parise and A. Ozdaglar. Analysis and interventions in large network games. *Annual Review of Control, Robotics, and Autonomous Systems*, 4(1), 2021.

[144] S. E. Parsegov, A. V. Proskurnikov, R. Tempo, and N. E. Friedkin. Novel multidimensional models of opinion dynamics in social networks. *IEEE Transactions on Automatic Control*, 62(5):2270–2285, May 2017.

[145] L. Pavel. *Game theory for control of optical networks*. Springer Science & Business Media, 2012.

[146] L. Pavel. Distributed GNE seeking under partial-decision information over networks via a doubly-augmented operator splitting approach. *IEEE Transactions on Automatic Control*, 2019.

[147] Z. Peng, Y. Xu, M. Yan, and W. Yin. Arock: An algorithmic framework for asynchronous parallel coordinate updates. *SIAM Journal on Scientific Computing*, 38(5):A2851–A2879, 2016.

[148] G. Piacentini, P. Goatin, and A. Ferrara. Traffic control via moving bottleneck of coordinated vehicles. *IFAC-PapersOnLine*, 51(9):13–18, 2018.

[149] B. Recht, C. Re, S. Wright, and F. Niu. Hogwild: A lock-free approach to parallelizing stochastic gradient descent. In *Advances in neural information processing systems*, pages 693–701, 2011.

[150] W. Riggs. Painting the fence: Social norms as economic incentives to non-automotive travel behavior. *Travel Behaviour and Society*, 7:26 – 33, 2017.

[151] J. Rivera, C. Goebel, and H. Jacobsen. Distributed convex optimization for electric vehicle aggregators. *IEEE Transactions on Smart Grid*, 8(4):1852–1863, 2017.

[152] J. Rosen. Existence and uniqueness of equilibrium points for concave n-person games. *Econometrica*, 33:520–534, 1965.

[153] R. W. Rosenthal. A class of games possessing pure-strategy nash equilibria. *International Journal of Game Theory*, 2:65–67, 1973.

[154] S. Sagratella. Algorithms for generalized potential games with mixed-integer variables. *Computational Optimization and Applications*, pages 1–29, 2017.

[155] F. Salehisadaghiani and L. Pavel. Distributed Nash equilibrium seeking: A gossip-based algorithm. *Automatica*, 72:209–216, 2016.

[156] A. Schroten, H. van Essen, L. van Wijngaarden, D. Sutter, and E. Andrew. Sustainable transport infrastructure charging and internalisation of transport externalities: Executive summary. Technical report, European Commission, May 2019.

[157] G. Scutari, D. P. Palomar, F. Facchinei, and J. Pang. Convex optimization, game theory, and variational inequality theory. *IEEE Signal Processing Magazine*, 27(3):35–49, 2010.

[158] C. Shapiro, S. Carl, H. R. Varian, et al. *Information rules: a strategic guide to the network economy*. Harvard Business Press, 1998.

[159] A. Simonetto and G. Leus. Distributed maximum likelihood sensor network localization. *IEEE Transactions on Signal Processing*, 62(6):1424–1437, March 2014.

[160] D. Smart. *Fixed Point Theorems*. Cambridge Tracts in Mathematics. Cambridge University Press, 1980.

[161] E. Sortomme and M. A. El-Sharkawi. Optimal scheduling of vehicle-to-grid energy and ancillary services. *IEEE Transactions on Smart Grid*, 3(1):351–359, 2012.

[162] G. Szabó and G. Fath. Evolutionary games on graphs. *Physics Reports*, 446(4-6):97–216, 2007.

[163] Tesla. Supercharger Tesla, 2020.

[164] R. Tibshirani. Regression shrinkage and selection via the lasso. *Journal of the Royal Statistical Society: Series B (Methodological)*, 58(1):267–288, 1996.

[165] G. R. Timilsina, L. Kurdgelashvili, and P. A. Narbel. Solar energy: Markets, economics and policies. *Renewable and Sustainable Energy Reviews*, 16(1):449 – 465, 2012.

[166] T. Ui. Bayesian Nash equilibrium and variational inequalities. *Journal of Mathematical Economics*, 63:139–146, 2016.

[167] U.S. Energy Information Administration (eia). eia Beta, 2020.

[168] P. van den Berg, L. Molleman, and F. J. Weissing. Focus on the success of others leads to selfish behavior. *Proceedings of the National Academy of Sciences*, 112(9):2912–2917, 2015.

[169] F. Vega-Redondo. The evolution of Walrasian behavior. *Econometrica*, 65(2):375–384, 1997.

[170] J. Von Neumann and O. Morgenstern. Game theory and economic behavior, 1944.

[171] M. Voorneveld. Best-response potential games. *Economics Letters*, 66(3):289–295, 2000.

[172] H. P. Williams. *Model building in Mathematical Programming*. John Wiley & Sons, 2013.

[173] H. Xing, M. Fu, Z. Lin, and Y. Mou. Decentralized optimal scheduling for charging and discharging of plug-in electric vehicles in smart grids. *IEEE Transactions on Power Systems*, 31(5):4118–4127, 2016.

[174] Y. Xu, S. Çolak, E. C. Kara, S. J. Moura, and M. C. González. Planning for electric vehicle needs by coupling charging profiles with urban mobility. *Nature Energy*, 3:484–493, 2018.

[175] M. Ye, J. Liu, C. Cenedese, Z. Sun, and M. Cao. A Network SIS Meta-Population Model with Transportation Flow. July 2020.

[176] P. Yi and L. Pavel. A distributed primal-dual algorithm for computation of generalized Nash equilibria via operator splitting methods. In *2017 IEEE 56th Annual Conference on Decision and Control (CDC)*, pages 3841–3846, Dec 2017.

[177] P. Yi and L. Pavel. Asynchronous distributed algorithms for seeking generalized Nash equilibria under full and partial-decision information. *IEEE Transactions on Cybernetics*, pages 1–13, 2019.

[178] P. Yi and L. Pavel. An operator splitting approach for distributed generalized Nash equilibria computation. *Automatica*, 102:111 – 121, 2019.

[179] P. You, Z. Yang, M. Chow, and Y. Sun. Optimal cooperative charging strategy for a smart charging station of electric vehicles. *IEEE Transactions on Power Systems*, 31(4):2946–2956, 2016.

[180] H. P. Young. The evolution of conventions. *Econometrica: Journal of the Econometric Society*, pages 57–84, 1993.

[181] H. P. Young. *Individual strategy and social structure: An evolutionary theory of institutions*. Princeton University Press, 2001.

[182] L. Zino, G. Como, and F. Fagnani. On imitation dynamics in potential population games. In *2017 IEEE 56th Annual Conference on Decision and Control (CDC)*, pages 757–762. IEEE, 2017.

[183] H. Zou and T. Hastie. Regularization and variable selection via the elastic net. *Journal of the royal statistical society: series B (statistical methodology)*, 67(2):301–320, 2005.

[184] S. Zou, Z. Ma, X. Liu, and I. Hiskens. An efficient game for coordinating electric vehicle charging. *IEEE Transactions on Automatic Control*, 62(5):2374–2389, 2017.

Summary

The growing complexity and globalization of modern society brought to light novel problems and challenges for researchers that aim to model real-life phenomena. Nowadays communities and even single individuals cannot be considered as a closed system, since one's actions create a ripple effect that ends up influencing the action of others. Therefore, the study of decision-making processes over networks became a pivotal topic in the research community. The possible applications are virtually endless and span into many different fields such as companies' competition over shared markets with limited resources, the evolution of individuals' opinion during the interaction on a social network, peer-to-peer energy market, and smart mobility. The recurring trends among these examples are the increment in the number of decision-makers involved, the complexity of the interactions, and the possible presence of an external policymaker (e.g. a service provider). Two of the most relevant examples that enclose all these aspects are smart mobility and energy management in highly populated cities that are the key applications on which we focus in this thesis.

The branch of mathematics that studies strategic decision-making processes is *game theory*. In this thesis, we focus on the class of *generalized noncooperative network games* where the players locally interact over a network structure, and the coupling among them arises in both the cost function and the constraints. The natural concept of equilibrium for these types of processes is the Generalized Nash Equilibrium (GNE), i.e., a state in which no agent can benefit by unilaterally changing their action. We analyze the convergence properties of such games using operator theory and potential games theory. Moreover, if the game does not naturally converge to a GNE then we design iterative algorithms, based on operator splitting methods, that generates behavioral rules for the players that, if followed, restore convergence.

The thesis is divided into two parts differentiating mainly by the theoretical tools used to tackle the problem but sharing several common aspects. In Part I, we focus on the convergence of network games under different update rules. Specifically, for a particular class of games (yet arising in several applications) we prove convergence of the unconstrained dynamics, under the mild assumption on the communication network, when the players update synchronously, asynchronously, and when the topology of the network varies over time. If coupling constraints are present then we design an iterative semi-decentralized GNE seeking algorithm that computes modified update rules that are guaranteed to converge to a GNE of the game. We then focus on a more general class of network games in which the cost function is required only to be differentiable. We propose an iterative GNE seeking algorithm, based on operator splitting methods, that ensures convergence under

synchronous/asynchronous update and it is robust to information delays. Furthermore, thanks to a deliberate choice of the auxiliary variables used, the algorithm is distributed, decentralized, and highly scalable.

Part II starts by questioning an assumption that is usually overlooked, i.e., the perfect players' rationality. We introduce novel dynamics, that we called *relative best response*, that models partial rationality in decision-making processes. We rely on the theory on potential games to establish convergence to a GNE for generalized ordinal potential finite games and for weighted convex potential games.

The remainder of the thesis is dedicated to two applications that will become crucial problems in the following years. First, we model the smart charging of Plug-In Electric Vehicles (PEV). We propose an energy price policy that aims at incentivizing the PEV owners to charge during the hours in which the demand is lower. The price dynamically changes following the total demand that the grid has to satisfy at that particular moment. This creates a coupling among the PEV and, as an emerging behavior, it flattens the curve of the energy demand, alleviating the problem of detrimental peaks in demand. Finally, we propose an Active Traffic Demand Management for a highway stretch based on nudging the PEVs to stop at a charging station during the moments of high traffic congestion. The incentive consists of a discount of the energy price that changes proportionally to the congestion level. This work is the first that links the energy market to the transportation facilities and provides rigorous analysis of the produced effects. We show via simulations that it is capable of reducing the congestion peaks and for all the drivers, on top of providing an advantageous service to the PEV owners. In both these applications, we rely on mixed-integer potential games to obtain a rigorous, yet very detailed and close to reality, model of the phenomena.

Samevatting

De groeiende complexiteit en globalisering van de moderne samenleving heeft nieuwe problemen en uitdagingen meegebracht voor onderzoekers die ernaar streven om realistische fenomenen te modelleren. Tegenwoordig kunnen gemeenschappen en zelfs individuen niet als een gesloten systeem worden beschouwd, omdat iemands acties een rimpeleffect creë rt dat uiteindelijk de acties van anderen beÃ¯nvloedt. Hierdoor werd de studie van besluitvormingsprocessen via netwerken een cruciaal onderwerp voor onderzoekers. De mogelijke toepassingen zijn vrijwel eindeloos en strekken zich uit over veel verschillende gebieden, zoals de concurrentie van bedrijven op gedeelde markten met beperkte middelen, de evolutie van de mening van individuen tijdens de interactie op een sociaal netwerk, tot peer-to-peer energiemarkt en slimme mobiliteit. De terugkerende trends bij deze voorbeelden zijn de toename van het aantal betrokken besluitvormers, de complexiteit van de interacties, en de mogelijke aanwezigheid van een externe beleidsbepaler (bijvoorbeeld een dienstverlener). Een van de meest relevante voorbeelden die al deze aspecten omvat, is slimme mobiliteit en energiebeheer in dichtbevolkte steden. Dit zijn dan ook de belangrijkste toepassingen waarop we ons in dit proefschrift richten.

De tak van de wiskunde die strategische besluitvormingsprocessen bestudeert, is *speltheorie*. In dit proefschrift richten we ons op de klasse van *gegeneraliseerde niet-coöperatieve netwerkspellen waarbij* de spelers lokaal communiceren via een netwerkstructuur, en er een koppeling tussen hen bestaat in zowel de kostenfunctie of criterium en randvoorwaarden. Het natuurlijke concept voor de evenwichtstoestand van dit soort processen is het gegeneraliseerde Nash-evenwichtstoestand (GNE), d.w.z. een toestand waarin geen een speler kan profiteren door eenzijdig hun strategie of actie te veranderen. We analyseren de convergentie-eigenschappen van dergelijke spellen met behulp van operatorentheorie en potentiële speltheorie. Voor spellen die van nature niet convergeren naar een GNE, ontwerpen we iteratieve algoritmen, gebaseerd op methoden voor operatorensplitsing, die gedragsregels genereren voor de spelers die, indien gevolgd, de convergentie herstellen.

Het proefschrift is opgedeeld in twee delen die zich voornamelijk onderscheiden door de theoretische hulpmiddelen die worden gebruikt om het probleem op te lossen, maar ook meerdere gemeenschappelijke aspecten hebben.

In deel I concentreren we ons op de convergentie van netwerkspellen onder verschillende updateregels. In het specifiek kijken we naar een bepaalde klasse van spellen (die nog steeds in verschillende toepassingen toepasbaar zijn), en bewijzen we convergentie van de dynamiek zonder randvoorwaarden, onder milde aannames over het communicatienetwerk, wanneer de spelers synchroon, asynchroon updaten en wanneer de topologie van het netwerk varieert in de tijd. Als er gekoppelde randvoorwaarden aanwezig zijn, ontwerpen we een iteratief half-gedecentraliseerd GNE-

zoekalgoritme dat aangepaste updateregels berekent die gegarandeerd convergeren naar een GNE van het spel. Vervolgens richten we ons op een meer algemene klasse van netwerkspellen waarin de kostenfunctie alleen maar differentieerbaar hoeft te zijn. We stellen een iteratief GNE-zoekalgoritme voor, gebaseerd op operatorensplitsingsmethoden, dat zorgt voor convergentie bij synchrone / asynchrone updates en dat bestand is tegen informatievertragingen. Bovendien is het algoritme, dankzij een bewuste keuze van de gebruikte hulpvariabelen, gedistribueerd, gedecentraliseerd en zeer schaalbaar.

Deel II begint met het in twijfel trekken van een aanname die meestal over het hoofd wordt gezien, namelijk de perfecte rationaliteit van de spelers. We introduceren een nieuwe dynamiek, die we de relatieve beste reactie noemen, die gedeeltelijke rationaliteit in besluitvormingsprocessen modelleert. We gebruiken de theorie van potentiële spellen om convergentie tot stand te brengen naar een GNE voor gegeneraliseerde ordinale potentiële spellen met een eindige strategie set en voor gewogen convexe potentiële spellen met een oneindige strategieset.

De rest van het proefschrift is gewijd aan twee toepassingen die in de komende jaren cruciale problemen zullen worden. Ten eerste modelleren we het slim opladen van plug-in elektrische voertuigen (PEV). We stellen een energieprijsbeleid voor dat erop gericht is de eigenaren van PEV's te stimuleren om te laden tijdens de uren dat de vraag lager is. De prijs verandert dynamisch volgens de totale vraag waaraan het net op dat moment moet voldoen. Dit creëert een koppeling tussen de PEV en, als een opkomend gedrag, vlakt het de curve van de energievraag af, waardoor het probleem van schadelijke pieken in de vraag wordt verlicht.

Ten slotte wordt een Active Traffic Demand Management voorgesteld voor een snelwegtraject op basis van het bemoedigen van de PEV's om te stoppen bij een laadstation tijdens momenten van hoge verkeersopstoppingen. De bemoediging bestaat uit een korting op de energieprijs die proportioneel verandert met het verkeerscongestie niveau. Dit werk is het eerste dat de energiemarkt koppelt aan de transportfaciliteiten en zorgt voor een grondige analyse van de geproduceerde effecten.

We laten via simulaties zien dat het in staat is om de congestiepieken te verminderen, naast het bieden van een voordelige service aan de PEV-eigenaren. In beide toepassingen maken we gebruik van spellen met gemengd geheelgetallig potentiële spellen om een rigoureus, maar zeer gedetailleerd en realistisch model van de verschijnselen te verkrijgen.

About the Author



Carlo Cenedese performed his PhD, from 2017 to 2020, with the Discrete Technology and Production Automation (DTPA) Group in the Engineering and Technology Institute (ENTEG) at the University of Groningen (NL), under the supervision of Prof. M. Cao and Prof J.M.A. Scherpen and external supervision of Prof. S. Grammatico (TU Delft).

From 2021, he is a researcher at the ETH Zürich under the supervision of Prof. J. Lygeros and take part of the NCCR Automation project "Coupled incentives to ease congestion on the electricity and road networks".

He was born in Treviso, Italy, in 1991, and received Bachelor's degree in Information Engineering in September 2013 and the Master's degree in Automation Engineering in July 2016, both at the University of Padova, Italy. From August to December 2016, Carlo worked as a research fellow for the company VI-grade s.r.l. in collaboration with the Automation Engineering group of Padova. In 2019, he visited the Department of Mathematical Sciences at the Politecnico di Torino.

His research interests include on the theoretical side: game theory, distributed optimization, and multi-agent network systems. He also worked on applications including: design of active traffic control management strategies, smart charging of EV, epidemics models and opinion dynamics.

Complete list of publications:

– 2021

[48] C. Cenedese, L. Zino, M. Cucuzzella and M. Cao, "Optimal policy design to mitigate epidemics on networks using an SIS model," 2021 IEEE 60th Annual Conference on Decision and Control (CDC), Austin USA (under review),

[44] C. Cenedese, M. Cucuzzella, J. M. A. Scherpen, S. Grammatico and M. Cao, "Highway Traffic Control via Smart e-Mobility – Part I: Theory," 2021 IEEE Transaction on Intelligent Transportation Systems (under review).

[45] C. Cenedese, M. Cucuzzella, J. M. A. Scherpen, S. Grammatico and M. Cao, "Highway Traffic Control via Smart e-Mobility – Part II: Case Study," 2021 IEEE Transaction on Intelligent Transportation Systems (under review).

– 2020

[41] C. Cenedese, G. Belgioioso, S. Grammatico and M. Cao, "An asynchronous distributed and scalable generalized Nash equilibrium seeking algorithm for strongly monotone games," 2020 European Journal of Control, doi: 10.1016/j.ejcon.2020.08.006.

[175] M. Ye, J. Liu , C. Cenedese, Z. Sun and M. Cao "A Network SIS Meta-Population Model with Transportation Flow," 2020 21st IFAC (Virtual) World Congress 2020, Berlin, Germany.

[42] C. Cenedese, G. Belgioioso, S. Grammatico and M. Cao, "An asynchronous, forward-backward, distributed generalized Nash equilibrium seeking algorithm," 2019 18th European Control Conference (ECC), Naples, Italy, pp. 3508–3513, doi: 10.23919/ECC.2019.8795952.

– 2019

[95] A. Govaert, C. Cenedese, S. Grammatico and M. Cao, "Relative Best Response Dynamics in finite and convex Network Games,"2019 IEEE 58th Conference on Decision and Control (CDC), Nice, France, pp. 3134–3139, doi: 10.1109/CDC40024.2019.9029821.

[46] C. Cenedese, F. Fabiani, M. Cucuzzella, J. M. A. Scherpen, M. Cao and S. Grammatico, "Charging plug-in electric vehicles as a mixed-integer aggregative game," 2019 IEEE 58th Conference on Decision and Control (CDC), Nice, France, pp. 4904–4909, doi: 10.1109/CDC40024.2019.9030152.

[33] M. Bruschetta, C. Cenedese and A. Beghi, "A real-time, MPC-based Motion Cueing Algorithm with Look-Ahead and driver characterization," 2019, Transportation Research Part F: Traffic Psychology and Behaviour, s.i. Driving simulation, v. 61, p. 38–52, doi: https://doi.org/10.1016/j.trf.2017.04.023.

– 2018

[47] C. Cenedese, Y. Kawano, S. Grammatico and M. Cao, "Towards Time-Varying Proximal Dynamics in Multi-Agent Network Games," 2018 IEEE 57th Conference on Decision and Control (CDC), Miami, USA pp. 4378–4383, doi: 10.1109/CDC.2018.8619670.

[34] M. Bruschetta, C. Cenedese, A. Beghi and F. Maran, "A Motion Cueing Algorithm With Look-Ahead and Driver Characterization: Application to Vertical Car Dynamics," 2018, IEEE Transactions on Human-Machine Systems, v. 48, n.1, p. 6–16, doi: 10.1109/THMS.2017.2776207.